A STUDY OF THE RECOMBINATION ACTIVATING GENE 1 IN THE ZEBRAFISH NERVOUS SYSTEM

FENG BO

A THESIS SUBMITTED FOR
THE DEGREE OF DOCTOR OF PHILOSOPHY
TEMASEK LIFE SCIENCES LABORATORY
NATIONAL UNIVERSITY OF SINGAPORE

2006

ACKNOWLEDGMENTS

I would like to thank my supervisor, Dr Suresh Jesuthasan. Without his constant support and guidance over these years, this dissertation would not have been possible. His patience and encouragement carried me on through difficult times, his insights and suggestions helped to shape my research skills, and his valuable feedback contributed greatly to this dissertation.

I thank my thesis committee members: Dr. Vladimir Korzh, Dr. Patrick Tan and Dr. Wen Zilong. Their valuable feedback helped me to improve this study in many ways.

I am grateful to Dr. Ding Shouwei, Dr. Liu Dingxiang for their guidance during the rotation period in my first year in IMA. In their labs I touched and learnt a lot of molecular techniques and knowledge that are very helpful to the work described in my thesis.

Many of my thanks also go to my friends who have given me various help during my graduate career. They are Mahendra Wagle, Cristiana Barzaghi, Caroline Kibat, Sylvie Le Guyader, Jasmine D'souza, Micheal Hendricks and Sarada Bulchand. I enjoyed all the vivid discussions we had on various topics and had lots of fun being a member of this fantastic group.

Last but not least, I thank my family for their understanding and supporting through all these years.

TABLE OF CONTENTS

CHAPTER 3 RESULTS_ PART 1 Analysis of *Rag* Expression in Zebrafish Nervous System

APPENDIXES

SUMMARY

Rag1 (recombination activating gene 1) plays a key role in V(D)J recombination and vertebrate adaptive immunity. Besides immune organs, *Rag1* transcripts have also been detected in the nervous system of vertebrates, where its function is not known. To investigate whether *Rag1* is functional and what role it could play in the nervous system, we initiated a study with zebrafish.

Firstly, we examined fluorescent transgenic zebrafish with laser scanning confocal microscopy, to document the expression of *Rag1* at single cell resolution.

Using a *Rag1:GFP* line, we found that *Rag1* was selectively expressed in many parts of the nervous system. The strongest expression appeared in the olfactory system, where *Rag1*-driven GFP was restricted only to a subset of microvillous OSNs (olfactory sensory neurons), which projected their axons to the lateral olfactory bulb. Experiments on RAG1 depleted fish (by morpholino or mutagenesis) demonstrated that axon pathfinding and amino acid detection in the olfactory system did not require RAG1. *Rag1*-driven GFP was also expressed in other parts of the nervous system, and restricted to subsets of neurons. These included RGCs (retina ganglion cell) and amacrine cells in the eye, cristae hair cells in the ear, some dorsal interneurons in spinal cord, and neurons in optic tectum, cerebellum and hypothalamus. By immunofluorescence, the RAG1 protein was detected in a portion of retinal and olfactory neurons, predominantly in the nucleus.

Rag2, an indispensable partner of *Rag1* in V(D)J recombination, was also detected in the nervous system, but was not co-expressed with *Rag1*. Both *Rag2*-driven GFP and DsRed

showed clear expression in the olfactory epithelium, which, however, was restricted to a group of ciliated OSNs projecting to ventral glomeruli.

To seek evidence for a neuronal function of *Rag1*, we carried out a microarray study and compared the overall gene expression between *Rag1* mutants and wt siblings, either in the olfactory epithelium of adults, or in the anterior regions of 3 day-old larvae.

The experiment with RNA isolated from adult olfactory rosettes revealed broad and complicated changes of gene expression. They mainly indicated an overall increase of innate immunity, activation of secondary responses upon infection, and a neuronal degeneration that was likely a consequence of the immune responses. All of these changes were possibly caused by the loss of adaptive immunity, which corresponds to *Rag1*'s immune function. *Rag1*'s neuronal function still remains obscure.

In the microarray with 3 dpf larvae, the transcription of one clone, named 12158, was revealed to be associated with *Rag1* integrity. This was also confirmed by RT-PCR.

All in all, our expression analysis suggests that *Rag1* is unlikely to mediate DNA rearrangement similar to V(D)J recombination in the nervous system. Instead, it may play some other function in selected groups of neurons. Our microarray experiments revealed the global effect of *Rag1* deficiency and suggested some candidates for *Rag1* downstream genes in neurons.

LIST OF TABLES

LIST OF FIGURES

LIST OF ABBREVIATIONS

A/P	Anterior/posterior
abcb3	ATP-binding cassette, subfamily B member 3
ACP	Annealing Control Primer
ANOVA	Analysis of Variance
AOB	Accessory Olfactory Bulb
AP	Alkline Phosphatase
ATM	Ataxia Telangiectasia Mutated Protein
BAC	Bacterial Artificial Chromosome
BBB	Brain blood barrier
Bcl	B-cell leukemia/lymphoma 1
BSA	Bovine Serum Albumin
CDK2	Cyclin-dependent kinase 2
cDNA	Complementary DNA
CNS	Central Nervous System
CoBL	Commissural Bifurcating Lateral Neuron
CR	Chicken Repeat
C-terminal	Carboxy-terminal
D/V	Dorsal/ventral
DAPI	4'6,-diamino-2-phenylindole

DEPC	Diethylpyrocarbonate
DIG	Digoxigenin
DMSO	Dimethylsulfoxide
DN	Double Negative
DNA	Deoxyribonucleic Acid
DNA-PKcs	DNA-Dependent Protein Kinase Catalytic Subunit
DNase	Deoxyribonuclase
dNTP	Deoxyribonucleoside Triphosphates
DP	Double Positive
dpf	Days Post Fertilization
DPP	Decapentaplegic gene
DSB	Double Strand Break
DSCAM	Down syndrome cell adhesion molecule
EB	Ethidium bromide
EDTA	Ethylenediamine tetraacetic acid
EGF	Epithelial Growth Factor
EST	Expressed Sequence Tag
FDR	False discovery rate
GABA	Gamma aminobutyric acid
GAP-43	Growth-associated protein-43
GCL	Ganglion Cell Layer
GFP	Green Fluorescent Protein
HMG1/2	High-Mobility-Group Protein 1/2
hpf	Hours post fertilization
HRP	Horseradish peroxidase
HuC	Hu protein C

Ig	Immunoglobulin
IgH	Immunoglobulin heavy chain
IgL	Immunoglobulin light chain
INL	Inner Nuclear Layer
IPTG	Isopropyl-1-thio-β-D-galactoside
Ku70/80	70 and 80 kD subunits of Ku antigen
LacZ	Bacterial β-galactosidase
LCR	Locus Control Region
LG	Linkage Group
log	Logarithm
LOWESS	Locally weighted scatterplot smoothing normalization
MHC	Major Histocompatibility Complex
MOE	Main Olfactory Epithelium
mRNA	Messenger RNA
NCBI	National Center for Biotechnology Information
NHEJ	Non-Homologous DNA End Joining
NWC	"very interesting" in Polish
OB	Olfactory Bulb
°C	Degree Celsius
OCAM	Olfactory cell adhesion molecule
OE	Olfactory Epithelium
OMP	Olfactory Marker Protein
ONL	Outer Nuclear Layer
OR	Odorant Receptor
ORF	Open Reading Frame
OSN	Olfactory Sensory Neuron

p53	Tumour Protein with a molecular weight of 53 kD
PAC	P1-derived Artificial Chromosome
Pcdh	Protocadherin
PCR	Polymerase Chain Reaction
PFA	Para-formaldehyde
PNS	Peripheral nervous system
POD	Horse-radish peroxidase
PSC	Post-cleavage synaptic complex
PTU	1-phenyl-2-thiourea
RACE	Rapid amplification of cDNA End
Rag1	Recombination activating gene 1
Rag2	Recombination activating gene 2
RAS	Rat Sarcoma
RGC	Retina gaglion cell
RING	Really interesting new gene
RNA	Ribonucleoside acid
RNase	Ribonuclease
rRNA	Ribosomal RNA
RSS	Recombination signal sequence
RT	Reverse transcription
RTase	Reverse transcriptase
SAM	Significance analysis of microarray
SCID	Severe combined immunodeficiency
Shh	Sonic Hedgehog
SOG	Short gastrulation
SPF	specific pathogen free

SSC	Sodium chloride-sodium citrate buffer
SV2	Synaptic vesicle-2 protein
TAP2B	Transporter associated with antigen processing 2 b
TCR	T-cell receptor
TCRα	T-cell receptor α chain
TCRβ	T-cell receptor β chain
TdT	Terminal deoxynuleotidyl transferase
TIGR	The Institute for Genomic Research
Tris	Tris (hydroxymethyl) aminomethane
Tris-HCl	Tris hydrochloride
TRPC2	Transient receptor potential channel C2
TSA	Tyramide signal amplification
TUNEL	Terminal deoxynucleotidyl Transferase Biotin-dUTP Nick End Labeling
UAS	Upstream Activating Sequence
UTR	Untranslated region
V2R	Vasopressin type 2 receptor
VNO	Vomeronasal Organ
wt	Wild type
X-gal	5-bromo-4-chloro-3-indolyl-β-D-galactoside
XRCC4	X-ray repair complementing defective repair in Chinese hamster cells 4

PUBLICATIONS

Feng, B., Bulchand, S., Yaksi, E., Friedrich, R. W. and Jesuthasan, S. (2005). The recombination activation gene 1 (Rag1) is expressed in a subset of zebrafish olfactory neurons but is not essential for axon targeting or amino acid detection. *BMC Neurosci* **6**, 46.

Feng, B., Schwarz, H. and Jesuthasan, S. (2002). Furrow-specific endocytosis during cytokinesis of zebrafish blastomeres. *Exp Cell Res* **279**, 14-20.

CHAPTER 1 INTRODUCTION

1.1 The Rag genes

Rag1 and *Rag2* (recombination activating gene 1 and 2) are well-known key players in V(D)J recombination, an essential process for developing adaptive immunity. They are found only in jawed vertebrates, and are thought to have evolved from ancient transposases. Consistent with their essential function in the immune system, they are highly conserved among different species. Although *Rag* genes were identified as lymphoid-specific genes, they are also detected in nervous system. This has attracted a lot of interest, but its significance is still poorly understood.

1.1.1 *Rag* function in the immune system

One of the intriguing features of the vertebrate adaptive immune system is its ability to generate specific responses to a tremendous number of antigens. The basis of this capability is the highly diversified B-cell receptor (immunoglobulin) and T-cell receptor proteins, which physically bind to specific target antigens and direct humoral or cellular responses to these stimuli (Fig. 1-1) (Bruce Alberts, 2002).

In the germline genome, immunoglobulin (Ig) and T-cell receptor (TCR) loci are composed of dispersed multiple variable (V), joining (J), and diversity (D) gene segments. For assembly of a complete antigen receptor gene, one V, one J and in some cases one D gene segment are joined by V(D)J recombination to create an exon that encodes the antigen binding portion. After transcription, this V(D)J exon is spliced to the exons encoding the constant region, producing the mature mRNA and subsequently the receptor polypeptide (Fig. 1-2) (Bruce Alberts, 2002; Fugmann et al., 2000; Gellert, 2002). Therefore, each receptor polypeptide contains a variable region and a constant

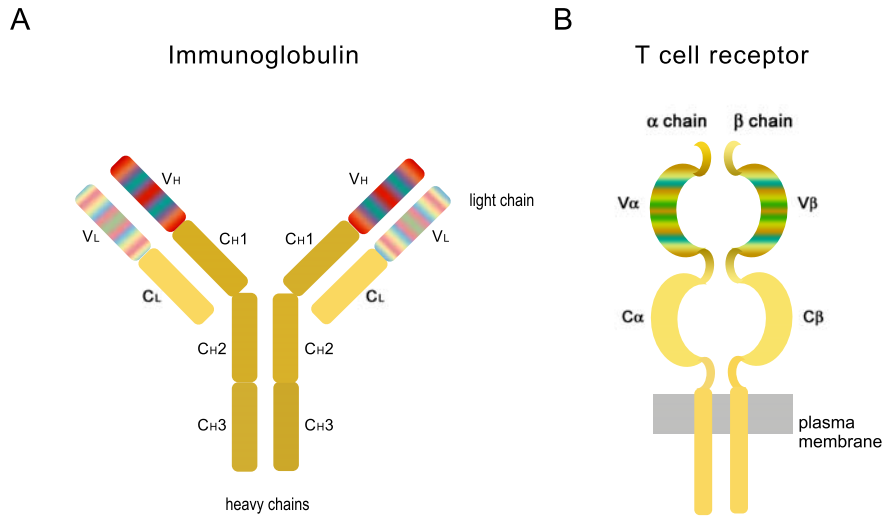

Figure 1-1. Immunoglobulin (Ig) and T cell receptor (TCR).

(A) Each Ig molecule contains two light chains and two heavy chains. The variable domains (highlighted as colorful squares) of the light and heavy chains (V_L and V_H) make up the antigen-binding sites. (B) The TCR is transmembrane protein that is composed of one α and one β poly-peptide chain. Each of them has one variable domain (V_α and V_β) on the extracellular part. It is thought that the V_α and V_β form an antigen-binding site similar to that from Ig molecules. Both the variable domains of Ig and TCR are translated from the V(D)J-joint exons that are created by the rearrangement of genomic DNA in developing lymphocytes (Bruce, 2002).

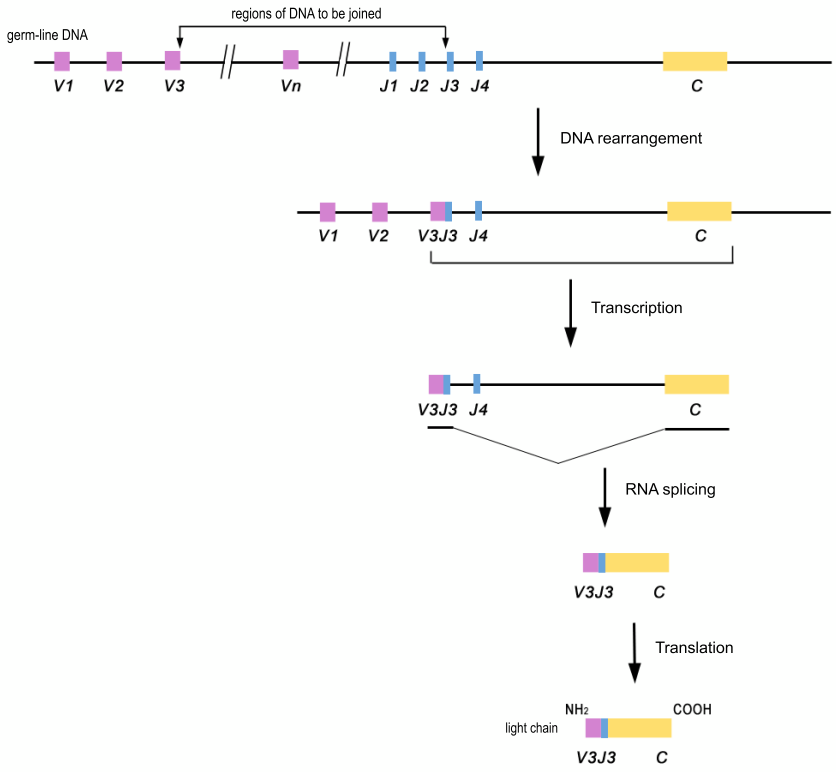

Figure 1-2. An example of V(D)J recombination: the V-J joining process involved in making a κ light chain of immunoglobulin in mouse.

In the developing B cells, the chosen V gene segment (V3 in this case) joins to the J gene segments (J3 in this case) by DNA recombination. The VJ joint-exon was transcribed together with a constant region C, as well as the intron and the "extra" J gene segment. By RNA splicing, the VJ exon joined the C region, with the intron and the "extra" J gene segment removed. The VJC joint mRNAs are then translated into κ light chain (Bruce, 2002).

region (Fig. 1-1). The variable regions created through V(D)J recombination directly provide the diversity of antigen receptors. The process of gene rearrangement via recombination is strictly regulated in a lineage-, locus- and stage-specific manner. The B cells and T cells rearrange specifically the immunoglobulin and T cell receptor genes respectively. The assembly of TCRβ genes happens earlier than TCRα genes during T cell development; IgH genes are assembled before IgL genes in developing B cells (Bassing et al., 2002). And, all of the rearrangements occur in the context of allelic exclusion. For example, a mature B cell expresses only one of its two IgH and one of its multiple IgL alleles (Gorman and Alt, 1998). This ensures that any mature T cell or B cell expresses only one type of antigen receptor.

V(D)J recombination is targeted by specific recombination signal sequences (RSSs) that lie adjacent to each gene segment. These RSSs consist of conserved heptamer (consensus 5'-CACAGTG) and nonamer elements (consensus 5'-ACAAAAACC) separated by a poorly conserved 12 or 23 nucleotides spacer. According to the length of its non-conserved spacer, an RSS is referred as 12-RSS or 23-RSS. Efficient V(D)J recombination take place only between a 12-RSS and a 23-RSS, a phenomenon known as the 12/23 rule (Fig. 1-3) (Fugmann et al., 2000; Gellert, 2002).

The process of V(D)J recombination can be considered as two phases, cleavage and joining. In the first phase, the two RSSs are recognized by the recombination machinery and form the synaptic complex, where DNA is cleaved precisely between the RSSs and their flanking coding element. In this process, the recognition of two RSSs and the cleavage of double strands DNA are mainly processed by RAG1 and RAG2 proteins; high-mobility-group protein 1 and 2 (HMG1/2) enhance the formation of synapsis and DNA cleavage. To cleave the DNA, RAG proteins bind to both RSSs and introduce a nick precisely at the 5' border of the heptamer of each RSS. This leads to the exposure of

a 3'-hydroxyl group on the coding flank, which subsequently attacks a phosphodiester bond on the other DNA strand and produces a covalently sealed hairpin coding end. The other side of the break remains as 5' phosphorylated blunt end, which terminates in the heptamer of the RSS and is referred as the signal end (Fig. 1-3) (Gellert, 2002). The second phase is a joining phase. Initially the four RAG-liberated DNA ends remain associated with RAG in a stable post-cleavage synaptic complex (PSC), which is important for coupling the cleavage and joining stages of V(D)J recombination (Ramsden et al., 1997). Then the factors that mediate non-homologous DNA end joining (NHEJ) are recruited and repair the DNA breaks. Ku70 and Ku80 are firstly recruited and form a complex at the double strand break (DSB) ends. They may play a function in protecting the broken DNA (Jones and Gellert, 2001; Walker et al., 2001). After the Ku complex, DNA-PKcs (DNA-dependent protein kinase catalytic subunit) and Artemis are recruited, but only to the coding ends. Within a complex, Artemis is phosphorylated by DNA-PKcs and acts as an endonuclease in cleaving the RAG-generated hairpins (Le Deist et al., 2004; Meek et al., 2004). At last, XRCC4 and DNA ligase 4 join and catalyze the ligation for both the coding ends and signal ends (Bassing et al., 2002). At this step, TdT (terminal deoxynucleotidyl transferase) is involved in the coding end joining and attributes the junction diversity by adding extra nucleotides (Komori et al., 1993). Therefore, the coding ends form imprecise coding joints and signal ends are fused as precise signal joints. (Fig.1-4) (Bassing et al., 2002; Jung and Alt, 2004).

Both *Rag1* and *Rag2* are essential for V(D)J recombination. Mice with either *Rag* gene depleted are completely defective in V(D)J recombination and produce no mature T cell and B cell (Mombaerts et al., 1992; Shinkai et al., 1992). RAG proteins are relatively large. For example, murine RAG1 and 2 consist of 1040 aa and 527 aa respectively. Full-length RAG1 and RAG2 protein are difficult to express and purify *in vitro*. Instead, a

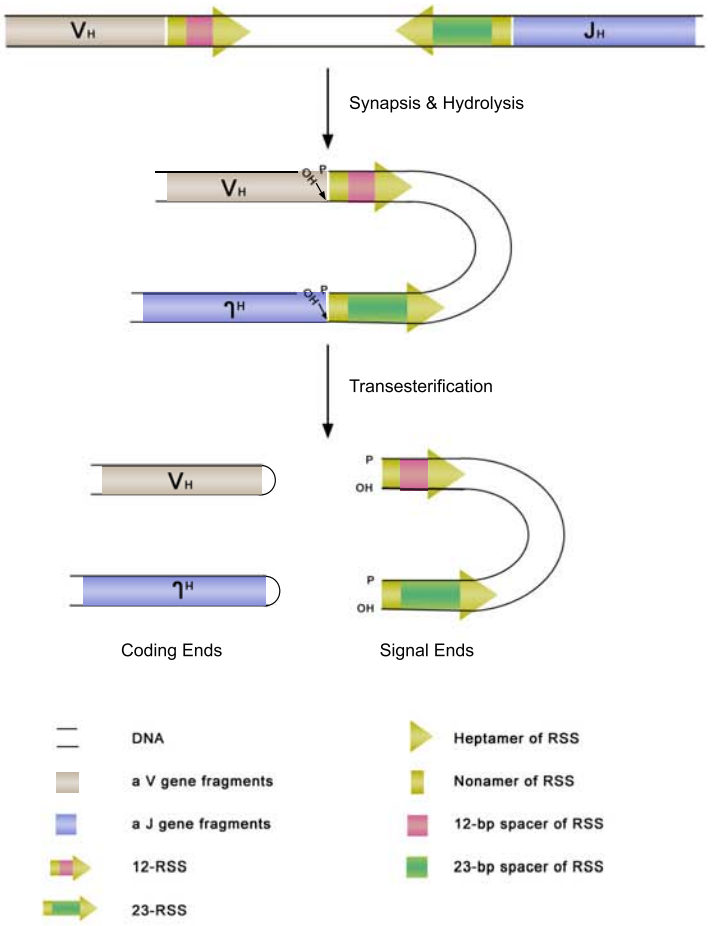

Figure 1-3. DNA cleavage by RAG proteins.

Schematic structures of 12-RSS and 23-RSS, flanking to a V and a J gene segment respectively, are shown. Firstly within a synapsis complex, a nick is made at the 5' end of the RSS heptamer, leaving a 3'-OH on the coding flank. Secondly, the left 3'-OH attacks the opposite strand and produce a hairpin coding end as well as a blunt signal end. This figure shows a coupled process at a pair of RSSs (Gellert, 2002).

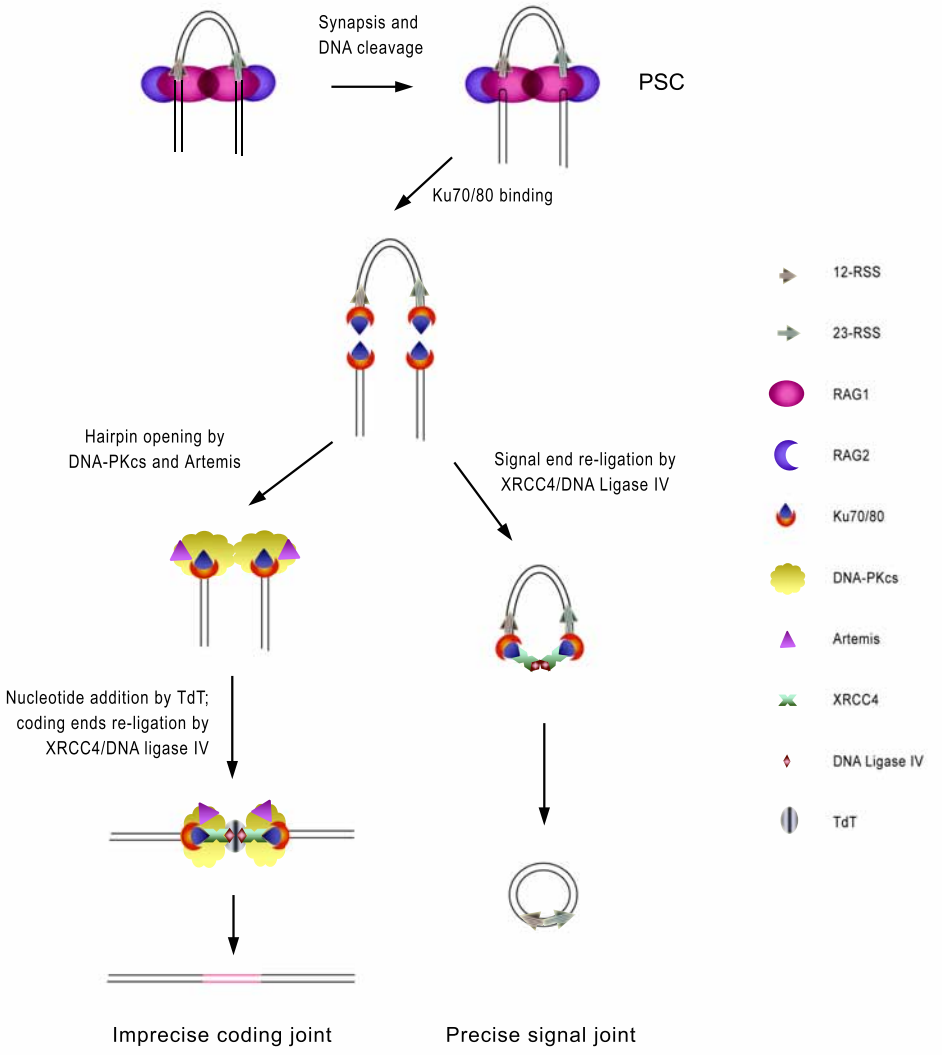

Figure 1-4. NHEJ proteins repair and join RAG-liberated coding and signal ends.

The Ku proteins, XRCC4 and DNA ligase IV are required for both coding and signal joins, while the DNA-PKcs and Artemis are more important for coding joins. The RAGs in the PSC (post-cleavage synapsis complex) are also important for joining both coding and signal ends (Bassing et al., 2002; Jung et al., 2004).

truncated “core” version of RAG1 and RAG2 are soluble and were found to retain all DNA cleavage activity in both *in vivo* and *in vitro* assays (Sadofsky et al., 1994; Silver et al., 1993). Thus biochemical characterization of RAG1 and 2 has largely focused on the core region of RAG1 (384-1008 aa) and RAG2 (1-387 aa). While the contribution of RAG2 to the V(D)J recombination is not clear, many aspects of core RAG1 and its function in V(D)J recombination are known. A catalytic triad of three residues, the DDE (aspartate-aspartate-glutamate) motif in RAG1 core region, is found essential for DNA cleavage. Mutation of any of the three residues (D600, D708, or E962) abolishes recombination of extra-chromosomal substrates *in vivo* as well as RSS cleavage by the purified protein (Kim et al., 1999; Landree et al., 1999). The core region of RAG1 also mediates the recognition of 12-RSS and 23-RSS. Two individual domains, the nomamer-binding domain and the central domain, were found to carry specific affinity to the conserved nonamer and heptamer elements of RSS respectively. In addition, the central domain also functions to recruit RAG2 to the recombination complex (Fig.1-5. B and C) (De and Rodgers, 2004).

Little is known about the non-core region of RAG proteins, however, available evidence clearly illustrate their importance in RAG function. The core RAG proteins perform V(D)J recombination less efficiently than the full-length proteins in the transgenic mice (Akamatsu et al., 2003; Dudley et al., 2003; Liang et al., 2002). Furthermore, the pathogenesis of some human SCID (severe combined immunodeficiency) and Omenn syndrome is linked to mutations in the non-core regions, e.g. at the N-terminal of RAG1 or C-terminal of RAG2 (Santagata et al., 2000; Schwarz et al., 1996; Villa et al., 2001). Recently an E3 ubiquitin ligase activity was assigned to a RING finger motif in the N-terminal non-core region of RAG1 (Fig.1-5. B and C), although its relationship with V(D)J recombination remains unknown (Yurchenko et al., 2003).

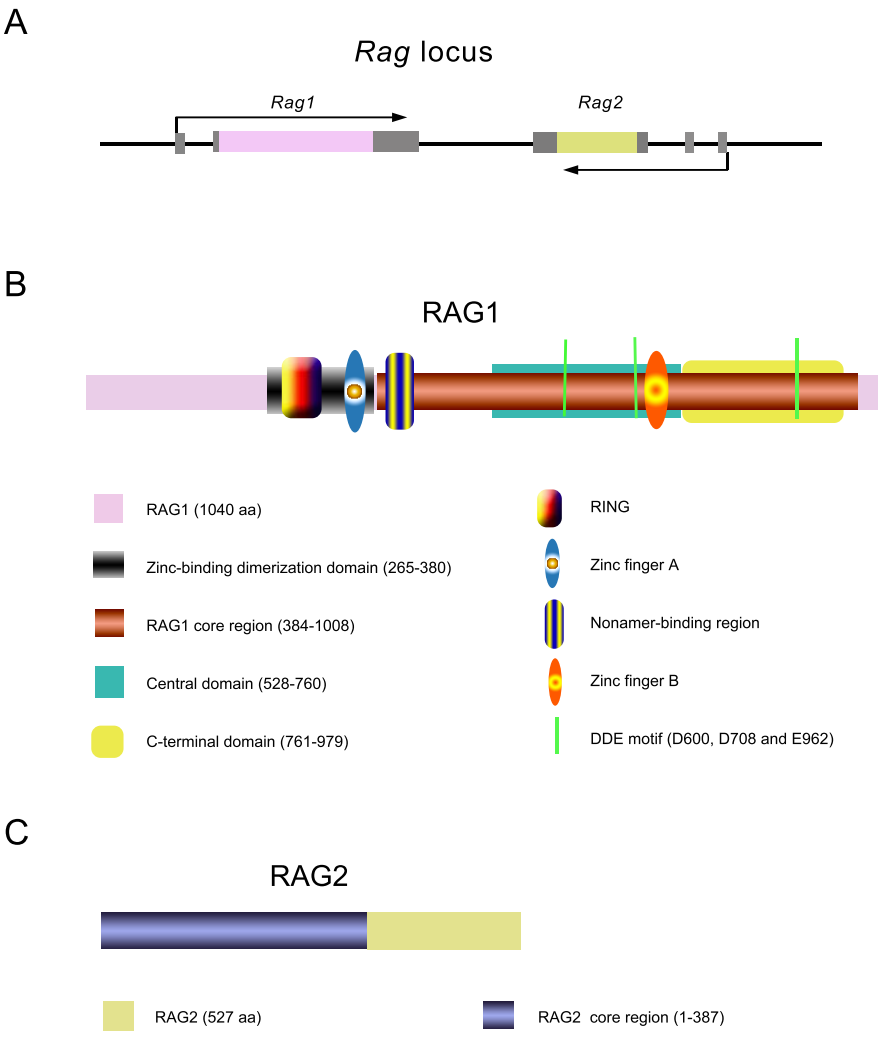

Figure 1-5. Schematic representations of murine *Rag* locus and RAG proteins.

(A) In *Rag* locus, *Rag1* and *Rag2* genes locate next to each other in opposite direction. In most species, the entire open reading frame (rectangles colored with pink for *Rag1* ORF, light green for *Rag2* ORF) is contained in a single large exon (Schatz, 2004). (B, C) The murine RAG1 and RAG2 proteins, with the core and non-core regions highlighted, are represented schematically as bars. The core regions of both RAGs are the minimal regions required for catalysis. The locations of the putative catalytic residues (D600, D708 and E962) in RAG1 are shown. Other function motifs are represented as indicated (De and Rodgers, 2004).

1.1.2 *Rag* genes may originate from ancient transposases.

A 25-year-old hypothesis that proposes a transposon-related beginning for the evolutionary origin of *Rag* genes and V(D)J recombination is highly favored (Brandt and Roth, 2004; Chatterji et al., 2004). It has been supported by many features of the *Rag* genes and V(D)J recombination. (i) In most species, including *Xenopus*, chicken, mouse and human, *Rag* genes do not contain introns in their open reading frame. Only the *Rag1* genes in zebrafish, fugu and rainbow trout are known to contain introns (Hansen and Kaattari, 1995; Willett et al., 1997). The compact nature of *Rag* genes suggests that they may evolve from a small transposable element. (ii) The unusual arrangement of RSSs in Ig and TCR loci (flanking to the V, D, J coding elements and being cut off during DNA recombination) highly resembles the inverted repeat sequences at either end of a transposon (Schatz, 2004). (iii) The DDE motif is an active catalytic site for a large family of transposases. It is highly conserved in the RAG1 core region among different species and is required for DNA cleavage during the V(D)J recombination (Jones and Gellert, 2004). (iv) The formation of hybrid joints in the recombination process and the way that RAG1 nicks the transferred strand and carries out strand transfer also exhibit similar biochemical features to transposition (Jones and Gellert, 2004). Furthermore, this hypothesis is strongly strengthened by the discovery of RAG-mediated transposition. Although RAG-mediated transposition was found to be inefficient *in vivo* (Messier et al., 2003; Schatz, 2004), the core regions of RAG1 and RAG2 indeed are able to carry out transposition *in vitro* (Agrawal et al., 1998; Hiom et al., 1998).

Some literature suggests that both *Rag* genes might have been introduced into the vertebrate genome by a horizontal transfer of a single ancient transposon. In the genome of all vertebrate species examined, *Rag1* and *Rag2* lie immediately adjacent to each other, separated only by a few kb in opposite orientation (Fig.1-5. A). No significant sequence

homology is found between these two genes, indicating that they are unlikely to be derived from gene duplication. These striking features suggest that *Rag1* and *Rag2* might have entered the genome of a vertebrate ancestor at the same time, possibly by the insertion of a single transposable element (Schatz, 2004). Moreover, *Rag* genes are found only in jawed vertebrates from the level of sharks (Bernstein et al., 1996; Greenhalgh and Steiner, 1995; Schluter and Marchalonis, 2003), and no close homolog of either *Rag* gene has been found in the lower eukaryotes (jawless vertebrates and invertebrates). The evolutionary discontinuity also indicates that *Rag* genes might have entered the vertebrate genome via a horizontal gene transfer event.

Data from other studies, however, have been used to propose that *Rag1* and *Rag2* might have been introduced into the vertebrate lineage by separate events. The transposases encoded by DNA transposons from the *Transib* superfamily have been found to be significantly similar to the *Rag1* core region, with an identity of 25~30% at the amino acid level (Kapitonov and Jurka, 2005). In addition, *Transib* transposons carry a pair of 38-bp terminal inverted repeats consisting of a conserved 5'-CACAATG heptamer and an AAAAAAATC-3' nonamer separated by a variable 23-bp spacer, which is highly similar to RSSs; *Transib* transposons prefer GC-rich regions and generate 5-bp target site duplication during transposition, both of which also have been found in RAG-mediated transposition. But different from the *Rag* locus that always contains both *Rag1* and *Rag2* genes, the *Transib* transposons identified so far encode only one protein, the *Rag1* "core"-like transposase. No homologous sequence to the 5' non-core *Rag1* or to *Rag2* has been located in *Transib* transposons. And no *Rag2*-like sequence has been found in the recently sequenced genomes, such as those from sea urchin, lancelet, hydra and sea anemone, which contain the *Transib* transposon and the *Rag1*-like sequence. One interpretation of this data is that *Rag1* evolved from a fusion of once separate proteins and originated separately from *Rag2* (Kapitonov and Jurka, 2005).

1.1.3 Diversity and conservation of *Rags* among organisms

Rag genes have been found in almost all jawed vertebrates examined so far, including those species that appeared in the last 4 million years and are mostly still prevalent on the earth (Bernstein et al., 1996; Schatz, 2004). Despite the broad distribution and the long period of evolution, *Rag* genes are highly conserved.

The basic organization of *Rag* locus in genome has remained among different species. (i) *Rag1* and *Rag2* genes are always located next to each other in opposite direction, although the size of the entire *Rag* locus and the length of the intergenic region between *Rag1* and *Rag2* vary in different organisms (Fig.1-5. A) (Peixoto et al., 2000). (ii) In most species the entire open reading frame and 3' UTR is fitted into a single exon. Introns have been only found in the *Rag1* gene of fishes. According to their position within *Rag1* coding sequence, two types were delineated. One is small and located in the N-ternimal part; the other lies in the middle and is relatively large. Chondrostei and Neopterygii fishes lack the first small intron, while teleosts have both (Venkatesh et al., 1999).

The protein sequences of both RAG1 and RAG2 are highly conserved in sharks, fish, amphibians, birds and mammals. The similarity of RAG1 proteins among different species is between 60~90%. Compared to RAG1, RAG2 is less conserved, with similarity ranging from 50% to 80%. The matches within RAG2 protein are mostly distributed evenly over the whole sequence, whereas in RAG1 protein, the N-terminal one third protein is significantly more divergent than the C-terminal two third (Frippiat et al., 2001; Schluter and Marchalonis, 2003; Willett et al., 1997). More detailed comparison between gene sequences in several organisms defines 6 distinct homology domains within the RAG1 protein (Bernstein et al., 1996). The strongly conserved fifth and sixth homology regions have been found to be indispensable for processing the recombination of RSS-substrate *in vitro*. The first and second homology regions are unnecessary in episomal

recombination, but are important for binding of nucleopore protein and potentially function in transportation of RAG1 into the nucleus. Homology region 3 contains a RING zinc finger motif, but its function, aside from acting as an E3 ligase (Yurchenko et al., 2003), still remains elusive. The region 4 has not been well-characterized.

The high-extent conservation of RAG protein sequences, genomic organization and gene structures indicates that the functions, as well as the regulation of *Rag* genes are important. It correlates well with the evolutionary stability of other components of adaptive immunity, which provides a great benefit for vertebrates. The diversity, despite the conservation of *Rag* genes, indicates the shaping of evolution and can be used as an indicator of evolutionary changes. A comparison of *Rag* genes across different species can suggest conserved structures that are potentially important for function. This may help us to understand any unknown functions and regulation of *Rag* genes.

1.2 Rags in the nervous system

1.2.1 The expression of *Rag* genes in the nervous system

Rag genes were initially identified as lymphoid-specific factors. Indeed, *Rag* genes are strongly expressed in immune organs of every jawed vertebrate species that have been tested so far. In mice, the co-expression of two *Rag* genes is found within the bone marrow and thymus (Oettinger et al., 1990) . In *Xenopus*, besides the thymus and bone marrow, slight expression of *Rags* was detected in the kidney of adult frog (Greenhalgh et al., 1993). In chickens, the transcripts of both *Rag1* and *Rag2* have been found in the thymus, and *Rag2* alone in Bursa of Fabricius (Pickel et al., 1993). In fish the expression of *Rag* genes is also confirmed in thymus and kidney (Hansen and Kaattari, 1996; Peixoto et al., 2000; Schluter and Marchalonis, 2003; Willett et al., 1997). Furthermore, within the immune organs *Rag* genes expression has only been found in the precursor B and T cells

where V(D)J recombination occurs, not in cells from other stages of lymphoid development (Lieber et al., 1987).

The conserved, highly restricted expression of *Rag* genes in the immune system correlates well with their function in V(D)J recombination. Because of their ability to rearrange the genome, *Rag* genes are dangerous, as unwanted rearrangement can be oncogenic. It would have become critical to keep *Rag* genes under tight regulation and expressed only in those cells that require their function (Barreto et al., 2001). In light of this, it is intriguing that the expression of *Rag1* was also detected in the brain and retina in a range of organisms. As early as 1991, David Baltimore's group reported the detection of *Rag1* transcripts in the murine central nervous system (CNS), by RT-PCR, in situ hybridization and Northern blot analysis. As revealed by in situ hybridization, the expression of *Rag1* in the mouse brain is widespread at a low level and most apparent in postnatal cerebellum and hipocampal formation. The *Rag2* transcripts, in contrast, were not detected by in situ hybridization and Northern blot analysis, and were only sporadically amplified by RT-PCR (Chun et al., 1991).

It was noticed for long time that the nervous system and immune system are both extreme complex, diverse and able to maintain memory. *Rag* genes and V(D)J recombination provide the major foundation of the immune diversity, while the mechanism to generate neuronal diversity is poorly understood. Further comparison between the nervous system and immune system revealed a variety of signaling molecules, transcription factors, cell surface antigens and receptors common for both systems (Boulanger and Shatz, 2004; Farrar et al., 1987; Loconto et al., 2003; Tordjman et al., 2002; Wekerle, 2005). This suggests that the two systems may use a similar strategy to achieve their diversity, and possibly also to encode memory. Given the central role of *Rag1* in V(D)J recombination,

its expression in the mouse brain directly raised the hypothesis that *Rag1* may mediate a similar DNA rearrangement process in the nervous system.

To test whether *Rag* genes play a function in mediating the site-specific recombination in the nervous system, transgenic mice carrying a modified RAG substrate were generated. These mice carried an inverted *LacZ* gene, driven by a universal promoter and flanked by a pair of RSSs, so that the RAG-recombination machinery can flip the *LacZ* gene at RSS sites and allow the promoter to transcribe *LacZ*. The translated protein, β-galactosidase, could be further detected by the substrate, X-gal. The results from these studies were exciting. Besides staining in the immune system, which was expected, X-gal staining was specifically detected in the brain and spinal cord among various non-lymphatic tissues. The distribution of X-gal labeling was widespread, but neither diffuse nor random. In the brain, more than 70 nuclei and tracts were selectively labeled (Abeliovich et al., 1992; Matsuoka et al., 1991). Similar studies were also carried out independently by two other groups. However, Tonegawa's group concluded that the expression of *LacZ* is due to the region- and neuron-specific backward transcription (Abeliovich et al., 1992); Honjo's group was unable to find any evidence of DNA recombination in the brain (Kawaichi et al., 1991). In addition, Papaioannou's group reported that the *Rag1*-knockout mice showed no obvious neuroanatomical and behavioral abnormalities (Mombaerts et al., 1992), which does not suggest that *Rag1* is functional in neurons.

The search for further evidence in support of "neuronal recombination" has proven very difficult, and no supporting data was produced in the following several years. In 1999, using transgenesis, Shuo Lin's group reported that the *Rag1* gene was also expressed in the zebrafish nervous system, in olfactory sensory neurons. They further confirmed the *Rag1* expression in olfactory epithelium by in situ hybridization and RT-PCR (Jessen et

al., 1999). This largely strengthened the report of *Rag1* transcripts in murine CNS, and led to the serious examinations of this phenomenon in other species. In 2000, when *Rag* genes of puffer fish were cloned, *Rag1* was detected in the brain and retina by RT-PCR (Peixoto et al., 2000) . In 2001, salamander *Rag1* was detected in the brain and retina by RT-PCR and in situ hybridization, although in a much less amount compared to its expression in thymus and kidney (Frippiat et al., 2001). These data indicate that the expression of *Rag1* in the nervous system is conserved among vertebrate species and suggest a function.

1.2.2 A brief overview of the nervous system

The nervous system is the most complex organ system in animals, and makes them distinguishable from other living organisms. Because of the nervous system, animals are able to receive information about the internal and external environments, to interpret it and make decisions, and to organize and carry out action. According to these functions, the nervous system is categorized as sensory system, integrating system and motor system respectively (Delcomyn, 1998). The structural organization of the nervous system is distinctive in different animals. But on general, they all can be divided into central and peripheral parts. The central nervous system (CNS) consists of the brain and the spinal cord (or nerve cord for invertebrates), which contains the main portion of neural tissue in the body and mostly carries out the function of integration. The peripheral nervous system (PNS) is defined to cover all neural tissues that lie outside the CNS, including the sensory and motor system. It functions in sensing stimuli, transmitting signals and carrying out response action (Delcomyn, 1998).

The structural and functional unit of the nervous system is the neuron. A neuron usually consists of a cell body (also called soma) containing the nucleus, one long process (axon) to transport information away from the cell body, and many short branches (dendrites) to

convey information toward the cell body (Delcomyn, 1998). The terminals of axon and dendrites can be extensively branched, and simultaneously connect many branches from many other neurons. The specialized connections between neural branches, called synapses, enable signal transmission between neurons and therefore establish neuronal communication (De Robertis, 1967; Jessell and Kandel, 1993). Based on function, neurons are classified into three types. Sensory neurons receive environmental stimuli and send out signals. Motor neurons deliver output signal to muscles or glands, and trigger action. Interneurons, in a general sense, refer to neurons that not belong to the class of sensory and motor neurons (Delcomyn, 1998). They transmit signals between neurons, and largely correspond to the integrative function of nervous system. Through specific synapses, these neurons build up the nervous system into a vast network with intricate connections, which functions in information communication.

1.2.3 Questions about the neuronal function of *Rag1*

The conserved expression of *Rag1* in the nervous system among vertebrates apparently indicates a function. Questions about this are interesting, but challenging. So far, the description and analysis of *Rag1*'s neuronal expression is limited, and the presence of *Rag2* in CNS is uncertain, largely due to the weak transcription of *Rags* in the nervous system. *Rag* genes are unique to vertebrates, thus may attribute some vertebrate specific features to the nervous system. Comparison between vertebrate and invertebrate nervous system revealed some difference. For example, the DsCAM (Down syndrome cell adhesion molecule) to generate neuronal diversity in *Drosophila* is not a diverse molecule in vertebrates. However, this provides no clear clue as to a possible role for *Rag1*. So far, it is not clear whether *Rag1* is functional, and what its function in the nervous system could be. To investigate these issues, models and techniques that provide higher sensitivity are required.

1.3 Advantages of using zebrafish

1.3.1 Zebrafish as a model for developmental and genetic research in vertebrates

Our understanding of many aspects of life has benefited from studies on model organisms. Each organism provides different advantages in laboratory experiments, but also has its own limitations. The fruit fly *Drosophila melanogaster* and nematode worm *Caenorhabditis elegans* have proven extraordinarily suitable for mutagenesis screens (forward genetics). Many fundamental signaling pathways in development were established from the analysis of mutated fly and worms, such as EGF (epidermal growth factor)/RAS (rat sarcoma), Notch, DPP (decapentaplegic)/SOG (short gastrulation) signaling pathways (Jorgensen and Mango, 2002; St Johnston, 2002). But these organisms are invertebrates; they cannot be used for studying vertebrate-specific features, such as a complex brain, notochord, multi-chambered heart, neural crest cells and kidney. Among models organisms, the mouse is a high vertebrate, which has been studied for more than 60 years and with it many exquisite methods have been established. But with this model it is difficult to study the early embryogenesis that occurs within the mother's uterus. Furthermore, an individual female produces a limited number of progeny, which makes the mouse also not suitable for genetic screens. In recent years, more and more animals have been explored and developed as research models. Among them, a small tropical fish, zebrafish (*Danio rerio*) has become an important model organism for biological research within the last decade.

Firstly noticed by George Streisinger, the zebrafish carries many features that are well suited for genetic and developmental studies. The embryos of this fish develop externally and are optically transparent. This provides easy access to all developmental stages, and facilitates embryological experiments and rapid screens of live embryos by morphology. Researchers can examine early embryogenesis without disrupting development. Zebrafish

are also robust and prolific breeders in the laboratory. Individual females can produce hundreds of progeny on a regular basis all year round and the young generation grows fast; they can reach sexual maturity in 3 months (Detrich et al., 1999; Grunwald and Eisen, 2002). Taking advantage of these features, many mutagenesis and genetic screens have been carried out. Just from the first two large-scale chemical mutagenesis screens, nearly 2000 mutations have been isolated. The phenotypic analyses of embryonic development in the obtained mutants were published in an entire issue of Development in Dec 1996 (Driever et al., 1996; Haffter et al., 1996).

Other studies demonstrate that zebrafish is also suited for cellular studies of vertebrate embryonic development. The embryos are simple and small. Their transparent cells are accessible for manipulative experiments, such as injection, ablation and transplantation (Mizuno et al., 1999). Moreover newly-developed tools greatly increased the utility of zebrafish as an experimental model. The zebrafish genome has been partially sequenced by the Sanger Center (Jekosch, 2004); full-length cDNA and multiple microarrays are available for expression profiling analysis (Lo et al., 2003; Ton et al., 2002); anti-sense morpholino oligonucleotides provide a method for reverse genetic studies (Nasevicius and Ekker, 2000). These advances enabled developmental and genetic research using zebrafish to be carried out with higher speed and more detail, and parallely expanded the studies on zebrafish to several other fields, including drug screens (Zon and Peterson, 2005), human disease studies (Ackermann and Paw, 2003; Dooley and Zon, 2000; Shin and Fishman, 2002) and neuroscience (Bilotta and Saszik, 2001; Malicki, 2000).

1.3.2 Advantages of zebrafish in experimental neuroscience research

Before zebrafish, frog tadpole, lamprey and some mammals were used for neuronal studies. Compared to them, zebrafish provides special advantages and is used as a model for neuronal experiments. Its externally fertilized, small transparent embryo is perfectly

suited for microscopic observations, which is further strengthened by the efficient transgenesis with fluorescent proteins under the control of various promoters. Fluorescent transgenic zebrafish enables *in vivo* observation of a particularly labeled cell or organ in detail, as well as the distribution pattern or the dynamics of gene expression through development (Kawakami, 2004; Tallafuss and Bally-Cuif, 2003); and also helps in addressing co-localization with simultaneous labeling of several genes in multiple colors. Besides transgenic labeling, small-molecule dyes also improve the observation studies of zebrafish. Lipophilic fluorescent dyes, which diffuse only within the labeled cells and could label neural axons, have been shown to be particularly useful in examining neuronal connections. Loading two different dyes (DiI and DiO) respectively into the anterior and posterior sides of eye, and checking the labeled retinal ganglion cell axons in the brain, has been used in genetic screens and defined many mutants defective in the retinal-tectal projections (Haffter et al., 1996). Introducing fluorescent labeling also benefits the observation of *in vivo* neuronal activity. For example, Calcium green is sensitive to the intracellular calcium concentration and fluoresces accordingly, and thus is used as an indicator of calcium change in neural cells. With Calcium green, studies of zebrafish has significantly improved the understanding of calcium signaling during *in vivo* development (Ashworth, 2004). For all of these labeling methods, the well-established laser scanning confocal microscopy technique provides a major means to observe, record and reconstruct the labeled details. With confocal microscopy, one can focus on a layer of tissue and obtain clean signal without the interference of out-of-focus labeling (Paddock, 2000). Given the complex structure of the nervous system and neural cells, the detailed direct observation of intact embryos or tissue with fluorescent labeling is significantly beneficial to neurobiological studies. In addition to observation, the small transparent zebrafish larvae also provide the possibility for precise manipulations, which is also useful in neuronal experiments. For example, non-invasive photo-ablation of

individual neurons in intact living fish will help to define accurate correlations between neurons and behaviors (Fetcho and Liu, 1998).

As a vertebrate model, zebrafish has a nervous system whose organization is highly similar to that of mammals. The understanding of *in vivo* neuronal properties from zebrafish, which is difficult to obtain from other models, can be an important reference for neurobiological studies on mammals.

1.4 Our aim for this study

Very few studies have described the expression of *Rag1* in the nervous system, and its function remains unknown. As a step towards understanding the role of *Rag1* in vertebrate nervous system, we have initiated a study using the zebrafish, with most analysis being concentrated on the olfactory system. We have attempted to define precisely where the gene is expressed, the extent of its co-expression with *Rag2*, and the effect of its absence.

CHAPTER 2 MATERIALS AND METHODS

2.1 Constructs

pCS2_5'RAG1-EGFP

First strand cDNA was synthesized from pooled 6 dpf larval RNA using random decamers. From this cDNA, a 350 bp 5' *Rag1* DNA fragment was amplified by PCR with *Pfu* DNA polymerase (Promega) using primer Rag1a and Rag1b. The PCR product was then digested with *Hae* III, phosphorylated with PNK (polynucleotides kinase; NEB) and inserted into *Sma*l I site of pEGFP-N1 (Clontech). In the resultant construct, 5' *Rag1* cDNA, including 5' UTR and partial coding sequence, was ligated to the downstream EGFP in the same reading frame. From this sequence, a fusion protein can be translated from the *Rag1* start codon.

For in vitro transcription, the entire 5'RAG1-EGFP fragment was cut out with *Not* I and *Bgl* II (the *Not* I end was blunted with Klenow) and cloned into *Bam*H I and *Stu* I sites of pCS2 (Rupp et al., 1994). From this construct, 5' RAG1-GFP fusion mRNA was synthesized from SP6 promoter for testing a morpholino, Rag1-mo1, which targets the *Rag1* ATG region.

pCS2_fullRAG1-EGFP

A full length zebrafish *Rag1* cDNA clone was obtained from RT-PCR in this lab. First strand cDNA was synthesized with random decamers, PCR was done with the Expand High Fidelity PCR system (Roche, Cat# 1732650). The entire *Rag1* cDNA could not be amplified in a single PCR reaction. Instead, 2 partial cDNA fragments were obtained separately. The 5' part was amplified with primer Rag1a and Rag1d, while the 3' part was amplified with primer Rag1c and Rag1-endR-BamH I (in this primer the *Rag1* stop codon

was replaced with a *Bam*H I site). Both were further sub-cloned into pGEM-T Easy vector (Promega, Cat# A1360), and several individual clones were picked out and sequenced. According to the published wt *Rag1* sequence, we chose the clone 37 (for 5' part) and 7 (for 3' part) for *Spe* I digestion. *Spe* I site is unique in the inserts as well as in the vector. From clone 37, a small fragment was cut off; the large portion of 5' *Rag1* remained together with the vector. From clone 7, a large 3' *Rag1* fragment was released and inserted to the clone 37. Thus we joined the two parts to generate a full length *Rag1* cDNA clone. This construct was named as pGEM-Te_fullRAG1.

To fuse to GFP, the full length *Rag1* cDNA (~3.2 kb) was released from this construct by *Not* I and *Bam*H I, with the *Not* I end blunted; the pGEM-T Easy backbone (~3 kb) was opened by *Pvu* I digestion and separated from the *Rag1* band. The previous pCS2_5'RAG1-EGFP construct was chosen as a recipient vector. It was digested with *Eco*R I, blunted and then digested with *Bam*H I. The previous *Rag1* full length cDNA was ligated to this vector and thus replaced the 5' *Rag1* fragment and fused to the EGFP in the new construct, pCS2_fullRAG1-EGFP. It was used to synthesis the full length RAG1-GFP fusion mRNA.

pCS2_RAG1^{797stop}

The PCR-based QuickChange site-directed mutagenesis (Stratagene) was used to introduce a C → T mutation in *Rag*1. It turned the 797 arginine into a stop codon.

Using 5 ng pCS2_fullRAG1-EGFP plasmid DNA as template, the mutation was introduced by a PCR with primers zfRag1_site-mut F and zfRag1_site-mut R, annealing at 55°C and cycling for 13 times. After *Dpn* I digestion, 2 µl PCR product was used for electroporation. 6 individual clones were picked out. 4 of them showed expected results

in allele-specific PCR, and were confirmed by sequencing to be successfully mutagenized.

pFBDa_2xUAS

pFBDa is a plasmid modified from pFastBac DUAL vector (Invitrogen). The original plasmid was sequentially digested with *Smal* I and *Stu* I. The small fragment was removed, while the remaining vector was self-ligated. This modification removed both P10 and Polyhedrin promoters and left the multiple cloning sites (MCS) in the vector.

UAS-unc76GFP fragment was cut from pBalphatubGalUASuncGFP (a gift from Dr. Reinhardt Koster) (D'Souza et al., 2005) by *Stu* I and *Not* I and cloned into *Pvu* II site of the pFBDa. Another UAS fragment was amplified from the same plasmid using SJ UAS primers, digested with *Spe* I and *Not* I, and then inserted into *Spe* I and *Not* I sites of the same vector. It resulted in a construct containing two UAS fragments in opposite directions. One drives unc76 fused to GFP, the other one can be used to drive any gene of choice. Thus the GFP can serve as a position indicator, and will not disturb the structure and function of the gene being tested.

pFBDa_UAS:uncGFP/UAS:Rag1

The full length *Rag1* cDNA was released from pGEM-Te_fullRAG1 with *Not* I digestion and cloned into the *Not* I site of the pFBDa_2xUAS construct. In the resultant construct *Rag1* was driven by one UAS and GFP was driven by another UAS. Thus *Rag1* and GFP will be activated by GAL4 at the same time, and GFP can be used as a visible indicator for *Rag1* expression.

pRag2:GFP & pRag2:DsRed

A ~7 kb 5' *Rag2* DNA fragment was obtained from the BAC clone 33K19 (Incyte Genomics Inc) by *Xho* I/*Eag* I digestion (Jessen et al., 2001a), and was sub-cloned into the *Xho* I and *Eag* I sites of pBlueScript II KS (Stratagene). This fragment contained a small part of the *Rag2* 5' coding sequence. At the 5' of the start codon, a nearby *Stu* I site was found to be unique within this fragment. To remove the *Rag2* coding sequence, the small fragment between *Stu* I and *Eag* I was replaced with a PCR-generated shorter fragment (with primer Rag2.Eag1), which covered the region between *Stu* I and the start codon and ended with an artificial *Eag* I site.

EGPF from pEGFP-N2 (Clontech) and DsRed from pDsRed-N1 (Clontech) were inserted respectively into *Eag* I site of the above construct. After that, a 2.6 kb PCR fragment from *Rag*-intergenic region was cloned into the *Sac* II site at 3' of EGFP or DsRed.

2.2 Fish stock

***Rag1:GFP* line:** a transgenic line kindly provided by Dr. Suo Lin (Jessen et al., 1999). It carries a PAC, in which the *Rag1* coding sequence was replaced with GFP (GFPmut3, U73901).

***Rag1* mutant line:** a zebrafish mutant line kindly provided by Dr. Brigitte Walderich (Wienholds et al., 2002). It carries a C → T mutation that results a premature stop codon at 797aa of RAG1.

***Rag2:GFP* line:** a transgenic line generated in this lab, with the previous pRag2:GFP construct. It carries a EGFP under the 7 kb *Rag2* promoter fragment.

***Rag2:DsRed* line:** a transgenic line generated in this lab, with the previous pRag2:DsRed construct. It carries a DsRed gene under the same *Rag2* promoter fragment.

***OMP:DsRed* line:** a transgenic line generated in this lab, with the construct kindly provided by Dr. Masayoshi Mishina (Yoshida et al., 2002). It carries a DsRed gene driven by an *OMP* (olfactory marker protein) promoter fragment.

2.3 Transgenesis

Sperm-mediated transgenesis was carried out as described previously (Jesuthasan and Subburaju, 2002).

For conventional transgenesis, 40~60 ng/µl DNA was injected into one-cell stage embryos, and progeny of injected fish were screened for fluorescence.

2.4 Imaging

The confocal microscopes used are Zeiss LSM 510 inverted, Zeiss Meta LSM 510 inverted, Zeiss Meta LSM 510 up-right and Bio-Rad.

Live zebrafish embryos and larvae were embedded in 1.5 % low-melting agarose (BioRad) and imaged with a Zeiss LSM 510 laser scanning confocal microscopy, using 40x (0.8 NA) or 63x (1.2 NA) water immersion objectives.

Isolated olfactory bulbs from larvae were imaged with a 20x (0.5 NA) water immersion objective.

Isolated olfactory rosettes and forebrains from adults were embedded in 3% methylcellulose in a glass-bottom dish (MatTek, Part# P35G-0-14-C), and imaged with 10x or 20x objectives using an inverted confocal microscope.

2.5 Lipophilic tracing of olfactory neurons

A saturated stock solution of DiI or Di8ANEPPQ (Molecular Probes) was prepared in ethanol. DiI was diluted 1:1000 in E3, while Di8ANEPPQ was diluted 1:5000, just before

use. Larvae were placed in this solution in mesh baskets for 3 minutes, and then rinsed several times in fresh E3. Bodipy labeling was carried out as described (Dynes and Ngai, 1998).

2.6 Antibodies and immunofluorescence

2.6.1 RAG1 and RAG2 antibodies

Rabbit polyclonal antibodies against the C-terminus of zebrafish RAG1 (amino acids 1042~1057), and the C-terminus of zebrafish RAG2 (amino acids 517~530) were generated by ZYMED Laboratory Inc. The RAG1 peptide antigen (**C**EETPEEADNSLDVPDF-COOH) was synthesized by Tufts University Core Facility; the RAG2 peptide antigen (**C**MTPAKKTFLRRLFD-COOH) was synthesized by ZYMED Laboratory Inc.

To test for specificity, the antibodies were incubated overnight at 4˚C with the corresponding antigen peptides at a concentration of 66.6 μg/ml. After a 30 minute spin at 16 000g, the supernatant was used for labeling thymocytes, which had been dissected from freshly killed 2~4 week-old zebrafish using tungsten needles.

2.6.2 Immunofluorescence on cryo-sectioned tissue

Brains from 3 month-old *Rag1:GFP* fish was dissected out in L-15 medium (Sigma), fixed in 4% PFA, embedded in tissue freezing medium (Jung, Cat# 0201-08926) and sectioned on a cryostat (Leica, CM3050S). The sections were incubated in rabbit anti-GFP (1:200) followed by Alexa488 anti-rabbit (1:300). Nuclei were stained with propidium iodide.

2.6.3 Immunofluorescence on neurons from retina

Retina from 3 day-old *Rag1:GFP* fish was dissected out in L-15 medium and dispersed with a mouth pipette (Sigma, Cat# A-5177). Cells were transferred to a polylysine-coated (50 µg/ml) glass-bottom dish (MatTek, Part# P35G-0-14-C), and kept in L-15 medium at room temperature for 40 minutes to allow them to settle and adhere. They were then fixed in 4% PFA, rinsed with PBS, permeablized with 0.2% Triton X-100, incubated with 1:200 anti-zfRAG1 (rabbit, Zymed) and 1:50 anti-GFP (mouse; Molecular Probes), followed by 1:300 Alexa568 anti-rabbit and 1:300 Alexa488 anti-mouse (Molecular Probes). Nuclei were stained with 100 ng/ml Hoechst.

2.6.4 Immunofluorescence on olfactory neurons

4 day-old *Rag1:GFP* fish were fixed in 4% PFA-PBS for 10 minutes. The olfactory epithelium was dissected out in Ringer's solution and transfered on Superfrost/Plus slides using a mouth pipette (Sigma Cat# A-5177). Extra solution was removed and the olfactory epitheliums were left to semidry and adhere to the slide. A drop of Ringer's solution was added and a cover slip was used to squash the epithelium gently, thus dispersing the cells and allowing them to adhere to the slide. The cover slip was gently removed and the cells were re-fixed in 4% PFA/PBS for another 5 minutes. They were then rinsed with PBS and permeabilized with 1% Triton X-100. The following antibodies were used: anti-zf RAG1 (rabbit, 1:200), anti-GFP (mouse, 1:50; Molecular Probes), anti $G\alpha_o$ (guinea pig, 1:200), $G\alpha_q$ and $G\alpha_{olf}$ (both rabbit, 1:200; Santa Cruz Biotech). The $G\alpha_o$ antibody [40] was made to a region of the protein that is 100% conserved between *Drosophila* (residues 345-354) and zebrafish. For detection, 1:500 Cy3 anti-guinea pig, 1:300 Alexa 568 anti rabbit and 1:300 Alexa 488 anti mouse (Molecular Probes) were used. Nuclei were stained with 100 ng/ml DAPI.

2.6.5 Immunofluorescent labeling of glomeruli

The brain of 4-day old *Rag1:GFP* fish larvae was dissected out in Ringers' solution and fixed for 1 hour in 4% PFA-PBS. Whole-mount antibody labeling was carried out using standard procedures, using the SV2 antibody (Developmental Studies Hybridoma Bank) at 1:500 dilution, and the Alexa 546 goat anti-mouse antibody (Molecular Probes) at 1:500 dilution.

2.7 in situ hybridization

2.7.1 Probe synthesis

A ~1.5 kb *Rag1* cDNA fragment was amplified by RT-PCR and cloned into pBlueScript II SK (Stratagene). From correct transformants, plasmids were purified, and linearized by *BamH* I for anti-sense probe synthesis with T7 RNA polymerase (NEB), or by *Xho* I for sense probe synthesis with T3 RNA polymerase (NEB).

For *Rag2* a 855 bp cDNA fragment was amplified and cloned into pGEM-T Easy vector (Promega). Then colony-PCR (35 cycles) was carried out to verify the transformants and amplify the inserts. Correct PCR products were cleaned up using QIAquick spin columns (Qiagen). The PCR product amplified with primer M13-20 Forward and Rag2a was used for anti-sense probe synthesis, while PCR product produced with M13-20 Forward and Rag2d was used for sense probe synthesis. Both sense and anti-sense RNA probe were synthesized using T7 RNA polymerase (NEB).

DIG-labeled probe was synthesized with DIG RNA labeling Mix (Roche).

2.7.2 Whole-mount in situ hybridization

Pre-processing of samples

3 dpf PTU treated wt larvae were fixed in 4% PFA/PBS at 4°C for overnight. The fixed samples were then washed with PBST at room temperature twice for 10 min, followed by dehydration with series washes of 30%, 50%, 70% and 100% methanol/PBST and stored at -20°C for at least 20 min. At this step, samples can be stored for months.

To start the *in situ* hybridization, the samples were rehydrated by series of washes with 70%, 50% and 30% methanol/PBST, with incubation at each step for 5 min, and re-fixed with 4% PFA/PBS at room temperature for 20 min. After wash with PBST, these samples were treated with 10 μg/ml proteinase K for 30 min at room temperature with agitation, and then re-fixed with 4% PFA/PBS for 20 min.

Hybridization

The re-fixed samples were washed with PBST twice for 5 min, and incubated in hybridization buffer (refer to Appendix 1) at 55°C for 3~5 hrs for pre-hybridization. Meanwhile, 0.5 μg/ml DIG-labeled RNA probe was denatured in hybridization buffer at 70°C for 5 min, and then immediately chilled on ice. The pre-hybridization buffer was removed, and the sample was incubated in hybridization buffer containing the probe, with agitation at 55°C overnight. In the second day, the probes were removed and the samples were washed sequentially with 2x SSCT and 0.2x SSCT at 68°C for 10 min.

Antibody staining

At room temperature, the samples were washed with PBST, and then incubated with 10% BCS/PBS for 2 hrs. The blocking buffer was then removed, the samples were incubated with 1:2000 diluted anti-DIG-AP (alkaline phosphotase conjugated anti-DIG antibody; Roche) at 4°C overnight. In the third day, the samples were washed with PBST, twice for 10 min, followed with buffer 9.5 T wash, also twice for 10 min; and then incubated with substrate BM purple (Roche Cat# 1442074) in darkness at room temperature. The developing was stopped when intense signal was seen.

2.7.3 TSA modification

A signal amplification step was adapted by using the TSA (Tyramide Signal Amplification) biotin system (NEN Cat# NEL700A) to replace the antibody staining step and enhance the sensitivity of *in situ* hybridization. After post-hybridization wash, the samples were washed in TNT wash buffer, and then blocked with TNB blocking buffer, incubated with anti-DIG-POD (instead of anti-DIG-AP), followed by incubation in biotinyl tyramide at room temperature for 15 min to amplify the signals. The conjugated biotin was then detected with Alexa 568-Streptavidin (Molecular Probes).

2.8 Microinjection

DNA injection

40~70 ng/μl plasmid DNA in H_2O was injected into the animal pole of one-cell stage embryos. The injection volume was approximately 1 nl, which was also used for mRNA and morpholino injections.

mRNA injection

Using SP6 mMESSAGE MACHINE (Ambion Cat# 1340), mRNA was synthesized in vitro, diluted as ~50 ng/μl in DEPC treated H_2O, and injected into the yolk of one-cell stage embryos.

Morpholino injection

Morpholinos (Gene-Tools) were diluted in H_2O and injected into the yolk of one-cell stage embryos. 50~100 embryos were injected with each morpholino, in concentration ranging from 0.2 to 1.0 μM. The following morpholinos were used in this study: **Rag1-mo1**: 5'-TTCTCCATGGCGTCAGCTTATTCTC-3' (targets the *Rag1* start codon). **Rag1-mo2**: 5'-TATTATACTCACTTGAGAAGATTCA-3' (targets the donor site of the

first intron of *Rag1*). **Rag1-mo3**: 5'-TCTTGGCAGTACCTTGCATCATTGC-3' (targets the donor site of the second intron of *Rag1*).

2.9 PCR

In my work, a general PCR reaction was run with 0.5 μM primers, 15 mM $MgCl_2$ and 200 μM of each dNTP, in a 0.2 ml PCR tube (Axygen) or 96-well PCR plates (MJ Research) sealed with Scotch tape. The volume for each PCR reaction ranged from 15 to 40 μl.

Colony-PCR

This is a PCR method specified to amplify a fragment directly from colonies on plates. It is normally used to screen for positive transformant colonies. The concentration of primers and dNTPs in PCR Mix were decreased to 0.1 μM and 80 μM respectively, so that good PCR products can be used directly in a sequencing reaction. Normally PCR master Mix was distributed into 96-well PCR plate as 25 μl per well. Individual colonies were picked with clean tooth-picks and briefly dipped into the PCR Mix in one well. Then, the entire PCR plate was sealed and run for 36 cycles in a themocycler. 50°C generally works as the annealing temperature for most primers and this method generally works for amplifying a fragment up to 2 kb.

2.10 Electrophoresis

According to the size of purpose DNA, 1~3% agarose / TAE gel containing 1:250 Gelstar (Molecular Probes) was used for electrophoresis. The voltage used ranged from 5 to 8 V/cm.

To monitor the quality of total RNA, the electrophoresis with 1.2% agarose gel was used. Before loading, ~ 1 μg total RNA was mixed with 2x RNA loading buffer (Ambion),

heated at 70°C for 3 min, and chilled immediately on ice. The gel was normally run at 8V/cm for 15 ~ 20 min.

2.11 Electroporation

Preparation of competent cells

E. coli Top10 stain was generally used for routine cloning during the course of this study. To prepare the competent cells for electroporation, 1 liter LB medium was inoculated with 1/100 volume of fresh overnight culture, and shaken at 37°C, 250 rpm until the OD_{600} of the culture reached about 0.6. The culture was then chilled on ice for 15 ~ 30 min, followed by spinning at 4°C, 4000x g for 5 min to harvest cells. The cell pellet was washed with 1 liter cold water, 0.5 liter cold water and 20 ml cold 10% glycerol serially. Spinning was repeated to collect cells from each wash. At last, the pellet was resuspended with 10% cold glycerol in a final volume of 2 ~ 3 ml, aliquot as 40 μl per tube, frozen in liquid nitrogen and stored at -80°C.

Electro-transformation

An aliquot of the frozen competent cells was thawed gently on ice. 1~2 μl DNA (ligation product can be used directly) was added into the cell suspension, mixed and transfered into a pre-chilled electroporation cuvette (Bio-Rad). Cuvettes with 0.1 cm gap were pulsed with 1.8 KV, 200 Ω and 25 μF; cuvettes with 0.2 cm gap were pulsed with 2.5 KV, 200 Ω and 25 μF. After the pulse, 1 ml SOC medium was added into the cuvette immediately; then the cells were transferred into a tube and allowed to recover at 37°C for 1 hr. At last, an appropriate amount of culture was spread on plates containing corresponding antibiotics to select correct transformants.

2.12 Storage of glyceral stock

Fresh overnight culture was mixed with 65% glycerol solution as 1:1, and frozen at -80°C.

2.13 Genotyping

2.13.1 Genotyping of the *Rag1* mutant zebrafish

We identified the *Rag1* mutant zebrafish (Wienholds et al., 2002) by genotyping, because they showed no morphological phenotype. The adult homozygous *Rag1* mutant fish are viable and fertile, but sensitive to the infection caused by fin-clip, thus we chose to identify them by genotyping their progenies.

Adult fish to be tested were crossed with wt fish in a single-pair manner. From the progenies, DNA was isolated from 8 individual embryos. With these DNA, either allele-specific PCR or sequencing was carried for genotyping. When all of tested embryos carry the mutant allele, the tested parent is likely to be a homozygous mutant; when they carry only wt alleles, the tested fish should be a wt sibling; if some embryos are wt and some are heterozygotes, the tested parent fish is surely a heterozygote.

2.13.2 DNA isolation from individual embryos

3~6 dpf single embryos were anesthetized with MS222 (tricaine; Sigma Cat# A-5040) in E3 water and transferred into 96-well PCR plates as 1 fish per well. Then the E3 water was removed and replaced with 50 μl TE buffer containing 200 μg/ml proteinase K. The plates containing fish in proteinase K were sealed and incubated at 55°C for 1~2 hour, 95°C for 5 minutes, and then short-spun. 2 μl of the clear liquid from each sample were used for one PCR reaction.

2.13.3 DNA isolation from clipped caudal fins

Individual adult fish was anesthetized with MS222 (tricaine; Sigma Cat# A-5040), taken out from water using a plastic spoon, and placed in a clean Petri dish. From each fish 1/3 caudal fin was cut with a pair of clean scissors. The fish was then released to a tank with fresh water, and kept individually until being identified. The clipped fin was transferred into 100 µl TE buffer containing 200 µg/ml proteinase K and 5% Chelex-100 (BioRad Cat#1432832) (Yue and Orban, 2001), incubated for 2 hour at 55°C with agitating, and then heated at 95°C for 5 minutes to inactivate the proteinase K. The debris was spun down, and 2 µl clear supernatant was used for each PCR reaction.

2.13.4 Allele-specific PCR

This is a PCR-based method, which is designed to distinguish the single-nucleotide difference between the *Rag1* mutant and wt allele(Kawakami and Hopkins, 1996). Totally four primers were used. Rag1E1 is the only forward primer. It works with Rag1f, a primer common for both mutant and wt alleles, to amplify a 770 bp band from *Rag1* 3rd exon. This band is used as an amplification control. Rag1wtR and Rag1mutR are allele-specific reverse primers. Rag1wtR contains a G at 3' end and matches only to wt allele; while Rag1mutR is almost same to Rag1wtR except containing a A at 3' end, which matches only to the *Rag1* mutant allele. PCR with Rag1wtR and Rag1E1 amplifies a 218 bp band only from wt allele; while Rag1mutR and Rag1E1 amplify a 218 bp band only from mutant allele.

In the allele-specific PCR, Rag1E1, Rag1f and Rag1wtR were used in one reaction to verify the presence of wt allele; whereas Rag1E1, Rag1f and Rag1mutR were used in another reaction to confirm the presence of *Rag1* mutant allele. PCR conditions (mainly the annealing temperature and the ratio of primers) were stringently optimized so that the

Rag1wtR only amplify the wt allele and the Rag1mutR only amplify the *Rag1* mutant allele, although the templates contain only a single-nucleotide difference. In both reactions the 770 bp band between Rag1E1 and Rag1f should be obtained robustly.

To test for the wt allele, 0.5 µl Rag1E1, 0.5 µl Rag1wtR, 0.3 µl Rag1f and 0.2 µl dNTP (10mM for each) were used for each 25 µl reaction, which was annealed at 67°C and run for 27 cycles. To test for the *Rag1* mutant allele, 0.5 µl Rag1E1, 1 µl Rag1mutR, 0.2 µl Rag1f and 0.3 µl dNTP (10mM for each) were used in one reaction, and the PCR was annealed at 68.5°C and run for 32 cycles.

2.13.5 Direct sequencing from PCR products

A 25 µl PCR reaction, with 80 µM dNTP and 80 nM of each primer, was run for 35 cycles and checked by electrophoresis. When a single band was clearly shown in the reaction, 1 µl PCR product was used directly in a sequencing reaction. For genotyping *Rag1* mutant, primer Rag1E1 and Rag1f were used for PCR, and Rag1E1 was used for sequencing.

2.14 RNA isolation:

From larvae

Freshly laid eggs were collected and raised in E3 water at density of 50~75 fish per 6 cm Petri dish. Larvae at desired stage were anesthetized with MS222 (tricaine, Sigma Cat# A-5040). Each 10 fishes were transferred with a mouth pipette (Sigma Cat# A-5177) into 250 µl Trizol (Invitrogen, Cat# 15596-018) containing 0.5 µg/ml glycogen, and were homogenized with pellet pestle motor (Kontes Cat# 749540-0000) immediately.

From 3 dpf fish heads

Rag1 mutants and wt sibling embryos were collected and raised as above. At 3 dpf, the larvae were anesthetized, and the fish heads were cut behind the ear in Ringer's solution using tungsten needles. 10 fish heads were pooled and transferred to 250 µl Trizol containing 0.5 µg/ml glycogen, and homogenized immediately.

From adult olfactory rosettes, retina or brain

Individual adult fish was killed by immersion ice into water. The fish head was cut off with a blade on a piece of tissue towel, and transferred into Ringer's solution. Under dissecting microscope, desired parts of tissue were dissected out using forceps or tungsten needles, transferred into a tube containing 250 µl Trizol with 0.5 µg/ml glycogen, and then homogenized immediately. For olfactory rosettes, 4 rosettes were pooled and homogenized in 250 µl Trizol containing 0.5 µg/ml glycogen.

After being kept at room temperature for 5 minutes, the above lysates (250 µl per tube) were kept on ice until the sample collection finished. Then 4 tubes of the lysates were combined, subjected to RNA isolation directly, or kept at -80°C for later use.

RNA isolation followed the Trizol protocol provided by Invitrogen (http://www.invitrogen.com/content/sfs/manuals/15596026.pdf).

2.15 RT-PCR

2.15.1 DNase I treatment

10 µl 10x DNase I buffer, 1 µl RNase-free DNase I (Roche) and 1 µl RNase inhibitor were used in a 100 µl reaction containing <50 µg total RNA. The reaction was incubated

at 37°C for 30 min. 5 µl 0.5M EDTA, 12.5 µl 4M LiCl and 375 µl chilled ethanol were then added and mixed. To facilitate RNA precipitation, the mixture was kept at -80°C for 40 min or longer. Then the RNA was pellet down by spinning at 4°C for 30 min.

2.15.2 First strand cDNA synthesis

First strand cDNA was synthesized with oligo dT20-VN or random decamer from 1~ 3 µg total RNA (DNase I treated), using Superscript II reverse transcriptase (Invitrogen). The working procedures followed the manual provided by Invitrogen (http://www.invitrogen.com/content/sfs/manuals/superscriptII_pps.pdf)

2.15.3 Semi-quantitative RT-PCR

To confirm the expression difference of candidate genes between *Rag1* mutants and wt siblings, semi-quantitative RT-PCR was carried out. Using PrimerSelect (from DNAstar software package), a pair of primers were designed for each gene to work at 50~55°C and amplify a 300~800 bp fragment. With these primers, PCR was carried out to amplify the candidate genes fragment from both *Rag1* mutants and wt siblings, using HotStartTaq DNA polymerase (Qiagen). To avoid the saturation of amplification, three batches of PCR product (10 µl each) was taken out from each reaction when it was cycled for 25, 28 and 31 times respectively, and then used for electrophoresis. The amount of input cDNA was monitored by the amplification of β-actin. –RT control was always kept for every reaction to monitor the contamination of genomic DNA. Used primers were listed in Appendix 4.

2.15.4 5' RACE for 12158

The 5'RACE of 12158 was adapted from the Smart RACE method from Clontech (http://www.clontech.com/clontech/techinfo/manuals/PDF/PT3269-1.pdf). First strand

cDNA was synthesized using 0.5 μM smart3 and 0.5 μM 12158R1. From that, a PCR using UPM (universal primers mix) primer mixture and 12158R2 was run under a touch-down program (from 68 to 50°C). The PCR product was diluted and used for the following nested PCR, which was run with primers 5smart3 and 12158R3. Two 12158 clones were obtained from this reaction. Primers used are listed in Appendix 3 and 4.

2.15.5 Real-time RT-PCR

To confirm and quantitate the reduction of 12158 expression in *Rag1* mutant zebrafish, real-time PCR was carried out using the iCycler iQ real-time detection system (Bio-Rad). Totally 3 pair of primers were used in this experiment. Actin-rtF and actin-rtR were used to amplify a 161 bp fragment from β-actin cDNA. This was used to monitor cDNA input and normalize data. 12158-rtF and 12158-rtR were used to amplify a 133 bp fragment within the original part of 12158 cDNA; while 12158-rpF2 and 12158-rpR were used for amplifying a 164 bp fragment within the part newly cloned by RACE in 12158B., 1:75,000 diluted Sybr Green (Molecular Probes) was used in PCR reactions to monitor the accumulation of DNA product. Annealing temperature, Mg^{2+}, primer and template concentration were optimized sequentially for each pair of primers. 2.5 mM $MgCl_2$ and 0.3 μM primers were found optimal for all of the three pairs of primers; 56°C, 54°C and 58°C were used respectively at annealing step for actin-rtF/R, 12158-rtF/R and 12158-rpF/R. Primers used are listed in Appendix 4.

2.15.6 RT-PCR with DEG kit

RNA from 3 dpf *Rag1* mutant and Wt sibling fish were used to synthesis the first strand cDNA, which were diluted 1 in 50 and used for PCR with annealing control primers (ACPs, from GeneFishing DEG kit). Totally 10 pairs of ACPs (a to j) were used in PCR according to the manual provided with the kit. PCR products were analysis by

electrophoresis with 2% agarose gel containing 0.5 μg/ml EB. The differentially amplified PCR products were extracted from the gel using QIAGEN gel extraction kit, and ligated into pGEM-T Easy vectors (Promega). The ligation products were then transformed into Top10 strain *E. coli* by electroporation, and spread on LB plate containing IPTG and X-gal. Individual white colonies were screened by colony-PCR. Only the PCR products with expected length were sequenced. The consensus sequence of majority colonies from one clone was used for designing a pair of primers. Semi-quantitative RT-PCR with these primers was used to confirm the expression difference between *Rag1* mutants and Wt siblings.

2.16 Microarray

2.16.1 Construction and hybridization of the zebrafish microarray

The microarray construction, cDNA synthesis and labeling, hybridization and data acquisition were done in the Microarray Core Facility of Kimmel Cancer Center (KCC) in Thomas Jefferson University (TJU). The zebrafish oligonucleotide probes used in our microarray experiments were designed by Compugen and synthesized by Sigma-Genosys. For each gene, one 65-mer 5' amine modified oligo was synthesized. Totally, each microarray chip containes 19200 spots, including 172 β-actin spots for positive controls, 2792 blanks for negative controls, and 16236 spots printed with oligos representing different genes. Estimated by LEADS clusters, the entire set of oligos covers 15,806 unique genes of zebrafish (http://www.labonweb.com/).

Total RNA were extracted from pooled 3 dpf fish heads (100~300 for each pool), or from pooled adult olfactory rosettes (32~48 for each pool) using Trizol reagent (refer to 2.14). For each experiment, 3 pairs (wt *vis Rag1* mutants) of independently isolated total RNA, ~10 μg for each samples, were collected in our lab and sent to KCC in TJU. Each of the

RNA samples was reverse-transcribed into biotin-labeled 1st strand cDNA, and then hybridized to an individual slide. The hybridization signals on the slide were further detected by Streptavidin-Alex conjugates. Thus in each experiment, six RNA sample was labeled individually, hybridized to six microarray chips, and the resultant six sets of data were collected respectively.

2.16.2 Microarray data analysis

The obtained microarray data were mainly processed with GeneSpring (Agilent Technologies) in our lab. Firstly, the background intensity individually measured for each spot was subtracted from the foreground signal intensity, to give a spot intensity for calculating the expression. Next, to control the variance between different hybridizations, Per-chip normalization was done according to the 50th percentile of all measurements in that sample, e.g. each spot intensity was divided by the 50th percentile of that chip; and the resultant data is further controlled by Per-gene normalization: each gene was divided by the median of its measurements in all samples. Then, signals with intensity lower than twice of the blanks in every hybridization were filtered out.

At this stage, the data quality and reproducibility were examined. For each experiment, 6 individual hybridizations were grouped into 3 pairs so that each of them contains 1 wt and 1 *Rag1* mutants hybridization result (Table 1). The overall distribution of the 3 pairs of data was examined in RI (ratio-intensity) scatter plot. In the RI plot, Log_2(Rag1/wt) ratio for each element on the array was displayed as a function of the Log_{10}(wt*Rag1) product intensity, thus revealing intensity-dependent effect in the Log_2(ratio) measurement. Further more, reproducibility among different hybridizations was examined by comparing logarithm ratios between two different pairs of samples in a plot. If the two pairs of data are perfectly reproduced, the ratio obtained from them should be equal, and the corresponding genes should locate along the line x = y in the plot. With reasonable imperfection, genes that

distribute close to this line are also acceptable. But the data scattering far from the x = y line will be considered as non-reproducible.

To enhance the identification of the most relevant genes, we focused only on data showing more than two fold changes between *Rag1* mutant and wt. The following statistic significance analysis was carried out with ANOVA (analysis of variance) and SAM (significance analysis of microarray).

The most recent annotations of the significants were obtained from Silicon-Genetics using the GeneSpider function in the GeneSpring software, and supplemented with the annotation database of GIS (Genome Institute of Singapore, http://giscompute.gis.a-star.edu.sg/~govind/zebrafish/).

CHAPTER 3 RESULTS_ PART 1 Analysis of *Rag* Expression in Zebrafish Nervous System

3.1 Expression of Rag1 and 2 in the zebrafish early embryo

At early stages, zebrafish embryos develop very fast. Around 10 hpf (hours post fertilization), some cells start to differentiate and establish the nervous system. Using RT-PCR we checked the expression of *Rag* genes at early embryonic stages. Total RNA was isolated at different stages from pooled wt (wild type) zebrafish embryos (n=10 for each sample); expression of *Rag1*, *Rag2* and β-actin (as a control) was examined by semi-quantitative RT-PCR; a parallel control without RTase (reverse transcriptase) during the first strand cDNA synthesis was kept for inspecting the amplification from genomic DNA.

Surprisingly, the transcripts of both *Rag1* and *Rag2* were detected within 24 hpf (Fig. 3-1). Even at 3 hpf, when the zygotic transcription has just initiated (Kane and Kimmel, 1993), certain amount of both *Rag1* and *Rag2* were detected. The expression level of both *Rag* genes drops down around 8 hpf, and begins to increase steadily afterwards. In contrast, the expression level of β-actin continuously increases with the embryo growth.

We next examined *Rag1:GFP* and *Rag2:GFP* transgenic zebrafish. The *Rag1:GFP* line was generated by Shuo Lin's group (Jessen et al., 1999). It carries a modified PAC, in which *Rag1* coding sequence was replaced by GFP. Given the large size of the PAC, it is likely that most, if not all, *Rag1* regulatory elements are present and play a role in regulating the GFP expression. The *Rag2:GFP* fish was generated in our lab. They carry EGFP driven by *Rag2* promoter. We found that the transgenic embryos indeed fluoresce weakly within 24 hpf. Before 10 hpf, GFP was present evenly among cells, but not in the yolk (Fig. 3-2A-D). Then GFP was gradually restricted to some areas. At 24 hpf,

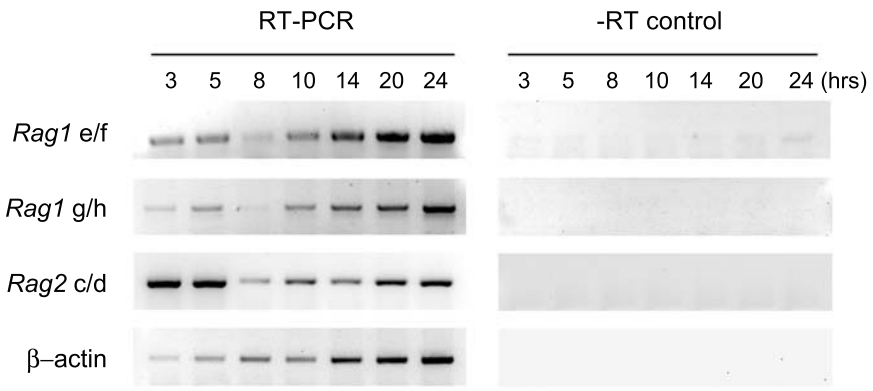

Figure 3-1. *Rag* transcripts were detected in the zebrafish early embryo.

RT-PCR detected the expression of *Rag1* and *Rag2* at early stages of zebrafish development. Two pairs of primers, Rag1e/Rag1f and Rag1g/Rag1h were used to detect *Rag1* transcripts. The amplification of β-actin was used as a loading control. -RT controls were kept for each sample to inspect the amplification from genomic DNA.

Rag1-driven GFP was present in the olfactory pit (Fig. 3-5A,B), the ventral part of forebrain (Fig. 3-2E) and somites (Fig. 3-2F), while *Rag2*-driven GFP was diffuse within whole neuronal tube (Fig. 3-2G).

These data suggest that *Rag* genes are expressed at early stages of zebrafish development in a broader range than previously reported.

3.2 Rags transcripts were detected in zebrafish larval nervous system by RT-PCR and in situ hybridization

At 3 dpf (days post fertilization), the nervous system of the zebrafish larvae is almost established. To examine the expression of *Rag* genes in the nervous system, we carried out RT-PCR using RNA isolated from the eye and brain of 3 dpf fish (Fig.3-3A, B). *Rag1* transcripts were detected in both eye and brain. *Rag2* was detected in the brain, and at very low level in the eye. Amplifications of β-actin were used as controls. *Rag1* and *Rag2* are not yet expressed in thymus and kidney at 3 dpf (Willett et al., 1997), which rules out the possibility that the positive result in RT-PCR might come from the contamination of lymphocytes in brain and eye.

We also carried out whole-mount *in situ* hybridization with DIG labeled *Rag1* anti-sense RNA probe. To use the newly formed thymus as a positive control for *Rag1* staining, we chose 4 dpf larvae for experiment. Hybridization with anti-sense *Rag1* probe showed strong staining in thymus and olfactory pit in these fish (Fig. 3-3C, D), whereas no obvious signal can be seen in other organs.

To increase the sensitivity of detection, we combined the TSA (Tyramide Signal Amplification) technique with *in situ* hybridization and used a fluorescent streptavidin (Aexa568-conjugated) to achieve better resolution under confocal microscopy. After

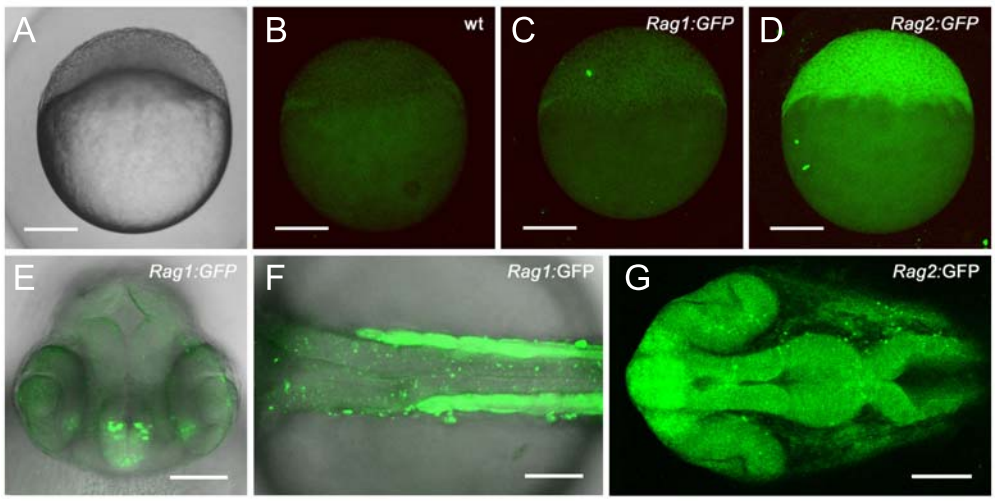

Figure 3-2. Expression of *Rag*-driven GFP in the zebrafish early embryo.

(A) A bright field image of wt 3 hpf zebrafish embryo. (B-D) Fluorescence images of wt, *Rag1:GFP* and *Rag2:GFP* 3 hpf embryos were taken under same conditions. (E-G) At 24 hpf, *Rag1*-driven GFP is visible in the ventral part of the diencephalon (E) and somites (F), whereas *Rag2*-driven GFP is present in neuronal tube (G).

hybridization, only the thymus (Fig. 3-3D arrows) and olfactory pit (Fig. 3-3D arrowheads) were stained over whole fish. A combination of *in situ* hybridization with the *Rag1* probe and immunofluorescence with an antibody against GFP on the *Rag1:GFP* fish revealed partial overlap of *Rag1* and GFP at cellular level in the olfactory pit (Fig. 3-3E arrows). The total number of GFP positive cell in the staining (27 ± 9) is much less than that detected in the live *Rag1:GFP* fish (91 ± 15) olfactory pit, suggesting that the tissue or the antigens were damaged during the staining process. This might lead to the incomplete overlap of staining in the olfactory pit (Fig. 3-3E).

Shuo Lin' group has successfully detected *Rag2* expression in the olfactory epithelium at the larval stages by *in situ* hybridization. To achieve higher resolution, we carried out the TSA modified *in situ* hybridization with DIG-labeled *Rag2* anti-sense RNA probe, but with the 4 dpf larvae, we failed to detect any apparent signal except in thymus. This suggests that the transcription of *Rag2* in olfactory pit is at a very low level, which might beyond the detection of *in situ* hybridization when the experiment is not perfectly optimized.

However, technical improvement of *in situ* hybridization seems not provide the potential to increase detection sensitivity significantly. Both Shuo Lin's group (Jessen et al., 2001a; Jessen et al., 1999) and our group have detected the *Rag1* expression in larval olfactory pit by *in situ* hybridization, but both of us did not notice signals in other parts of the nervous system. Whereas, revealed by our RT-PCR, *Rag* genes are also expressed in retina and brain. These suggest that *Rag1* and *2* are transcribed in other parts of the nervous system at a level even lower than that in the olfactory epithelium, and *in situ* hybridization is not sufficient to detect them. To study the detailed expression of *Rag* genes in the entire nervous system, a more sensitive approach is required. One possibility is the analysis of *Rag*-driven reporters in transgenic fish.

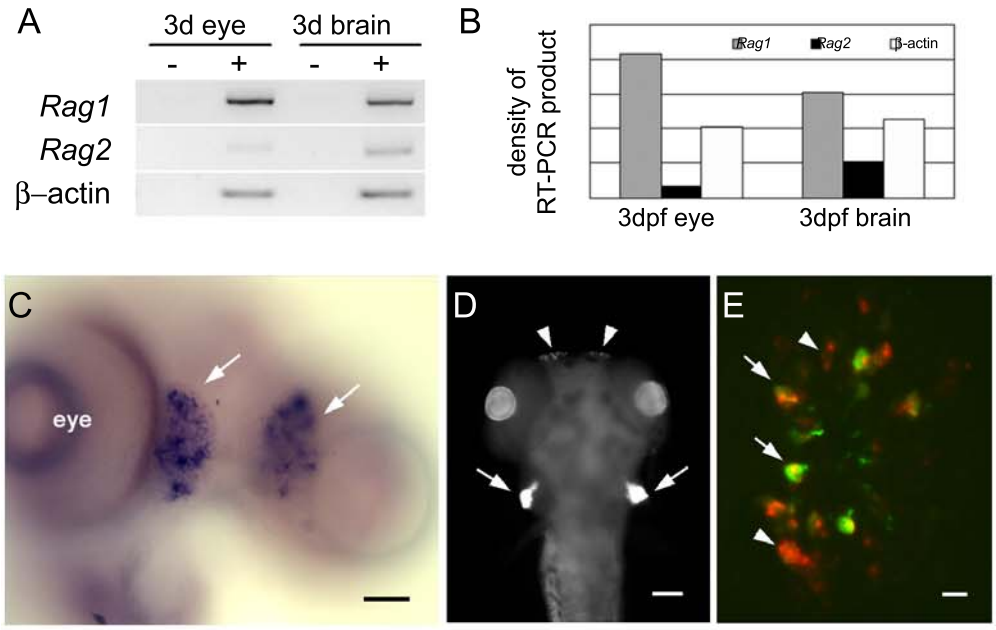

Figure 3-3. *Rag* genes were detected in the nervous system of zebrafish larvae by RT-PCR and *in situ* hybridization.

(A) Expression of *Rag* genes in 3 dpf fish eye and brain were detected by RT-PCR. (B) Diagram sowing the relative density of RT-PCR amplification for *Rag1*, *Rag2* and β-actin. (C) Olfactory pit (arrows) stained by in situ hybridization with *Rag1* anti-sense probe. A 5 day-old embryo is shown here in frontal view. (D) Thymus (arrows) and olfactory pits (arrowheads) were stained by TSA *in situ* with *Rag1* anti-sense probe. The fish was shown in dorsal view. Signals in lens came from artificial autofluorescence. It was also present in the sense probe controls. (E) *Rag1:GFP* fish double labeled with TSA in situ (*Rag1*, red) and immunoflourescence (GFP, green). In the olfactory pit *Rag1* co-localized with reporter GFP in some cells (arrows), but there was also some non-overlapping staining (arrowheads). Bar = 50 μm (C); 100 μm (D); 20 μm (E).

3.3 Transgenesis reveals that Rag1 is expressed in a restricted manner in the zebrafish nervous system

To identify which regions of the nervous system might express *Rag1*, we re-examined the *Rag1:GFP* line in detail. We found that in fact *Rag1* is expressed in only a subset of OSNs, and in many other parts of the zebrafish nervous system.

3.3.1 Expression of *Rag1-driven GFP* in zebrafish olfactory epithelium is restricted to a subset of microvillous neurons

3.3.1.1 The zebrafish olfactory system

The olfactory system is an important chemosensory system, which enables animals to perceive diverse chemical stimuli in the environment. Usually it is composed of a pair of peripheral olfactory epithelia (OE) in nasal cavities and a pair of olfactory bulbs (OB) in the forebrain. The OE arises outside the central nervous system (CNS) from an olfactory placode (a thickening of the ectoderm), a thin columnar epithelium that is four or five cells high. In adult zebrafish, as in other teleosts, the OE is a rosette with lamellae radiating from a midline raphe. Each lamella contains both sensory and non-sensory area. The sensory portion lies close to the central raphe, while the non-sensory area covers the distal part of the lamella (Fig. 3-4A, B) (Byrd and Brunjes, 1995; Morita and Finger, 1998).

Despite the difference of structures, the basic organization of zebrafish olfactory system is similar to that of mammals (Byrd and Brunjes, 1995). The sensory portion of the peripheral OE contains a large number of olfactory sensory neurons (OSN), which have dendrites exposed to the epithelial surface and send axons to the ipsilateral OB. In mammals, each OSN expresses a single allele of one odorant receptor (OR) from a large gene family (Chess et al., 1994). The selectively expressed ORs are present on dendrites

exposed to the external world, as well as on axon tips extending into the brain (Barnea et al., 2004; Menco et al., 1997). The interaction of odorants and OR on the dendrites surface triggers a cascade of intracellular signals. In most OSNs a receptor-coupled $G\alpha_{olf}$ protein is activated and stimulates type III adenylyl cyclase to produce second messenger cAMP (Bakalyar and Reed, 1990), which then triggers opening of the cyclic nucleotide-gated cation channels (OCNC) (Dhallan et al., 1990; Firestein et al., 1991; Goulding et al., 1992). The resultant action potential is sent through axons to the OB (Levy et al., 1991; Prasad and Reed, 1999; Reed, 1992). Guidance of these axons is tightly controlled by a combination of factors, including the odorant receptors themselves as well as other proteins (Cutforth et al., 2003; Singer et al., 1995).

The overall projection of OSNs is highly ordered. Firstly, it follows a "zone-to-zone projection" principle. The OE is divided into four spatially segregated zones that are defined by the expression of OR and other molecules, like OCAM (olfactory cell adhesion molecules). Similar zonal organization is also preserved in the OB. OSNs expressing a given OR are distributed within one zone in the OE and send their axons to the corresponding zone in the OB (Ressler et al., 1993; Vassar et al., 1993). Secondly, the axons projection follows the "glomerular convergence" principle. A glomerulus is typically a spherical neuropil where the incoming axons terminate and synapse with the dendrites of second-order neurons. From one OE, all OSNs expressing a given OR, although distributed randomly within a zone, normally converge their axons to a single glomerulus in the ipsilateral OB (Fig. 3-4C) (Mombaerts et al., 1996; Wang et al., 1998; Yoshihara and Mori, 1997). Moreover, the relative positions of glomeruli in the OB are constant among individuals (Baier and Korsching, 1994). As a result of this well-ordered projection, chemical information is presented to the brain as spatial map composed of activated glomeruli in the OB (Rubin and Katz, 1999; Uchida et al., 2000).

These are common features of the main olfactory system among many vertebrates. In some higher eukaryotes a distinct accessory olfactory system, comprising the vomeronasal organ (VNO) and accessory olfactory bulb (AOB), is specialized in the perception of pheromones (Brennan, 2001; Halpern and Martinez-Marcos, 2003). Some pheromonal responses, however, are also detected by specialized cells that lie in the main olfactory epithelium (MOE) (Restrepo et al., 2004). The pheromone-detecting cells in both MOE and VNO are microvillous neurons. They are morphologically distinguishable from the major type of OSNs in MOE, which are ciliated cells and known to mediate the detection of volatile odorants in mammals. Ciliated and microvillous OSNs utilize different families of receptors and G-proteins, and respond to different classes of odorants (Bargmann, 1997; Dulac and Axel, 1995; Matsunami and Buck, 1997; Prasad and Reed, 1999).

Teleosts, including zebrafish, do not have a separate vomeronasal system. Both general odorants and intra-species pheromones are detected by the MOE, where morphologically diverse OSNs , including ciliated, microvillous and crypt neurons, are intermingled (Asano-Miyoshi et al., 2000; Hansen and Zeiske, 1998). However, among these intermixed cells, a strong correlation exists between cell morphology, distribution in the height of OE, expression of receptor class and G-protein type, ligand spectrum and target location in the OB (Hansen et al., 2004; Hansen et al., 2003; Morita and Finger, 1998). Tall ciliated OSNs usually have their nuclei located in the basal half of the OE and extend slender dendrites to the epithelial surface. They express receptors similar to those found in MOE of mammals, express the $G\alpha_{olf}$ subunit, and respond to amino acids or nucleotides. Microvillous neurons are relatively short, situated within the superficial half of the OE and carry small apical endings. They express receptors belonging to the V2R family (which are largely restricted to the VNO in mammals), express $G\alpha_o$, $G\alpha_q$ or $G\alpha_{i-3}$

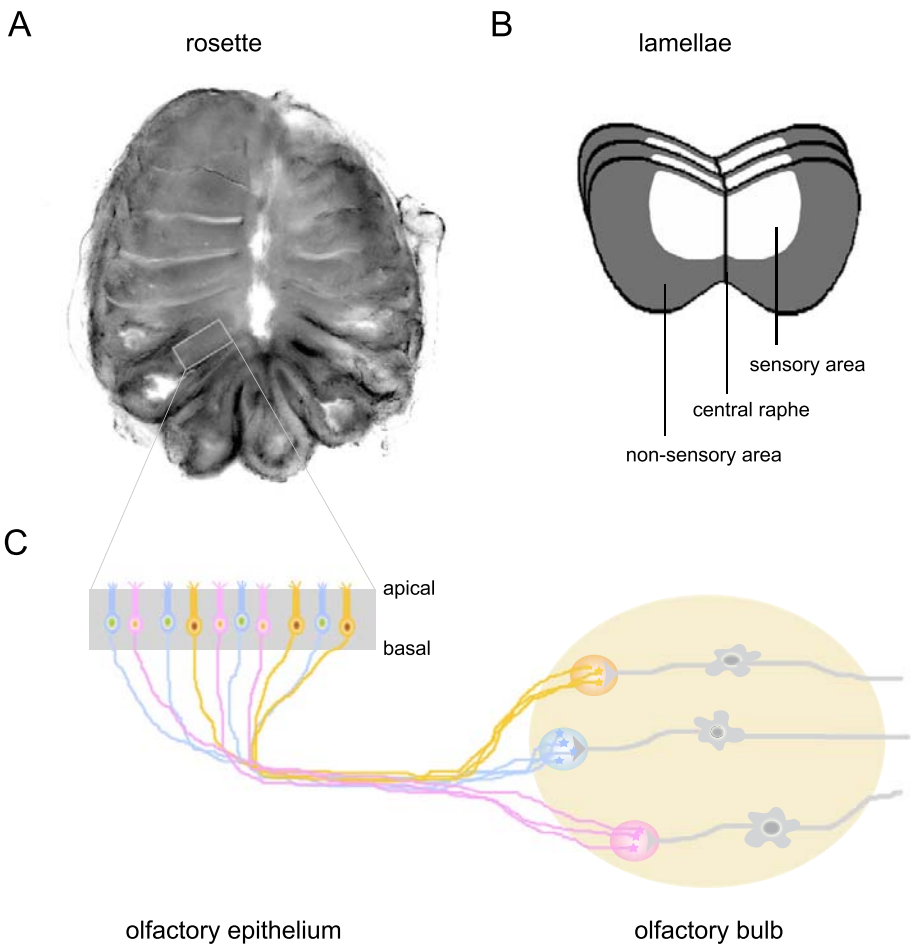

Figure 3-4. The organization of zebrafish olfactory system.

(A) A bright field image of an olfactory rosette from an adult zebrafish. The lamella are folded radialy around the central midline raphe and form a rosette structure (Weth et al., 1996). (B) Each lamella is composed of a sensory (white area) and a non-sensory (grey area) region of the epithelium (Morita and Finger, 1998). (C) Olfactory sensory neurons (OSNs) that express the same odorant receptor (OR) gene distribute mosaic in the OE, but converge their axons to a single glomerulus in the ipsilateral olfactory bulb. Three population s of OSNs, each expressing a different OR, are illustrated in different color. Their axons project to specific glomeruli, where they form synapsis with the dendrites of the second-order neurons (in grey) (Mombaerts, 1999).

subunit, and respond to pheromones, amino acids or bile acids (Lipschitz and Michel, 2002). Crypt neurons have been found only in fish OE (Hansen and Finger, 2000). They have a distinct ovoid shape, contain $G\alpha_o$ or $G\alpha_q$ in the apical region and are located in the basal and sensory segments within the OE (Hansen et al., 2004; Hansen et al., 2003). Their function is not known yet.

3.3.1.2 Expression of *Rag1*-driven GFP in zebrafish OSNs

To understand the expression of *Rag1* in the zebrafish olfactory system, we imaged the *Rag1:GFP* fish at high magnification. We found that very few OSNs start fluorescing around 22 hpf, when the olfactory placode is still a simple single-layered epithelium. In addition, these cells carry newly extending short axons (Fig. 3-5A), when they appear as GFP-positive. Given the fact that zebrafish OSNs start to express OR and mature from 22 hpf to 3 dpf (Hansen and Zeiske, 1993), this suggests that GFP driven by the *Rag1* promoter is turned on among the earliest batch of OSNs. With fish growth, the number of GFP positive cells in the OE increased and the GFP positive axons extended (Fig. 3-5B). These fluorescent axons reached the OB at 2 dpf and relatively stable projections were established at 3 dpf (Fig. 3-5C, D). At this stage, two kinds of GFP positive cells were visible in OE, bright and dim. Surprisingly, all of the bright GFP labeled axons from one OE converged to a single target in the lateral region of the ipsilateral OB (Fig. 3-5D, F, arrows), while the dim GFP positive axons terminated at the adjacent area (Fig. 3-5D, F, arrowheads). Staining with the synaptic vesicle maker SV2 (Buckley and Kelly, 1985) confirmed that the intense GFP-positive target is a glomerular neuropil (Fig. 3-5G). The projection of bright GFP axons in OB remains stable and visible *in vivo* until at least one month, as determined by the direct observation in live *Rag1:GFP* fish.

In adult zebrafish, the expression of *Rag1:GFP* was also detectable in the olfactory system. Most GFP positive OSNs have their cells bodies close to the apical surface in the

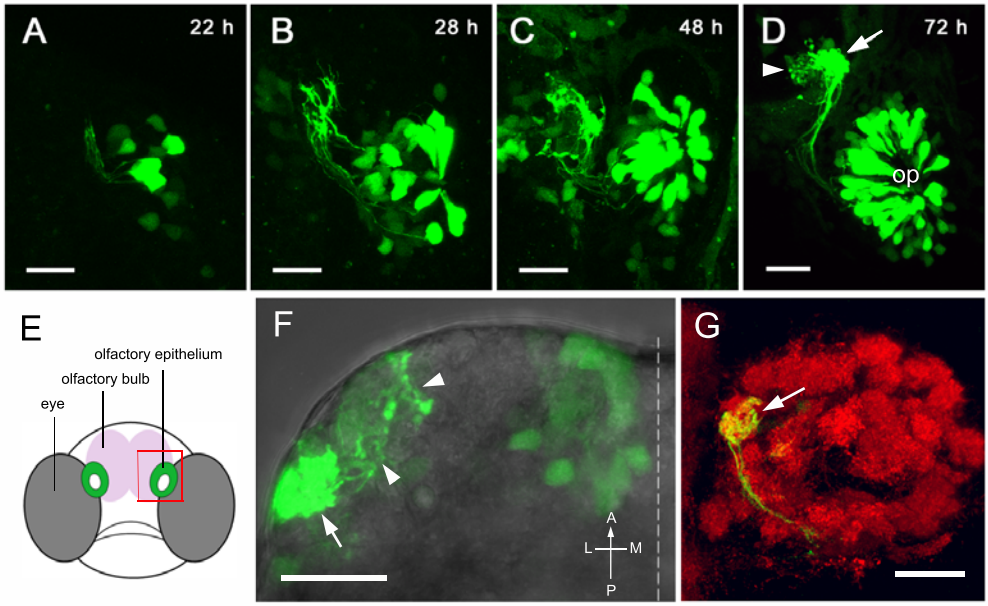

Figure 3-5. Expression of *Rag1*-driven GFP in the embryonic zebrafish olfactory system.

(A) At 22 hours post-fertilization, a few olfactory sensory neurons express GFP under the control of *Rag1* promoter. (B) At 28 hpf in the olfactory placode, both the number of GFP-positive and length of GFP-positive axons increased. (C) At 2dpf, GFP-positive axons reached ipsilateral olfactory bulb. (D) At 3 dpf, strong fluorescing olfactory sensory neurons converge their axons to a single target (arrow) in the ipsilateral OB. (E) Schematic drawing of the front view of a zebrafish embryo. The red box indicates the regions that were imaged in (A-D). (F) Dorsal view of an isolated forebrain from a 4 day-old fish, showing the left olfactory bulb. Anterior is to the top and the midline is indicated by the dotted line. Axons with strong GFP project to a single target in the lateral bulb (arrow), while axons with lower levels of GFP innervate other regions of the lateral bulb (arrowheads). (G) Frontal view of glomerular structures in the olfactory bulb of a 4-day fish, labeled with an antibody to SV2. Only one lateral structure is innervated by OSNs with strong GFP expression (arrow). Lateral is to the left, while dorsal is to the top. ob: olfactory bulb; op: olfactory pit. Bar = 20 μm.

OE and carry dendrites of intermediate length; a few cells, however, have their soma deep in the epithelium (Fig. 3-6A, B). GFP positive axons project only to the lateral area of OB, as can be seen in dissected forebrains (Fig. 3-6C, E) or using immunofluorescence on sections (Fig. 3-6D). A subset of axons projecting to a target in the lateral OB contained high levels of GFP (Fig. 3-6E), which is similar to the GFP positive projection in larvae. These observations suggest that some aspects of *Rag1:GFP* expression established in the embryo remain in adulthood.

3.3.1.3 Characterization of *Rag1:GFP* positive OSNs

Zebrafish OSNs have dendrites exposed to the outside, which can take up lipophilic dyes dissolved in water. Then, diffusion of this dye in the entire cells, including the axons, can make the whole structure of OSNs visible (Dynes and Ngai, 1998). We stained the *Rag1:GFP* fish with DiI. When higher concentration of DiI (1:1000 dilution) was used, the OE was heavily stained and many axon targets (glomeruli) in the OB were labeled (Fig. 3-7A, B, arrow). However, the target of GFP positive axons was hardly labeled with DiI (Fig. 3-7B, arrowheads). When the *Rag1:GFP* fish was stained with less concentration of DiI (1:5000 dilution), the labeled OSNs in the OE can be clearly seen. We found that DiI rarely labeled the strong GFP expressing neurons (13.8%, n=58; Fig. 3-7C). This indicates that the GFP positive cells have lower accessibility to outside, which was confirmed later by another experiment (done by S.Bulchand): even when incubated in Di8ANEPPQ, a lipophilic dye with higher solubility, only a limited number (53.8%, n=26) of GFP positive cells were labeled (Fig. 3-7D, E) (Feng et al., 2005).

With a construct provided by Dr Masayoshi Mishina, we generated a stable transgenic line expressing tau-DsRed under the control of the OMP (olfactory marker protein) promoter fragment. In this fish, tau-DsRed is expressed in most OSNs except for a sub-population projecting to a lateral area in the developing OB (Yoshida et al., 2002). By

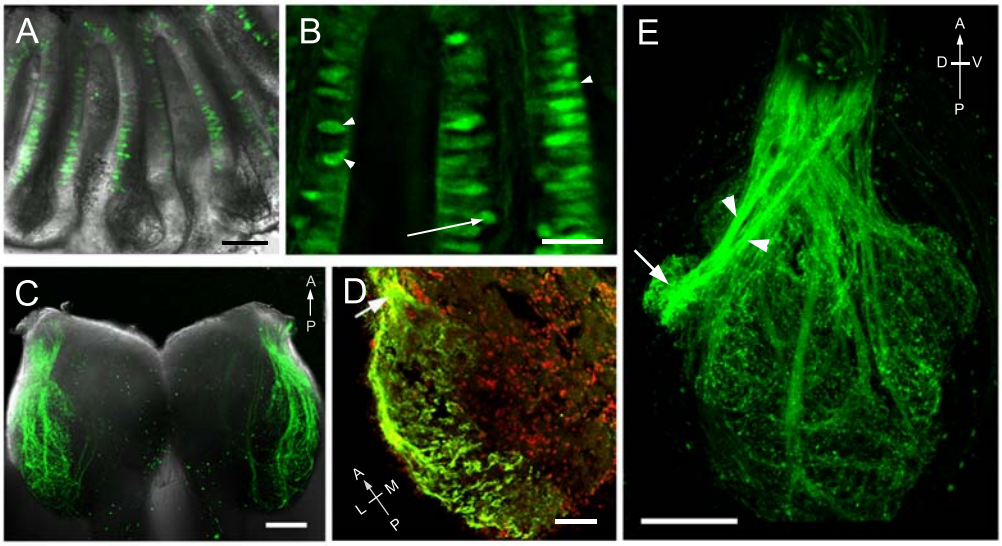

Figure 3-6. Expression of *Rag1*-driven GFP in the adult zebrafish olfactory system.

(A) An olfactory rosette isolated from an adult *Rag1:GFP* fish. GFP-expressing cells are located in the sensory region of the lamella and midline raphe. Most cell bodies are located apically. (B) High magnification of lamella from another adult olfactory rosette. GFP-expressing cells have different morphologies. Many have the cell body close to the apical surface (arrowheads). The arrow indicates one neuron with a deep cell body. (C) The ventral view of an isolated forebrain from a *Rag1:GFP* adult fish. GFP positive axons innervate only the lateral region of both olfactory bulbs. (D) Anti-GFP immuno-fluorescence on a horizontal section through the olfactory bulb of an adult. Label is detectable only in olfactory sensory neurons innervating the lateral bulb. The incoming olfactory nerve is visible at the upper left (arrow). Anterior is to the top-left; lateral to the bottom-left. Nuclei are labeled with propidium iodide (red). (E) Lateral view of an olfactory bulb dissected from a 1.5-year-old *Rag1:GFP* male. Axons innervate a large portion of the lateral bulb, but axons with the highest levels of GFP (arrowheads) form two bundles that innervate a single region (arrow). Other glomeruli are innervated by dimmer axons. Dorsal is to the left; ventral is to the right. Bar = 20 μm (B); 50 μm (A, D); 100 μm C, E).

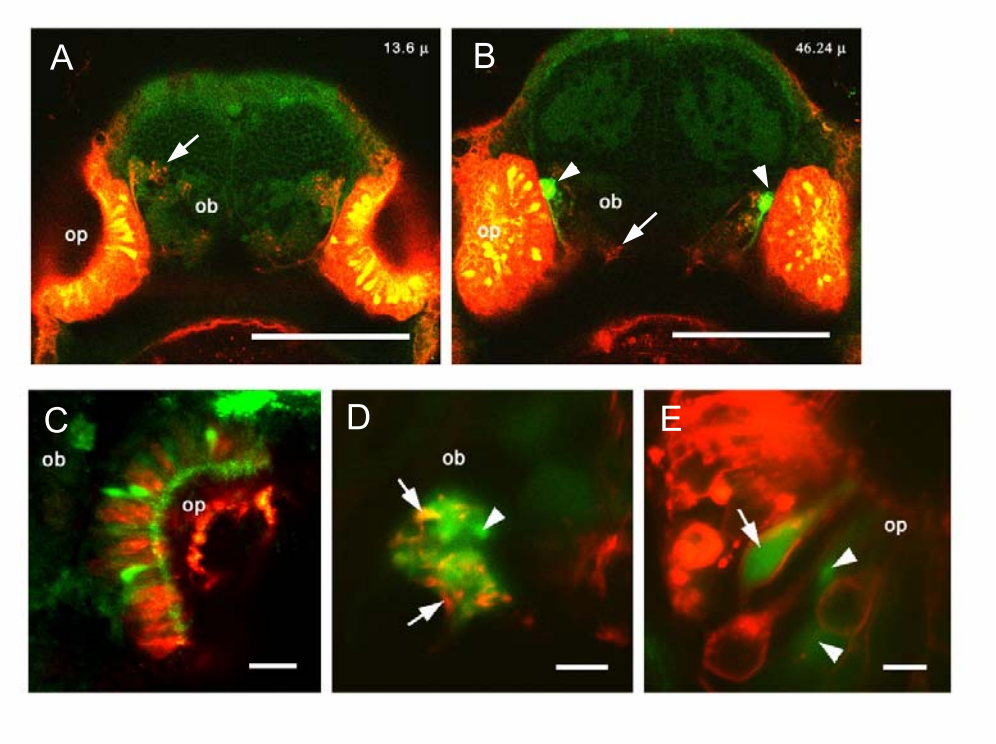

Figure 3-7. The DiI/Di8-labeled olfactory system of *Rag1:GFP* fish.

(A.B) The frontal view of an 8-day old larva, with DiI labeling of olfactory sensory neurons (red) and Bodipy labeling of inter-cellular spaces (dim green). (A) In a shallow section of the labeled forebrain, many DiI-labeled olfactory axons are visible (arrows). (B) In a deeper section, the GFP-containing axons (arrowhead) can be seen, along with other DiI-labeled axons (arrow). (C) In the DiI-labeled olfactory pit of Rag1:GFP fish larvae, most GFP-expressing cells (green) have not taken up DiI (red). (D.E) The Di8ANEPPQ-labeled olfactory system of a *Rag1:GFP* transgenic fish. In the olfactory bulb (D), some axons with strong GFP expression (green) are also labeled with Di8ANEPPQ (red; arrow), whereas others are not (arrowhead). (E) In this section through the olfactory epithelium, a GFP-expressing neuron was labeled with Di8ANEPPQ (arrow), whereas two others were not (arrowheads). Bar = 50 µm (A, B); 20 µm (C); 5 µm (D, E).

crossing to *Rag1:GFP* fish, we obtained the double transgenic fish, *OMP:tauDsRed*/*Rag1:GFP*. In the OE of these fish, *Rag1:GFP* was detected in a distinct population of OSNs that have shorter cell body than tauDsRed positive neurons (Fig. 3-8). OMP is known to be a marker of the ciliated OSNs. *Rag1:GFP* expressing cells were OMP-negative and showed different morphology, indicating that they are not ciliated OSNs.

We next tried the immunofluorescence with antibodies to different G-alpha subunits. Cells with strong GFP expression were found to be negative in all $G\alpha_{olf}$, $G\alpha_o$ and $G\alpha_q$ staining (Fig. 3-9). Crypt cells or other neurons that were labeled by the $G\alpha_q$ antibody were GFP-negative (Fig. 3-9D, E). 36 out of 85 neurons containing $G\alpha_o$ expressed GFP at low levels (Fig. 3-9A-C), while the remaining cells had no GFP. An additional 13 cells had low GFP expression, but did not express $G\alpha_o$. The absence of $G\alpha_{olf}$ and $G\alpha_q$ indicate that these *Rag1:GFP* cells are not ciliated or crypt neurons, while the heterogeneity in $G\alpha_o$ expression suggests that they could be microvillous neurons, but heterogeneous in some respects.

3.3.1.4 Summary

In larval stages, *Rag1:GFP* positive OSNs send axons to only few glomeruli, while DiI labeled OSNs project to many glomeruli, indicating that GFP labeled neurons account only for a subset OSNs. The strong GFP expression in the OE appears to define a special sub-population of OSNs of zebrafish, which have less access to the external environment, are OMP-negative and $G\alpha_{olf}$, $G\alpha_o$ and $G\alpha_q$ -negative; the dim GFP-expressing cells are OMP, $G\alpha_{olf}$, $G\alpha_q$ -negative, but heterogeneous in $G\alpha_o$ expression. In adulthood, the projection of GFP positive axons is still restricted to the lateral region in OB; the GFP expressing OSNs are located mainly at the apical layer in OE. The absence of OMP and

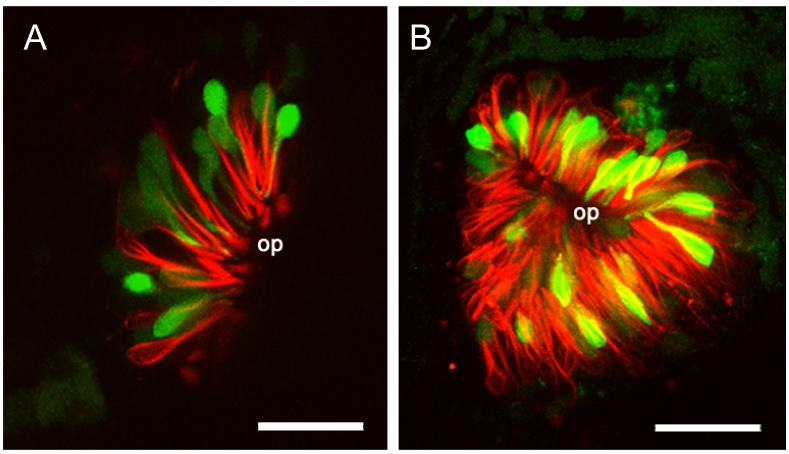

Figure 3-8. *Rag1:GFP*-positive OSNs do not express OMP.

(A, B) In the olfactory pit of a fish transgenic for *Rag1:GFP* and *OMP:tauDsRe*d, GFP expressing cells (green) are distinct from those labeled with DsRed. Panel A is a projection reconstructed from 3 continuous sections ; panel B is from the Z stack that covers entire olfactory pit. ob: olfactory bulb; op: olfactory pit. Bar = 20 μm.

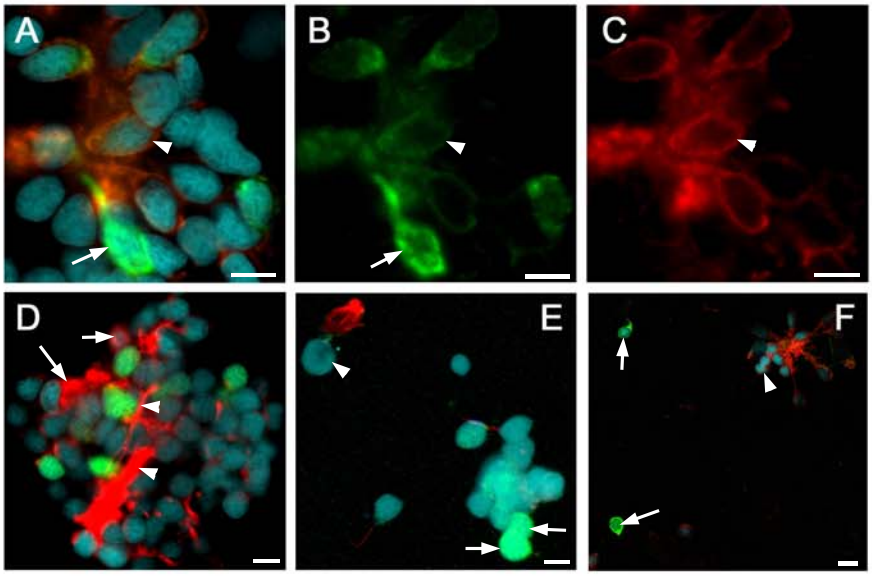

Figure 3-9. Expression of G alpha subunits in larval olfactory neurons.

(A-C) $G\alpha_o$ (red fluorescence, C) is present in a subset of *Rag1*-expressing cells (green fluorescence, B; arrowheads) isolated from the olfactory epithelium of a *Rag1:GFP* zebrafish. A cell with bright GFP (arrow), however, does not contain $G\alpha_o$. (D) $G\alpha_q$-positive neurons (arrows) do not express GFP, and vice-versa. Axons are strongly labeled (arrowhead). (E) A crypt cell (arrowhead), with $G\alpha_q$ label in the dendrites, lacks GFP. Two cells with bright GFP (arrows), in contrast, lack $G\alpha_q$ label. (F) $G\alpha_{olf}$ label, seen here in axons and some cell bodies (arrowheads), was not detected in cells strongly expressing GFP (arrows). Bar = 5 μm (A-E); 10 μm (F).

$G\alpha_{olf}$, as well as apical localization in adult OE indicate that these *Rag1:GFP* expressing cells are microvillous OSNs.

In addition, first few GFP positive OSNs fluoresce around the time when their axons extend out; suggesting that *Rag1* is expressed in these neurons at the post-mitotic stage, thus its function probably is irrelevant to the early neurogenesis of OSNs.

All together, these data indicate a selective expression of *Rag1* among OSNs, and suggest that *Rag1* may play a role in specifying a particular group of neurons in olfactory system, but is unlikely to have a general function in neurogenesis or in olfactory function.

3.3.2 *Rag1*-driven GFP is selectively expressed in many parts of the zebrafish nervous system

To further understand the selective expression of *Rag1* indicated by the observation in olfactory system, careful examination was carried out in other parts of zebrafish, which revealed that in fact *Rag1* is selectively expressed in many parts of the nervous system.

3.3.2.1 Eye

Similar to other vertebrates, the zebrafish retina is composed of seven major cell types: rod and cone photoreceptors, bipolar cells, amacrine cells, ganglion cells, horizontal cells and Müller glia. These cells are arranged precisely in three major layers, ganglion cell layer (GCL), inner nuclear layer (INL) and outer nuclear layer (ONL) (Fig. 3-10A, B) (Dyer and Cepko, 2001; Neumann, 2001). Neurogenesis in the zebrafish retina is initiated with retina ganglion cells (RGC) around 30 hpf. It starts from ventral center, close to the optic stalk, and spreads as a wave towards the peripheral retina. This is followed with the second and third waves of differentiation in the inner (INL) and outer nuclear layer (ONL). These neurogenesis waves are mainly controlled by a short-range signal, Sonic

Hedgehog (Neumann and Nuesslein-Volhard, 2000). The overall laminar architecture of zebrafish retina is essentially established by 60 hpf (Malicki, 2000).

In *Rag1:GFP* fish, GFP signals in the retina start to show up around 48 hpf, mainly in ganglion cell layer and amacrine cell layer (Fig. 3-10C). The axon bundles that extend from RGCs to the contralateral optic tectum in the midbrain also contain GFP (Fig. 3-10C, arrow). With fish growth, the fluorescence in RGCs and their axons gradually dimmed down. From 3 dpf onwards, there were very few fluorescent cells in the GCL. Amacrine cells turned on GFP expression slightly later than RGCs. The peak of expression appeared around 52 hpf, when the expression in the RGC layer began to decrease. At 8 dpf (the last time point examined[1]), the GFP signal remained strong in amacrine cell layer (Fig. 3-10D, arrow) and the inner plexiform layer, which contains axons extended from amacrine cells (Fig. 3-10D, arrowhead). In RGC layer very few GFP positive cells were visible, and they are probably not RGCs but displaced amacrine cells, because they send axons to the IPL instead of optic tectum. No GFP was detected in the bipolar cell layer and outer nuclear layer. With an antibody, GFP was also detected in sections of 21 dpf fish retina, mainly restricted to the amacrine cell layer (data not shown).

These observations indicate that in zebrafish retina the expression of *Rag1* is transient in the developing RGC, but is relatively stable in the amacrine cell layer.

3.3.2.2 Ear

The ear of zebrafish develops from an ectodermal thickening, the otic placode, whichbecomes visible from 16 hpf. This placode cavitates and forms the otic vesicle, the

[1] Zebrafish eyes start to be covered with heavy black pigments (melanophore) from 28 hpf. To image the internal structure of the live fish eye, 0.003% 1-phenyl-2-thiourea (PTU) in 10 % Hank's saline is routinely used to block the melanophore formation. But PTU is a hormone inhibitor, and will harm the fish if the treatment lasts too long. So no image was obtained from live fish older than 8 dpf.

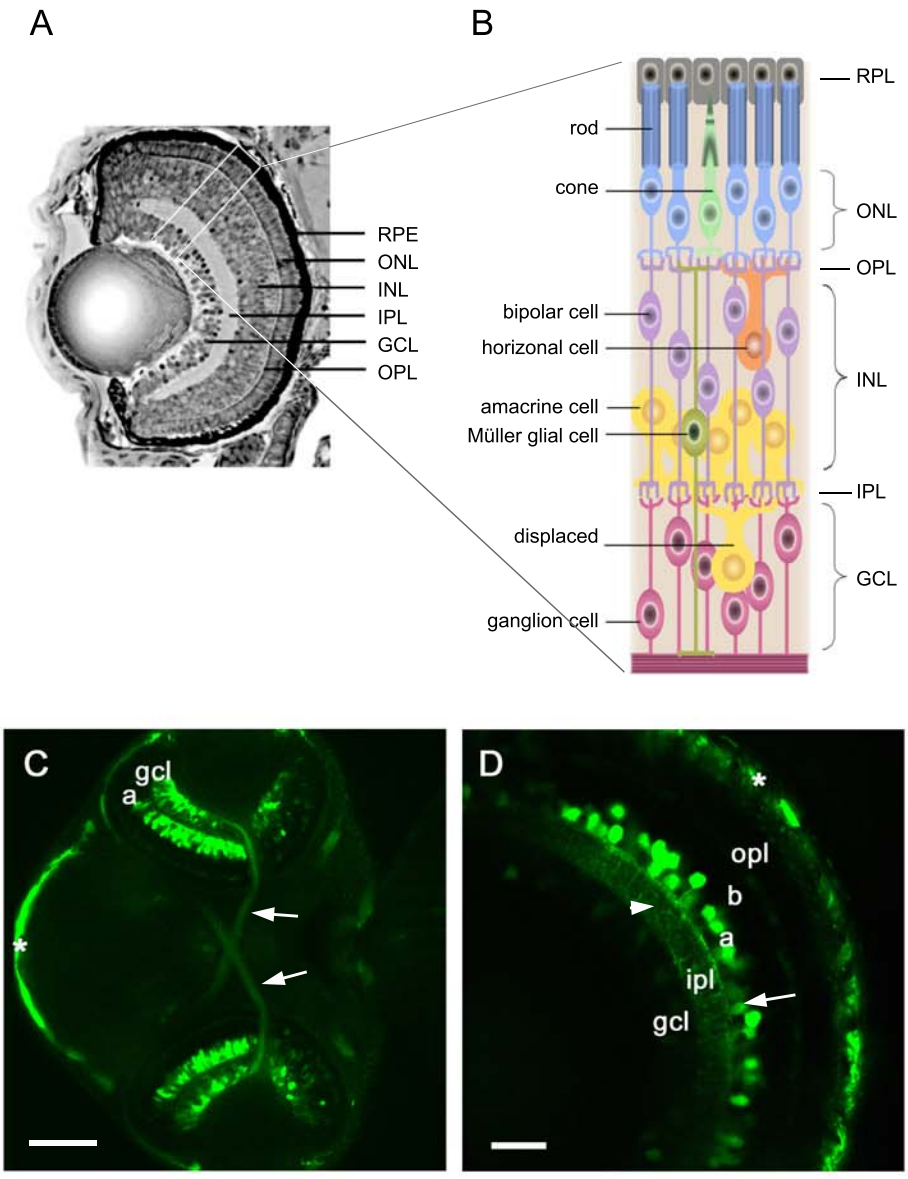

Figure 3-10. Expression of *Rag1*-driven GFP in zebrafish retina.

Figure 3-10. Expression of *Rag1*-driven GFP in zebrafish retina.

(A) A section of a zebrafish larval eye at 76 hpf, showing the characteristic lamination of a vertebrate retina (Neumann, 2001). GCL: ganglion cell layer; IPL: inner plexiform layer; INL: inner nuclear layer; OPL: outer plexiform layer; ONL: outer nuclear layer; RPE: pigmented epithelium of the retina. (B) Schematic representation of the vertebrate retina structure. The seven main classes of cell types found in the vertebrate retina (rod and cone photoreceptors, bipolar cells, ganglion cells, amacrine cells, horizontal cells and Müller glia) are organized into three distinct cellular layers (Dyer and Cepko, 2001). Photoreceptor cell bodies (rods and cones) make up the outer nuclear layer (ONL) of the retina. They receive stimuli and transmit signals through bipolar cells, whose cell bodies are found in the inner nuclear layer (INL), to the ganglion cells. From the ganglion cell layer (GCL), these signals make their way along the optic nerve to the brain. (C, D) GFP is expressed in the retina of *Rag1:GFP* fish. (C) At 2dpf, GFP was expressed in the retina ganglion cell layer (gcl) and amacrine cell layer (a). The axon bundles (arrow) from RGC to brain were visible. (D) At 8 dpf, the expression of GFP dropped down in the ganglion cell layer, but was maintained in the amacrine cell layer (arrow) and inner plexiform layer (arrowhead). a: amacrine cell layer; b: bipolar cell layer; *: skin auto-fluorescence. Bar = 100 μm (C); 20 μm (D).

larval ear of zebrafish. Each otic vesicle contains five sensory patches of epithelium, two maculae and three cristae, which consist of groups of hair cells and supporting cells (Fig. 3-11A). Hair cells are the sensory neurons that transduce small movements triggered by sound or body dis-equilibrium into an electrical signal. The hair cells in the maculae differentiate from about 24 hpf, whereas in cristae they become visible between 42 and 74 hpf (Haddon and Lewis, 1996; Whitfield et al., 2002).

Besides the ear, hair cells also exist in zebrafish lateral line. The lateral line is a unique sensory system in fish and amphibians, which is specialized in detecting changes in the motion of water. It comprises a set of neuromasts, where hair cells form the core and are surrounded by support cells (Ghysen and Dambly-Chaudiere, 2004).

In *Rag1:GFP* fish, only 3 clusters of hair cells that locate in the cristae of otic vesicle express GFP (Fig. 3-11B). The hair cells in the maculae and lateral line do not fluoresce.

3.3.2.3 Brain

The zebrafish brain shares many common features with other vertebrate brains in patterning during development. They all start with the progressive subdivision of the neural tube. The constrictions along the neural tube form the primordia of the telencephalon, diencephalon, midbrain and hindbrain rhombomeres (Kimmel, 1993). Each of them undergoes further morphogenesis and all work together as a functional brain. The molecular regulatory mechanism behind the morphogenesis of the zebrafish brain also shows evident similarity with other vertebrate brains. For example, a zinc-finger transcription factor *krox-20*, which was initially found in mouse embryos (Wilkinson et al., 1989) and is known to be expressed in the rhombomere r3 ands r5 and play an important role in hindbrain patterning in all examined vertebrate embryos, was

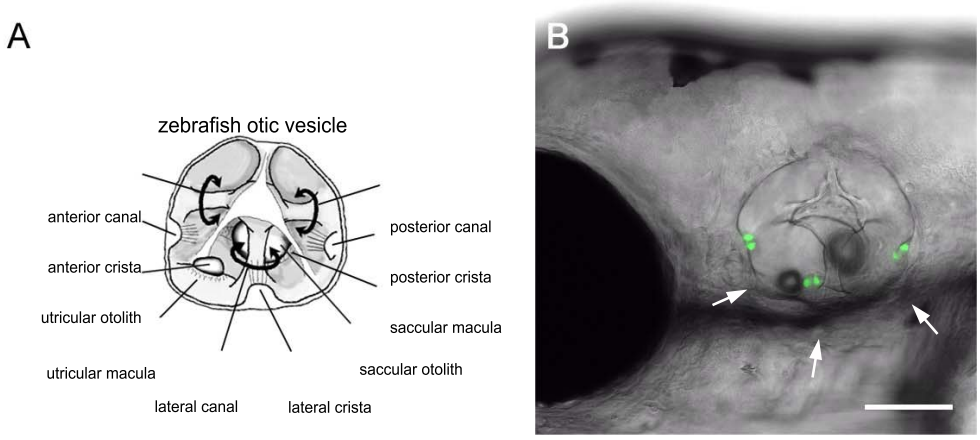

Figure 3-11. Expression of *Rag1*-driven GFP in zebrafish otic vesicles.

(A). Drawing of a wild-type zebrafish ear at 4 days postfertilisation (dpf), to give a three-dimensional impression of the structures within the vesicle. Epithelial pillars within the ear form hubs of the developing semicircular canals (curved arrows). Each canal (anterior, lateral and posterior) is associated with a small sensory patch or crista, whereas each otolith overlies a larger sensory patch or macula (Whitfield et al., 2002). (B) The otic vesicle of a 3-day old fish, shown in lateral view, with GFP-positive cells in the three cristae (arrow). Bar = 100 μm.

also identified in zebrafish and has been proven to play the same role (Costagli et al., 2002; Moens and Prince, 2002; Oxtoby and Jowett, 1993).

As a vertebrate model for developmental neurobiology research, zebrafish shows growing importance. Pioneering works by Kimmel on the embryonic brain (Kimmel, 1993) and Wullimann on the postembryonic and adult zebrafish brain (Rupp et al., 1996) have contributed a lot to our understanding of the organization of the zebrafish brain. However, detailed knowledge about neural development in postembryonic zebrafish brain is still limited, and this places a constraint on a full description of where *Rag1* is expressed.

At early stages, the zebrafish brain develops very fast. Around 24 hpf, scaffold of tracts and commissures of primary neurons have formed (Kimmel, 1993). By 72 hpf, the further sculptured brain primordia are more integrated by neuronal connections and some functions have been enabled (Mueller and Wullimann, 2005; Westerfield, 2000). In the brain of *Rag1:GFP* fish, the earliest GFP signal appears in the hypothalamus of the ventral diencephalon around 26 hpf. Between 48 to 54 hpf, many other parts of the brain start to fluoresce. The most prominent one is the optic tectum in the midbrain, which is the primary higher-order brain structure for visual processing in zebrafish (Rupp et al., 1996). RGCs in the retina send their axons into 10 distinct arborization fields (AFs) in the contralateral forebrain and midbrain. Among these AFs the largest is optic tectum, e.g. AF10 (Burrill and Easter, 1994). *Rag1:GFP* was expressed in many neurons in the optic tectum. Most of them extend long GFP-positive processes radially into the tectal neuropil (Fig. 3-12C). These signals start to show up around 46 hpf, reach their expression peak around 52 hpf, then gradually drop down. In addition to the optic tectum, the *Rag1:GFP* are also expressed in several other parts in the brain, including hypothalamus (Fig 3-12D), cerebellum (Fig 3-12C), two groups of cells that symmetrically located in the

forebrain (fig.3-12B), and two groups of cells (close to the skin, not shown) and an axon bundle at the level of the otic vesicle (Fig 3-12C).

The adult brain is not transparent, so GFP expression could not be examined in detail in live tissue. Immunofluorescence with an antibody against GFP on sections showed that in the adult zebrafish brain some neurons still express *Rag1:GFP*. In the tectum GFP was detected in a layer specific manner (Fig. 3-12E). In the central part of the midbrain, some groups of neurons, which could not be identified, were also GFP positive (Fig. 3-12F).

When *Rag1* transcripts were detected in the mouse brain in 1991, it was shown by *in situ* hybridization that *Rag1* was intensely expressed in hippocampal formation and cerebellum (Chun et al., 1991). Our above observations indicate that *Rag1* is selectively expressed in the zebrafish brain, which is consistent with this report. But further comparison is largely blocked because of the limited anatomical information in zebrafish.

3.3.2.4 Spinal cord

In the trunk, expression of *Rag1:GFP* was found only in some spinal interneurons. Their cell bodies lie in the dorsal part of the neural tube, while axons extend ventrally and form a bundle near the ventral midline of the spinal cord. These features are very close to those found in the commissural bifurcating lateral neuron (CoBL, Fig. 3-13)(Bernhardt et al., 1990; Downes et al., 2002).

3.4 Immunofluorescence confirmed the selective expression of Rag1 in neuronal nucleus

To confirm the fidelity of the reporter gene in *Rag1:GFP* transgenic fish and to characterize the distribution of endogenous RAG1 protein among zebrafish neurons, an antibody against the C-terminal 15 amino acids of zebrafish RAG1 protein was generated.

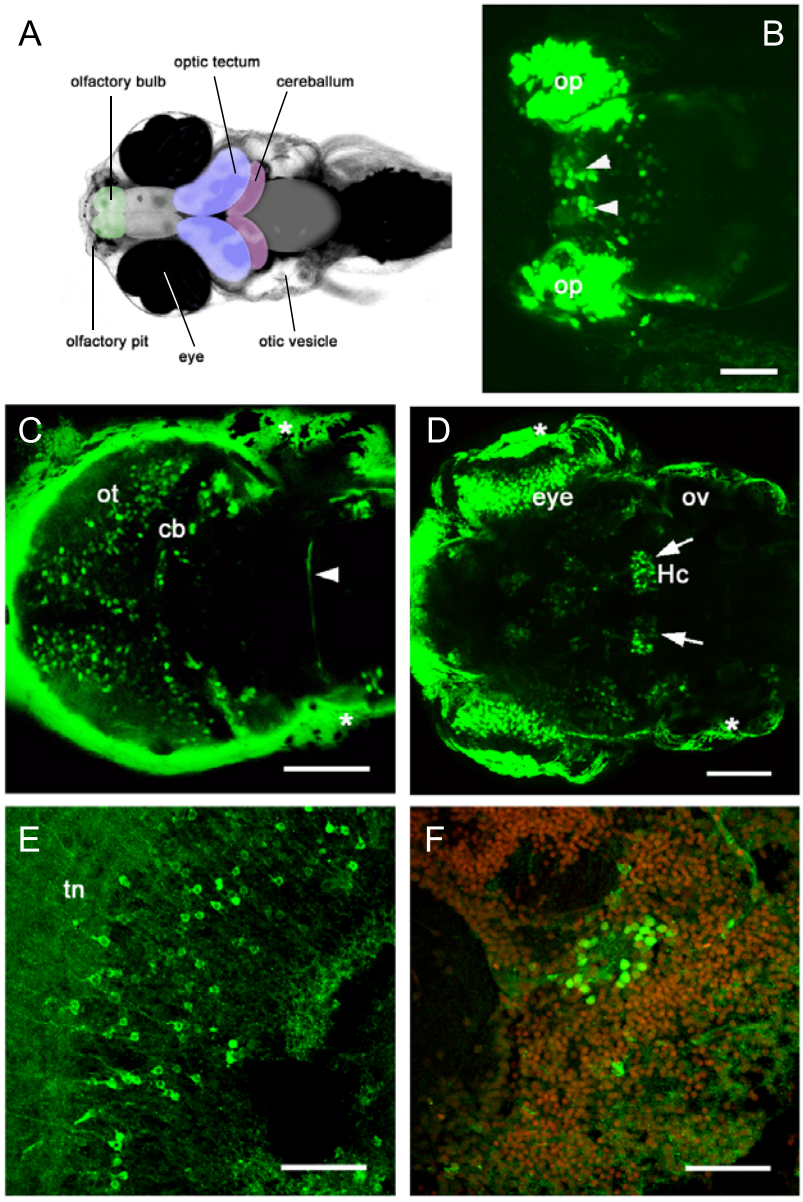

Figure 3-12. Expression of *Rag1*-driven GFP in zebrafish brain.

Figure 3-12. Expression of *Rag1*-driven GFP in zebrafish brain.

(A) The dorsal view of a 4 dpf fish head. Colored patches indicate different parts of the brain (Mathieu et al., 2002). (B-D) Images of live *Rag1:GFP* larval fish. (B) Dorsal view of the forebrain of an 8-day old fish. Two groups of cells, on either side of the midline, express GFP (arrowheads). The expression level in these cells is lower than olfactory sensory neurons, where the signal is saturated in this image. (C) Dorsal view of the tectum of a 3-day old fish, with many fluorescing tectal neurons. In the hindbrain, an axon bundle (arrowhead) at the level of the otic vesicle, is the only labeled structure. (D) Dorsal view of the midbrain/hindbrain boundary at 3 dpf; with labeling of discrete, deep structures (caudal hypothalamus; arrow). (E, F) Expression of *Rag1* in adult zebrafish, as detected by anti-GFP immunofluorescence on brain sections of transgenic fish. (E) A sagital section through the tectum, with numerous GFP-positive cells projecting into the tectal neuropil. (F) A section through the cerebellum, showing a cluster of GFP-positive cells. Nuclei are stained with propidium iodide. op: olfactory pit; ot: optic tectum; cb: cerebellum; ov: otic vesicle; Hc: caudal hypothalamus; tn: tectal neuropil; *: skin auto-fluorescence. Bar = 50 μm (B, E, F); 100 μm (C, D).

A

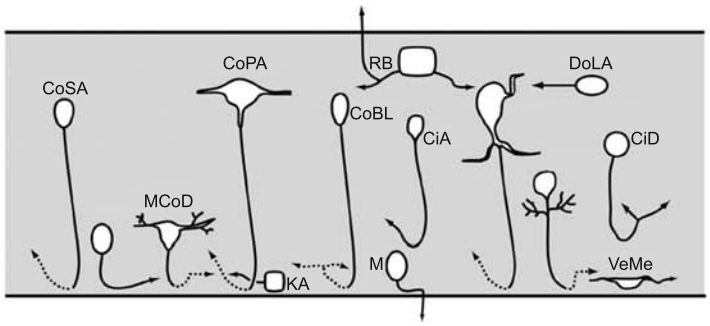

CiA: circumferential ascending
CoBL: commissural bifucating longitudinal
CiD: circumferential descending
CoLA: commissural longitudinal ascending
CoPA: commissural primary ascending
CoSA: commissural secondary ascending
DoLA: dorsal lateral ascending
KA: Kolmer-Agduhr
M: motoneuron
MCoD: multipolar commissural descending
RB: Rohon-Beard
UCoD: unipolar commissural descen
VeLD: ventral longitudinal descending
VeMe: ventral medial

B

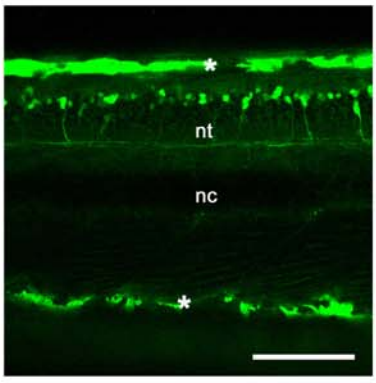

Figure 3-13. Expression of *Rag1*-driven GFP in zebrafish spinal cord.

(A) Summary diagram of the known zebrafish spinal cord neurons. Dashed lines indicate commissural projections (Benhardt et al., 1990; Downes et al., 2002). (B) Lateral view of the trunk of a 3 dpf *Rag1:GFP* fish. Some dorsal interneurons within the neural tube express GFP. Their axons form a longitudinal fascicle in the ventral neural tube. nt: neural tube; nc: notocord; *: skin auto-fluorescence. Bar = 100 μm.

The specificity of this antibody was tested on thymocytes from 2 week-old zebrafish, in which *Rag1* is intensely expressed. This antibody stains the thymocytes, and its activity is specifically abolished by the pre-absorption with the synthesized RAG1 C-terminal peptide (Fig. 3-14A, B).

Using this antibody together with an antibody against GFP, we carried out double immunofluorescence. Olfactory epithelia and retina from 3-4 dpf zebrafish were dissected out, dispersed on slides, fixed and double labeled. In both experiments, some cells were clearly labeled by RAG1 antibody, with staining mainly in the nucleus; and among these cells there was a clear overlap of RAG1 (red) and GFP (green) immunofluorescence (Fig. 3-14C-H). From 3 experiments on OE, 100 out of 105 cells that carried high level of GFP were found to be RAG1 positive. The overlap of GFP and endogenous RAG1 protein proves that the GFP expression in *Rag1:GFP* transgenic zebrafish is a reliable indicator for endogenous RAG1.

RAG1 protein has been heavily studied for more than 20 years. Its transcripts in the murine nervous system were also noticed fifteen years ago. But so far there had been no direct evidence showing the presence of RAG1 protein in the nervous system. Our antibody staining on the dispersed zebrafish neurons is the first evidence for the presence of RAG1 protein in neurons, predominantly in the nuclei.

3.5 Transgenesis shows that Rag2 is expressed in subsets of neurons distinct from Rag1

In the immune system, RAG2 works together with RAG1 to cleave and rejoin DNA at specific signal sequences (RSS), which leads to the rearrangement of genomic DNA and the assembly of Ig and TCR genes (Gellert, 2002; Kim et al., 2000). In this process RAG2 was shown to stabilize and enhance RAG1's function in the DNA- protein complex, and

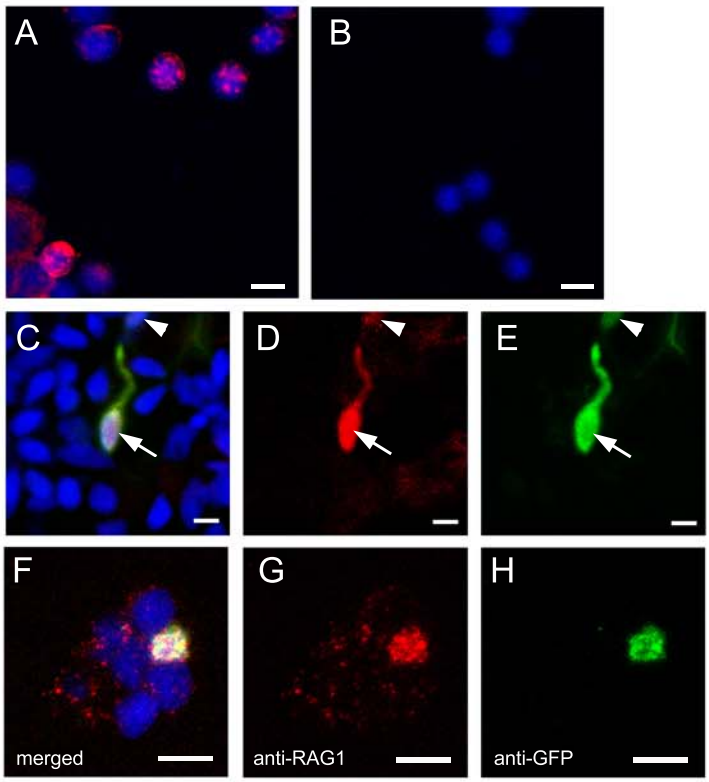

Figure 3-14. Immunofluorescence with antibody against RAG1.

(A) Isolated zebrafish thymocytes, labeled with the antibody to RAG1 (in red) and DAPI (blue). (B) After pre-absorption with the peptide used for immunization, no labeling was detected with this antibody. (C-E) Olfactory epithelial cells from a *Rag1:GFP* transgenic fish were double-labeled with anti-zf RAG1 (D) and anti-GFP (E) antibodies. RAG1 protein (C, D; red) is present in the GFP-positive (C, E; green) neurons (arrow and arrowhead), with high (arrow) or low (arrowhead) levels of GFP. (F-H) Double-label of retinal cells isolated from a 3-day old *Rag1:GFP* fish. The GFP-positive cell also contains RAG1, which is nuclear localized. DAPI (A, B, C, F; blue) is used to stain nuclei. Bar = 5 μm.

possibly to play an essential role in the joining step (Qiu et al., 2001). When *Rag2* was knocked out, V(D)J recombination was completely blocked and no mature T cells and B cells were produced in mice (Shinkai et al., 1992). Consistent with its indispensable function, RAG2 has been reported to be present and functional together with RAG1 in immune organs among different organisms. To establish whether in the nervous system *Rag1* plays a function similar to the V(D)J recombination in the immune system, we chose to check whether *Rag2* is co-expressed with *Rag1* in neurons. *Rag1* was known to be expressed at very low level in the nervous system, where *Rag2* could not be detected by traditional in situ hybridization in the mouse (Chun et al., 1991). To achieve higher sensitivity, we examined transgenic fish that carry GFP or DsRed under the zebrafish *Rag2* promoter.

3.5.1 *Rag2* is expressed in a group of ciliated OSNs

Firstly, sperm-mediated transgenesis was carried out (Jesuthasan and Subburaju, 2002). The zebrafish *Rag2* promoter, a ~7 kb fragment immediately upstream of *Rag2* coding sequence, was cloned and used to express DsRed in the *Rag1:GFP* line. Expression of DsRed in the thymus at 5 dpf was used as an indicator of successful transgenesis. In fish with co-expression of GFP and DsRed in thymocytes (Fig. 3-15B), very little overlapping expression was seen in the olfactory pit (Fig. 3-15C).

To confirm this observation, stable transgenic lines containing GFP or DsRed driven by *Rag2* promoter were generated. Totally one *Rag2:GFP* line and two *Rag2:DsRed* lines were examined. All these fishes showed the expression of reporter gene in thymus from 4 dpf (Fig. 3-16A). But the reporter expression in nervous system is different between DsRed and GFP fish. Both DsRed lines carried only few fluorescent neurons in the larval stage; and the red fluorescence in OSNs began to show up around 2 dpf. In contrast, in the *Rag2:GFP* line, the fluorescence wa s detected in many parts of nervous system, and

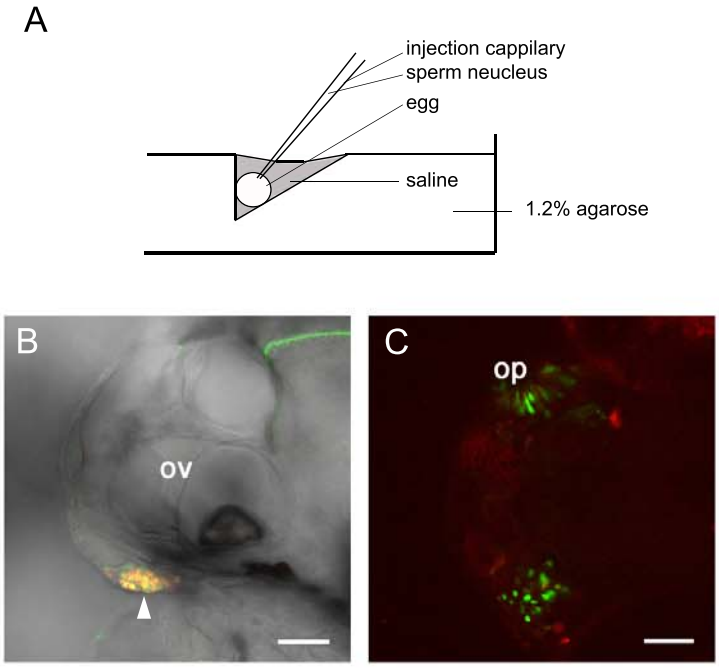

Figure 3-15. Expression of *Rag2*-driven DsRed in the *Rag1:GFP* fish, revealed by sperm mediated transgenesis.

(A) Schematic drawing to illustrate the sperm mediated transgenesis. Zebrafish sperm nuclei were isolated, incubated with purpose DNA, and then injected into freshly squeezed egg. The embryos developed from these eggs have higher probability to express the purpose gene (Jesuthasan and Subburaju 2002). (B) Lateral view of the midbrain region, showing that at 5th day post injection, *Rag2*-driven DsRed was expressed in the thymus, overlapping with the *Rag1*-driven GFP. (C) Dorsal view of the forebrain region showing that in the olfactory pit of the same fish, DsRed (*Rag2*, red) was expressed in very few cells and hardly overlap with GFP (*Rag1*, green). ov: otic vesicle; op: olfactory pit. Bar = 50 μm.

GFP was visible in the olfactory pit before 24 hpf. It is known that after translation, DsRed protein takes longer time than GFP to fold and oligomerize before it can fluoresce (Sacchetti et al., 2002). This might lead to the different expression of DsRed and GFP, even though they are under the same *Rag2* promoter fragment. Nevertheless, in both cases, the expression pattern of *Rag2*-driven reporters was distinct from that seen with the *Rag1* promoter.

In the larval olfactory pit, *Rag2:GFP* is expressed in many cells at a relatively low level. The overall expression reaches its peak at 2 dpf (Fig. 3-16B), then gradually becomes weak. This is different from the *Rag1:GFP* embryos, whose GFP expression in a group of OSNs remains strong. Among the GFP positive cells in *Rag2:GFP* fish OE, some cells do express GFP at higher level than others. But, different from *Rag1:GFP* fish, no distinct projection is formed with the GFP positive axons at this stage. Furthermore, different from *Rag1:GFP* positive OSNs (refer to 3.1.3.1) that didn't express OMP, some *Rag2:GFP* positive cells in OE also express *OMP:DsRed* in the double transgenic fish (Fig. 3-16D).

In the *Rag2:DsRed* lines, only few red fluorescent OSNs are visible at larval stage, and they do not overlap with GFP positive OSNs in the *Rag1:GFP/Rag2:DsRed* double transgenic fish (Fig. 3-16C).

The expression of *Rag2*-driven reporters was also examined in the adult olfactory system. Both the DsRed and GFP are expressed in a subset of OSNs which carry slender dendrites and have soma located in the basal OE (Fig. 3-17A). These morphological features suggest that they are ciliated OSNs (refer to 3.1.3.1). Imaging of the dissected OB revealed that these OSNs project their fluorescent axons to only few glomeruli in the ventral OB (Fig. 3-17B). Both *Rag2:DsRed* lines were crossed to *Rag2:GFP* fish for generating double transgenic fish, and they all showed overlapping expression with the

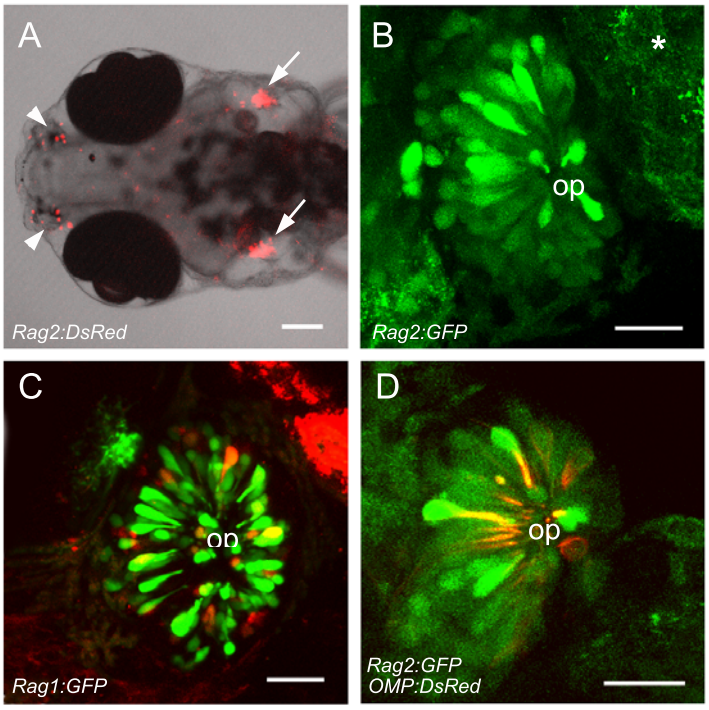

Figure 3-16. In stable transgenic lines, the expression of *Rag2*-driven reporters is different from the *Rag1*-driven GFP in the embryonic olfactory system.

(A) The dorsal view of a 5 day-old *Rag2:DsRed* fish, showing the expression of DsRed in thymus (arrow) and olfactory pit (arrowhead). (B) In a 2-day old *Rag2:GFP* fish. A number of cells are labeled with GFP in the olfactory pit, but no obvious projection of the GFP-positive axons can be seen. (C) The olfactory pit of a 3 day-old fish that carries both *Rag1:GFP* and *Rag2:DsRed*. Very few DsRed-positive cells (red) are visible and they hardly overlap with the GFP expressing cells (green). (D) In a fish with both *Rag2:GFP* and *OMP:DsRed* transgenes, the *Rag2*-driven GFP (green) is expressed in the OMP-positive (red) OSNs. op: olfactory pit; *: auto-fluorescence of the skin. Bar = 100 μm (A); 20 μm (B-D).

Rag2:GFP. In the OE, red and green fluorescence are partially overlapped among OSNs, while in the OB, red and green axons project to same sets of glomeruli, although some terminals are not double labeled (Fig. 3-17C-E). This indicates that the *Rag2* promoter drives the reporters in the same group of OSNs in all these three transgenic lines, and suggests that the expression is not due to the genomic context of integration.

The cell morphology, location and axon projection of these *Rag2*-positive OSNs are all different from the *Rag1:GFP* expressing OSNs. This was further confirmed by observation of adult fish labeled with both *Rag2:DsRed* and *Rag1:GFP*. From the overview of the olfactory rosette, the *Rag2* positive cells (red) mainly occupied the middle part of the lamella, while the *Rag1* positive cells (green) distributed broadly along the lamella, with higher density at the narrow region close to the central raphe (Fig. 3-18A). Under high magnification, the *Rag2:DsRed* expressing OSNs were seen to be embedded deeper from the apical surface and carry long narrow dendrites; whereas *Rag1:GFP* positive OSNs were mainly located at the apical half of the OE and had relatively short small dendrites(Fig. 3-18B, C). In the OB, *Rag2:DsRed* positive axons converge to only few ventral glomeruli; while *Rag1:GFP* labeled axons project to the broad lateral region (Fig. 3-18D).

Based on these observations we speculate that the expressions of *Rag1* and *Rag2* in the olfactory system are not co-localized; they are restricted to different subsets of OSNs.

3.5.2 *Rag2* is expressed distinctly from *Rag1* in many parts of zebrafish nervous system

In other parts of the nervous system, very few neurons express *Rag2:DsRed* and they do not co-localize with *Rag1:GFP* in the double transgenic fish. *Rag2:GFP* showed obvious

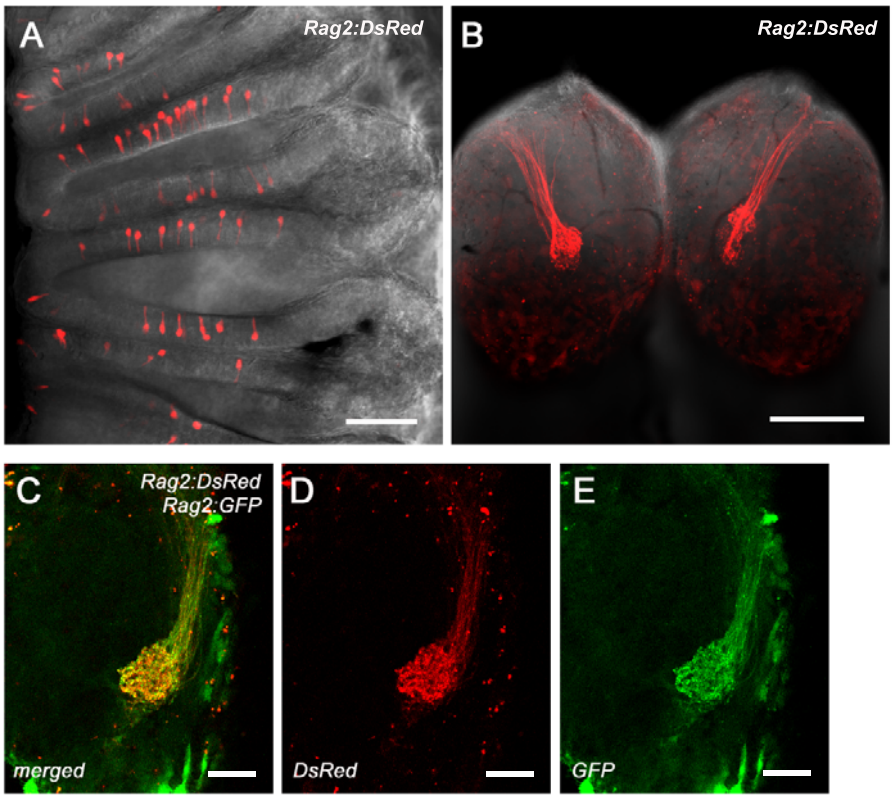

Figure 3-17. Expression of *Rag2*-driven reporters in the adult olfactory system.

(A) In the olfactory epithelium, *Rag2*-driven DsRed was expressed in a subset of OSNs that carry a long dendrite and a deep-located cell body. (B) Ventral view of the olfactory bulb of *Rag2:DsRed* adult fish. The DsRed-positive axons project into few glomeruli on the ventral OB. (C-E) In the olfactory bulb of a fish that carry both *Rag2:GFP* and *Rag2:DsRed*, the GFP-positive axons (green) and DsRed-positive axons (red) project into the same set of glomeruli. Bar = 50 μm (A, C-E); 200 μm (B).

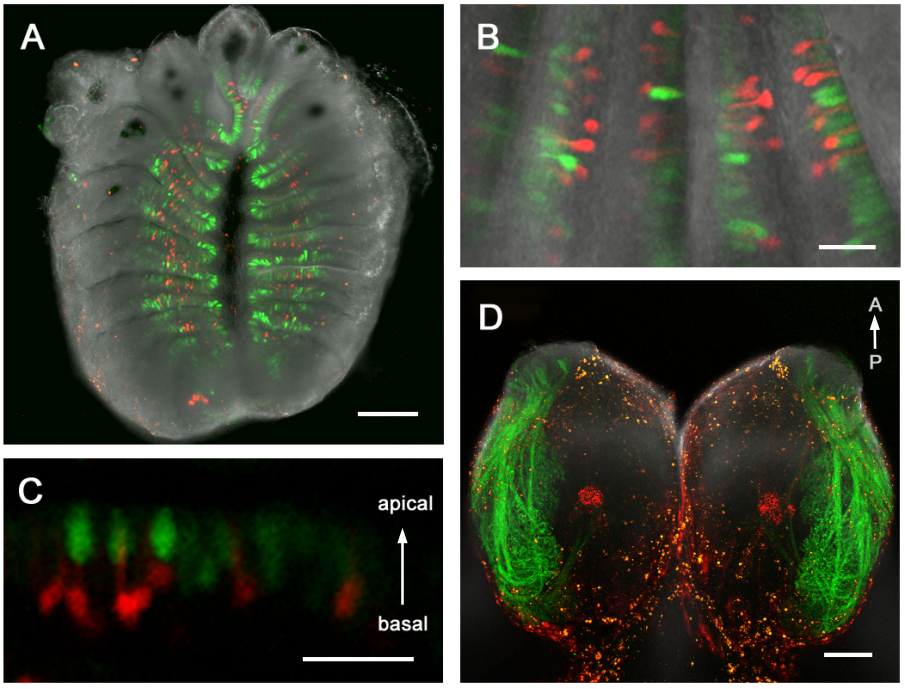

Figure 3-18. The different expression of *Rag2*-driven DsRed and *Rag1*-driven GFP in adult olfactory system.

(A-C) Olfactory epithelium of fish that carried both *Rag1:GFP* and *Rag2:DsRed*. (A) An entire olfactory rosette with bright field and fluorescent image merged. (B, C) High magnification images of a double labeled OE. *Rag1*-driven GFP (green) is mainly expressed in a subset of OSNs that located in the apical part of the OE and carry a small short dendrite on the apical surface, whereas *Rag2*-driven DsRed (red) is expressed in a distinct subset OSNs that carry a long dendrite with the cell body in the basal part of the OE. (D) Ventral view of the olfactory bulb of a double transgenic fish. Axons expressing *Rag1:GFP* project to the lateral region of the OB (green), whereas the axons with *Rag2*-driven DsRed converge into few ventral glomeruli (red). Bar = 100 μm (A, D); 20 μm (B, C).

expression in many parts of nervous system, and thus was examined in detail at larval stages.

In the retina, only a very low level of GFP was detected in the bipolar layer (Fig. 3-19A), different from the restricted expression of *Rag1:GFP* in RGCs and amacrine cells. According to the relative position of lens and outer pigment layer, we combined the retina images of *Rag1:GFP* fish and *Rag2:GFP* fish in pseudocolor, which illustrates the non-overlapping expression of GFP under the two different promoters (Fig. 3-19B).

Rag2:GFP was also seen in the brain (Fig. 3-19C, D), but very few cells expressed GFP brightly. In the forebrain, a group of GFP positive cells were located at the posterior part of the telencephalon, where no *Rag1:GFP* cells were seen. Some *Rag2:GFP* expressing cells also appeared in the hypothalamus and optic tectum, where also many *Rag1:GFP* neurons were located. Co-localization of *Rag1* and *Rag2* in brain cells could not be determined, because *Rag2:DsRed* could not be detected here.

In the trunk, many cells express *Rag2:GFP* in the spinal cord, but at different levels. Some motoneurons, which have cell bodies in the ventral spinal cord and carry axons innervating myotomes, express higher level of GFP (Fig. 3-19E). These neurons are different from those expressing *Rag1:GFP*, which are located in the dorsal spinal cord and do not project axons to myotomes.

These observations indicate that the expression of *Rag2* and *Rag1* are not correlated in the zebrafish nervous system, thus *Rag1* is unlikely to play the same role (e.g. mediating V(D)J recombination) in the nervous system as it does in immune system.

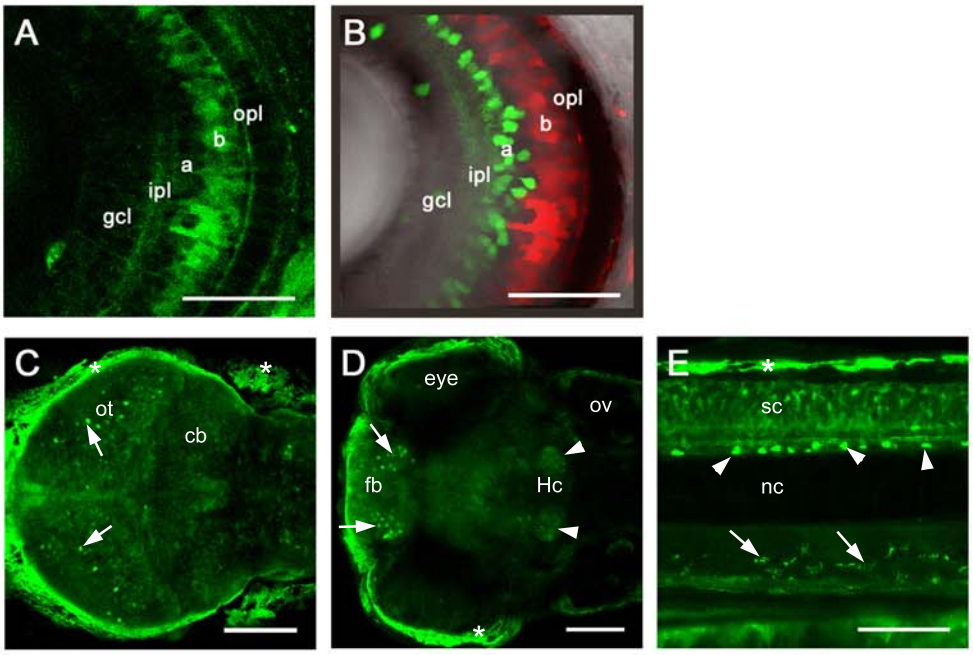

Figure 3-19. Expression of *Rag2*-driven GFP in other parts of zebrafish embryonic nervous system.

(A) The retina of a 3-day old *Rag2:GFP* fish, with very weak expression of GFP in bipolar cells. (B) A combined picture, showing that *Rag1*-driven GFP (green) and *Rag2*-driven GFP (red, pseudocolor) are expressed in different layers in zebrafish retina. (C) Dorsal view of the tectum, with weak label in few cells (arrows); most cells have background levels of fluorescence. (D) Dorsal view of deep¬ regions of the brain. GFP-positive cells are visible in the forebrain (arrow) and caudal hypothalamus (arrowhead). (E) Lateral view of the spinal cord of a 3-day old fish. Strong GFP expression is visible in the ventral motoneurons (arrowheads), and in axons innervating myotomes (arrows). Low level of fluorescence is visible in the entire neural tube and longitudinal fascicles. gcl: ganglion cell layer; ipl: inner plexiform layer; a: amacrine cell layer; b: bipolar cell layer; opl: outer plexiform layer; ot: optic tectum; cb: cerebellum; fb: forebrain; ov: otic vesicle; op: olfactory pit; ob: olfactory bulb; Hc: caudal hypothalamus; *: auto fluorescence of the skin. Bar = 50 μm (A, B); 100 μm (C-E).

3.5.3 RAG2 antibody failed to detect signals in the olfactory epithelium

An antibody was also generated against the C-terminal 15 amino acids of zebrafish RAG2. Its binding to isolated thymocytes (known to express high level of *Rag2*) can be abolished by pre-absorption with the antigen peptide, indicating that this antibody labels the thymocytes specifically (Fig. 3-20). But, using this antibody on the dispersed olfactory epithelium, we failed to detect any specific signal, but only dim and broad staining. RAG2 protein in OSNs may thus be present at very low level (i.e. below our detection limit), or the mRNA may not be translated.

3.5.4 Summary

Shuo Lin's group has showed the presence of *Rag1* and *Rag2* in zebrafish OSNs and speculate that they are concurrently expressed (Jessen et al., 2001b; Jessen et al., 1999). In our study, analysis of *Rag2* expression was based on a similar promoter. But our detailed observation of three transgenic lines revealed that the expression of *Rag2* in zebrafish OE is distinct from *Rag1* expression. Two *Rag* genes are restricted to different subsets of OSNs. In a broader view, *Rag2* is detected in many parts of the nervous system. In the caudal hypothalamus and optic tectum, *Rag2* maybe co-localized with *Rag1* in some neurons, which, however, can not be confirmed. We lack the information on endogenous RAG2 protein distribution. This might be solved with another high-quality antibody. But it could not be done here due to time constraint.

Nevertheless, our observation indicates that, as a general rule, *Rag2* is not co-localized with *Rag1* in the nervous system. This suggests that *Rag1* is unlikely to mediate a V(D)J-like DNA recombination in the nervous system, nor to function in general neurogenesis, but might be involved in the function of some groups of neurons.

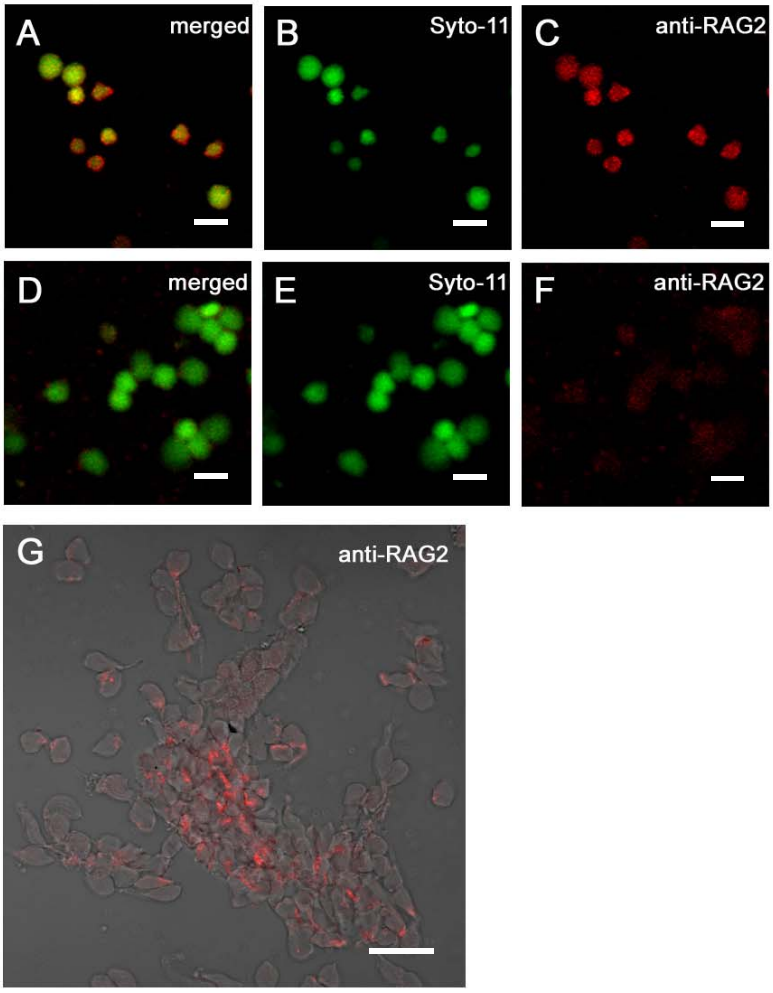

Figure 3-20. Immunofluorescence with the antibody against RAG2.

(A-C) Isolated zebrafish thymocytes, labeled with the antibody against RAG2 (in red) and Syto-11 (green). (D-F) After pre-absorption with the peptide used for immunization, there is no labeling was detected with this antibody. Syto-11 (green) was used to stain nuclei. (G) Immunofluorescence with this antibody on the olfactory epithelial cells from wt fish. No specific signals were detected. Bar = 10 μm (A-F); 20 μm (G).

3.6 No obvious neuronal defect was detected when RAG1 was depleted

3.6.1 Depletion of RAG1 doesn't affect the axon targeting of the GFP positive OSNs

Within one OE, OSNs with the same identity, which is specified by the odorant receptor together with other proteins, always converge their axons to the same glomerulus in the OB (Wang et al., 1998). The high-level of *Rag1* in a subpopulation of OSNs that project to one glomerulus raises the possibility that RAG1 is itself somehow involved in specifying the identity and hence the targeting of these neurons. To investigate this issue, we examined the effect of RAG1 depletion on the projection of these OSN.

3.6.1.1 Effect of knocking-down RAG1 by morpholinos

Morpholinos are chemically modified oligonucleotides. They are assembled from four different subunits, each of which contains one of the four genetic base (Adenine, Cytosine, Guanine and Thymine) linked to a 6-membered morpholinine ring instead of 5-membered ribose or deoxyribose in natural RNA and DNA. They thus keep the base-stacking abilities of natural genetic material. Morpholinos have been shown to bind to and block translation of mRNA in vitro, in tissue culture cells, and in vivo among several organisms (Heasman, 2002). From 2000, it became an important reverse genetic tool in zebrafish (Nasevicius and Ekker, 2000). In our study we used this approach to examine *Rag1*'s function in nervous system, mainly focusing on the olfactory system.

Three morpholinos were used to knockdown RAG1. The first morpholino (mo1) was targeted to the start codon of *Rag1*. However, the use of internal ATGs, which has been

reported for some forms of Omenn's syndrome in human (Santagata et al., 2000), might obscure the effects of the mo1. Thus we designed and tested two more morpholinos, mo2

and mo3, which target to splice donor sites of the first and second exons of *Rag1* coding sequence respectively (Fig. 3-22A).

Rag1-mo1, the morpholino against *Rag1* start codon, was tested using a fusion of the *Rag1* 5'-end to GFP. Injection of mRNA for the fusion alone led to a strong green fluorescence (Fig. 3-21A1), whereas co-injection with the Rag1-mo1 suppressed the fluorescence (Fig. 3-21A3). A standard control morpholino was also tested and had no effect (Fig. 3-21A2). These results demonstrate that Rag1-mo1 can target the *Rag1* 5' part and block the translation of the fusion protein.

Unexpectedly, injection of mo1 into *Rag1:GFP* fish caused a reduction in the level of GFP, despite there being a 8 nucleotide contiguous mismatch between mo1 and the transgene (Fig. 3-21C). The decrease of GFP in OE was evident for the first three days after injection (Fig. 3-21B), and recovered from the 4^{th} day. To check whether the reduction of GFP is a direct consequence of mo1 injection, we cloned the transgene fragment from *Rag1:GFP* line (including the putative mo1 binding site) and generated mRNA by intro transcription. After injection into embryos, the mRNA was translated into GFP (Fig. 3-21D1); while in the embryos co-injected with mo1, the GFP signal was reduced in a dosage-dependent manner. This confirmed that the injection of mo1 directly reduced GFP level in the *Rag1:GFP* fish, presumably because the mismatch is contiguous and exclusively at one end of the morpholino. Despite the reduction in fluorescence, convergence of labeled axons to the lateral glomerulus persisted (Fig. 3-21B2; 15 embryos imaged at high magnification). Aside from the decrease in GFP expression, no other defect could be detected.

The second morpholino (mo2) was designed to target the splice donor site of the first exon (Fig. 3-22A). Injection of this morpholino led to failure in splicing out the first

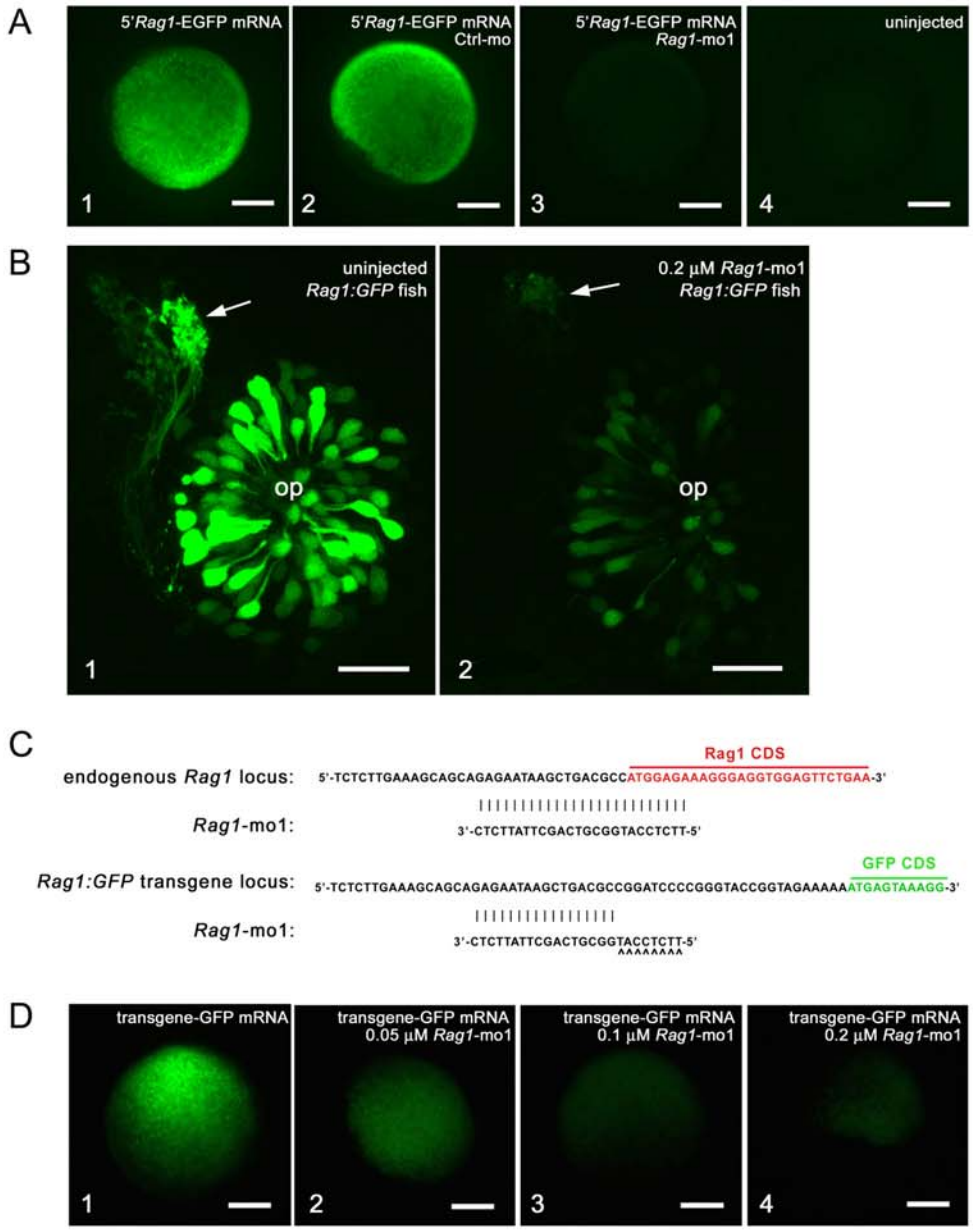

Figure 3-21. The effect of RAG1 depletion on the olfactory projection, revealed by the morpholino against *Rag1* ATG region.

Figure 3-21. The effect of RAG1 depletion on the olfactory projection, revealed by the morpholino against *Rag1* ATG region.

(A) A morpholino against the *Rag1* ATG region (Rag1-mo1) blocked the translation of mRNA encoding the 5' end of *Rag1* fused to EGFP. (A1) An embryo injected with the mRNA expresses the fusion protein and shines the green fluorescence. (A2) Co-injection with the control morpholino didn't affect the translation of the fusion protein. (A3) When co-injected with Rag1-mo1, the mRNA couldn't be translated into the fluorescent fusion protein. (A4) An uninjected embryo was imaged as a control. (B) Rag1-mo1 reduced the GFP expression in the *Rag1:GFP* fish. (B1) Olfactory neurons labeled with GFP under the *Rag1* promoter, with brightly labeled axons projecting to a single target (arrowhead), at 3 dpf. (B2) In a transgenic embryo injected with mo1, axons still project to the same target (arrowhead), but the intensity of GFP fluorescence is reduced. (C) Rag1-mo1 was designed against the *Rag1* ATG region. It partially matches to the 5' region of the transgene GFP in the *Rag1:GFP* fish. (D) Rag1-mo1 reduces the translation of the transgene GFP mRNA, which contains the indicated 5' region. (D1) An embryo injected with the mRNA encoding the transgene GFP. (D2-4) Embryos co-injected with the trasngene GFP mRNA and Rag1-mo1. The GFP translation was reduced by the Rag1-mo1 in a dosage-dependent manner.

intron, which was revealed by RT-PCR (Fig. 3-22B) and confirmed by sequencing (data not shown). The consequent aberrant mRNA contains a stop codon within the un-spliced intron. Monitored by RT-PCT, the effect of Rag1-mo2 was maintained until 2 dpf, and dropped down from 3 dpf. Injections of 0.8 μM caused slight non-specific morphological abnormalities, such as small eyes, but no defect in the projection of GFP positive axons was detected at 3 dpf (data not shown). Since the mo2 effect only last to 2 dpf, we can not rule out the possibility that the projection of GFP-positive axons formed after the RAG1 depletion was recovered.

Injection of the third morpholino (mo3), which was designed to the donor site of the second exon, resulted in loss of the normal transcript and stronger abnormalities (not shown). Less abnormality was seen when a mixture of mo2 and mo3 was injected. Using RT-PCR, the morpholino effect on mRNA splicing was examined for different dosage and ratios. It was found that injection of a mixture with high concentration of mo2 and mo3 led to a dramatic loss of normally spliced *Rag1* mRNA till 3 dpf (Fig. 3-23B, highlighted with red brackets). However, the weak amplification of the un-spliced mRNA (Fig. 3-23B, in blue brackets) indicates that the Rag1-mo3 not only blocked the splicing of the second intron, but also introduced abnormal splicing events. That resulted in some short aberrant amplification, which was confirmed by the amplification using primers that amplify across both introns (Fig. 3-23B, highlighted with green brackets). Among the injected fish, those injected with 0.6 μM mo2 and 0.6 μM mo3 showed least abnormality, and they showed no defect in axon projection of the *Rag1* expressing OSNs (n=50).

3.6.1.2 Analysis of zebrafish *Rag1* mutant

As an additional step in analyzing the role of *Rag1* in establishing the olfactory projection, a *Rag1* mutant line was examined. This line of fish carries a C→T mutation,

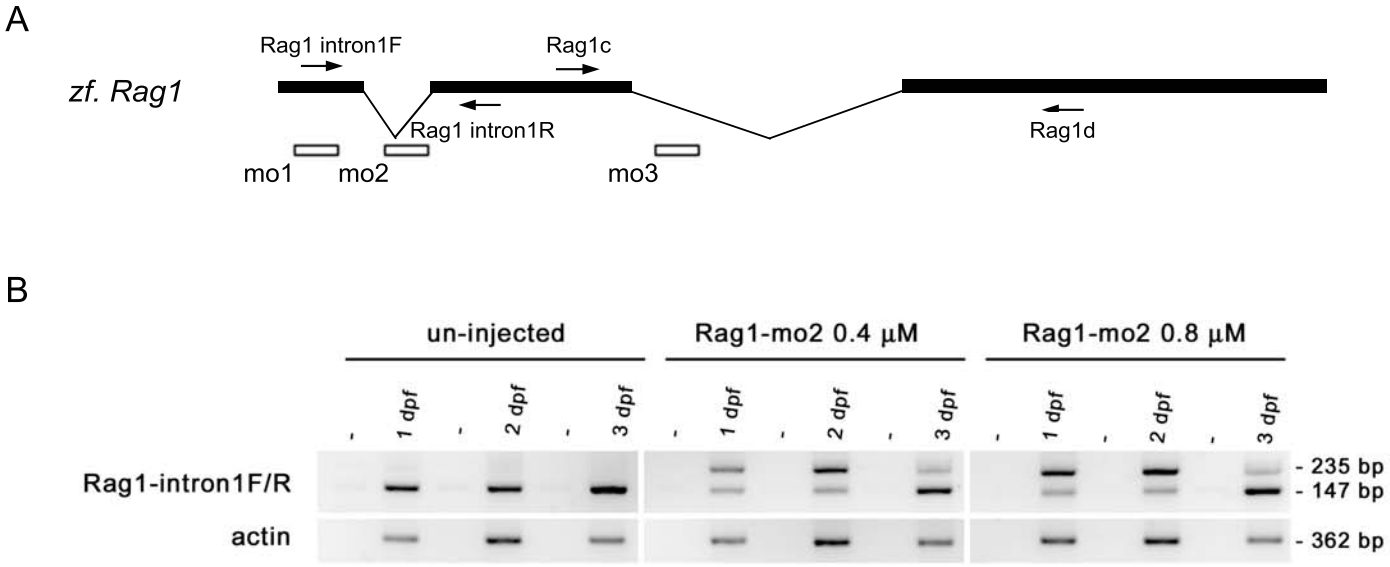

Figure 3-22. The splicing of *Rag1* mRNA was blocked by the morpholino Rag1-mo2, which is against the first intron donor site.

(A) A schematic diagram of the *Rag1* gene, showing the location of morpholinos and primers that were used to analyze morpholino-injected fish. (B) RT-PCR on control or Rag1-mo2 injected embryos. Abnormal splicing occured in the morpholino-injected fish, leading to a premature stop codon, as indicated by sequencing of the upper band. By the time-lapse, the effect of morpholino was maintained for the first two days, and then dropped down on the 3rd day after injection. -: control for the right neighbor lane, without reverse transcriptase in the first strand cDNA synthesis reaction.

A

primers	length of amplicon (bp)	
	from normal spliced *Rag1* mRNA	from un-spliced *Rag1* mRNA
Rag1 intron1F/R	147	235
Rag1 c/d	920	1769
Rag1 intron1F/ Rag 1d	1965	2902

B

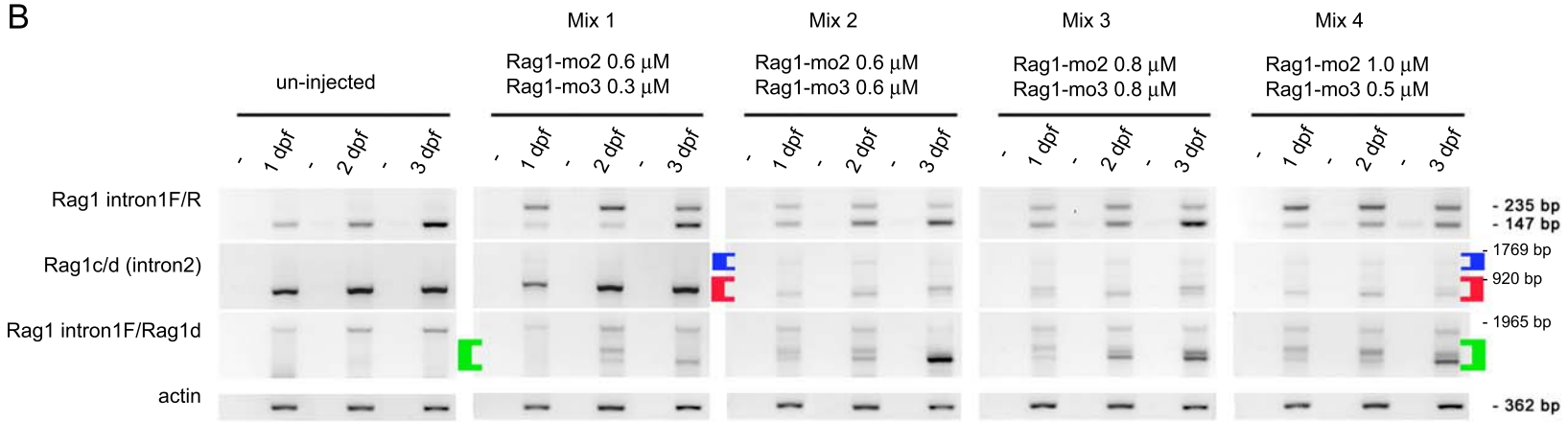

Figure 3-23. Co-injection of Rag1-mo2 and mo3 caused the loss of normal *Rag1* transcripts.

(A) The expected amplicon length with different primer pairs. Rag1 intron1F/R, Rag1c/d were used to amplify a fragment cross the first and second intron respectively; while Rag1 intron1F and Rag1d were used to amplify a longer fragment cross both the first and the second introns. (B) Different dosage of Rag1-mo2 and mo3 were injected, and the effect of morpholino on the mRNA splicing was examined by RT-PCR with three pairs of primers, at different stages. After injection of a mixture of Rag1-mo2 and mo3, the normal *Rag1* transcripts was largely lost (shown in red brackets); both unspliced (shown in blue brackets) and abnormal spliced mRNA (shown in green brackets) were detected. -: -RT control for the next right lane.

which turns R797 into a stop codon in the catalytic domain of RAG1 core region and abolishes RAG1 function (Wienholds et al., 2002). The *Rag1* mutant fish are immunodeficient, but viable and fertile.

We examined the entire olfactory projection. Firstly, the live, transparent larvae were exposed to freshly diluted lipophilic tracer Di8ANEPPQ. In these fish, only the neurons exposed to the water took up the dye, which then diffused and labeled the axon projections. The labeling pattern in the OB was examined directly under confocal microscope. The staining in *Rag1* mutants and wt siblings were carefully compared, but no obvious difference could be seen (Fig. 3-24A). Secondly, the larval forebrains, including olfactory bulbs, were isolated and labeled with SV2 antibody. This is a marker for synaptic vesicles and labels the glomeruli. Consistently, the SV2 staining didn't reveal any obvious difference between *Rag1* mutants and wt siblings. The lateral neuropil structure that is innervated by neurons expressing high level of GFP still could be visualized in the mutants (Fig. 3-24C-E). These data indicates that *Rag1* is not required for path finding of OSN axons.

3.6.2 No other neuronal defect was detected in *Rag1* mutant fish

The odor-evoked activity of the OSNs was examined by Calcium imaging (Friedrich and Korsching, 1997) in the *Rag1* mutant fish and wt siblings. The results showed that the amino acid evoked activity, which predominantly locates in the ventral lateral region of the OB, where also the *Rag1:GFP* positive axons target to, was present in the *Rag1* mutants (done by Bulchand S, Yaksi E and Friedrich R. W; refer to the attached paper) (Feng et al., 2005).

Furthermore, this *Rag1* mutant fish was also crossed to *Shh:GFP* and *islet:GFP* transgenic fish. *Shh* (sonic hedgehog) is a signaling molecule that plays important

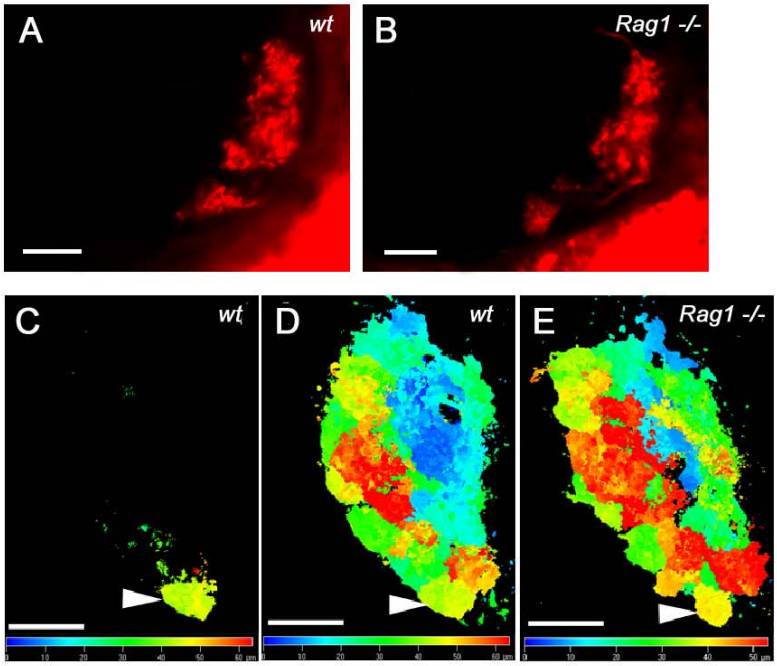

Figure 3-24. No defect in olfactory projection was detected in *Rag1* mutant fish.

(A, B) A subset of Di8ANEPPQ-labeled olfactory sensory neurons in 7-day old wild type and *Rag1* mutant fish. Axons innervate all target structures detectable in this optical plane in the mutant. (C-E) SV2-labelled 4 day-old *Rag1:GFP* transgenic (C, D) and *Rag1* mutant (E) forebrains, shown in dorsal view. The images are colour-coded according to depth. The glomerulus innervated by the strong GFP-positive neurons (E) is indicated by the arrowhead. Bar = 20 μm. The colour bars in C-E indicate depth. Embryos in this figure are shown in dorsal view, with anterior to the left.

functions in many developmental processes including the differentiation of many types of neurons. Thus *Shh*-driven GFP labels many neurons in the transgenic fish (Shkumatava et al., 2004). *Islet* is a transcription factor that is mainly expressed in motoneurons, and thus its promoter drives GFP expression in many motoneurons (Higashijima et al., 2000). We obtained the transgenic *Rag1* mutant fish for both lines, but no obvious alteration was detected in the morphology and pattern of GFP expression (data not shown). This indicates that global neuronal development and patterning in the *Rag1* mutant fish is normal.

We also tried to cross the *Rag1* mutants with the *Rag1:GFP* fish, but failed to get the transgenic mutant fish. The reason is not clear.

During maintenance of the *Rag1* homozygote mutant fish, no obvious defect was detected in response to tapping or sudden movement of objects in the visual field. They also appeared to swim normally.

3.7 Conclusions

Using transgenesis we found that *Rag1* is selectively expressed in the zebrafish nervous system. The most intriguing expression appeared in the olfactory system, where the *Rag1:GFP* signal was restricted to a subset of microvillous OSNs and their axons, which projected only to the ventral lateral OB. This region of the bulb has been shown to be innervated by neurons expressing TRPC2, a member of microvillous neurons (Sato et al., 2005). In addition, the *Rag1:GFP* was also detected in RGCs and amacrine cells in retina, cristae hair cells in ear, some dorsal interneurons in spinal cord, and some neurons in the optic tectum, hypothalamus and cerebellum.

In transgenic fish, reporters driven by a *Rag2* promoter fragment were also found to be expressed in the nervous system, but did not appear to correlate with the expression of

Rag1:GFP. Both *Rag2:GFP* and *Rag2:DsRed* showed clear labeling in the OE, but the signal appeared restricted to a group of ciliated OSNs, which sent their axons to a few ventral glomeruli. Observation in other parts of the nervous system also did not support the correlation between two *Rag* genes.

Immunofluorescence confirmed the selective presence of RAG1 in retinal and olfactory neurons, predominantly in the nucleus, but failed to detect RAG2.

Furthermore, the depletion of RAG1, either by morpholino or by mutagenesis, did not alter the olfactory projection and amino acids detection. There was also no other obvious morphological and behavioral defects noticed when RAG1 was depleted.

Thus we conclude that *Rag1* is expressed in a selective manner in the zebrafish nervous system; its expression is not correlated with *Rag2*; and the expression of *Rag1* is not required for path finding as well as amino acids detection of OSNs. This strongly suggests that *Rag1* is unlikely to mediate a V(D)J-like DNA recombination in the nervous system. Any function of *Rag1* is likely to be specific to subsets of neurons.

CHAPTER 4 RESULTS_PART 2 Searching for *Rag1* Downstream Genes in the Nervous System by Microarray

4.1 Two sets of microarray experiments were done to search for Rag1-downstream genes in the nervous system

As indicated by the previous observations in *Rag1:GFP* fish, *Rag1* appears to be expressed in a subset of neurons in many parts of the nervous system. To seek evidence for a function, we carried out microarray experiments.

Microarray hybridization is a technology developed in the past several years and has now become a standard tool in genomics research. It normally involves a large number of DNA probes, which are immobilized to a solid surface in a very high density, and a set of labeled DNA or cNDA samples, usually in a mixture, to hybridize to the probes. Thus massive complementary bindings between the immobilized probes and samples are parallely determined, providing a platform for scientists to study tens of thousands of genes at once. This technology has been successfully used in monitoring expression of many thousands of genes simultaneously, polymorphism screening and genotyping on a genomic scale(Ramsay, 1998; Schena et al., 1998).

We used this approach to screen for genes with expression changes in *Rag1* mutant fish. The *Rag1* mutant fish carry a point mutation in the catalytic domain of the RAG1 core region, which thus generates a premature stop cordon and abolishes RAG1's function. This fish has been shown to be unable to rearrange T-cell receptor genes (Wienholds et al., 2002). By global comparison of gene expression between *Rag1* mutants and wt siblings, we set out to find genes with altered expression in the nervous system of *Rag1* mutant fish.

The microarray that we used is an oligonucleotide microarray, which is built from the Compugen/Sigma-Genosys oligo sets (http://www.labonweb.com/). Comparing to cDNA, for

which each clone has its own hybridization character, oligos are easier to be designed to have similar hybridization temperature and binding affinity, and therefore produce a meaningful result.

Totally two sets of microarray hybridization were done. One was carried out with RNA samples from anterior parts of 3 dpf larva; and the other was done with RNA from adult olfactory rosettes. Using larva at 3 dpf should allow us to access the main tissues in the nervous system, which is roughly established at 3 dpf; and at the same time avoid the interference of defects in the immune system, which starts to develop at 4 dpf. We also chose the adult olfactory rosette, because it is a peripheral sensory organ, which hardly contains immune tissues and expresses a significant level of *Rag1* in the adult.

For both larva and adult OE experiments, 3 pairs of total RNA samples were isolated independently and sent for hybridization. All of these RNA samples showed two clear bands of rRNA on electrophoresis gel (Fig. 4-1), indicating that their quality is acceptable.

4.2 Data normalization and statistical analysis

4.2.1 Data preprocess and normalization

Our microarray experiments were done in the Microarray Core Facility of the Kimmel Cancer Center (KCC) in Thomas Jefferson University. We obtained the raw data and carried out processing and analysis mainly with GeneSpring, a microarray analysis software purchased from Agilent Technologies.

Firstly, the signal intensity was subtracted to background to give a spot intensity for calculating the expression. Then from the subtracted spot intensity, we performed data normalization. This is to adjust the hybridization intensity obtained from individual chips so as to exclude systematic errors that might be introduced by imprecise probe input, inconsistent wash or some imperfection in microarray chip production. In the literature,

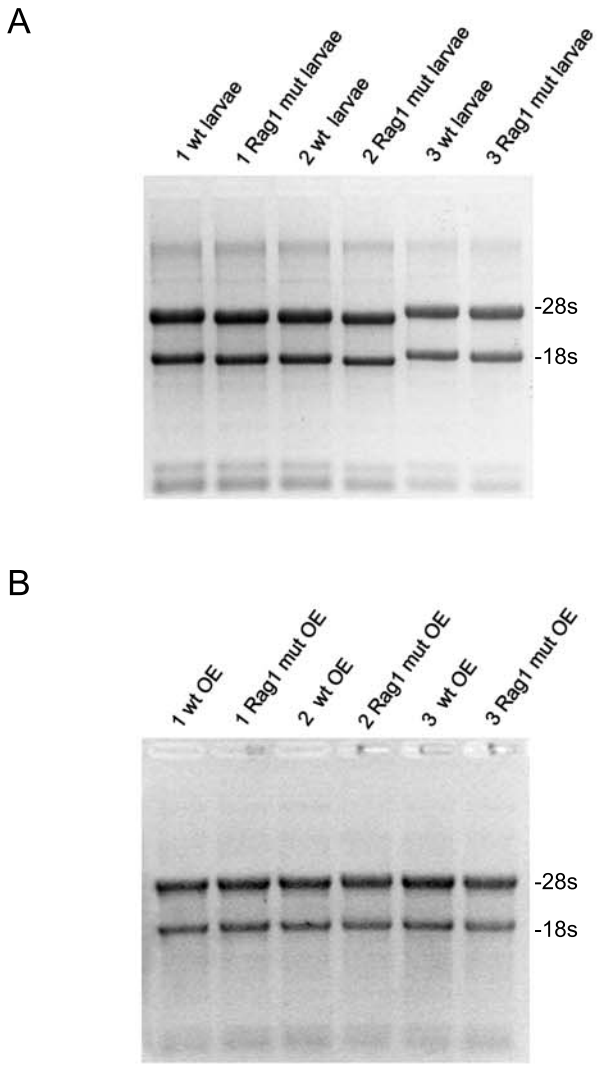

Figure 4-1. Electrophoresis of RNA samples used in microarray experiments.

(A) 3 pairs of total RNA samples were isolated from 3 dpf larval heads. (B) Total RNAs isolated from adult olfactory rosettes. The two apparent bands consist of 18S and 28S tRNA, which are typically abundant in fish total RNA samples.

several methods have been utilized for this purpose and their advantages and flaws have been discussed. Basically, normalization can be done according to the global intensity on an array, or according to a set of invariant genes, such as housekeeping genes or internal controls (Leung and Cavalieri, 2003). For two-color hybridization, two sets of probes are labeled with two different fluorescence dyes respectively, which usually introduce the difference in dye incorporation efficiency. To reduce the dye-related bias problem, a method called locally weighted scatterplot smoothing (LOWESS) normalization was developed and is widely accepted (Leung and Cavalieri, 2003; Quackenbush, 2002). Our microarray was hybridized with single-colored cDNA. Dye-related bias is not a problem. Therefore, we chose the default Per-chip and Per-gene normalization provided by GeneSpring to control the variance between different samples (for details, refer to Chapter 2.15)

Next, to avoid the interference of the basal level of noise, signals with intensity lower than 2 folds of the blanks in every sample were removed from the data for further analysis, which are 5496 and 3562 measurements for larvae and adult OE microarray respectively (Table 2). At this stage, the remained normalized data of every chip distributed around "1" (the normalized median intensity) symmetrically, indicating that the data obtained from different hybridizations are globally comparable (Fig. 4-2).

For each experiment, 6 individual hybridizations were grouped into 3 pairs (Table 1). Their overall distribution of ratio-intensity was examined in RI (ratio-intensity) scatter plot. In our experiments, no obvious intensity-dependent bias was seen, but some variance existed among the 3 pairs of data (Fig. 4-3).

To further examine the reproducibility of these data, we compared the logarithm ratios between two different pairs of samples in a plot. With reasonable imperfection, genes that distribute close to the line x = y are acceptable, while the data scattering far from the x = y line will be considered as non-reproducible. Generally they will not pass through the following statistical analysis. We did the comparison for pair 1 *vis* pair 2 and pair 1 *vis* pair 3

Table 1. Microarray experiments design.

Experiments	Pairs	Conditions	
		Wt siblings	***Rag1* mutants**
Microarray with RNA from 3 dpf larval heads	Pair 1	1 wt	1 Rag1
	Pair 2	2 wt	2 Rag1
	Pair 3	3 wt	3 Rag1
Microarray with RNA from adult olfactory epithelium	Pair 1	1 wt	1 Rag1
	Pair 2	2 wt	2 Rag1
	Pair 3	3 wt	3 Rag1

Table 2. Summary of microarray data analysis.

Experiments		Total spots	Positive controls	Blanks	Total measurements	Low intensity signals	After density filter	< 2 fold change	> 2 fold change	Anova p>0.05	Anova p<0.05
Microarray with RNA from 3dpf larval heads	Filtered out	-	172	2792	-	5496	-	10703	-	22	-
	Balanced	19200	-	-	16236	-	10740	-	37	-	15
Microarray with RNA from adult olfactory epithelium	Filtered out	-	172	2792	-	3562	-	12124	-	209	-
	Balanced	19200	-	-	16236	-	12674	-	550	-	341

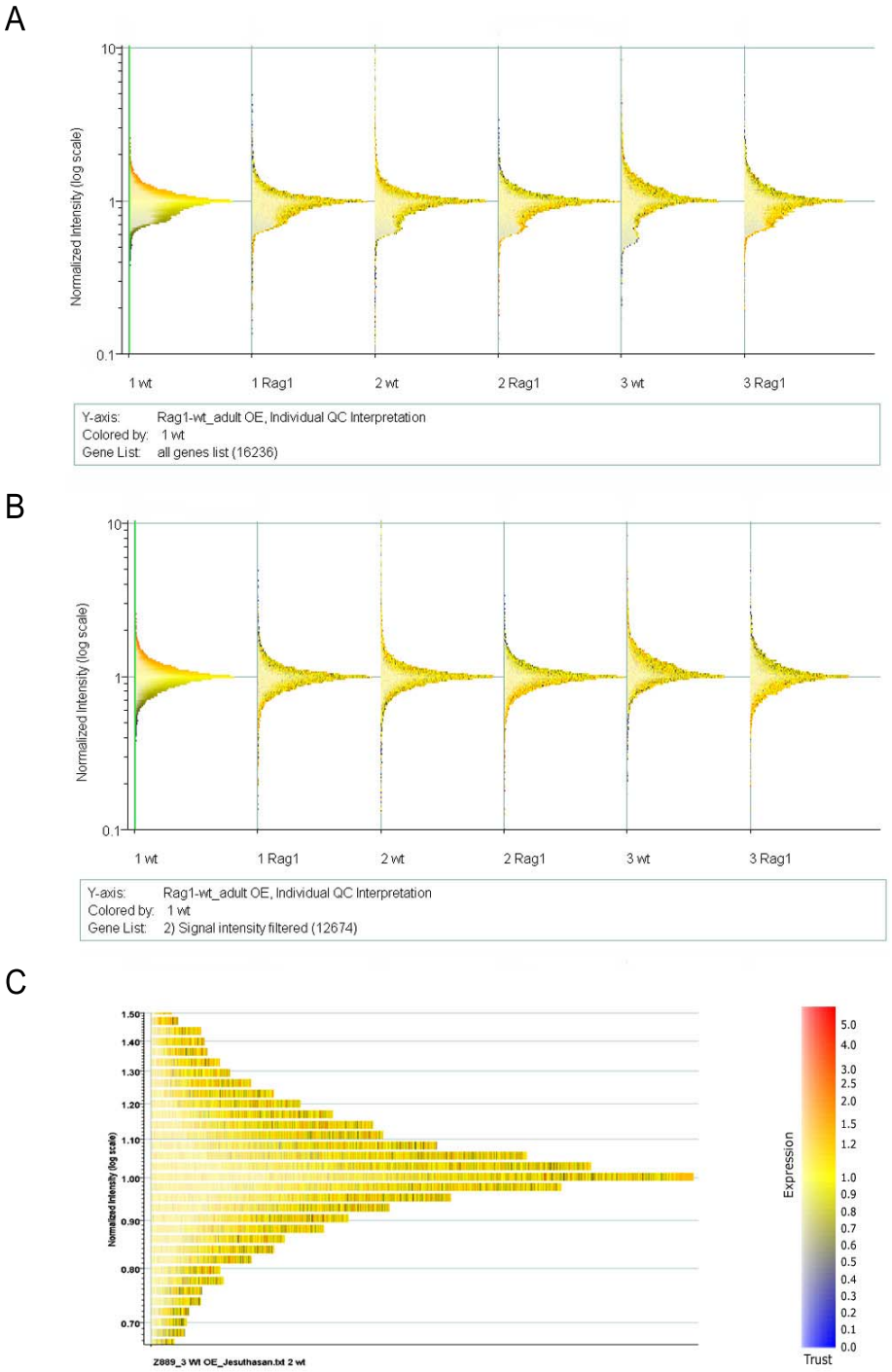

Figure 4-2. Data filtering by signal intensity.

(A) The overview of all 6 hybridizations in the adult OE microarray experiment was build according to the distribution of measurements among different intensity (log scaled). In this panel, all measurements (16236) in a hybridization were exhibited. (B) After low intensity signals were filtered out, the overall distribution of data in every hybridization became symmetrically around the median. (C) A zoom-in picture showing the distribution of measurements intensity in the 2nd wt hybridization.

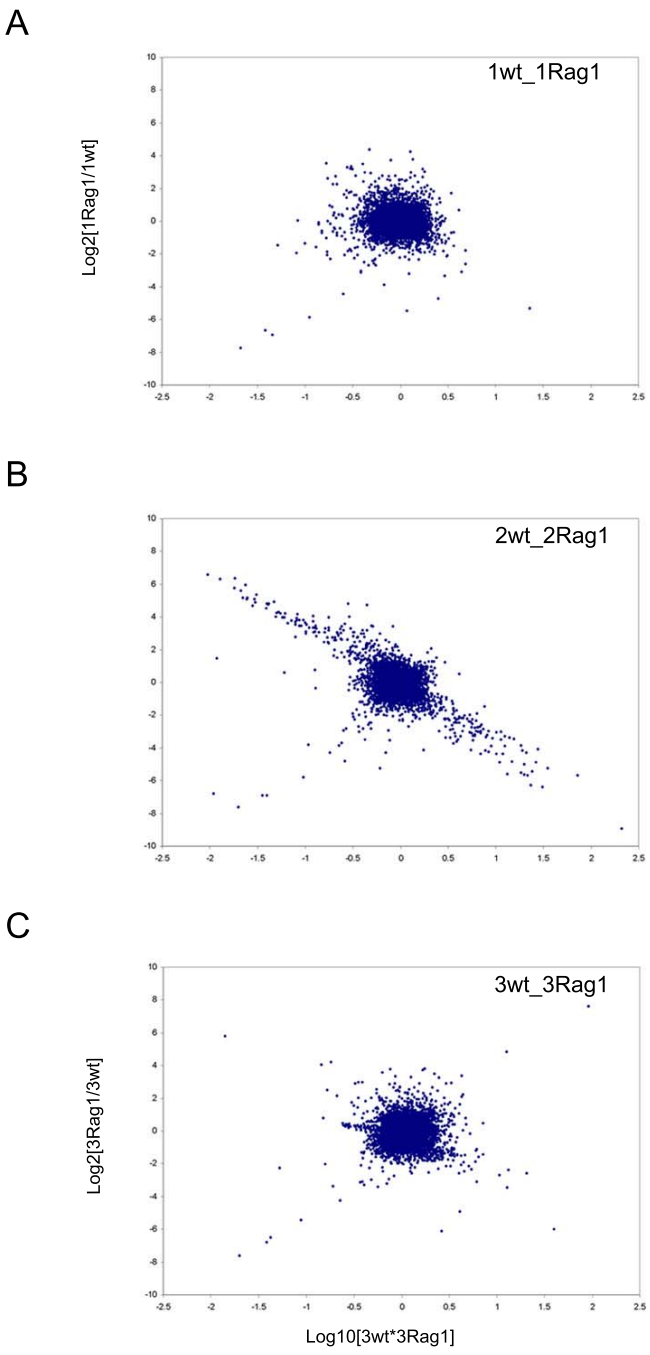

Figure 4-3. RI scatter plot of three pairs of hybridizations in the adult OE microarray.

6 individual hybridizations were considered as three pairs, e. g. 1wt & 1Rag1 (A), 2wt & 2Rag1 (B), and 3wt & 3Rag1 (C). Within each pair, the Log2(Rag1/wt) for each element was displayed as a function of the Log10(wt*Rag1), and the distribution of every valid element (low intensity signal were filtered out) was built together as the ratio-intensity (RI) plot.

(Fig. 4-4). It was shown that most data are reproducible between these three pairs of data, and only a small group of signals varied too much in pair 2. We tried and found that removing these data for significance analysis did not change the following result.

4.2.2 Statistical significance analysis

For microarray experiments, the large volume of data and complicated intrinsic variation make it necessary to recruit a statistical method to extract biological information systematically. Our experiments were carried out to detect the difference in expression between two conditions. Theoretically the differentially expressed genes can be referred to by a fixed threshold cut-off method, but it is inefficient. The main reason is the numerous variations occurred during a microarray experiment. Although some systemic variations can be removed by proper normalization, but random sample to sample variations are mostly beyond notice and control. Thus it is essential to have replicates in a microarray experiment. The variation in a gene expression, which is obtained from the replication, enables statistic analysis for computing a possibility of differential expression. This has been proven more powerful and reliable than the simple fold changes in determining the significants. The combination of both also has been used, in which the cut-off according to fold changes narrows down the data set and strengthens the following statistic analysis. Here we did our analysis in this way to enhance the identification of the most relevant genes, e.g. only data showing more than two fold changes in expression between wt and *Rag1* mutants were picked for significance statistic analysis.

Many statistic method have been developed for microarray significance analysis (Cui and Churchill, 2003). We used the ANOVA model provided by GeneSpring and the SAM program proposed by Tusher et al. in Stanford University.

A

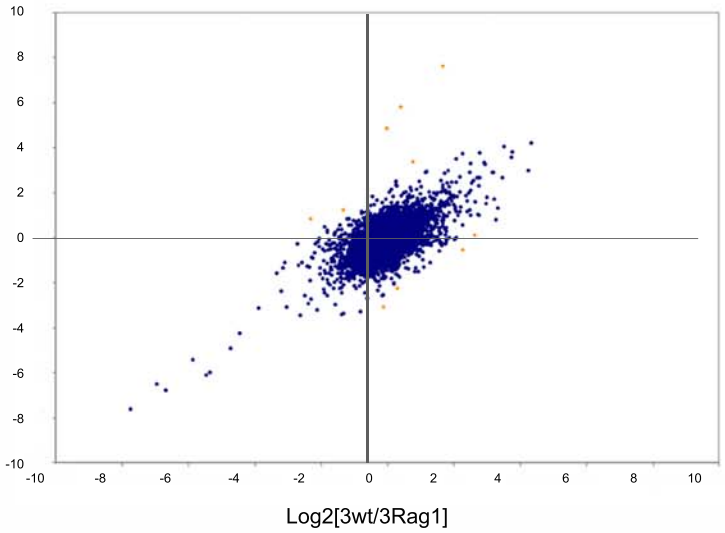

B

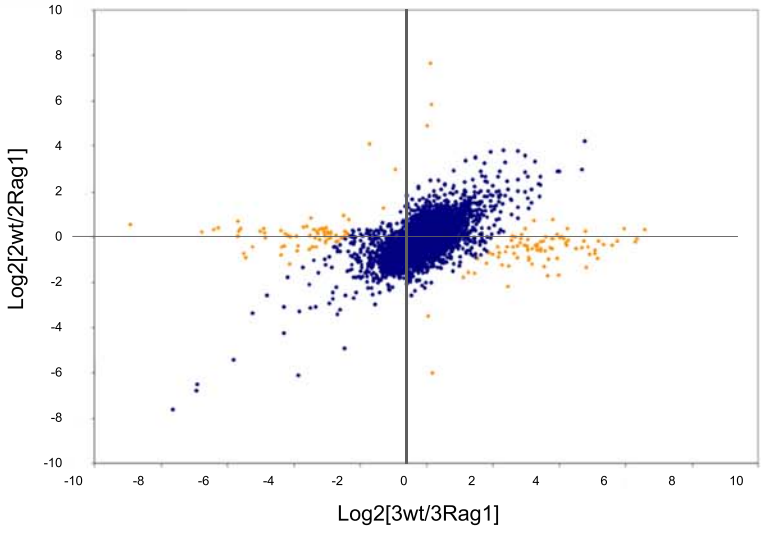

Figure 4-4. The duplicibility examination for the adult OE microarray.

Log2(ratio) of each pair of samples were further paired for comparison. Here we compared Pair 1 vis Pair3 (A), and Pair 1 vis Pair 2 (B). The reproducible data were consistent in every pair of sample and colored as dark blue, whereas the non-reproducible data were variable and were colored as yellow in this figure.

ANOVA (analysis of variance) is an approach that can be applied to cDNA microarray data from any experimental design. In complicated microarray experiment with multiple categorical factors, such as sex, age and genotype arranged as eight conditions in a 2 by 2 by 2 factorial design, ANOVA is a powerful model to address difference among conditions. In this model, the relative expression of a gene is calculated according to the overall measurements in a chip and the weighted average expression of that gene over all samples in the experiment (Cui and Churchill, 2003; Kerr and Churchill, 2001). It is also suitable to the analysis of single-colored microarray.

Using one-way ANOVA provided by GeneSpring, we tested data obtained from both larvae microarray and adult OE microarray. For the larvae experiment, 15 clones pass the test ($p<0.05$); for the adult OE experiment, 341 was selected ($p<0.05$) as significant differently expressed (Table 2; Fig. 4-5).

To verify these results, another well-accepted statistic analysis method SAM (significance analysis of microarray) was used. The SAM program utilizes a FDR (false discovery rate) concept to control the possibility of a non-differentially expressed gene to be chosen as a significant. Based on the FDR, users can choose the cut-off of significance by tuning a parameter Δ (delta), so to balance the result between having false positives and losing true significants. We obtained the SAM (2.0 version) program from the web (http://www-stat.stanford.edu/~tibs/SAM/index.html) and used it in analysis of the above normalized and intensity-filtered adult OE microarray data (total 12674 measurements). The Δ was set as 0.89 to produce 341 significants with more than 2 fold change in expression (the number produced in ANOVA analyses). Within these genes, the FDR computated by

SAM is 1.22% (Fig. 4-6A). Comparing the 341 significants produced in SAM and ANOVA, we found that they are 93.3% overlapped (Fig. 4-6B). This indicates that both of the results are largely reliable.

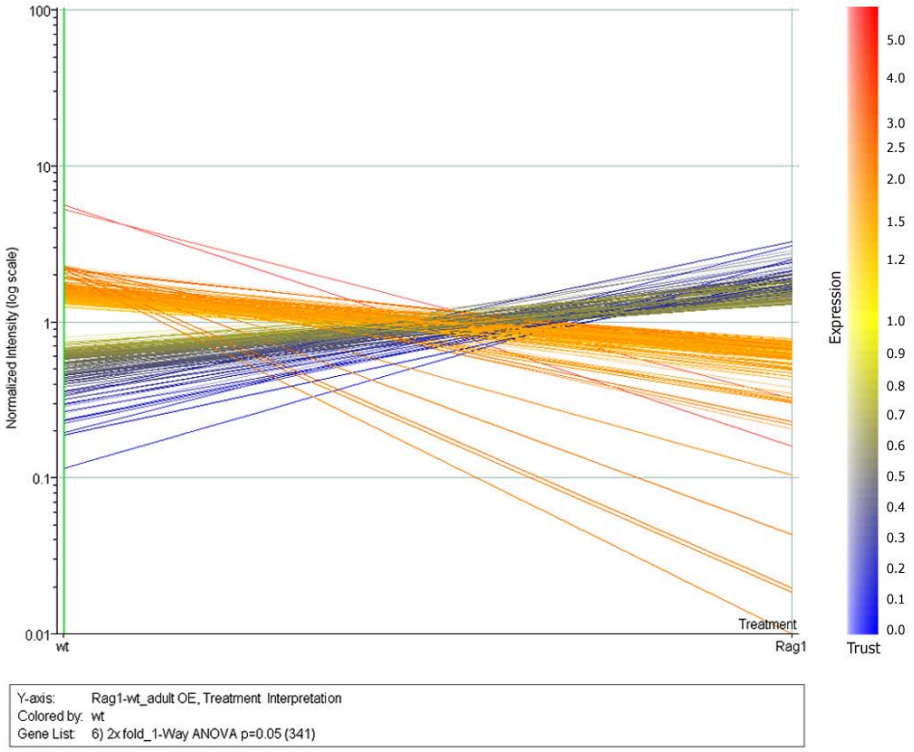

Figure 4-5. The expression changes of the 341 singnificants in wt and *Rag1* mutants.

341 genes were identified to be significantly changed in expression by ANOVA analysis. Their expression (intensity) changes are shown in the picture. The measurements for one gene were respectively averaged among wt and *Rag1* mutant replicates, and connected by a line. These lines were colored according to the wt results. Thus, the orange and red lines stand for genes expressed at high level in wt siblings, but down-regulated in the *Rag1* mutants, while the green and blue lines stand for genes that changed oppositely.

A

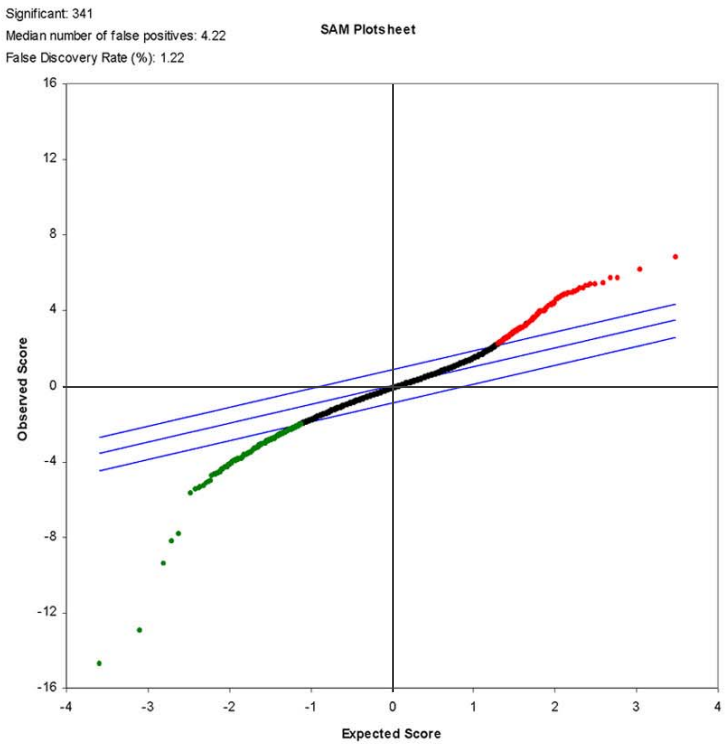

B

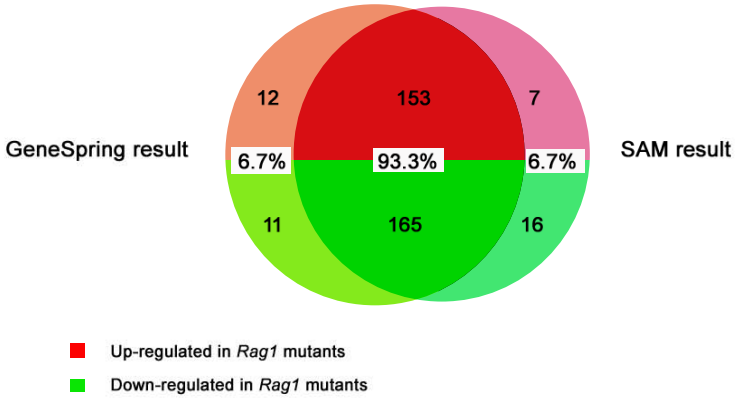

Figure 4-6. SAM analysis result for the adult OE microarray.

(A) The same data from the adult OE experiment was also used for SAM analysis. When Δ was set as 0.89 to produce 341 significants with more than two fold change in expression, the false discovery rate (FDR) was 1.22%. (B) The 341 significants produced in ANOVA and SAM analysis were compared. 93.3% of these two sets of genes are same.

4.3 Interpretation of the adult OE microarray result

The significant differently expressed 341 genes produced in the ANOVA analysis from adult OE microarray were annotated with the information obtained from NCBI (National Center for Biotechnology Information), TIGR (The Institute for Genomic Research) and Silicon Genetics. These 341 genes contain 28 well-known genes and 311 ESTs that mostly haven't been characterized.

The EST clones were found to be obtained from different libraries, some of which are tissue-specific. From a summary that classified these ESTs according to their sources and up- or down-regulation in the *Rag1* mutant fish, we noticed that genes from fin, embryo, testis, ovary and heart libraries were equivalently up- or down-regulated; whereas genes from kidney and regenerating fins were largely up-regulated, and genes from some neuronal tissue, including brain, retina and olfactory epithelium, were mostly down-regulated (Fig. 4-7). This is consistent with our understanding. In mutant fish, the mutated RAG1 failed to mediate V(D)J recombination and support the adaptive immunity. To compensate this loss, the innate immunity, including several general host defense systems, was up-regulated when infection occurred. The kidney is an immune organ, producing a lot of immune molecules, including those functioning in the adaptive immunity as well as those mediating innate immunity. The biased up-regulation of ESTs from kidney (30 of 40) might correspond to the up-regulation of innate immunity. Zebrafish fin is a tissue that generally is not related to immunity. But during its regeneration, some stress-responding genes are activated. The large up-regulation of ESTs obtained from regenerated fins (16 of 23) might correlate to the stress response that had been triggered in the *Rag1* mutant fish.

However further interpretation of the microarray data is largely blocked by the limited annotation (only 28 well-known genes from 341) and poor characterization of the

Summary

Source	Up-regulated in *Rag1* mutants	Down-regulated in *Rag1* mutants
SK	15	16
WU	27	25
ICRF	3	0
SE	1	1
	4	5
r-fin	16	7
kidney	30	10
embryo	9	8
testis	9	4
ovary	7	5
male	6	5
heart	4	2
OE	11	17
brain	5	24
retina	1	26
neuronal	3	4
known gene	13	17
	165	176

Abbreviation & terms:

SK: Sugano Kawakami zebrafish DRA Danio rerio cDNA clone
WU: Zebrafish WashU MPIMG EST Danio rerio cDNA clone
ICRF: Zebrafish ICRFzfls Danio rerio cDNA clone
SE: Steve Ekker Danio rerio cDNA clone
fin: adult pectoral fin Danio rerio cDNA
Zebrafish Research Genetics C32 fin Danio rerio cDNA
r-fin: zebrafish fin regeneration Danio rerio cDNA
embryo: Zebrafish shield stage whole embryo cDNA
testis: Gong zebrafish testis Danio rerio cDNA clone
ovary: Gong zebrafish ovary Danio rerio cDNA clone
Campbell zebrafish ovary Danio rerio cDNA clone
male: Sugano SJD adult male Danio rerio cDNA clone
cDNA clone
Zebrafish Kidney cDNA random primed
heart: ZF adult heart library Danio rerio cDNA
Zebrafish Embryonic Heart cDNA Library
OE: Zebrafish adult olfactory Danio rerio cDNA clone
brain: zebrafish adult brain Danio rerio c
retina: Zebrafish adult retina cDNA Danio rerio cDNA clone
neuronal: Zebrafish neuronal Danio rerio cDNA clone

Figure 4-7. A summary of the 341 significants produced in ANOVA analysis from the adult OE amicroarray.

The 341 significantly changed genes were grouped according to their origins and expression changes. ESTs from kidney and regenerating fins were mostly up-regulated (highlighted with green color), while ESTs from olfactory epithelium, brain and retina were largely down-regulated (highlighted with red color).

majority of ESTs. To circumvent this problem, information obtained from homologous genes in other organisms was given to the uncharacterized ESTs to assign putative function. This helped to annotate additional 182 ESTs. While this might introduce some errors, it provides a potential overview and better understanding of the microarray results.

4.3.1 Expression alteration in the *Rag1* mutant fish was detected at different regulation levels.

With the functional information, including both known and putative, the consequence of loss of RAG1 in adult zebrafish was revealed to be broad and complicated. Expression alteration was detected among genes functional in different regulation levels, including genome maintenance, transcription regulation, translation regulation and protein processing (Table 3).

In the genome level, *Mcm3*, a gene that controls DNA replication and its correlation with cell cycle, was up-regulated; EST homologues of *Tep1*, a protein component that functions in adding a new telomere to the chromosome end, methyltransferase *Dnmt3bl* and CpG DNA methylase, which might have function in modifying the genome and affecting transcription by methylation, were down-regulated. At the transcription level, many transcription factors were found to be significantly changed in expression. These include the increase of an EST homologous to *Brf1*, a general activator of RNA polymerase III; as well as the decrease of homologues of *Nrip2*, a negative regulator of transcription from RNA polymerase II promoter, *NF-YB*, a factor that binds to CCAAT motif in promoters and stimulates transcription, and *Bteb1*, a transcription activator selectively recognizing tandem repeats of GC box in promoters. At the translation level, an EST homolog of *Bzw2*, a factor that functions in activating translation initiation, was found up-regulated. At the post-translation level, EST homologues of *P4Ha2* and *AP-B* were up-regulated. *P4Ha2*encodes a component of an enzyme that catalyses the post

Table 3. Expression changes of genes involved in different level of regulations.

Functional classes		Genebank Acc	Ratio (Rag1/wt)	wt average intensity	t-test *P* value	Rag1 average intensity	t-test *P* value	Symbol	Description
Maintainess of genome		AI958242	0.42	1.42	0.018	0.6	0.027	si:tep1	similar to Telomerase associated protein 1
		BI889166	2.32	0.58	0.108	1.36	0.12	mcm3	MCM3 minichromosome maintenance deficient 3
Transcription regulation	**Methylation**	AI884262	0.51	1.37	0.046	0.7	0.067	si:dnmt3bl	similar to DNA (cytosine-5-)-methyltransferase 3 beta
		AI641534	0.5	1.32	0.075	0.65	0.145	si:sss1m	CpG DNA methylase (cytosine-specific methyltransferase)
	Transcription factor	BI888606	0.47	1.48	0.067	0.7	0.121	si:nf-yb	similar to NF-YB, Nuclear transcription factor Y subunit beta
		BI846800	0.46	1.51	0.08	0.7	0.049	si:nrip2	similar to Nrip2; Neuronal interacting factor X 1 (NIX1)
		AW018991	2.3	0.6	0.014	1.39	0.006	si:brf1	BRF1 homolog, subunit of RNA polymerase III transcription initiation factor IIIB
		AI979399	0.38	1.56	0.092	0.59	0.103	si:bteb1	similar to BTEB1, basic transcription element binding protein 1
Translation regulation		BM156974	0.35	1.52	0.028	0.53	0.048	si:bzw2	similar to BZW2 Basic leucine zipper and W2 domains 2
Protein processing		BI980545	9.28	0.23	0.007	2.15	0.038	si:p4ha2	similar to Prolyl 4-hydroxylase alpha-2 subunit precursor (4-PH alpha-2)
		BI673608	2.16	0.64	0.016	1.37	0.015	si:ap-b	similar to Arginyl aminopeptidase (aminopeptidase B)

translational formation of 4-hydroxyproline in collagen and other proteins; *AP-B* is an enzyme that catalyses the release of N-terminal Arg and Lys from oligopepetides.

The overall consequence of these complex changes is not clear from this view. These genes might participate in different biological processes that occur in different type of cells. Next, we tried to interpret the result by grouping genes according to their biological function and expression changes.

4.3.2 Innate immunity was largely up-regulated in the *Rag1* mutant fish

Among the function alterations that have been noticed in the *Rag1* mutant fish, the most obvious change is the significant up-regulation of *Rag1*-independent innate immunity. It can be understood as a compensatory consequence of the loss of RAG1, and has been indicated by the biased up-regulation of ESTs from kidney.

Besides the specific adaptive immunity, which is mediated by RAG proteins and has been depleted in the *Rag1* mutant fish, vertebrate hosts are also equipped with a general defense system, the innate immunity. It includes complement system, inflammation and interferon-mediated immune response. The complement system mainly functions in attacking the membrane of microbial cells. It can be indirectly activated by the antibody-antigen binding through the classical pathway, or directly activated by the polysaccharides in microorganisms, which is known as the alternative pathway (Bruce Alberts, 2002). Inflammation is a defense reaction of living tissue to injury. Through multiple interactions, it enables localization and removal of the irritant (Cruse, 1999). Interferons are a group of proteins that function in immune modulation. By activating a response cascade, they can enhance the ability of macrophages to destroy viruses, bacteria and tumor cell (Cruse, 1999).

Totally, 59 from 341 genes were identified to be functional in the immune response,

excluding MHC class I molecules whose difference in expression was introduced by a polymorphism (data not shown), and antigen receptors (TCR and Ig) that are directly assembled by RAG-mediated V(D)J recombination (refer to Chapter 1.2). From these 59 genes, 54 were up-regulated in the *Rag1* mutant fish (Table 4; Fig. 4-8), which include 6 ESTs similar to different complement components; 2 genes (*Irf7* and *Stat1*) and 9 ESTs that are relevant to interferon function or homologous to interferon induced proteins; as well as 10 EST clones that respectively resemble *Flap*, *Pbef, Tnf* and different *Galectins*, a group of genes that are involved in the inflammatory response. These molecules mainly function in triggering the immune response. The up-regulation of innate immunity was also reflected in the expression alteration of downstream responding molecules. An indispensable step in the development of immune response is the migration of leukocytes from blood to target tissue. This process involves the regulation and reorganization of cytoskeleton (Vicente-Manzanares and Sanchez-Madrid, 2004). In our microarray, the EST homologues of *Epb41l3*, a structural constituent of actin cytoskeleton, and *Plecktrin 2*, a molecule that contributes to the lamellipodia formation during cell migration, were up-regulated. These changes might correspond to the cytoskeleton reorganization triggered by immune response, while other explanations also remain possible.

Among the innate immune reactions, inflammation usually causes a series of consequences, including cell damage and cell adhesion breakdown, which then trigger the secondary responses to eliminate the damaged tissue, repair it with new cells and reconstruct the cell adhesion. Repetitive infection and chronic inflammation may induce an overall up-regulation of apoptosis and cell proliferation, as well as a fast turnover of cell adhesion matrix.

Cornifelin is a gene associated with the epidermal hyperproliferation that usually is caused by a chronic inflammatory disease. In *Rag1* mutant fish, 2 EST homologues of

cornifelin were found to be up-regulated, indicating the presence of chronic inflammation. It is likely caused by the loss of RAG1 and adaptive immunity, and to which the increase of innate immunity failed to compensate. In addition to cornifelin, EST homologues of another 4 genes that function in stimulating cell proliferation were also found to be up-regulated in the *Rag1* mutant fish. *Epiregulin* and *Epiprofin* are genes functional in the epithelia cell proliferation; *Tspan-3* regulates the proliferation and migration of oligodendrocytes; *N-myc* plays a critical role in promoting the proliferation of undifferentiated neuroblasts and is notably associated with neuroblastomas (Kobayashi et al., 2006; Rudie Hovland et al., 2001). Consistenly, an EST similar to *Rbbp6*, which encodes a retinoblastoma tumor suppressor (pRB) protein that suppress cellular proliferation, is down-regulated. These suggest a compensatory increase of cell proliferation in response to the chronic inflammation caused by immune defect.

In addition, the expression alteration observed in apoptosis related genes also indicates the presence of chronic inflammation. *Caspb* (Caspase b), an EST homologue of *Card4* (Caspase recruitment domain 4) and NACHT, which are gene triggering the apoptosis, are up-regulated; whereas *Tradd*, a gene that stimulates and blocks apoptosis through two different pathways, and 2 EST homologues of *Ddit4*, a gene that functions in protecting cells from hypoxia and H_2O_2-triggered apoptosis, were down-regulated. These suggest a general increase of apoptosis, which might be involved in the constitutive clearance of the inflamed tissue.

Furthermore, alteration in expression of cell adhesion molecules also supports the presence of repetitive infection and inflammation. Collagen in the extracellular matrix is mainly found in a fibrillar form, which provides the stiff resilient part of many tissues (Wess, 2005). Two clones that correspond to *Mmp13*, the interleukin-1 induced collagenase 3 that mediate the degradation of collagen, were up-regulated. While the up

Table 4. Expression alteration of immunity-relevant genes in the *Rag1* mutants.

Functional classes	Genebank Acc	Ratio (Rag1/wt)	wt average intensity	t-test *P* value	Rag1 average intensity	t-test *P* value	Symbol	Description
Complement system	AA497156	2.75	0.66	0.015	1.82	0.085	si:c7	Complement protein component C7
	AW116315	2.35	0.59	0.032	1.39	0.015	si:c4-1	similar to Complement C4-1
	BI672168	3.56	0.54	0.067	1.91	0.067	si:c4-2	similar to Complement C4-2
	BI473395	6.82	0.35	0.009	2.38	0.062	si:h2-bf	similar to Histocompatibility 2, complement component factor B
	BI475655	2.68	0.57	0.02	1.54	0.045	si:c1qg	similar to Complement component 1, q subcomponent, gamma polypeptide
Interferon induced respouns	BE605965	5.97	0.31	0.04	1.83	0.027	irf7	Interferon regulatory factor 7
	AW343772	4.4	0.42	0.004	1.84	0.019	stat1	STAT1, Signal transducer and activator of transcription 1
	BM095893	2.47	0.59	0.039	1.46	0.013	si:isgf3	similar to Interferon-stimulated transcription factor 3
	AW077455	3.54	0.47	0.022	1.66	0.022	si:ifit2	Interferon induced protein 2
	BG738260	22.4	0.12	0.005	2.58	0.031	si:ifi56	similar to Interferon-inducible protein IFI56
	BI847099	6.76	0.36	0.048	2.42	0.086	si:ifi44	
	AW019242	2.71	0.62	0.019	1.68	0.07	si:ifi44	
	AI331804	2.6	0.62	0.004	1.62	0.037	si:ifi44	similar to P44, Interferon-induced protein 44 (microtubular aggregate protein; histocompatibility 28)
	AW019056	2.83	0.59	0.011	1.66	0.038	si:ifi44	
	BI877941	10.4	0.19	0.032	1.94	0.033	si:ifi44	
	AW018470	2.26	0.7	0.035	1.57	0.069	si:ifit1	similar to interferon inducible protein with tetratricopeptide repeats 1
Inflammatory response	AW077834	2.33	0.58	0.09	1.34	0.103	si:flap	similar to FLAP, 5-lipoxygenase activating protein (FLAP)
	AI641272	2.27	0.59	0.1	1.35	0.023	si:pbef	
	AA495032	2.61	0.54	0.09	1.41	0.043	si:pbef	similar to PBEF, pre-B cell enhancing factor
	AI883105	2.19	0.65	0.055	1.41	0.035	si:pbef	
	AI883323	2.17	0.62	0.115	1.34	0.081	si:pbef	
	BM155827	2.91	0.66	0.015	1.93	0.097	si:gal1-l1	Lectin, galactoside-binding, soluble, 1 (galectin 1)-like 1
	BI885986	2.69	0.59	0.086	1.6	0.09	si:gal1-l1	
	AW420718	4.19	0.41	0.012	1.74	0.025	si:gal9-l1	Lectin, galactoside-binding, soluble, 9 (galectin 9)-like 1
	AW019034	2.72	0.57	0.106	1.54	0.234	si:gal9	similar to Galectin-9
	BM096075	7.24	0.28	0.018	2.05	0.021	si:tnfaip1	similar to tumor necrosis factor, alpha-induced protein 2
Cytoskeleton	BM185873	2.07	0.65	0.016	1.34	0.004	si:epb41l3	similar to Erythrocyte membrane protein band 4.1-like 3
	BG728481	2.38	0.6	0.085	1.42	0.193	si:plecktrin2	similar to Pleckstrin 2

(Continued)

Cell proliferation	BE557057	3.19	0.6	0.023	1.92	0.078	si:cornifelin	similar to cornifelin [Homo sapiens]; and Placenta-specific
	BI844331	2.97	0.52	0.009	1.54	0.009	si:cornifelin	gene 8 protein PLAC8-like 1 (C15 protein)
	BE605410	2.43	0.59	0.075	1.43	0.048	si:epiregulin	similar to epiregulin; Epithelial mitogen
	AW466712	2.36	0.61	0.042	1.45	0.076	si:epiprofin	similar to Epiprofin
	AI964296	2.83	0.6	0.009	1.69	0.055	si:tspan3	similar to Transmembrane 4 superfamily member 8 (Tetraspanin 3) (Tspan-3)
	AI721479	2.17	0.64	0.069	1.39	0.081	nmyc1	Neuroblastoma myc-related oncogene 1
	AI959474	0.5	1.27	0.105	0.63	0.107	si:rbbp6	similar to Retinoblastoma binding protein 6
Apoptosis	AF327410	2.49	0.59	0.04	1.48	0.022	caspb	Caspase b
	BI427786	2.2	0.68	0.095	1.5	0.164	si: card4	similar to Caspase recruitment domain 4
	AI793577	9.32	0.22	0.028	2.06	0.026	si:nacht	NACHT, leucine rich repeat and PYD containing 5; Ribonuclease/angiogenin inhibitor
	AF231014	0.46	1.67	0.089	0.76	0.006	tradd	Death domain-containing adaptor molecule; Danio rerio Tradd (tradd) gene, complete cds.
	BF158442	0.06	5.15	0.104	0.32	0.002	si:ddit4	similar to DNA-damage-inducible transcript 4 and HIF-1
	BI843145	0.03	5.43	0.097	0.16	0.004	si:ddit4	responsive RTP801
Cell adhesion	AW420822	6.9	0.4	0.008	2.75	0.073	mmp13	Matrix metalloproteinase 13
	AW305943	5.32	0.5	0.01	2.65	0.082	mmp13	
	BF717537	3.52	0.52	0.003	1.82	0.053	si:mfap4	similar to Microfibrillar-associated protein 4
	BI980545	9.28	0.23	0.007	2.15	0.038	si:p4ha2	similar to Prolyl 4-hydroxylase alpha-2 subunit precursor (4-PH alpha-2)
Other	AF402599	10	0.33	0.001	3.29	0.073	lyz	Lysozyme
	AF349034	6.46	0.45	0.002	2.89	0.088	mpx	Myeloid-specific peroxidase
	AI641426	3.71	0.43	0.06	1.59	0.012	si:rifin	similar to Repetitively Interspersed Family
	AI616686	2.07	0.66	0.098	1.36	0.079	si:hapln1	Hyaluronan and proteoglycan link protein 1 precursor (Proteoglycan)
	AW077654	2.65	0.61	0.036	1.62	0.08	spi1	Spleen focus forming virus (SFFV) proviral integration oncogene
	AW173887	3.69	0.46	0.004	1.71	0.017	si:zc3hav1	similar to Zinc finger CCCH type, antiviral 1
	BG303313	2.84	0.63	0.002	1.79	0.108	si:f13a1	similar to Coagulation factor XIII, A1 subunit
	BM036395	2.71	0.6	0.091	1.62	0.092	vg1	Vitellogenin 1
	BM157226	3.72	0.42	0.066	1.56	0.037	si:cd83	similar to CD83 antigen
	BI865595	3.4	0.44	0.041	1.51	0.013	si:icsbp	similar to interferon consensus sequence binding protein
	BI880782	2.24	0.63	0.093	1.42	0.082	si:cxcr3	similar to C-X-C chemokine receptor type 3
	AF253046	2.43	0.6	0.035	1.45	0.03	syk	Spleen tyrosine kinase
	AW421020	2.14	0.68	0.049	1.45	0.068	si:cyp2e1	similar to cytochrome P450, family 2, subfamily F, polypeptide 1

regulation was also seen in the expression of EST homologues of *Mfap4*, an extracellular matrix protein that binds to collagen, and *P4Ha2* that encodes a component of the key enzyme in collagen synthesis. These changes indicate a fast turnover of collagen, e.g. both the degradation and synthesis were up regulated, in the *Rag1* mutant fish, which usually associated with inflammation (Havemose-Poulsen and Holmstrup, 1997).

Besides these changes, two enzymes that function in the general host defense system against a wide range of bacteria, *Mpx* and *Lyz*, were also up-regulated. *Mpx* (myeloid specific peroxidase) catalyses the production of many toxic intermediates in enhancing the microbicidal activity of polymorphonuclear leukocytes; *Lyz* (lysozyme C) has a primary bacteriolytic function and may associate with the monocyte-macrophage system to enhance their immune activity.

4.3.3 Expression of a large group of neuronal genes decreased in the *Rag1* mutants

The second large group of genes that were altered in the *Rag1* mutant fish is relevant to neuronal functions (Table 5). First of all, genes involved in neuronal differentiation were mostly down-regulated. These include *Her6* and EST homologues of *Siah2, Stmn4, S100a, Ndr2. Her6* is a zebrafish homologue of mammalian *Hes-1*, which encodes a HLH factor. Persistent expression revealed *Hes-1*'s function in suppressing neurogenesis (Tomita et al., 1996), while in the *Hes-1* null mutant mice, postmitotic neurons appeared prematurely (Ishibashi et al., 1995). Recently, *Hes-1* is found to be transiently up-regulated upon the differentiation of neuronal cells, which is thought to be critical in controlling the proper timing of neurogenesis (Axelson, 2004; Grynfeld et al., 2000). *Siah2* encodes an E3 ubiquitin ligase that is required for the specification of r7 photoreceptor cell in the eye. *Stmn4* encodes a *Stathmin* like protein RB3, which is mainly expressed in mature neurons and may play a role in activity induced neuronal

plasticity and neuronal differentiation (Beilharz et al., 1998; Ozon et al., 1999). *S100a* encodes a protein that belongs to a large subfamily of EF-hand Ca^{2+}-binding proteins. These proteins are known to associate with differentiated neurons (Donato, 2001), and their immunoactivity has been detected in zebrafish crypt olfactory neurons (Germana et al., 2004). *Ndr2*, a member of the NDR subfamily of serine/theonine protein kinases, has been proven to have a function in regulating the structural process of differentiating and mature neurons (Stork et al., 2004). These changes indicate a decrease of neural differentiation.

Consistently, several genes involved in neurite growth were also found to be down-regulated. These include *Thy1* and 3 ESTs homologous to *Ulk1/2* (unc-51-like kinase 1 and 2). *Thy1* is an abundant neuronal glycoprotein in mammals, and is known to be implicated in axon regeneration and outgrowth (Barlow et al., 2002). *Ulk*, the mammalian homologue of *Unc-51* from *C. elegans*, is also known to play a role in neurite extension (Okazaki et al., 2000).

Furthermore, many genes functional in neuronal signaling and synapses, which mainly are functions of mature neurons, were found to be down regulated in the *Rag1* mutants. This is also consistent with the decrease of neural differentiation. The decreased neuronal signaling molecules include 5 different odorant receptors (*Or2.1*, *Or2.6*, *Or2.7*, *Or3.1* and *Or9.1*), *Ocnc* and an EST homologue of an orphan receptor. Odorant receptors (OR) enable the recognition of odorants, where the *Ocnc* is a part of the signal cascade downstream of ORs. The orphan receptors belong to the nuclear hormone receptor family, but their function in the brain hasn't been well elucidated. In neuronal synapses, *Syp1* (Synaptophysin 1) is one of the most abundant protein of the synaptic vesicle membrane (Thiel, 1993); *Vamp2* (Synaptobrevin 2) is the major SNARE protein of synaptic vesicles (Quetglas et al., 2000); *Syt* (Synaptotagmin) is a Ca^{2+} sensor that directly couples the Ca^{2+}

influx and synaptic vesicles fusion (Koh and Bellen, 2003); and *Cplx2* (Complexin 2) is the modulator of the synaptic vesicle release (Hu et al., 2002). They are all required for fast Ca^{2+}-triggered synaptic vesicle exocytosis. In our microarray result, 3 individual clones representing *Vamp2*, 2 ESTs similar respectively to *Syt1* and *Syt11*, 1 EST homologue of *Syp1* and 1 EST homologue of *Cplx2* were found to decrease significantly in the *Rag1* mutants. In addition, EST homlogues of several membrane transporting ATPase and pump molecules, including H^+-transporting ATPase, Ca^{2+}-transporting plasma membrane ATPase and solute carrier family 6, were also found to be down-regulated.

Besides these, *Chga* (chromogranin A) and *Eno2* (enolase 2), which have long been used as markers for neurons and neoplastic neuroendocrine cells (De Block et al., 2004), were also down-regulated.

All in all, from 39 genes that are classified as neuronal genes, 36 were down-regulated. This strongly suggests a degeneration of the nervous system, which might be caused by infections. Accumulated data has revealed that infection and injury triggered increase of immunity, especially the complement system, may selectively cause neural damage and trigger neuronal degeneration in CNS (Lucas et al., 2006; van Beek et al., 2003). This suggests that the neuronal degeneration, revealed by the microarray in OE, might be caused by chronic infection in the *Rag1* mutant fish. There is no direct evidence for this in the PNS, and the possibility that *Rag1* has a direct function in regulating neuronal genes cannot be ruled out.

4.3.4 Other alterations in the *Rag1* mutant fish

Expression change of other genes was also noticed in the *Rag1* mutant fish. A small group of ESTs homologous to GTPase and relevant regulators, including *Rhobtb1*, *Rgs2*,

Table 5. Expression alteration of neuronal genes revealed in the adult OE microarray.

Functional classes	Genebank Acc	Ratio (Rag1/wt)	wt average intensity	t-test *P* value	Rag1 average intensity	t-test *P* value	Symbol	Description
Signaling	U42393	0.43	1.41	0.015	0.61	0.038	ocnc	Danio rerio olfactory cyclic-nucleotide gated channel
	U72685	0.49	1.43	0.108	0.7	0.116	or3.1	Danio rerio odorant receptor 3 (ZOR3) gene, partial cds.
	AF283560	0.47	1.39	0.039	0.65	0.03	or9.1	Odorant receptor, family 9, member 1
	AF012761	0.48	1.38	0.046	0.66	0.059	or2.7	Danio rerio olfactory receptor protein 2.7 gene, complete cds.
	AF012760	0.47	1.57	0.097	0.74	0.1	or2.6	Danio rerio olfactory receptor protein 2.6 gene, complete cds.
	AF012748	0.49	1.44	0.069	0.7	0.137	or2.1	Odorant receptor, family 2, member 1
	AW154394	0.51	1.45	0.054	0.74	0.022	si:gpr63	similar to G protein-coupled receptor 63
Synaptic transportation	BI670974	0.5	1.35	0.098	0.68	0.155	si:syp	similar to Synaptophysin
	BG305533	0.42	1.54	0.053	0.65	0.044	vamp2	Vesicle-associated membrane protein 2
	AW305605	0.44	1.38	0.007	0.6	0.028	vamp2	Vesicle-associated membrane protein 2
	BM035348	0.5	1.38	0.138	0.69	0.149	vamp2	Vesicle-associated membrane protein 2
	AW826278	0.43	1.66	0.099	0.72	0.045	si:syt1	similar to Synaptotagmin I (p65)
	AI793746	0.47	1.64	0.105	0.77	0.028	si:syt11	similar to Synaptotagmin XI
	BI982411	0.41	1.61	0.089	0.67	0.077	si:cplx2	similar to Complexin 2 (Synaphin-1)
	AI722383	0.49	1.35	0.021	0.67	0.018	si:slc6a6	similar to Solute carrier family 6, member 6
	AW233556	0.48	1.49	0.153	0.72	0.054	si:vpp1	similar to Vacuolar H(+)-transporting ATPase 116 kDa subunit, a1 isoform
Neurotransmitter receptor	AW076828	0.49	1.5	0.077	0.73	0.03	si:gag2	similar to GABA-A receptor gamma-2 subunit
Membrane transporation	BI710377	0.46	1.63	0.108	0.75	0.044	si:atp2b1	similar to ATPase; Ca++ transporting, plasma membrane 1
	BI864494	0.31	2.15	0.12	0.67	0.067	si:atp2b2	similar to ATPase, Ca++ transporting, plasma membrane 2
	BI842255	2.78	0.57	0.057	1.59	0.069	si:clic6	similar to Chloride intracellular channel 6

(Continued)

Neurogenesis (differnetiation)	AI721479	2.17	0.64	0.069	1.39	0.081	nmyc1	Neuroblastoma myc-related oncogene 1
	X97333	0.42	1.57	0.042	0.66	0.013	her6	Hairy-related 6
	BI430135	0.43	1.42	0.011	0.61	0.015	stmn4	Stathmin-like 4
	BM181692	0.5	1.34	0.016	0.67	0.023	si:siah2	similar to Ubiquitin ligase SIAH2 (Seven in absentia homolog 2)
	BM156040	0.48	1.34	0.01	0.64	0.023	si:ndr2	similar to Serine/threonine kinase 38; large tumor suppressor 2;protein kinase Ndr
	AW076585	0.49	1.41	0.195	0.69	0.163	si:s100a	similar to S-100 protein, alpha chain
Neuronal migration	BI890456	4.22	0.43	0.004	1.84	0.04	si:pafah1b1	similar to platelet-activating factor acetylhydrolase, isoform 1b, beta1 subunit
Neurites growth	BM181792	0.27	1.95	0.061	0.53	0.016	thy1	Thy-1 cell surface antigen
	BI876180	0.5	1.45	0.085	0.72	0.04	si:ulk1	similar to unc-51-like kinase 1
	BG306394	0.33	1.52	0.189	0.5	0.125	si:ulk2	similar to Unc-51 like kinase 2
	AI332046	0.29	1.71	0.108	0.5	0.024	si:ulk2	similar to Unc-51 like kinase 2
Neuroendocrine	AW203029	0.49	1.22	0.046	0.59	0.108	chga	Chromogranin A
	BI878329	0.47	1.35	0.041	0.64	0.056	eno2	Enolase 2
Neurol metablism	BG985485	0.42	1.52	0.09	0.64	0.035	sult2st	Sulfotransferase family, cytosolic sulfotransferase 2
	BI533409	0.48	1.35	0.011	0.64	0.026	si:sult4a1	similar to sulfotransferase family 4A, member 1
Otolith formation	AI544512	0.43	1.44	0.061	0.61	0.07	otop1	Otopetrin 1
	BI890046	0.42	1.35	0.034	0.57	0.059	otop1	Otopetrin 1
Other	BI846800	0.46	1.51	0.08	0.7	0.049	si:nrip2	similar to Nrip2; Neuronal interacting factor X 1 (NIX1)
	BI707699	0.16	1.85	0.033	0.3	0.009	si:a13	similar to Annexin A13

Sept3 and *Rasrgp1*, were found to be up-regulated in the *Rag1* mutant fish. But, since these molecules are known to function in many different biological processes, the implication of these changes is not clear. Similarly, *inhibin b*, *integrin* and *Cxcr4* play multiple functions in both immune and nervous system, thus their decrease in the *Rag1* mutants is also difficult to explain.

In addition, a few ESTs similar to genes required in maintaining adult fertility, including *Tesk2*, *Pl10* and *Ptx3,* were found to be down-regulated in the *Rag1* mutant fish. *Tesk2* and *Pl10* are two genes enriched in male germ lines and play important role in spermatogenesis (Leroy et al., 1989; Rosok et al., 1999). *Ptx3* is a tumor necrosis factor (TNF)-stimulated gene, playing important role in inflammation as well as female fertility (Garlanda et al., 2005; Salustri et al., 2004). Here we list *Ptx3* as a fertility gene, because its expression change is different from the increase of immune genes, but similar to the decrease of fertility relevant genes. The overall down-regulation of these genes in the *Rag1* mutants revealed by microarray is consistent with our observation that the *Rag1* mutant homozygote fish are fertile, but their fertility is maintained for only 3~5 months (data not shown), which is much shorter compared to wt siblings (1~2 years) (Westerfield, 2000). By current knowledge, these alterations are not directly linked to the immunity changes in the mutants. Whether they are an unknown consequence of the immune defect, or linked to an unknown function of *Rag1*, still remains elusive.

4.3.5 Summary

Our microarray results revealed broad and complicated alterations of gene expression in adult olfactory rosettes. These included an overall increase of innate immunity, activation of secondary responses (e.g. enhanced apoptosis, cell proliferation and cell adhesion turnover), which is known and expected in a tissue under infection (The mutant fish are not housed in a specific pathogen free environment.). Meanwhile, a large group of

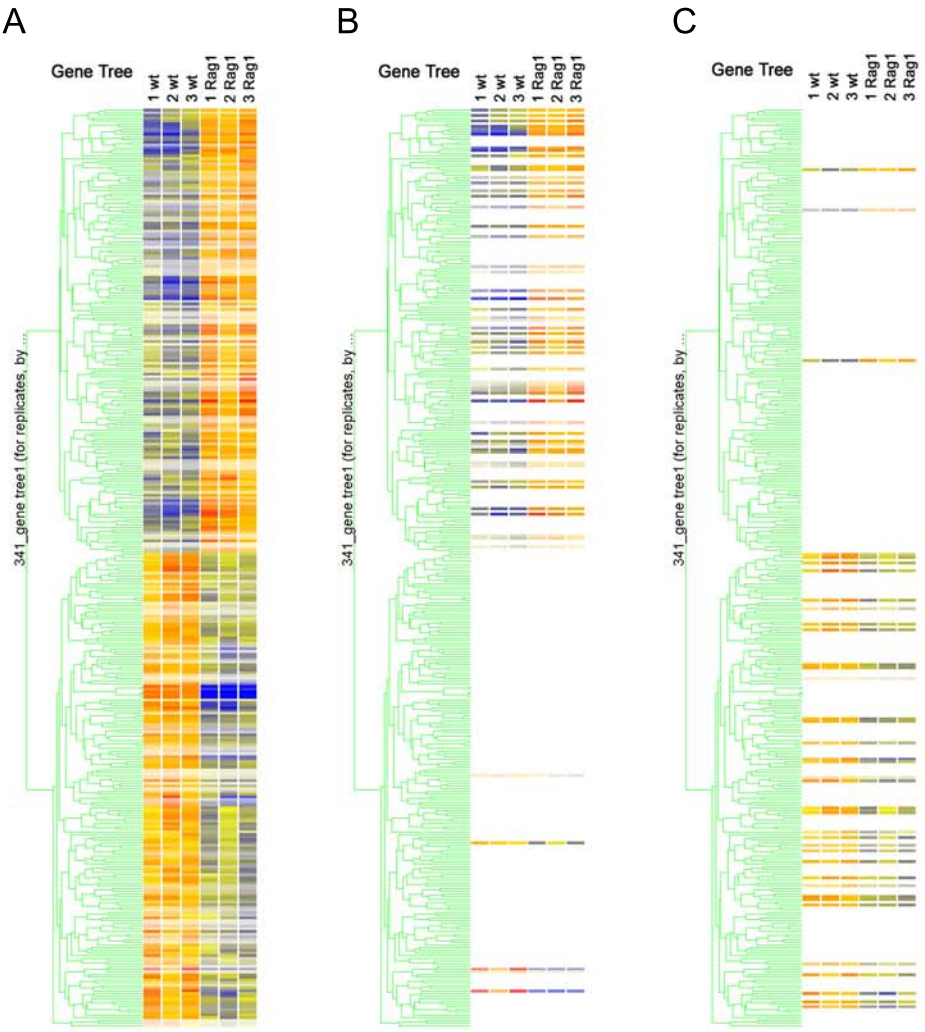

Figure 4-8. The distribution of immune genes and neuronal genes in the 341-gene tree.

(A) The 341 significants were built into a gene tree according to the standard correlation in their expression. Two large groups were formed for up- and down-regulated genes. (B) Genes involved or related to immune functions largely fell into the up-regulated group. (C) Neuronal genes were mostly categorized into the down-regulated group.

neuronal genes were also found to be down-regulated in the mutants, indicating a neuronal degeneration. As suggested by the literature, this may be caused by the increased immune responses. Thus all of these changes were possibly consequences of the loss of adaptive immunity, which corresponds to *Rag1*'s immune function. *Rag1*'s neuronal function remains obscure.

4.4 Characterization of 12158, a candidate downstream gene of Rag1

4.4.1 Two versions of 12158 were cloned

Clone 12158 was one of the significants picked up by 2 fold change cut-off from 3 dpf larvae microarray experiment. Its expression change between wt and *Rag1* mutants was confirmed by RT-PCR, thus it was analyzed in detail.

The 12158 clone was generated from a zebrafish EST BI865569, which contains 243 bp nucleotides and a putative polyA tail. From this sequence we did 3'RACE and obtained 2 clones, 12158A and 12158B (Fig. 4-9A). 12158A contains additional 160 bp nucleotides at 5' of the original EST sequence (Fig. 4-9B). The entire fragment can be amplified by PCR from genomic DNA, but not from cDNA (Fig. 4-9C), which indicates that the 5'part of 12158A might be picked up from genomic DNA in the RACE reaction. 12158B contains a longer 5' fragment (656 bp; Fig. 4-9D), which is totally different from 12158A. With primers covering both the newly-cloned and previously identified sequences, 12158B can be amplified from both cDNA and genomic DNA. The amplifications from cDNA confirmed the decreased expression of 12158 in the *Rag1* mutant fish (Fig. 4-9E). Surprisingly, the PCR product amplified from cDNA and genomic DNA for 12158B are same. This suggests that the 5' part of 12158A was not amplified from an intron, but from another allele, which was not transcribed.

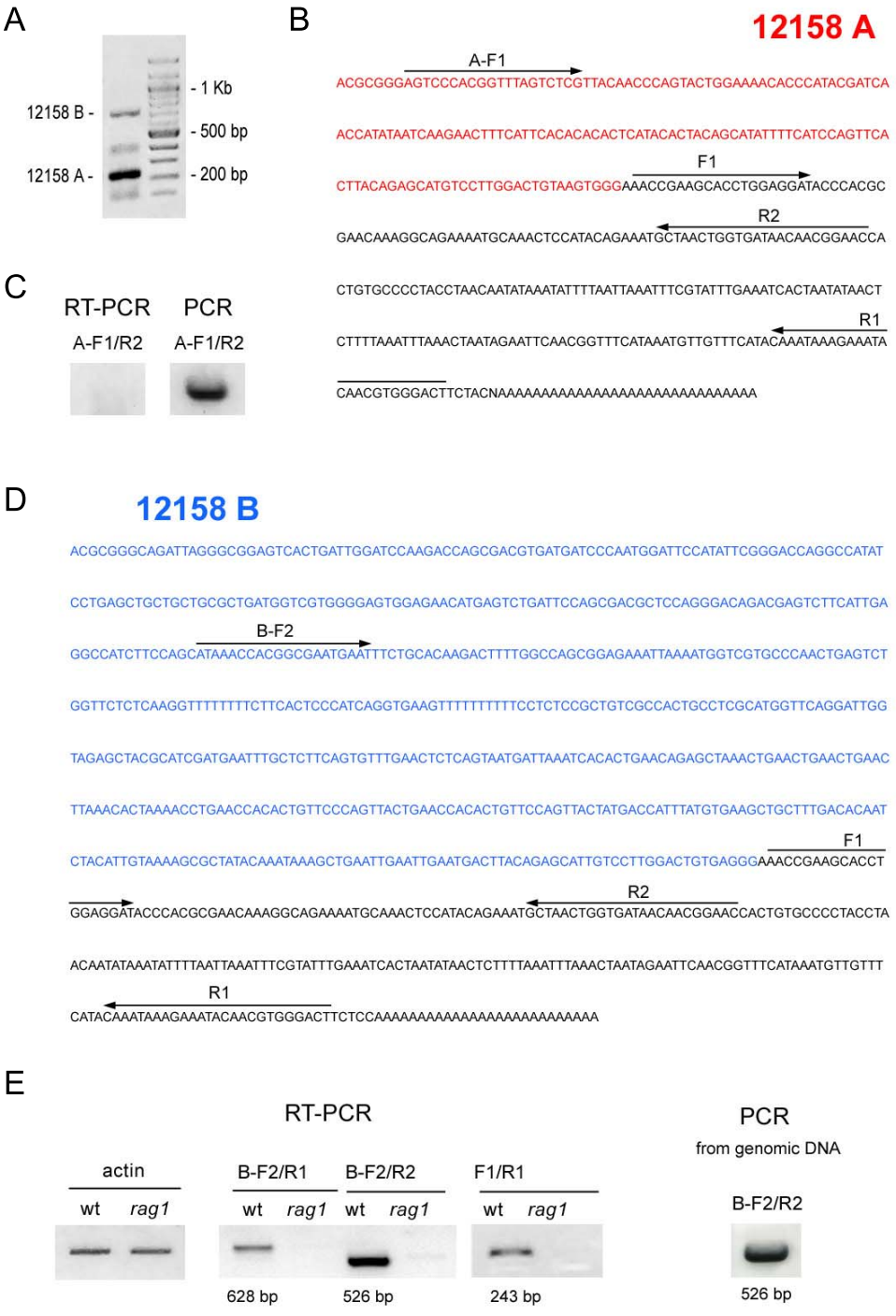

Figure 4-9. 5' RACE of clone 12158.

Figure 4-9. 5' RACE of clone 12158.

(A) By 5'RACE, two PCR bands containing the original 12158 sequence were amplified. (B) Sequence of clone 12158A. The original 12158 sequence is colored in black; the newly cloned sequence is in red. Name and locations of the relevant primers are indicated. (C) With primers A-F1 and R2, clone 12158A can be amplified from genomic DNA (the PCR), but not from cDNA (the RT-PCR). (D) Sequence of clone 12158B. The original 12158 sequence is in black; the newly cloned sequence is in blue. Name and locations of the relevant primers are indicated. (E) By RT-PCT, 12158B was amplified with 3 pairs of primers, and its decreased expression in *Rag1* mutant was confirmed in all of these reactions. β-actin was used as loading control. –RT controls were not shown. With primers B-F2 and R2, a band with equal length (526 bp) was also amplified from genomic DNA (the PCR).

4.4.2 12158B might be evolved from transposition of a LINE element in the 12158A allele

Blast search with the 12158B sequence picked up a BAC clone, CH211-206E6. As revealed by GeneScan analysis, 12158B matches to the 3' UTR of a predicted protein, which contains a reverse transcriptase domain (rvt; Fig. 4-10C, red bar). Further Blast search revealed that the predicted ORF and 3'UTR contain several highly repetitive sequences (Fig. 4-10B) that match to zebrafish genome at more than 100 locations with more than 90% identity (data not shown). Consistently, in the zebrafish EST database, the predicted ORF matches to hundreds of clones, suggesting high abundance of this transcript (Fig. 4-10D); 12158B, which matches to 3'UTR of the predicted ORF, appears to be a chimera in transcription. The newly cloned 5' part (Fig. 4-11A, blue box) was equally abundant as the ORF (Fig. 4-11B), while the 3'original part (Fig. 4-11A, grey box) was rarely transcribed and only appeared in the original EST clones (Fig. 4-11B). This observation suggests that in some situations the 5' part might be transcribed independently of the 3' 12158 sequence, although the joined transcript of the predicted ORF and 12158 has been proven here by RT-PCR (Fig. 4-10E). One possible explanation is that the 5' predicted ORF and UTR belong to a repetitive element that is also located and transcribed in other loci. This is further supported by real-time PCR. The amplification with primer rtF and rtR (designed to amplify the 3' 12158 sequence; Fig. 4-11A) confirmed the decrease of 12158 expression in *Rag1* mutant fish (Fig. 4-11C, F); whereas the amplification with rpF and rpR (for amplifying the 5' repetitive part of 12158B; Fig. 4-11A) didn't show significant difference between *Rag1* mutant and wt sibling (Fig. 4-11D, F). This indicates that the 5' repetitive part was not unique to the 12158B, but exists in many other transcripts, whose total expression level was not significantly decreased in *Rag1* mutants. All of these results suggest that the 12158B allele contains a repetitive element.

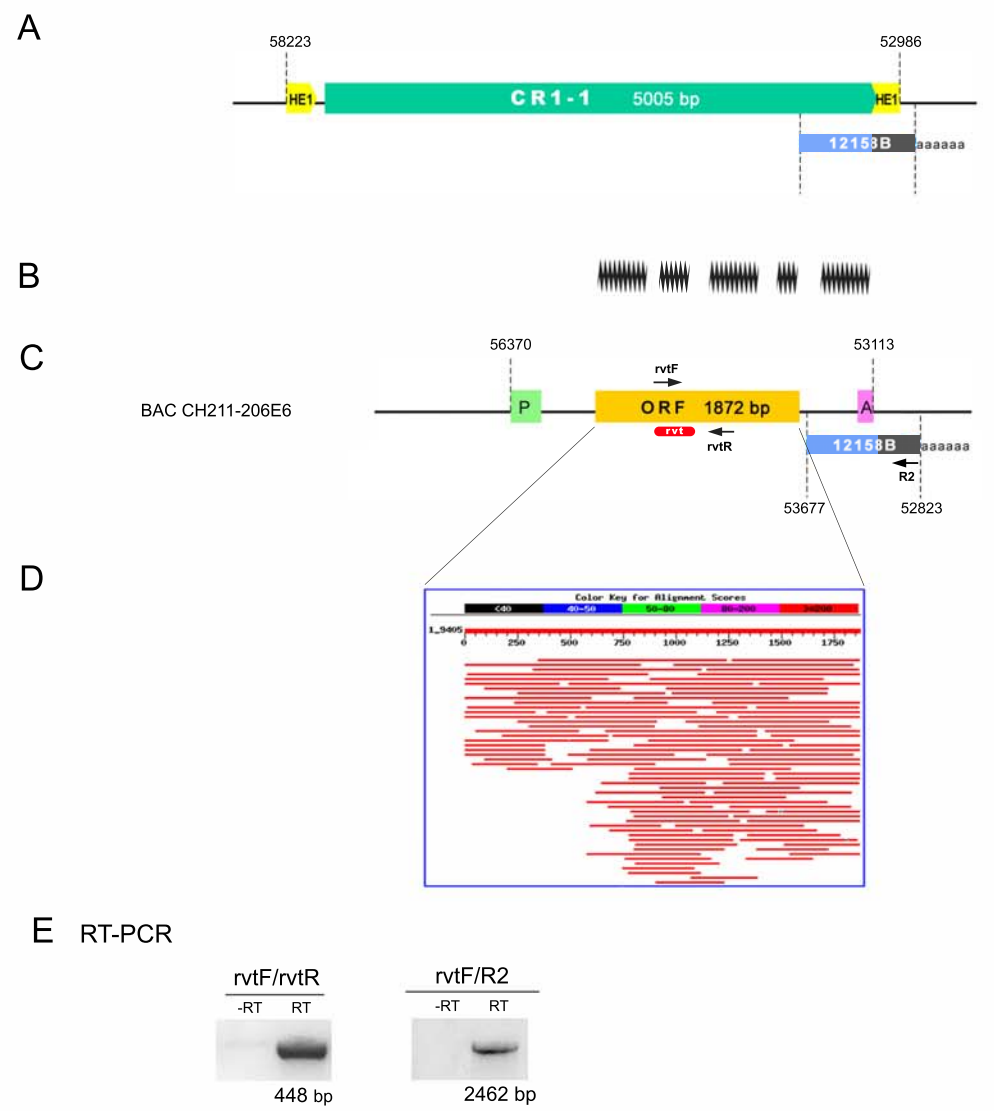

Figure 4-10. Clone 12158B matches to BAC clone CH211-206E6.

(A) Result presented by RepeatMasker. Some repetitive elements were found in the BAC CH211-206E6. 12158B matches to a part of a LINE element CR1-1 and a part of a broken SINE element EH1. (B) Highly repetitive sequences were found in 12158B and its 5' region. (C) The analysis result of GeneScan. 12158B was found to match to the 3'UTR of a predicted gene, which carries a reverse transcriptase domain (rvt, red bar). The predicted promoter was shown as a green box; ORF was a yellow box and polyA signal was a pink box. (D) Blast result of the predicted ORF to zebrafish EST database indicates that this gene is abundantly transcribed. (E) RT-PCR confirmed the transcription of the predicted gene. Amplification with primers rvtF and R2 proved that the 12158 and its 5' gene exist in a single transcript. Primers are indicated in panel C.

Furthermore, in the BAC CH21-206E6, RepeatMasker analysis revealed a LINE element CR1-1 (5005 bp) at the 5' of 12158B, and two parts of a HE1 SINE element in the regions flanking to the CR1-1. LINE and SINE stand for long and short interspersed repetitive elements respectively. They are both mobile genetic elements, which normally comprise a significant part of the genome in higher eukaryotes. Both LINEs and SINEs are retrotransposons, but LINEs range from 3 to 7 KB in length and each contains an ORF to encode a reverse transcriptase; whereas SINEs are only 100 ~ 500 bp in length and do not encode any protein (Deininger and Batzer, 2002). CR1 (chicken repeat 1) family LINE elements have been found in many organisms and are suggested to be an ancient repetitive element (Hodgetts, 2004). HE1 is a newly identified SINE family, which is designated for higher elasmobranch family 1(Ogiwara et al., 1999). Alignment of BAC CH21-206E6 (representing the 12158B allele) and 12158A revealed two homologous regions separated by a 5034 bp fragment (Fig. 4-12). The CR1-1 element is located in this 5034 bp region, while the flanking regions that match to 12158A contain the two parts of the HE1. Rejoining the separated two parts of this HE1 perfectly forms a complete HE1 as it is in 12158A allele, which suggests that 12158B allele is evolved from transposition of a CR1-1 element in the middle of a HE1 element in 12158A allele.

This is further supported by sequencing of PCR products, which revealed that the genomic sequences flanked 12158A were identical to the corresponding regions in the BAC CH21-206E6, and a two-nucleotide repeat AC appears precisely in the junctions at both sides of the 5034 bp fragment (Fig. 4-12A), indicating target specificity of the transposition. In addition, by Blast search CR1-1 element was found highly abundant in zebrafish genome, whereas the flanking sequences were unique to the CH21-206E6 clone (Fig. 4-13). Thus we propose that this 5034 bp fragment in 12158B allele was resulted from a transposition of CR1-1 into 12158A allele, and the transcription of this CR1-1 was carried out to the downstream flanking region, which lead to the expression of 12158.

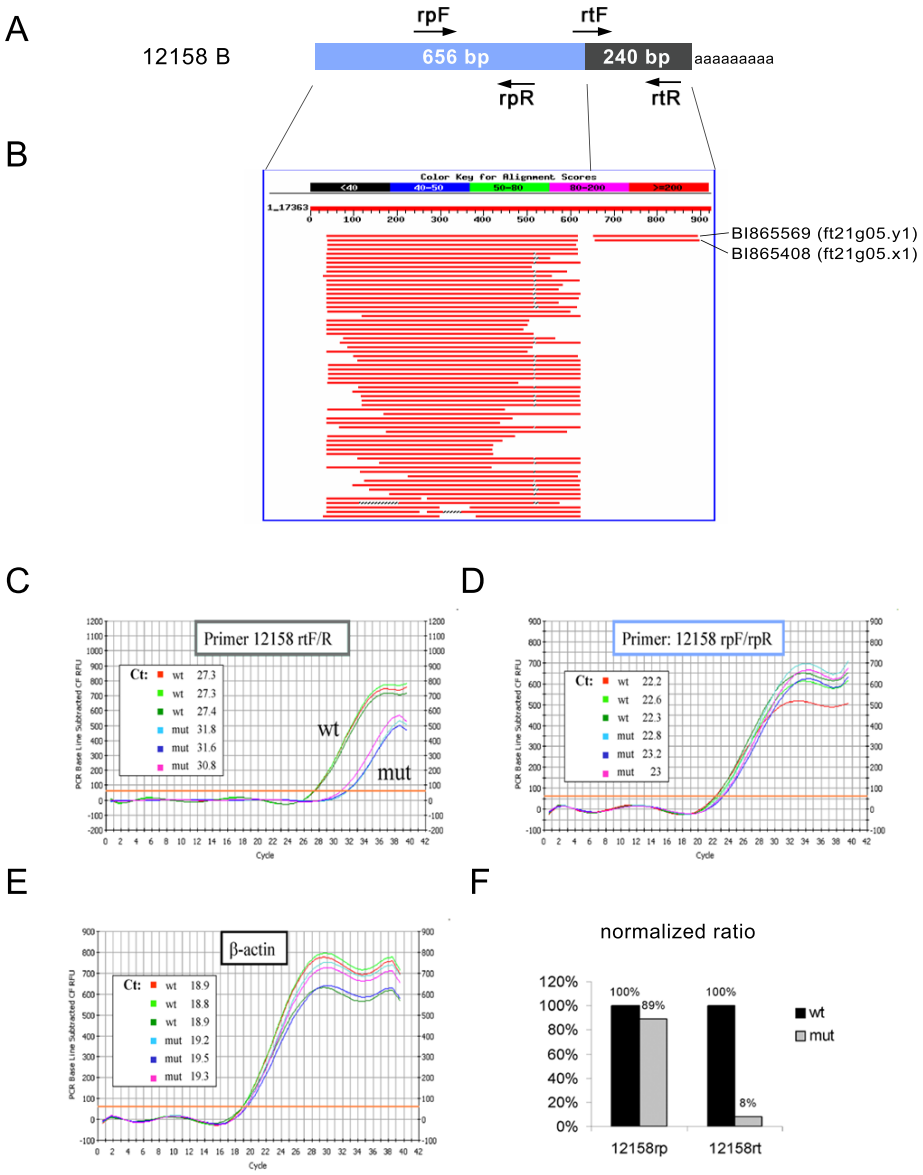

Figure 4-11. The 5' part and 3' part of 12158B are unequally transcribed.

(A) Schematic representation of 12158B. The original part of 12158 is shown as a grey bar, while the part newly-coned in the RACE reaction is illustrated as a blue bar.
(B) Blast search of 12158B sequence to zebrafish EST database. The result shows that the 5' part of 12158B matches to many different EST clones, whereas the 3' part only matches to two sequences that came from the same EST clone (written at the right side).
(C-F) Results of real-time PCR. The used primers are indicated in panel A; for each sample (Rag1 mutant vis wt) 3 repeat reactions was run; records from different reactions were distinguished by colors; the Cycle Numbers at Threshold (Ct) for each reaction are listed. (C) Amplification with primers rtF and rtR shows that the transcription of 3' 12158B is decreased in Rag1 mutant fish. (D) The amplification with primers rpF and rpR shows that the expression of 5' part of 12158B is not significantly changed in Rag1 mutants. (E) Amplifications from β-actin was used as loading controls.
(F) Summary chart to present the relative levels of different parts of 12158B, normalized according to the β-actin amplification.

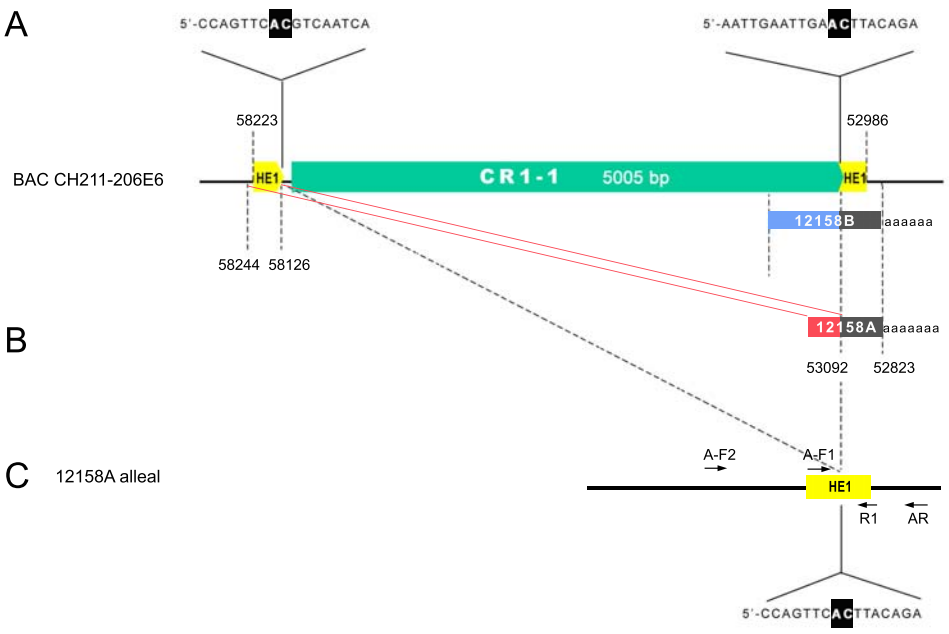

Figure 4-12. 12158A matches to the flanking regions of the CR1-1 element in BAC CH211-206E6.

(A) Schematic representation of the relative position of 12158A and BAC CH211-206E6. 12158A matches to the same fragment that 12158B matches to, but in two regions that separated by a 5034bp fragment containing a CR1-1 element. The boundary sequences were illustrated, and AC was found exactly at both junctions. (B) The 12158A clone. The original 12158 region was shown as a grey bar, matching to the right flank of the CR1-1; while the part cloned by RACE was presented as a red bar, matching to the left flank of the CR1-1. (C) The proposed 12158A allele, containing the complete HE1 element that is separated by a CR1-1 in 12158B allele. Primers used for PCR confirmation were indicated as arrows.

4.4.3 The two versions of 12158 are two alleles in the same locus

Next, we examined whether the 12158A and the stably transposed 12158B locate in the same locus of zebrafish genome. By PCR screening with DNA from clipped fins, we identified some 12158A positive adult fishes. They were crossed as single-pairs, and the progenies were tested by A-F1/R1 PCR. In a population of progeny from a single pair of parents, the amplifications with A-F1/R1 are positive in ~75% embryos (35/48, Fig.4-14), which fit perfectly with the Mendellian principles of inheritance(Klug, 2000) and suggest that the 12158A allele is single-copied in the genome. The same batch of progenies was also tested by the PCR with primers B-F2/R2 and the result showed that also 75% of the embryos (36/48) are positive (Fig.4-14A). Thus both 12158A and 12158B are likely to be single-copy alleles. If 12158A and 12158B are located in the same locus, among a haploid of genome, whenever 12158A is positive, 12158B should be negative, *vise versa*. We thus built a model (Fig. 4-14B). $A^+(b^-)$ stands for 12158A positive allele, which is also 12158B negative; $B^+(a^-)$ stands for 12158B positive and 12158A negative. By Mendel's segregation postulate for single-paired factors(Klug, 2000), a pair of heterezygote parents $A^+(b^-)$ /$B^+(a^-)$ should give 25% $A^+(b^-)/A^+(b^-)$, 25% $B^+(a^-)/B^+(a^-)$ and 50% $A^+(b^-)$ /$B^+(a^-)$ progenies. Since in PCR test, both homozygote and heterozygote are present as positive, there will be 75% 12158A positive (A^+) and 75% 12158B positive (B^+) and 50% double positives among these progenies. Indeed, among the ~75% 12158A positives and 75% 12158B positives, we found that 23 from 48 (~50%) are double positives (Fig. 4-14C). This fits well with the proposed model and strongly suggests that 12158A and 12158B are single copy alleles in the same locus among the genome. Thus we speculate that 12158B is evolved from a transposition of CR1-1 into 12158A allele.

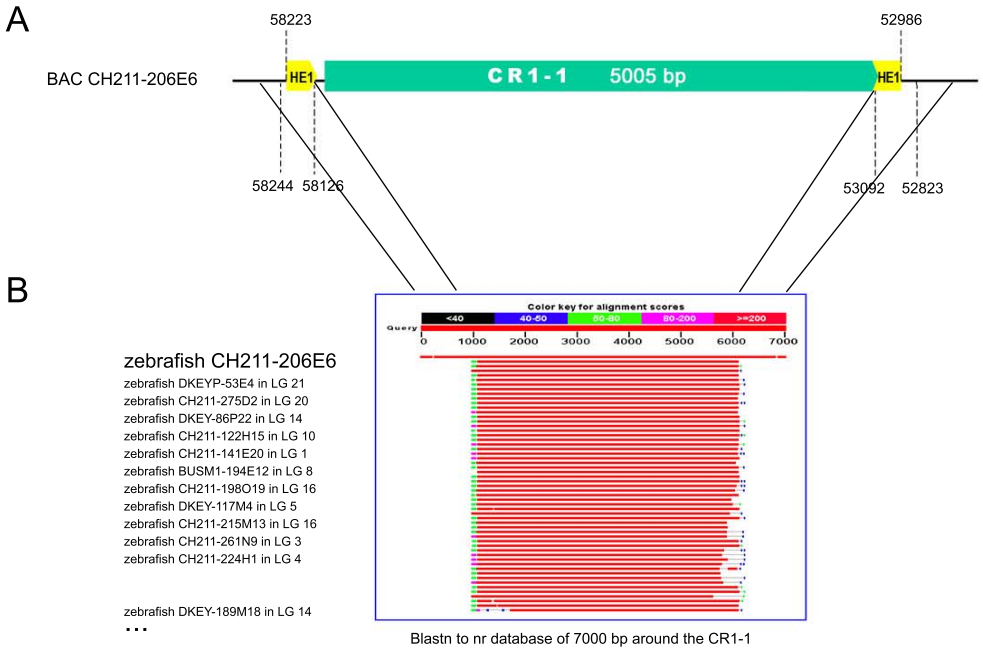

Figure 4-13. Blast result of the CR1-1 and flanking regions.

(A) A 7000 bp sequence, which covers the entire fragment described previously, was used for Blast search. (B) The Blast result shows that the CR1-1 within this fragment is a highly repetitive element among zebrafish genome. It exists in many different loci among different Linkage Groups (LG). Some Blast hits and locations are listed in the left side of this panel. However, the flanking regions are unique in the BAC CH211-206E6, which matches to 12158.

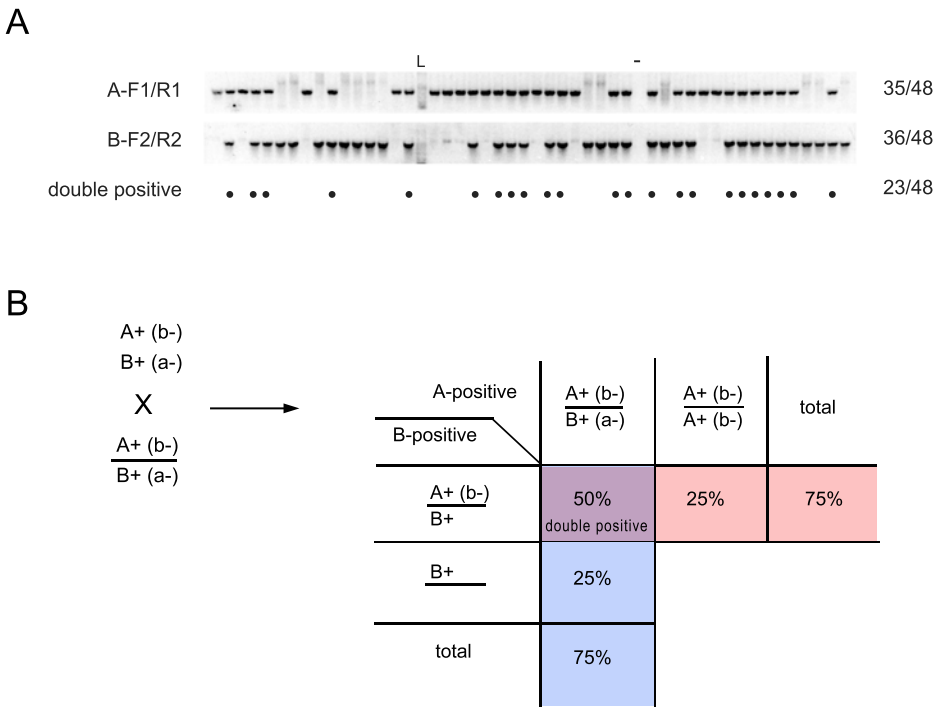

Figure 4-14. 12158A and 12158B are single-copy alleles and locate in the same locus of zebrafish genome.

(A) In the cross of two 12158A positive fishes, individual embryos were tested by PCR with A-F1/R1 and B-F2/R2 primer pairs. Positive amplifications were show as a clear single band; the double positive individuals were marked with black dots. In the gel picture, Lane 17 was loaded with DNA ladder (L), Lane 34 was empty (-). Total number of fishes positive in PCR and fishes tested were summarized and written on the right side of gel pictures. (B) The model to illustrate the inheritance of 12158A and 12158B, which are proposed to be single-copy alleles.

4.4.4 12158 transcript is down-regulated in *Rag1* mutant fish

12158A allele was found only in the wt siblings population, but not in the *Rag1* mutants (n = 285). The down-regulation of 12158 in *Rag1* mutant fish was revealed by microarray and confirmed by RT-PCR (Fig. 4-9E), even though the *Rag1* mutants are all 12158B homozygotes, while among the wt siblings, some fish carry only one allele of 12158B. The reason behind this is not clear.

Progenies from the incross of 12158A positive fish were examined, and no defect in morphology and viability was detected, although at least 25% among them should be 12158A homozygote embryos, which do not carry CR1-1 element in this locus and produce no 12158 transcripts. This suggests that the presence of CR1-1 element in this locus and the 12158 transcripts are not essential. But whether they play any non-essential function remains elusive.

4.5 Summary

Comparing *Rag1* mutants and wt siblings, our microarray experiments revealed the global effect of *Rag1* deficiency on gene expression and suggested some candidates of *Rag1* downstream genes in the nervous system.

In adult olfactory rosettes, alterations of gene expression are broad and complicated. They mainly indicated an overall increase of innate immunity, activation of secondary responses upon infection, and a neuronal degeneration that was likely a consequence of the immune responses. All of these changes were possibly caused by the loss of *Rag1* in immune system; *Rag1*'s function in the nervous system was not clear.

In the microarray with 3 dpf larvae RNA, difference between *Rag1* mutants and wt siblings was little. The transcription of a clone, 12158, was revealed to be decreased in

the *Rag1* mutants, which was also confirmed by RT-PCR. Further characterization revealed that 12158 is a part of the transcript of a CR1-1 repetitive element. The reason behind the association of its transcription and *Rag1* integrity is not clear.

CHAPTER 5 DISCUSSION

5.1 Hypothesis about DNA recombination in the nervous system

One obvious hypothesis to explain the neuronal expression of *Rag1* is: a RAG-mediated genomic recombination, similar to V(D)J recombination in the immune system, also exists in the nervous system. This was proposed 15 years ago and was heavily debated since then.

5.1.1 The presence of DNA rearrangement in the nervous system

The strongest support for the above hypothesis comes from the studies on transgenic mice. They carried an inverted *LacZ* gene flanked with RSSs so that the RAG-mediated recombination will flip and activate the *LacZ* gene. In these mice, the translated β-galactosidase activity and rearranged DNA were only detected in the nervous system and immune organs (Matsuoka et al., 1991). This strongly suggests that DNA rearrangement, possibly similar to the V(D)J recombination, exists in the nervous system. However, using the same approach, Tonegawa's group speculated that the activation of *LacZ* gene is due to special backward transcription (Abeliovich et al., 1992); Honjo's group was unable to detect DNA rearrangement in the mouse brain (Kawaichi et al., 1991). So far, there is still no evidence to further prove whether the recombination detected in Matsuaka's work are relevant to RAG1 protein or not, or if endogenous sequences are rearranged. Moreover, no neuronal and behavioral defect was seen in the *Rag1*-knockout mice (Mombaerts et al., 1992), which did not support the idea about *Rag1*'s function in neurons.

The same RSS-*LacZ* reporter cassette has also been used in P19 cells for the same purpose (Kawabata et al., 2004). The β-galactosidase activity was detected specifically

during retinoic acid induced neural differentiation. Further analysis revealed that the activation of *LacZ* is more likely due to DNA re-integration, rather than the RSS-mediated recombination. This suggests that an alternative, less stringent DNA recombination might occur specifically during neural differentiation.

There is also other evidence for the presence of neuronal DNA recombination. As we know, the non-coding signal ends are often excised as circular DNA molecules in V(D)J recombination, which can be used as an indicator for DNA recombination events (Okazaki et al., 1987; von Schwedler et al., 1990). Similar extrachromosomal circular DNA have also been found in *Drosophila* embryo (Degroote et al., 1990), *Xenopus* embryo (Cohen and Mechali, 2001), human bone marrow (Lou et al., 1993) and mammalian cell lines (Stanfield and Helinski, 1986; van Loon et al., 1994). They are possibly generated from genomic DNA via mechanisms including reverse transcription, replicon misfiring or DNA recombination. Recently, Suzuki's group detected some circular DNA molecules in mouse brain tissue (Maeda et al., 2004). Although the formation mechanism and significance are not clear, the stage specificity revealed by clone BC-1 and the genomic deletion detected at this locus suggest that a neurogenesis-specific DNA rearrangement might exist.

5.1.2 Mutations in NHEJ pathway cause the increase of neural apoptosis

Data obtained from the NHEJ (non-homologous end-joining) pathway mutants has been proposed as another support for the neuronal DNA recombination hypothesis.

Un-repaired double–strand breaks (DSBs) of genomic DNA may cause cell death. In eukaryotic cells, DSBs can be repaired by either homologous recombination or non-homologous end-joining (NHEJ) pathway. NHEJ is particularly engaged to repair the RAG-labered DSB during V(D)J recombination. Mutations in NHEJ components,

including XRCC4, DNA ligase IV, Ku 70, Ku 80 and DNA-PKs, cause the failure of V(D)J recombination and lead to premature death of lymphocytes. Intriguingly, analysis of mice embryo carrying these mutations also revealed an aberrant increase of neural apoptosis, which likely to be caused by the un-repaired DSBs (Gao et al., 1998; Sekiguchi et al., 1999). DSBs can be induced in mammalian cells by various mechanisms, including RAG-mediated cleavage. The expression of *Rag1* in the nervous system raised the possibility that RAG proteins generate DSBs in neural cells as the first step for DNA recombination.

However, some recent evidence, including our unpublished data, indicates that *Rag1* is irrelevant to the increase of neural apoptosis in those NHEJ mutants. When we knocked-down XRCC4 and DNA-ligase IV in zebrafish early embryo using anti-sense morpholino, the increased apoptosis was detected by TUNEL staining at 24 hpf (Cole and Ross, 2001), mainly in neural tube (data not shown). This does not correlate with the *Rag1* expression. According to our observation of the *Rag1:GFP* fish, *Rag1* is mainly expressed in the olfactory pit, ventral part of brain and somites, not in the neural tube around 24 hpf (refer to 3.1.2). This suggests that *Rag1* is not the cause of increased cell death in neural tube of these fish. Furthermore, we couldn't detect any *Rag1*-specific DSBs in zebrafish nervous system, either by immunofluorescence with antibodies against phosphorylated histone γ-H2AX and NBS1 (Nijmegen breakage syndrome protein) (Chen et al., 2000), nor by the end-labeling with TdT (data not shown). These data were consistent with the observation that a mutation in *Rag1* does not suppress the neural apoptosis phenotype in NHEJ mutants (Sekiguchi et al., 1999).

Although the direct cause has not been revealed, other data have suggested that the intense neuronal DSBs revealed in the NHEJ mutants are being tightly monitored. ATM (ataxia telangiectasia mutated protein) is a kinase of p53. Both of them are involved in

monitoring DSBs and mediating the apoptosis triggered by damaged DNA. In mutant mice, the deficiency of p53 and ATM was found to be able to rescue the abnormal neurogenesis caused by NHEJ mutations, but not the immune defect in these mutants (Gao et al., 2000; Lee et al., 2000b). Consistently, p53- and ATM-deficient mice show other types of neuronal abnormalities, neurobehavioral disorders and ataxia respectively (Amson et al., 2000; Borghesani et al., 2000). These data indicate a function of p53 and ATM in preventing the accumulation of neurons carrying damaged DNA, suggesting that DSBs are generated during neurogenesis under tight control and proper repair of these DSBs is critical. This also supports the presence of neurogenesis-specific DNA rearrangement, since the generation and repair of DSBs could be a part of the process.

5.1.3 Neuronal diversity

Unlike the immune system, the mechanisms to create diversity and complexity in the nervous system are largely remained unknown. Some neuronal molecules were found highly diverse and thus were regarded as the candidate substrates of the proposed "neuronal DNA recombination". Two popular examples are the odorant receptors (OR) and protocadherins (*Pcdh*).

5.1.3.1 OR genes

Odorant receptor (OR) genes form the largest gene family in the mammalian genome (Buck and Axel, 1991; Dugas and Ngai, 2001; Glusman et al., 2001; Godfrey et al., 2004; Zhang and Firestein, 2002). However, from such a large, highly dispersed repertoire, each olfactory sensory neuron (OSN) expresses only one OR gene in a mutually exclusive and monoallelic manner (Serizawa et al., 2004; Shykind, 2005). The expression of *Rag1* in the zebrafish olfactory epithelium, whose organization is highly similar to that in

mammals, suggests that DNA rearrangement is a possible mechanism for the regulation of OR genes.

However, in our study, the selective expression of *Rag1* in a sub-population of neurons in the OE (refer to 3.3.1) indicates that *Rag1*, and therefore RAG1-mediated DNA recombination, do not play essential role, such as the regulation of OR genes, in every OSN. And the fact that knocking-down *Rag1* didn't affect the axon projection of the *Rag1*-possitive neurons further confirmed that *Rag1* doesn't play a role in regulation of OR genes, which is involved in the axon projection of OSNs.

This is consistent with the studies reported in 2004 (Eggan et al., 2004; Li et al., 2004). Jaenisch's and Mombaerts's groups independently cloned mice from post-mitotic OSN nuclei. These mice expressed a normal range of OR genes instead of the expected single subtype of OR in the donor OSN, in contrast to the mice cloned from lymphocyte nuclei, which express the one type of antigen receptor in whole body (Hochedlinger and Jaenisch, 2002). This excludes the DNA rearrangement model for OR gene activation.

Now, more and more data support a new model. By sequence comparison of mouse and human genomes, a 2-kb homology (H) region far upstream of the MOR28 OR gene cluster was found to be critical in activating the downstream OR genes (Nagawa et al., 2002), indicating that a cis-acting locus control region (LCR) activates the OR genes. After an OR has been chosen, a negative feedback mechanism is proven essential in maintaining the mutual exclusive expression of the OR: the functional OR proteins were postulated to prevent further activation of other OR genes in the cells (Lewcock and Reed, 2004; Serizawa et al., 2003; Shykind et al., 2004). These are thus two parts of the theory: stochastic selection of an OR gene is mediated by a cis-acting LCR; negative feedback regulation by the OR gene product suppresses other OR genes and stabilizes the

chosen one. Together they ensure the maintenance of the one neuron-one receptor rule in the olfactory system (Serizawa et al., 2004).

5.1.3.2 Protocadherins

Protocadherins (*Pcdh*) are another family of genes that have been regarded as putative substrates of DNA recombination in the nervous system.

In both human and mice, the *Pcdh-α, β, γ* genes are clustered and display a striking genomic organization, which highly resembles the immunoglobulin and T-cell receptor loci (Wu et al., 2001). Especially in the *Pcdh-α* and *γ* clusters, large variable (V) exons are tandemly arranged and followed by three small constant region exons. Each of the V exons separately joins a constant exon to generate diverse *Pcdh* mRNA. Recent studies located a conserved regulatory motif upstream of the each V exon and proposed a multiple promoter and *cis*-alternative splicing model (Wang et al., 2002). But the high rate of somatic mutations of *Pcdh* molecules and a significant number of DSBs within *Pcdh* locus in the mouse cerebral cortex, still indicate that DNA rearrangement in *Pcdh* genes might exist (Yagi, 2003).

5.1.4 Our data suggest a modification for the old hypothesis

5.1.4.1 The restricted expression in zebrafish nervous system does not support a universal function of *Rag1* in all neurons

As revealed by transgenesis and confirmed by immunofluorescence in our study, the expression of *Rag1* was restricted to subsets of neurons in zebrafish nervous system (refer to Chapter 3). It appears in sensory organs (the OE, retina and otic vesicle) as well as the CNS (the spinal cord and brain), but only restricted to particular subsets of neurons (e.g., the microvillous OSNs in OE, RGC and amacrine cells in the retina, crista hair cells in the

otic vesicle and dorsal interneurons in the spinal cord). The selective expression of *Rag1* in the OE was maintained till adulthood. These observations indicate that any function of *Rag1* is not common for all neurons.

5.1.4.2 The non-overlap expression between *Rag1* and *Rag2* among neurons does not support the presence of neuronal V(D)J recombination

A critical requirement for V(D)J recombination in the immune system is the presence of RAG2 protein. *Rag2* transcripts had been detected in zebrafish OSNs by Shuo Lin' group (Jessen et al., 2001b). We independently generated 3 transgenic lines to examine the expression of *Rag2* in the nervous system and to examine if *Rag1* and *Rag2* are co-expressed. It was clearly seen in OE that the *Rag2*-driven reporters are not correlated with the *Rag1* expression. All three *Rag2* transgenic lines express the reporter in the same subset of ciliated OSNs, which project to a few glomeruli in the ventral OB. These OSNs are distinct from the *Rag1:GFP* expressing microvillous OSNs in cell morphology, cell location and axon projection. The expression of *Rag2*-driven reporters was also found in other parts of the nervous system at larval stages, but no obvious correlation with *Rag1* expression was detected. These data suggest that *Rag1* is unlikely to mediate V(D)J recombination in the nervous system.

5.1.4.3 Summary

Although several issues have been clarified, the nervous recombination model still remains a possibility. Our studies suggest that a modification of the old hypothesis is required. A universal DNA recombination, which acts via a mechanism similar to V(D)J recombination and is essential in creating the diversity in whole nervous system, is unlikely to exist. Instead, an alternative *Rag1*-independent or selective *Rag1*-mediated somatic DNA rearrangement in some neurons might occur.

5.2 The maturity and identity of the Rag1:GFP positive neurons in olfactory epithelium

5.2.1 GFP-positive olfactory neurons are mature

Given the fact that in the immune system *Rags* are expressed in immature lymphocytes undergoing V(D)J recombination, the presence of *Rag1* in a sub-population of neurons in olfactory epithelium (OE) raised a possibility that these cells are also immature neurons, which might undergo a type of *Rag1*-dependent genomic rearrangement. But further examination demonstrates that the *Rag1*-positive cells in OE are mature neurons.

Mature olfactory sensory neurons (OSN) are bipolar cells. They extend axons to olfactory bulb (OB) to form synapses with second-order neurons in glomeruli and terminate the knob-like dendrites with cilia or microvilli on the epithelial surface to sense chemical odorants (Farbman, 1994). By our observations, the *Rag1:GFP* positive neurons in the OE are bipolar cells. Most of them have a visible GFP-positive axon extending to the OB. These axons terminate at a few targets in the OB and the projection structures are relatively stable. The co-localization with the synapse marker SV2 proves that those GFP-positive targets are glomeruli. The dendritic end of the *Rag1:GFP* positive cells are exposed to the epithelial surface, although with lower accessibility than those GFP-negative OSNs. When fish was left in the water containing lipophilic dye such as DiI or Di8, the OSNs exposed to the water will take up these dyes and get labeled. Among the massive number of labeled cells, some GFP-positive cells also became stained and the staining could be traced to the axon terminal. The bipolar structure suggests that these GFP positive cells are mature OSNs.

In addition, the apical-basal position of the *Rag1:GFP* cells in adult OE suggests that they are mature OSNs. The proliferation, differentiation and death of neurons proceed

throughout life in the olfactory epithelium. Globose progenitor cells located in the basal layer undergo mitotic division and continually produce pro-neurons, which migrate apically in the epithelium, and then grow axon and dendrites, ultimately reach their maturity and become OSNs (Beites et al., 2005; Byrd and Brunjes, 2001; Farbman, 1994). By our observations, the *Rag1:GFP* positive neurons are located in apical layer in the adult OE. This resembles the distribution of mature neurons, not immature neurons.

We tried to further clarify this issue using immunofluorescence with an antibody against GAP-43, a maker for immature neurons. But the antibody showed a lot of non-specific staining and failed to work on zebrafish OSNs. Nevertheless, even without molecular confirmation, the bipolar cellular structure and apical localization still strongly indicate that these *Rag1:GFP* positive cells in olfactory epithelium are mature sensory neurons.

5.2.2 The *Rag1:GFP* positive cells in OE are microvillous OSNs

In teleosts OE, there are three morphologically different types of OSNs: ciliated, microvillous and crypt cells. The *Rag1:GFP* positive OSNs in adult are mainly located in the apical half of the adult OE, with a relative short dendrites and small apical endings. This cellular morphology and position along the apical-basal axis of OE strongly resemble the microvillous OSNs described in catfish and goldfish (Hansen et al., 2004; Hansen et al., 2003).

Microvillous and ciliated OSNs are the two major types of neurons in the OE. Several lines of evidence suggest that they express different signal transduction machineries and project axons to different region in the OB (Hamdani et al., 2001; Hansen et al., 2003; Morita and Finger, 1998). In zebrafish, the ciliated OSNs express OR-type odorant receptors, cyclic nucleotide-gated channel A2 subunit, olfactory marker protein (OMP), and project axons mostly to the dorsal and medial regions of the OB; whereas the

microvillous OSNs express V2R-type receptors, transient receptor potential channel C2 (TRPC2), and project axons to the lateral region of the OB. Furthermore, it has been shown recently that axons from different types of OSNs target different glomeruli in a mutually exclusive manner, from a very early stage (Sato et al., 2005). In our study we noticed that the *Rag1:GFP* positive neurons are OMP-negative; they show distinct morphology from OMP-positive OSNs, which are mainly ciliated neurons; from embryonic stage to adulthood, the *Rag1:GFP* positive axons target to a distinct set of glomeruli in the lateral OB, which highly resembles the axonal projection pattern of TRPC2 positive microvillous OSNs (Sato et al., 2005).

The cell morphology of OSNs was also known to correlate with the expression of G proteins. Ciliated OSNs express $G\alpha_{olf,}$ while microvillous OSNs are heterogenous in carrying $G\alpha_o$ and $G\alpha_q$ (Hansen et al., 2004; Hansen et al., 2003). We checked the expression of different $G\alpha$ subunit in these GFP expressing neurons and found that all GFP positive cells are $G\alpha_{olf}$ negative, $G\alpha_q$ negative, but heterogeneous in carrying $G\alpha_o$. It is consistent with the former observations and suggests that these GFP positive cells are not ciliated, but microvillous OSNs.

Despite that the expression of OR genes, odorants spectrum and the related behavior haven't been tested; the cell morphology, position in the OE, the absence of OMP and $G\alpha_{olf,}$ as well as the axonal projection to the lateral OB, all strongly suggest that these *Rag1:GFP* positive cells are microvillous OSNs.

5.3 The regulations of Rag expression

5.3.1 *Rag genes* are under complicated regulation

In the immune system, *Rag1* and *Rag2* are expressed in a stringent lineage- and stage-specific manner, which is essential for the proper control of V(D)J recombination. This

manner of *Rag* expression is accomplished through transcription regulation as well as post-translational modification.

Examination of the *Rag* locus has revealed an unusual complicated regulatory mechanism for both *Rag1* and *Rag2* transcription, which is still not fully understood. Firstly, studies on human and mouse have shown that *Rag1* and *Rag2* core promoters alone are not sufficient to drive the lymphoid-specific expression of reporter genes *in vitro*. *Rag1* promoters in human and mouse are highly conserved and active in both lymphoid and non-lymphoid cell lines (Brown et al., 1997; Zarrin et al., 1997). The *Rag2* promoter from human shows robust activity in both lymphoid and non-lymphoid cell lines (Fong et al., 2000), whereas the mouse *Rag2* promoter is lymphoid specific and behaves differentially in B and T cells (Lauring and Schlissel, 1999). Secondly, the tissue- and stage-specificity of *Rag1* and *2* expression is accomplished by a selective usage of a series of *cis* elements. Several distal regulatory elements have been identified in the *Rag2* side of the locus. In mouse, a proximal enhancer, 2.6 kb 5' upstream of *Rag2*, confer specific expression of *Rag1* and *Rag2* in B-lymphoid, but not in T- or non-lymphoid cell lines (Wei et al., 2005); whereas a distal element, 8 kb 5' of *Rag2*, is able to direct reporter expression in both B and T cell lines (Monroe et al., 1999; Wei et al., 2002). In addition, a distal silencer at *Rag1* side was found in human and zebrafish to restrict *Rag1* expression to immune tissue (Jessen et al., 1999; Zarrin, 1998). Thirdly, other careful studies further demonstrate that the two *Rag* genes, closely linked and convergently transcribed, actually undertake an unusual coordinate regulation in immune system. In the mouse, a 55 kb region, covering both *Rag1* and *Rag2*, 10 kb 5' of *Rag2* and 20 kb 5' of *Rag1*, is sufficient to direct both *Rag1* and *Rag2* expression in pro-B, pre-B and DN T cells ($CD4^-$ $CD8^-$ double negative T cells), but not in DP T cells ($CD4^+$ $CD8^+$ double positive T cells) (Yu et al., 1999). Subsequent analysis revealed that, within this region, the intergenic segment between *Rag1* and *Rag2* contains a Runx-dependent silencer, which suppresses

Rag expression in DP T cells; whereas out of this region, a *cis* element between 71 and 86 kb 5' of *Rag2* serves as an anti-silencer to counteract the silencing effect, and thus is essential for *Rag* expression in DP T cells (Yannoutsos et al., 2004). Besides these, another element located 20~25 kb 5' of *Rag2*, has been independently shown to be necessary for optimal expression of both *Rag* genes in developing B cells (Hsu et al., 2003).

Besides the complicated transcription regulation, post-translational modification is also involved in controlling the level of RAG proteins. In 1993, Desiderio's group found that RAG2 was regulated at protein level by phosphorylation (Lin and Desiderio, 1993). Subsequent studies refined and expanded this conclusion. RAG2 protein is phosphorylated by cyclin A-associated CDK2 at Thr-490 (mouse RAG2), which is located within a conserved signal sequence S/T-P-X-K/R (Li et al., 1996; Lin and Desiderio, 1994). The Thr-490 phosphorylation mediates the translocation of RAG2 from nucleus to cytoplasm and triggers its subsequent degradation through the ubiquitin/proteasome system (Mizuta et al., 2002). Since cyclinA/CDK2 activity increases sharply at the G1/S boundary, is maintained until M phase entry and eliminated at G0/G1 phase, the RAG2 accumulation and V(D)J recombination are thus coupled to the cell cycle, specifically at G0/G1 phase (Lee and Desiderio, 1999).

Some studies suggest that RAG1 protein might undergo post-translational regulation as well. As measured by pulse-chase, RAG1 is a short-lived protein, with a half life of 15 minutes (Sadofsky et al., 1993). Recent assignment of the E3 ligase function to the N-terminal RING domain of RAG1 and discovery of *Rag1* auto-ubiquitylation further suggested that *Rag1* might undergo auto-regulation (Jones and Gellert, 2003; Yurchenko et al., 2003), although the possibility that RAG1 RING domain ubiquitylates RAG2 and leads to its degradation also exists (Sadofsky, 2004).

5.3.2 Mis-regulation of *Rags* and consequence

Systematic tight regulation stringently restricts RAG proteins to specific cell lineages at specific developmental stages and phase of the cell cycle, where and when V(D)J recombination is required. RAG proteins themselves have endonuclease activity(McBlane et al., 1995). The RAG complex is able to recognize a collection of diverse RSSs, the so-called cryptic RSSs, which has been estimated to be frequent in normal genome (Lewis et al., 1997). Mis-regulation of *Rags* at any level might lead to serious consequences, such as translocation.

Demongeot's group generated transgenic mice that carries ubiquitously and constitutively co-expressed *Rag1* and *Rag2* (Barreto et al., 2001). In these mice a severe block in both B and T cell lymphopoiesis was detected, indicating that down-regulation of *Rags* at proper stages is also essential for lymphocyte development. Furthermore, these mice died between three and four weeks, much shorter than the normal lifespan of two years. This phenotype is similar to that reported in the NHEJ (non-homologous end-joining) mutant mice, suggesting the presence of an excess of un-repaired DSBs (double strand break). These DSBs might be generated through the mis-recognization of abundant cryptic RSSs (that normally are not exposed to RAGs) by the ectopically expressed RAGs.

Consistent with that, enforced expression of RAG2 throughout the cell cycle is associated with accumulation of aberrant recombination products, which were also formed in the NHEJ mutants (Lee and Desiderio, 1999).

5.3.3 Implications of *Rags* regulation

5.3.3.1 The presence of RAG2 in the OE

To examine the expression of Rag2 in detail, we generated *Rag2* transgenic zebrafish in this study. These fish carried EGFP or DsRed under the control of a ~7 kb *Rag2* promoter fragment. Totally, 3 independent lines that showed the expected reporter expression in thymus from 4 dpf were examined: one *Rag2:GFP* line and two *Rag2:DsRed* lines. All these three lines similarly expressed the reporter in a subset ciliated OSNs, which project their axons to a few ventral glomeruli. In the fish that carry both *Rag2:GFP* and *Rag2:DsRed*, the red and green OSNs partially overlapped, whereas the red and green glomeruli are completely co-localized. This suggests that the GFP and DsRed are expressed in the same subset of OSNs; their partial overlapping within this group of cells might be caused by difference in their stability and post-translational processing. The consistent expression in 3 different lines rules out the possibility that the restricted expression of *Rag2*-driven reporter in a subset OSNs comes from the integration of the transgene in different genomic locations (Wakimoto, 1998).

Another possible artificial effect might be introduced by the use of a truncated *Rag2* promoter. However, *Rag2* transcripts has been detected by both Shuo Lin and us in zebrafish OE, which proves that endogenous *Rag2* is transcribed in the OE; also the truncation of a promoter and loss of regulatory elements normally lead to expanded gene expression. This is opposite to the restricted expression of *Rag2* in zebrafish OE suggested by the transgenics. Hence, unless the promoter used contains a silencer element, the transcription activity seen in the OE is probably real.

The post-translational regulation of RAG2 is unlikely to be reflected by this transgenesis. Thus the fidelity of the reporter gene still remains to be examined. To confirm it at

protein level, we generated an antibody against a 15-aa peptide antigen within zebrafish RAG2. This antibody recognized thymocytes specifically, but failed to stain any OSNs. Thus whether endogenous RAG2 proteins exist in neurons still remains an open question.

5.3.3.2 Specific expression of *Rag1* in the nervous system

Compared to the broad yet restricted distribution of *Rag1* in the nervous system, *Rag1* can hardly be detected in other tissues. We have checked skin and muscle by confocal microscope and RT-PCR. Consistent with the reports in mice (Chun et al., 1991) and amphibian (Frippiat et al., 2001), no *Rag1* was detected in these tissues of zebrafish larvae. This suggests that the expression of *Rag1* in the nervous system is specific, not a consequence of loss of control.

5.3.3.3 Ectopic over-expression of *Rag1* showed no effect on neurons

The ubiquitous constitutive expression of both *Rag1* and *Rag2* caused early death and immune defect of the host. Since the immune defect in *Rag*-depleted mice showed no effect on the host lifespan, the early death of these mice should be caused by other reasons. By the phenotype similarity between these mice and the NHEJ mutants, it was proposed that ectopically expressed *Rags* might cause neuronal defect and lead to the early death of host (Barreto et al., 2001). In addition, the selective presence in the nervous system (Chun et al., 1991) (also refer to our data in Chapter 3) indicates that *Rag1* might have some functions restricted to a group of neurons, thus the ectopic expression might be intolerable for other neurons.

To clarify this possibility, we tried to over-express *Rag1* in neurons using the GAL4/UAS system (Scheer and Camnos-Ortega, 1999). We constructed the plasmid pFBDa_UAS:uncGFP/ UAS:Rag1, in which two UAS elements drive GFP and zebrafish *Rag1* separately, so that GFP will be turned on parallely to *Rag1* and indicate its over-

expression. This plasmid was injected into one-cell stage embryos together with the pHuC:GAL4 plasmid, which carries GAL4 driven by a neural specific HuC promoter (Park et al., 2000). 1-day after injection, RNA was isolated from these embryos and used for RT-PCR to monitor the *Rag1* over-expression. As indicated by the amplification with a pair of primers within *Rag1* coding sequence, the *Rag1* mRNA level was significantly increased in the injected embryos (Fig. 5-1). Parallely, some injected embryos were kept for observation. At 2-day after injection, GFP was clearly seen in some well differentiated neurons, but no obvious morphological defect was noticed.

Another approach was also used to over-express *Rag1*. GFP was ligated to the C-terminus of the full length *Rag1* cDNA. From this sequence, RAG1-GFP fusion mRNA was transcribed and injected into one-cell stage embryos, in which GFP signal was examined to monitor the presence of the RAG1-GFP fusion protein. In the injected embryos, some faint GFP expression was distinguishable, but no morphological phenotype was detected at early stages. The presence of faint GFP indicates that the fusion mRNA was made properly and fusion protein was translated. However, it remains to be examined whether the ectopically expressed *Rag1* is subjected to post-translational control.

5.3.3.4 The *Rag1* mutant rescue experiments

The above two approaches have also been applied to *Rag1* mutants to achieve a rescue. Several putative *Rag1* downstream genes (revealed by the microarray with larval tissue), including the 12158 (refer to 4.4), were examined to verify the rescue effect. But in both experiments, the pFBDa_UAS:uncGFP/ UAS:Rag1 and pHuC:GAL4 mixed plasmid injection and the RAG1-GFP fusion mRNA injection, no obvious rescue was detected by RT-PCR (data not shown).

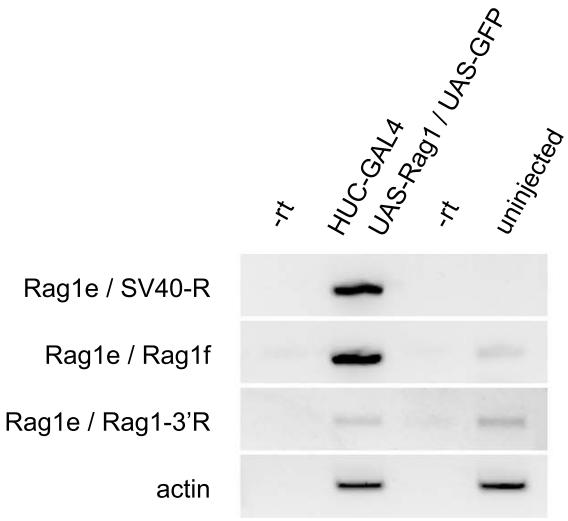

Figure 5-1. Over expression of *Rag1* in early zebrafish embryo.

Rag1e and Rag1f are respectively a forward primer and reverse primer within the *Rag1* coding sequence. The amplification with these two primers indicates the total *Rag1* expression, i.e. the mRNA transcribed from both endogenous and exogenous *Rag1* genes (row 2). SV40-R is reverse primer in the SV-40 polyA tail. Together with Rag1e, its amplification only indicates the exogenous (from plasmid) *Rag1* transcription (row 1). Rag1-3'R is reverse primer in the endogenous *Rag* intergenic region, its amplification indicates only the endogenous *Rag1* (row 3). Actin amplification was used as a loading control (row 4).

There are several possible reasons. 1) Since the expression of *Rag1* in neurons is highly restricted, the random mosaic expression provided by plasmid and mRNA injection was not sufficient to rescue the *Rag1* deficiency, which is only critical in a group of neurons. 2) The expression provided by plasmid and mRNA is transient, possibly initiate from 3~5hpf and fade on 2~3 dpf. As revealed by transgenesis, *Rag1* is expressed in different sets of neurons at different time, most of them appearing from 2 dpf onwards. Thus the above transient expression may not sufficient to rescue the *Rag1* deficiency all the time. 3) It is also possible that the *Rag1* mutants contain some other mutations in their genome, which contribute to the decrease of those candidate genes.

To prove that a gene is a specific downstream target of *Rag1*, the rescue experiment is necessary. A good choice is to generate a transgenic *Rag1* mutant line, which carries a wt *Rag1* allele as a transgene. Considering the complicated regulation of *Rag1*, it may be safe to introduce a BAC clone covering the *Rag* locus as a transgene. But this could not be done in this study due to the time constrains.

5.3.4 The understanding of *Rag* is far from complete

Although *Rag* genes were identified as early as in 1989 (Jung and Alt, 2004; Schatz et al., 1989), current studies on *Rags* are still refining our understanding.

Firstly, *Rags* function seems not to be restricted to the immune system. Besides the previously described *Rags* expression in the nervous system, low level *Rag1* or *Rag2* transcripts also have been detected in zebrafish ovary (Willett et al., 1997), *Xenopus* oocytes (Greenhalgh et al., 1993) and mouse early embryo (Hayakawa et al., 1996). This is consistent with our observation that the *Rags* transcripts are present in zebrafish early embryo. Moreover, our RT-PCR was done with zebrafish externally developed embryos, detection of *Rag1* in mouse blastocytes was confirmed by in situ hybridization

(Hayakawa et al., 1996). These ruled out the doubt that the *Rag* signals in oocytes and ovary might come from blood-borne cells. However, the function of *Rags* in germ cells and early embryo is not clear. The presence of partially joined Ig gene in shark germ cell genome suggests that *Rags* might work as a recombinase at this stage (Lee et al., 2000a).

Secondly, the properties of RAG1 and RAG2 are still under investigation. So far, V(D)J recombination is the only sequence-directed DNA rearrangement found in vertebrates. It is initiated with the recognization of specific RSS by the RAG complex. However, this recognization is not simple, because RSSs are highly variable, inspite of the specificity of recombinase targeting. In an alignment of RSSs from different species, all four nucleotides were observed at 22 of 28 12-RSS positions and 34 of 39 23-RSS positions. In mice, fewer than 16 % of RSSs carry consensus heptamers and nonamers; none contains a consensus spacer sequence. Currently, the mechanism for the RAG complex to recognize such diverse RSSs with significant specificity is not clear (Cowell et al., 2004). In addition, some studies suggest that RAG complex may have a function in recognizing other sequence or structure in the genome. Cyptic RSSs are also diverse and exist frequently in non-Ig and TCR loci of genomes (Lewis et al., 1997). They are not adjacent to V, D and J gene segments, but may also be recognized by RAG complex. Some of them were shown to have physiological functions, such as chromosome translocation and receptor editing (Davila et al., 2001; Fanning et al., 1998), which were suspected to be RAG-mediated. Meanwhile, other studies demonstrated that the RAG complex is involved in cleaving a non-B-form DNA structure within *Bcl-2* Mbr locus (containing no RSSs) of human chromosome. This cleavage might subsequently lead to the reciprocal translocation between chromosome 14 and 18, which was found to be the most common chromosomal abnormality in human cancer (Raghavan et al., 2004).

Thirdly the conserved *Rag* locus is undergoing further characterization. Besides the well studied *Rag1* and *Rag2* genes, many conserved cis-elements have also been identified in this locus and have revealed a complicated regulatory mechanism for *Rag1* and *Rag2*, but so far the characterization is not enough to fully explain the regulation of *Rags*. Moreover, another evolutionarily conserved gene, NWC (which means "very interesting' in Polish), was identified within *Rag* locus recently (Cebrat et al., 2005). It spreads over a distance of 70 kb, with gene structures highly conserved among mouse, human, chimpanzee and dog. In non-lymphoid tissue, NWC is ubiquitously expressed under control of a promoter located in the *Rag* intergenic region; whereas in T and B lymphocytes, it is regulated by the *Rag1* promoter (Cebrat et al., 2005). Studies of this new gene have just been initiated; further characterization and examination of this gene and its relationship to *Rags* should reveal more interesting knowledge.

5.4 About the microarray experiments

5.4.1 Implications of our experiments

5.4.1.1 Immune interference in isolating *Rag1* downstream neuronal genes

Our microarray with RNA isolated from adult olfactory rosettes revealed broad and complicated changes in genes expression in the *Rag1* mutant fish. These changes reflected the expected increase of innate immunity, activation of corresponding secondary responses (e.g. enhanced apoptosis and cell proliferation), as well as neuronal degeneration.

As suggested by the literature, the neuronal degeneration might be also a consequence of the increase of innate immunity. It was speculated for long time and strengthened recently, that immune response, especially the complement-mediated inflammation, may occur in CNS and selectively cause neuronal degeneration (Lucas et al., 2006; van Beek

et al., 2003). Normally the CNS is protected by the BBB (brain blood barrier), and in CNS inflammation mediators are expressed, if any, at very low level. Only in response to injury, infection or disease, which rarely occurs in CNS, is inflammation activated. So far, inflammation has been known to associate with the neuronal degeneration in many CNS diseases (Lucas et al., 2006; van Beek et al., 2003). The olfactory rosette is a sensory organ in PNS. It has not been proposed that inflammation causes neuronal degeneration in PNS. However, this might be because the efficient repair masks the phenomenon. In *Rag1* mutants, the repair response may not have been sufficient to repair the repetitive infections that occurred in the olfactory rosette, and thus causes chronic inflammation. This might make the neuronal degeneration become apparent. Furthermore, those neuronal genes down-regulated in the *Rag1* mutants are relevant to many different biological functions, and their combined loss is more likely to occur in a neuronal degeneration rather than in a decrease of a specific function. Thus we speculate that the decrease of neuronal genes in the *Rag1* mutants was mainly an indirect consequence of the adaptive immune deficiency. Using adult *Rag1* mutants for the microarray introduced interference of the immune defect. A clear analysis of *Rag1*'s neuronal function may require a mosaic rescue experiment, in which the immune defect of the *Rag1* mutants is rescued, for example, by kidney-transplantation (Langenau et al., 2004).

To avoid the effect of immune deficiency, we had tried a microarray with RNA isolated from the larvae at 3 dpf, when the adaptive immune system hasn't initiated, but the nervous system is largely established. However, from this experiment only 15 genes were identified to be significantly changed by ANOVA analysis, and 14 of them are poorly annotated ESTs. The computation result with the SAM program is highly similar, suggesting that between wt and *Rag1* mutants, very little difference can be detected by microarray at this stage. This is likely due to the fact that a lot irrelevant tissue, such as non-neural tissue and non-*Rag1*-expressing neural tissue, were included in the

microarray, where they diluted and masked the possible neuronal function of *Rag1*. Further purification of *Rag1*-expressing tissue might improve the microarray result, but this is technically difficult currently.

5.4.1.2 Gene expression beyond the tissue restriction

In our adult OE microarray, RNA used for hybridization was extracted from isolated adult olfactory rosettes. However, minority of genes, which are known to be enriched and functional in other tissue, were also present and showed expression changes in this microarray result. For example, *Tesk2* and *Pl10*, two genes expressed in testis and known to function in spermatogenesis; *Siah2*, a gene encoding an E3 ubiquitin ligase and required for the specification of r7 photoreceptor cells in the eye, were found to be present in wt olfactory samples, but decreased in the *Rag1* mutant rosettes. This suggests an unknown function of these genes in the OE. But, currently no evidence is available to verify these results.

5.4.2 Microarray with zebrafish

Zebrafish is an important vertebrate model for developmental and genetic studies. In recent years, the genome sequencing project and several EST (expressed sequence tag) projects accumulated a large amount of genomic information and also established zebrafish as a genomic model. High intensity microarray for genome wide gene expression analysis has been established for zebrafish, and has been used in mapping the transcriptom profiles during different embryonic stages (Mathavan et al., 2005) and systematic analysis of the downstream effect of a mutated gene (Qian et al., 2005; Sumanas et al., 2005). However, ESTs, the major contributors in zebrafish microarray (in our experiments, 14309 from 16399 oligo probes were designed from EST sequences), are still poorly annotated. This largely preventes further analysis of the microarray result,

and limits the usage of microarray in zebrafish. In our experiments, the original annotation of the Compugen-Sigma oligo set was out of date. The most recent annotations were obtained from Silicon-Genetics using the GeneSpider function in the GeneSpring software, and supplemented with the annotation database of GIS (Genome Institute of Singapore, http://giscompute.gis.a-star.edu.sg/~govind/zebrafish/), which combined recent annotations from several databases (including Entrez Gene, Zebrafish UniGene Cluster and Zebrafish Gene Index) and was used in a recent publication (Mathavan et al., 2005). After all of these efforts, there were still 131 genes from 341 significants totally un-annotated. These may contain a critical clue for the neuronal function of *Rag1*. Further effort on the characterization of these ESTs might thus be of use.

5.5 Abundant polymorphism in zebrafish genome

5.5.1 Abundant nucleotide sequence polymorphism revealed by GeneFishing technology

Before we started the microarray experiments, we have tried another approach to search for *Rag1*-downstream genes in the nervous system. This is a RT-PCR based differential screening with a set of specially designed degenerate primers (GeneFishing, DEG kit). These primers, named as ACPs (annealing control primers), contain three parts. The regulator between the core and the universal sequence plays the key role in annealing of each portion to a template, thus increases the specificity and fish out differentially expressed genes.

To avoid immune system effects, RNA from 3 dpf embryos was used. RT-PCR products differentially amplified from *Rag1* mutant and Wt siblings were sub-cloned and sequenced. From this, a pair of internal primers were designed and used in RT-PCR to confirm the expression difference.

The RT-PCR with ACP primers looked promising. Some different amplifications were detected between *Rag1* mutants and Wt siblings (Fig. 5-2A, B; red and green arrowheads), and they were reproducible in different PCR reactions (Fig. 5-2A, B; red arrowheads). But, RT-PCR with internal primers designed from the cloned fragments didn't show any significant difference between *Rag1* mutants and Wt siblings (Fig. 5-2C). This indicates that the difference displayed in the RT-PCR with ACP primers might come from nucleotide sequence polymorphism between *Rag1* mutants and Wt siblings. Totally 20 clones were checked. None of them confirmed the expression difference. This suggests that sequence polymorphism in the zebrafish genome is abundant, and that this approach is unsuitable.

5.5.2 A repetitive element generated polymorphism was found in 12158 locus

Clone 12158, which was picked out from the larva microarray as a gene down-regulated in the *Rag1* mutant, was also found to be polymorphic among wt siblings. Two alleles (12158A and 12158B) were identified to be single-copy alleles at the same locus in zebrafish genome (Fig. 4-11C, D). Comparison between these two alleles indicates that 12158B is generated from the insertion of a repetitive element CR1-1 in the 12158A allele (refer to Chapter 4.4). Thus the 12158B can be considered as a repetitive element generated polymorphic allele in this locus.

5.6 Overall conclusion

Using transgenesis and immunofluorescence, we found that *Rag1* is expressed in the zebrafish nervous system in a selective manner, which does not correlate with the *Rag2* expression indicated by transgenesis. These data strongly suggest that *Rag1* in the nervous system is unlikely to mediate DNA rearrangement similar to V(D)J recombination in the immune system, but may play a role restricted to subsets of neurons.

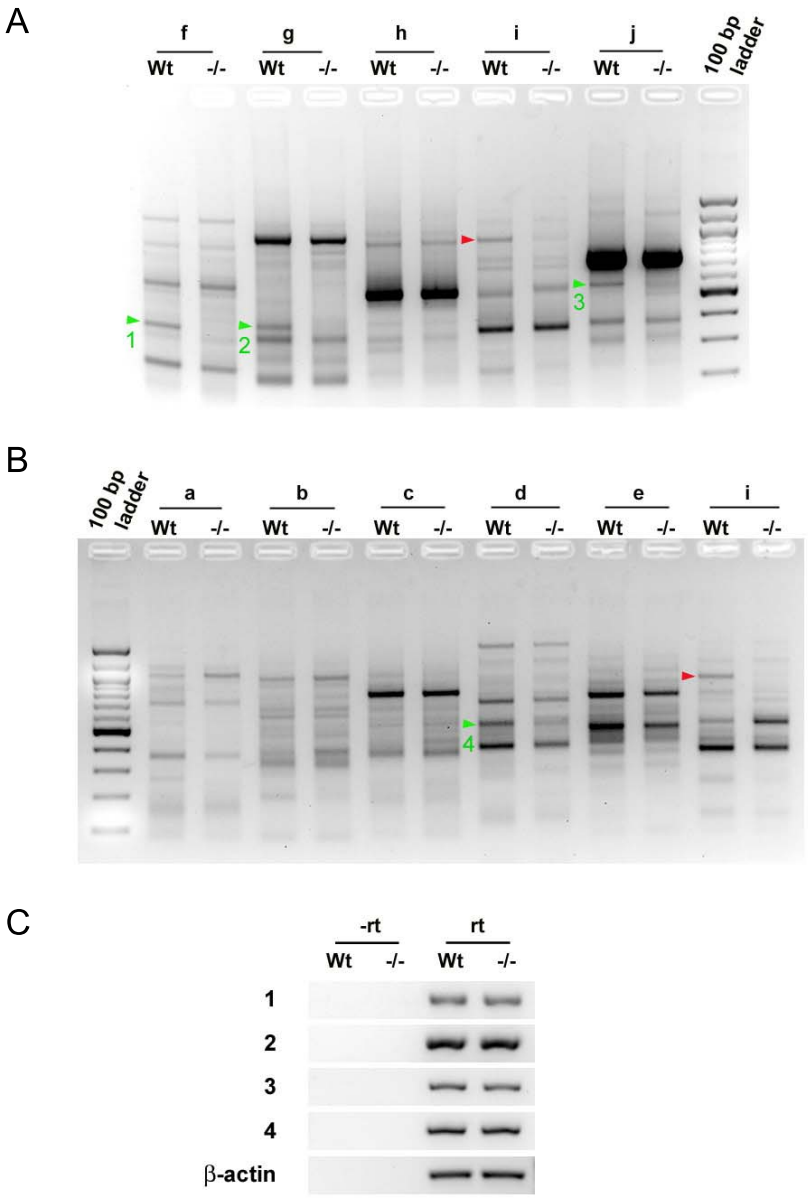

Figure 5-2. Polymophism revealed by the GeneFishing DEG kit.

(A, B) RT-PCR with annealing control primers (APC) a to j for Rag1 mutants (-/-) and Wt siblings (wt). Some different amplifications were indicated with red and green arrowheads. (A) and (B) showed results from different PCR reactions. A reproducible differentially amplified band with primer i was indicated with red arrowhead. (C) RT-PCR with internal primers from clone 1-4 (green arrowheads in panel A and B) didn't show significant difference between Rag1 mutants and wt siblings.

Overall gene expressions in adult olfactory rosettes were compared between *Rag1* mutants and wt siblings by microarray. The complicated changes revealed in the experiment indicated an overall increase of innate immunity, activation of secondary responses, and a neuronal degeneration that was also likely a consequence of the increase of innate immunity. In the microarray with 3 dpf larvae RNA, the transcription of clone 12158 was revealed to be associated with *Rag1* integrity, which was also confirmed by RT-PCR.

All in all, our expression analysis suggests that *Rag1* may play a function in selected groups of neurons; our microarray experiments revealed the global effect of *Rag1* deficiency and some candidates for *Rag1* downstream genes in neurons.

REFERENCES

Abeliovich, A., Gerber, D., Tanaka, O., Katsuki, M., Graybiel, A. M. and Tonegawa, S. (1992). On somatic recombination in the central nervous system of transgenic mice. *Science* **257**, 404-10.

Ackermann, G. E. and Paw, B. H. (2003). Zebrafish: a genetic model for vertebrate organogenesis and human disorders. *Front Biosci* **8**, d1227-53.

Agrawal, A., Eastman, Q. M. and Schatz, D. G. (1998). Transposition mediated by RAG1 and RAG2 and its implications for the evolution of the immune system. *Nature* **394**, 744-51.

Akamatsu, Y., Monroe, R., Dudley, D. D., Elkin, S. K., Gartner, F., Talukder, S. R., Takahama, Y., Alt, F. W., Bassing, C. H. and Oettinger, M. A. (2003). Deletion of the RAG2 C terminus leads to impaired lymphoid development in mice. *Proc Natl Acad Sci U S A* **100**, 1209-14.

Amson, R., Lassalle, J. M., Halley, H., Prieur, S., Lethrosne, F., Roperch, J. P., Israeli, D., Gendron, M. C., Duyckaerts, C., Checler, F. et al. (2000). Behavioral alterations associated with apoptosis and down-regulation of presenilin 1 in the brains of p53-deficient mice. *Proc Natl Acad Sci U S A* **97**, 5346-50.

Asano-Miyoshi, M., Suda, T., Yasuoka, A., Osima, S., Yamashita, S., Abe, K. and Emori, Y. (2000). Random expression of main and vomeronasal olfactory receptor genes in immature and mature olfactory epithelia of Fugu rubripes. *J Biochem (Tokyo)* **127**, 915-24.

Ashworth, R. (2004). Approaches to measuring calcium in zebrafish: focus on neuronal development. *Cell Calcium* **35**, 393-402.

Axelson, H. (2004). The Notch signaling cascade in neuroblastoma: role of the basic helix-loop-helix proteins HASH-1 and HES-1. *Cancer Lett* **204**, 171-8.

Baier, H. and Korsching, S. (1994). Olfactory glomeruli in the zebrafish form an invariant pattern and are identifiable across animals. *J Neurosci* **14**, 219-30.

Bakalyar, H. A. and Reed, R. R. (1990). Identification of a specialized adenylyl cyclase that may mediate odorant detection. *Science* **250**, 1403-6.

Bargmann, C. I. (1997). Olfactory receptors, vomeronasal receptors, and the organization of olfactory information. *Cell* **90**, 585-7.

Barlow, J. Z., Kelley, K. A., Bozdagi, O. and Huntley, G. W. (2002). Testing the role of the cell-surface molecule Thy-1 in regeneration and plasticity of connectivity in the CNS. *Neuroscience* **111**, 837-52.

Barnea, G., O'Donnell, S., Mancia, F., Sun, X., Nemes, A., Mendelsohn, M. and Axel, R. (2004). Odorant receptors on axon termini in the brain. *Science* **304**, 1468.

Barreto, V., Marques, R. and Demengeot, J. (2001). Early death and severe lymphopenia caused by ubiquitous expression of the Rag1 and Rag2 genes in mice. *Eur J Immunol* **31**, 3763-72.

Bassing, C. H., Swat, W. and Alt, F. W. (2002). The mechanism and regulation of chromosomal V(D)J recombination. *Cell* **109 Suppl**, S45-55.

Beilharz, E. J., Zhukovsky, E., Lanahan, A. A., Worley, P. F., Nikolich, K. and Goodman, L. J. (1998). Neuronal activity induction of the stathmin-like gene RB3 in the rat hippocampus: possible role in neuronal plasticity. *J Neurosci* **18**, 9780-9.

Beites, C. L., Kawauchi, S., Crocker, C. E. and Calof, A. L. (2005). Identification and molecular regulation of neural stem cells in the olfactory epithelium. *Exp Cell Res* **306**, 309-16.

Bernhardt, R. R., Chitnis, A. B., Lindamer, L. and Kuwada, J. Y. (1990). Identification of spinal neurons in the embryonic and larval zebrafish. *J Comp Neurol* **302**, 603-16.

Bernstein, R. M., Schluter, S. F., Bernstein, H. and Marchalonis, J. J. (1996). Primordial emergence of the recombination activating gene 1 (RAG1): sequence of the complete shark gene indicates homology to microbial integrases. *Proc Natl Acad Sci U S A* **93**, 9454-9.

Bilotta, J. and Saszik, S. (2001). The zebrafish as a model visual system. *Int J Dev Neurosci* **19**, 621-9.

Borghesani, P. R., Alt, F. W., Bottaro, A., Davidson, L., Aksoy, S., Rathbun, G. A., Roberts, T. M., Swat, W., Segal, R. A. and Gu, Y. (2000). Abnormal development of Purkinje cells and lymphocytes in Atm mutant mice. *Proc Natl Acad Sci U S A* **97**, 3336-41.

Boulanger, L. M. and Shatz, C. J. (2004). Immune signalling in neural development, synaptic plasticity and disease. *Nat Rev Neurosci* **5**, 521-31.

Brandt, V. L. and Roth, D. B. (2004). V(D)J recombination: how to tame a transposase. *Immunol Rev* **200**, 249-60.

Brennan, P. A. (2001). The vomeronasal system. *Cell Mol Life Sci* **58**, 546-55.

Brown, S. T., Miranda, G. A., Galic, Z., Hartman, I. Z., Lyon, C. J. and Aguilera, R. J. (1997). Regulation of the RAG-1 promoter by the NF-Y transcription factor. *J Immunol* **158**, 5071-4.

Bruce Alberts, A. J., Julian Lewis, Martin Raff, Keith Roberts, and Peter Walter. (2002). Molecular Biology of the Cell: Taylor & Francis Group Ltd.

Buck, L. and Axel, R. (1991). A novel multigene family may encode odorant receptors: a molecular basis for odor recognition. *Cell* **65**, 175-87.

Buckley, K. and Kelly, R. B. (1985). Identification of a transmembrane glycoprotein specific for secretory vesicles of neural and endocrine cells. *J Cell Biol* **100**, 1284-94.

Burrill, J. D. and Easter, S. S., Jr. (1994). Development of the retinofugal projections in the embryonic and larval zebrafish (Brachydanio rerio). *J Comp Neurol* **346**, 583-600.

Byrd, C. A. and Brunjes, P. C. (1995). Organization of the olfactory system in the adult zebrafish: histological, immunohistochemical, and quantitative analysis. *J Comp Neurol* **358**, 247-59.

Byrd, C. A. and Brunjes, P. C. (2001). Neurogenesis in the olfactory bulb of adult zebrafish. *Neuroscience* **105**, 793-801.

Cebrat, M., Miazek, A. and Kisielow, P. (2005). Identification of a third evolutionarily conserved gene within the RAG locus and its RAG1-dependent and -independent regulation. *Eur J Immunol* **35**, 2230-8.

Chatterji, M., Tsai, C. L. and Schatz, D. G. (2004). New concepts in the regulation of an ancient reaction: transposition by RAG1/RAG2. *Immunol Rev* **200**, 261-71.

Chen, H. T., Bhandoola, A., Difilippantonio, M. J., Zhu, J., Brown, M. J., Tai, X., Rogakou, E. P., Brotz, T. M., Bonner, W. M., Ried, T. et al. (2000). Response to RAG-mediated VDJ cleavage by NBS1 and gamma-H2AX. *Science* **290**, 1962-5.

Chess, A., Simon, I., Cedar, H. and Axel, R. (1994). Allelic inactivation regulates olfactory receptor gene expression. *Cell* **78**, 823-34.

Chun, J. J., Schatz, D. G., Oettinger, M. A., Jaenisch, R. and Baltimore, D. (1991). The recombination activating gene-1 (RAG-1) transcript is present in the murine central nervous system. *Cell* **64**, 189-200.

Cohen, S. and Mechali, M. (2001). A novel cell-free system reveals a mechanism of circular DNA formation from tandem repeats. *Nucleic Acids Res* **29**, 2542-8.

Cole, L. K. and Ross, L. S. (2001). Apoptosis in the developing zebrafish embryo. *Dev Biol* **240**, 123-42.

Costagli, A., Kapsimali, M., Wilson, S. W. and Mione, M. (2002). Conserved and divergent patterns of Reelin expression in the zebrafish central nervous system. *J Comp Neurol* **450**, 73-93.

Cowell, L. G., Davila, M., Ramsden, D. and Kelsoe, G. (2004). Computational tools for understanding sequence variability in recombination signals. *Immunol Rev* **200**, 57-69.

Cruse, J. M. L., Robert E. (1999). Atlas of Immunology. Boca Raton, London, New York, Washington, D.C.: CRC Press LLC.

Cui, X. and Churchill, G. A. (2003). Statistical tests for differential expression in cDNA microarray experiments. *Genome Biol* **4**, 210.

Cutforth, T., Moring, L., Mendelsohn, M., Nemes, A., Shah, N. M., Kim, M. M., Frisen, J. and Axel, R. (2003). Axonal ephrin-As and odorant receptors: coordinate determination of the olfactory sensory map. *Cell* **114**, 311-22.

Davila, M., Foster, S., Kelsoe, G. and Yang, K. (2001). A role for secondary V(D)J recombination in oncogenic chromosomal translocations? *Adv Cancer Res* **81**, 61-92.

De Block, C. E., Colpin, G., Thielemans, K., Coopmans, W., Bogers, J. J., Pelckmans, P. A., Van Marck, E. A., Van Hoof, V., Martin, M., De Leeuw, I. H. et al. (2004). Neuroendocrine tumor markers and enterochromaffin-like cell hyper/dysplasia in type 1 diabetes. *Diabetes Care* **27**, 1387-93.

De, P. and Rodgers, K. K. (2004). Putting the pieces together: identification and characterization of structural domains in the V(D)J recombination protein RAG1. *Immunol Rev* **200**, 70-82.

De Robertis, E. (1967). Ultrastructure and cytochemistry of the synaptic region. The macromolecular components involved in nerve transmission are being studied. *Science* **156**, 907-14.

Degroote, F., Renault, S. and Picard, G. (1990). Nucleotide sequence of circular DNA molecules homologous to the 240 bp tandem repeats of the intergenic spacer of Drosophila melanogaster ribosomal DNA. *Biol Cell* **69**, 69-70.

Deininger, P. L. and Batzer, M. A. (2002). Mammalian retroelements. *Genome Res* **12**, 1455-65.

Delcomyn, F. (1998). Foundations of Neurobiology. New York: W. H. Freeman and Company.

Detrich, H. W., 3rd, Westerfield, M. and Zon, L. I. (1999). Overview of the Zebrafish system. *Methods Cell Biol* **59**, 3-10.

Dhallan, R. S., Yau, K. W., Schrader, K. A. and Reed, R. R. (1990). Primary structure and functional expression of a cyclic nucleotide-activated channel from olfactory neurons. *Nature* **347**, 184-7.

Donato, R. (2001). S100: a multigenic family of calcium-modulated proteins of the EF-hand type with intracellular and extracellular functional roles. *Int J Biochem Cell Biol* **33**, 637-68.

Dooley, K. and Zon, L. I. (2000). Zebrafish: a model system for the study of human disease. *Curr Opin Genet Dev* **10**, 252-6.

Downes, G. B., Waterbury, J. A. and Granato, M. (2002). Rapid in vivo labeling of identified zebrafish neurons. *Genesis* **34**, 196-202.

Driever, W., Solnica-Krezel, L., Schier, A. F., Neuhauss, S. C., Malicki, J., Stemple, D. L., Stainier, D. Y., Zwartkruis, F., Abdelilah, S., Rangini, Z. et al. (1996). A genetic screen for mutations affecting embryogenesis in zebrafish. *Development* **123**, 37-46.

D'Souza, J., Hendricks, M., Le Guyader, S., Subburaju, S., Grunewald, B., Scholich, K. and Jesuthasan, S. (2005). Formation of the retinotectal projection requires Esrom, an ortholog of PAM (protein associated with Myc). *Development* **132**, 247-56.

Dudley, D. D., Sekiguchi, J., Zhu, C., Sadofsky, M. J., Whitlow, S., DeVido, J., Monroe, R. J., Bassing, C. H. and Alt, F. W. (2003). Impaired V(D)J recombination and lymphocyte development in core RAG1-expressing mice. *J Exp Med* **198**, 1439-50.

Dugas, J. C. and Ngai, J. (2001). Analysis and characterization of an odorant receptor gene cluster in the zebrafish genome. *Genomics* **71**, 53-65.

Dulac, C. and Axel, R. (1995). A novel family of genes encoding putative pheromone receptors in mammals. *Cell* **83**, 195-206.

Dyer, M. A. and Cepko, C. L. (2001). Regulating proliferation during retinal development. *Nat Rev Neurosci* **2**, 333-42.

Dynes, J. L. and Ngai, J. (1998). Pathfinding of olfactory neuron axons to stereotyped glomerular targets revealed by dynamic imaging in living zebrafish embryos. *Neuron* **20**, 1081-91.

Eggan, K., Baldwin, K., Tackett, M., Osborne, J., Gogos, J., Chess, A., Axel, R. and Jaenisch, R. (2004). Mice cloned from olfactory sensory neurons. *Nature* **428**, 44-9.

Fanning, L., Bertrand, F. E., Steinberg, C. and Wu, G. E. (1998). Molecular mechanisms involved in receptor editing at the Ig heavy chain locus. *Int Immunol* **10**, 241-6.

Farbman, A. I. (1994). Developmental biology of olfactory sensory neurons. *Semin Cell Biol* **5**, 3-10.

Farrar, W. L., Hill, J. M., Harel-Bellan, A. and Vinocour, M. (1987). The immune logical brain. *Immunol Rev* **100**, 361-78.

Feng, B., Bulchand, S., Yaksi, E., Friedrich, R. W. and Jesuthasan, S. (2005). The recombination activation gene 1 (Rag1) is expressed in a subset of zebrafish olfactory neurons but is not essential for axon targeting or amino acid detection. *BMC Neurosci* **6**, 46.

Fetcho, J. R. and Liu, K. S. (1998). Zebrafish as a model system for studying neuronal circuits and behavior. *Ann N Y Acad Sci* **860**, 333-45.

Firestein, S., Darrow, B. and Shepherd, G. M. (1991). Activation of the sensory current in salamander olfactory receptor neurons depends on a G protein-mediated cAMP second messenger system. *Neuron* **6**, 825-35.

Fong, I. C., Zarrin, A. A., Wu, G. E. and Berinstein, N. L. (2000). Functional analysis of the human RAG 2 promoter. *Mol Immunol* **37**, 391-402.

Friedrich, R. W. and Korsching, S. I. (1997). Combinatorial and chemotopic odorant coding in the zebrafish olfactory bulb visualized by optical imaging. *Neuron* **18**, 737-52.

Frippiat, C., Kremarik, P., Ropars, A., Dournon, C. and Frippiat, J. P. (2001). The recombination-activating gene 1 of Pleurodeles waltl (urodele amphibian) is transcribed in lymphoid tissues and in the central nervous system. *Immunogenetics* **52**, 264-75.

Fugmann, S. D., Lee, A. I., Shockett, P. E., Villey, I. J. and Schatz, D. G. (2000). The RAG proteins and V(D)J recombination: complexes, ends, and transposition. *Annu Rev Immunol* **18**, 495-527.

Gao, Y., Ferguson, D. O., Xie, W., Manis, J. P., Sekiguchi, J., Frank, K. M., Chaudhuri, J., Horner, J., DePinho, R. A. and Alt, F. W. (2000). Interplay of p53 and DNA-repair protein XRCC4 in tumorigenesis, genomic stability and development. *Nature* **404**, 897-900.

Gao, Y., Sun, Y., Frank, K. M., Dikkes, P., Fujiwara, Y., Seidl, K. J., Sekiguchi, J. M., Rathbun, G. A., Swat, W., Wang, J. et al. (1998). A critical role for DNA end-joining proteins in both lymphogenesis and neurogenesis. *Cell* **95**, 891-902.

Garlanda, C., Bottazzi, B., Bastone, A. and Mantovani, A. (2005). Pentraxins at the crossroads between innate immunity, inflammation, matrix deposition, and female fertility. *Annu Rev Immunol* **23**, 337-66.

Gellert, M. (2002). V(D)J recombination: RAG proteins, repair factors, and regulation. *Annu Rev Biochem* **71**, 101-32.

Germana, A., Montalbano, G., Laura, R., Ciriaco, E., del Valle, M. E. and Vega, J. A. (2004). S100 protein-like immunoreactivity in the crypt olfactory neurons of the adult zebrafish. *Neurosci Lett* **371**, 196-8.

Ghysen, A. and Dambly-Chaudiere, C. (2004). Development of the zebrafish lateral line. *Curr Opin Neurobiol* **14**, 67-73.

Glusman, G., Yanai, I., Rubin, I. and Lancet, D. (2001). The complete human olfactory subgenome. *Genome Res* **11**, 685-702.

Godfrey, P. A., Malnic, B. and Buck, L. B. (2004). The mouse olfactory receptor gene family. *Proc Natl Acad Sci U S A* **101**, 2156-61.

Gorman, J. R. and Alt, F. W. (1998). Regulation of immunoglobulin light chain isotype expression. *Adv Immunol* **69**, 113-81.

Goulding, E. H., Ngai, J., Kramer, R. H., Colicos, S., Axel, R., Siegelbaum, S. A. and Chess, A. (1992). Molecular cloning and single-channel properties of the cyclic nucleotide-gated channel from catfish olfactory neurons. *Neuron* **8**, 45-58.

Greenhalgh, P., Olesen, C. E. and Steiner, L. A. (1993). Characterization and expression of recombination activating genes (RAG-1 and RAG-2) in Xenopus laevis. *J Immunol* **151**, 3100-10.

Greenhalgh, P. and Steiner, L. A. (1995). Recombination activating gene 1 (Rag1) in zebrafish and shark. *Immunogenetics* **41**, 54-5.

Grunwald, D. J. and Eisen, J. S. (2002). Headwaters of the zebrafish -- emergence of a new model vertebrate. *Nat Rev Genet* **3**, 717-24.

Grynfeld, A., Pahlman, S. and Axelson, H. (2000). Induced neuroblastoma cell differentiation, associated with transient HES-1 activity and reduced HASH-1 expression, is inhibited by Notch1. *Int J Cancer* **88**, 401-10.

Haddon, C. and Lewis, J. (1996). Early ear development in the embryo of the zebrafish, Danio rerio. *J Comp Neurol* **365**, 113-28.

Haffter, P., Granato, M., Brand, M., Mullins, M. C., Hammerschmidt, M., Kane, D. A., Odenthal, J., van Eeden, F. J., Jiang, Y. J., Heisenberg, C. P. et al. (1996). The identification

of genes with unique and essential functions in the development of the zebrafish, Danio rerio. *Development* **123**, 1-36.

Halpern, M. and Martinez-Marcos, A. (2003). Structure and function of the vomeronasal system: an update. *Prog Neurobiol* **70**, 245-318.

Hamdani, E. H., Alexander, G. and Doving, K. B. (2001). Projection of sensory neurons with microvilli to the lateral olfactory tract indicates their participation in feeding behaviour in crucian carp. *Chem Senses* **26**, 1139-44.

Hansen, A., Anderson, K. T. and Finger, T. E. (2004). Differential distribution of olfactory receptor neurons in goldfish: structural and molecular correlates. *J Comp Neurol* **477**, 347-59.

Hansen, A. and Finger, T. E. (2000). Phyletic distribution of crypt-type olfactory receptor neurons in fishes. *Brain Behav Evol* **55**, 100-10.

Hansen, A., Rolen, S. H., Anderson, K., Morita, Y., Caprio, J. and Finger, T. E. (2003). Correlation between olfactory receptor cell type and function in the channel catfish. *J Neurosci* **23**, 9328-39.

Hansen, A. and Zeiske, E. (1993). Development of the olfactory organ in the zebrafish, Brachydanio rerio. *J Comp Neurol* **333**, 289-300.

Hansen, A. and Zeiske, E. (1998). The peripheral olfactory organ of the zebrafish, Danio rerio: an ultrastructural study. *Chem Senses* **23**, 39-48.

Hansen, J. D. and Kaattari, S. L. (1995). The recombination activation gene 1 (RAG1) of rainbow trout (Oncorhynchus mykiss): cloning, expression, and phylogenetic analysis. *Immunogenetics* **42**, 188-95.

Hansen, J. D. and Kaattari, S. L. (1996). The recombination activating gene 2 (RAG2) of the rainbow trout Oncorhynchus mykiss. *Immunogenetics* **44**, 203-11.

Havemose-Poulsen, A. and Holmstrup, P. (1997). Factors affecting IL-1-mediated collagen metabolism by fibroblasts and the pathogenesis of periodontal disease: a review of the literature. *Crit Rev Oral Biol Med* **8**, 217-36.

Hayakawa, S., Tochigi, M., Chishima, F., Shiraishi, H., Takahashi, N., Watanabe, K., Fujii, K. T. and Satoh, K. (1996). Expression of the recombinase-activating gene (RAG-1) in murine early embryogenesis. *Immunol Cell Biol* **74**, 52-6.

Heasman, J. (2002). Morpholino oligos: making sense of antisense? *Dev Biol* **243**, 209-14.

Higashijima, S., Hotta, Y. and Okamoto, H. (2000). Visualization of cranial motor neurons in live transgenic zebrafish expressing green fluorescent protein under the control of the islet-1 promoter/enhancer. *J Neurosci* **20**, 206-18.

Hiom, K., Melek, M. and Gellert, M. (1998). DNA transposition by the RAG1 and RAG2 proteins: a possible source of oncogenic translocations. *Cell* **94**, 463-70.

Hochedlinger, K. and Jaenisch, R. (2002). Monoclonal mice generated by nuclear transfer from mature B and T donor cells. *Nature* **415**, 1035-8.

Hodgetts, R. (2004). Eukaryotic gene regulation by targeted chromatin re-modeling at dispersed, middle-repetitive sequence elements. *Curr Opin Genet Dev* **14**, 680-5.

Hsu, L. Y., Lauring, J., Liang, H. E., Greenbaum, S., Cado, D., Zhuang, Y. and Schlissel, M. S. (2003). A conserved transcriptional enhancer regulates RAG gene expression in developing B cells. *Immunity* **19**, 105-17.

Hu, K., Carroll, J., Rickman, C. and Davletov, B. (2002). Action of complexin on SNARE complex. *J Biol Chem* **277**, 41652-6.

Ishibashi, M., Ang, S. L., Shiota, K., Nakanishi, S., Kageyama, R. and Guillemot, F. (1995). Targeted disruption of mammalian hairy and Enhancer of split homolog-1 (HES-1) leads to up-regulation of neural helix-loop-helix factors, premature neurogenesis, and severe neural tube defects. *Genes Dev* **9**, 3136-48.

Jekosch, K. (2004). The zebrafish genome project: sequence analysis and annotation. *Methods Cell Biol* **77**, 225-39.

Jessell, T. M. and Kandel, E. R. (1993). Synaptic transmission: a bidirectional and self-modifiable form of cell-cell communication. *Cell* **72 Suppl**, 1-30.

Jessen, J. R., Jessen, T. N., Vogel, S. S. and Lin, S. (2001a). Concurrent expression of recombination activating genes 1 and 2 in zebrafish olfactory sensory neurons. *Genesis* **29**, 156-62.

Jessen, J. R., Jessen, T. N., Vogel, S. S. and Lin, S. (2001b). Concurrent expression of recombination activating genes 1 and 2 in zebrafish olfactory sensory neurons. *Genesis* **29**, 156-62.

Jessen, J. R., Willett, C. E. and Lin, S. (1999). Artificial chromosome transgenesis reveals long-distance negative regulation of rag1 in zebrafish. *Nat Genet* **23**, 15-6.

Jesuthasan, S. and Subburaju, S. (2002). Gene transfer into zebrafish by sperm nuclear transplantation. *Dev Biol* **242**, 88-95.

Jones, J. M. and Gellert, M. (2001). Intermediates in V(D)J recombination: a stable RAG1/2 complex sequesters cleaved RSS ends. *Proc Natl Acad Sci U S A* **98**, 12926-31.

Jones, J. M. and Gellert, M. (2003). Autoubiquitylation of the V(D)J recombinase protein RAG1. *Proc Natl Acad Sci U S A* **100**, 15446-51.

Jones, J. M. and Gellert, M. (2004). The taming of a transposon: V(D)J recombination and the immune system. *Immunol Rev* **200**, 233-48.

Jorgensen, E. M. and Mango, S. E. (2002). The art and design of genetic screens: caenorhabditis elegans. *Nat Rev Genet* **3**, 356-69.

Jung, D. and Alt, F. W. (2004). Unraveling V(D)J recombination; insights into gene regulation. *Cell* **116**, 299-311.

Kane, D. A. and Kimmel, C. B. (1993). The zebrafish midblastula transition. *Development* **119**, 447-56.

Kapitonov, V. V. and Jurka, J. (2005). RAG1 Core and V(D)J Recombination Signal Sequences Were Derived from Transib Transposons. *PLoS Biol* **3**, e181.

Kawabata, M., Kawabata, T. and Saeki, K. (2004). DNA rearrangement activity during retinoic acid-induced neural differentiation of P19 mouse embryonal carcinoma cells. *Acta Med Okayama* **58**, 263-70.

Kawaichi, M., Oka, C., Reeves, R., Kinoshita, M. and Honjo, T. (1991). Recombination of exogenous interleukin 2 receptor gene flanked by immunoglobulin recombination signal sequences in a pre-B cell line and transgenic mice. *J Biol Chem* **266**, 18387-94.

Kawakami, K. (2004). Transgenesis and gene trap methods in zebrafish by using the Tol2 transposable element. *Methods Cell Biol* **77**, 201-22.

Kawakami, K. and Hopkins, N. (1996). Rapid identification of transgenic zebrafish. *Trends Genet* **12**, 9-10.

Kerr, M. K. and Churchill, G. A. (2001). Statistical design and the analysis of gene expression microarray data. *Genet Res* **77**, 123-8.

Kim, D. R., Dai, Y., Mundy, C. L., Yang, W. and Oettinger, M. A. (1999). Mutations of acidic residues in RAG1 define the active site of the V(D)J recombinase. *Genes Dev* **13**, 3070-80.

Kim, D. R., Park, S. J. and Oettinger, M. A. (2000). V(D)J recombination: site-specific cleavage and repair. *Mol Cells* **10**, 367-74.

Kimmel, C. B. (1993). Patterning the brain of the zebrafish embryo. *Annu Rev Neurosci* **16**, 707-32.

Klug, W. S. C., Micheal R. (2000). Concepts of Genetics. New Jersey: Prentice hall.

Kobayashi, M., Hjerling-Leffler, J. and Ernfors, P. (2006). Increased progenitor proliferation and apoptotic cell death in the sensory lineage of mice overexpressing N-myc. *Cell Tissue Res* **323**, 81-90.

Koh, T. W. and Bellen, H. J. (2003). Synaptotagmin I, a Ca2+ sensor for neurotransmitter release. *Trends Neurosci* **26**, 413-22.

Komori, T., Okada, A., Stewart, V. and Alt, F. W. (1993). Lack of N regions in antigen receptor variable region genes of TdT-deficient lymphocytes. *Science* **261**, 1171-5.

Landree, M. A., Wibbenmeyer, J. A. and Roth, D. B. (1999). Mutational analysis of RAG1 and RAG2 identifies three catalytic amino acids in RAG1 critical for both cleavage steps of V(D)J recombination. *Genes Dev* **13**, 3059-69.

Langenau, D. M., Ferrando, A. A., Traver, D., Kutok, J. L., Hezel, J. P., Kanki, J. P., Zon, L. I., Look, A. T. and Trede, N. S. (2004). In vivo tracking of T cell development, ablation, and engraftment in transgenic zebrafish. *Proc Natl Acad Sci U S A* **101**, 7369-74.

Lauring, J. and Schlissel, M. S. (1999). Distinct factors regulate the murine RAG-2 promoter in B- and T-cell lines. *Mol Cell Biol* **19**, 2601-12.

Le Deist, F., Poinsignon, C., Moshous, D., Fischer, A. and de Villartay, J. P. (2004). Artemis sheds new light on V(D)J recombination. *Immunol Rev* **200**, 142-55.

Lee, J. and Desiderio, S. (1999). Cyclin A/CDK2 regulates V(D)J recombination by coordinating RAG-2 accumulation and DNA repair. *Immunity* **11**, 771-81.

Lee, S. S., Fitch, D., Flajnik, M. F. and Hsu, E. (2000a). Rearrangement of immunoglobulin genes in shark germ cells. *J Exp Med* **191**, 1637-48.

Lee, Y., Barnes, D. E., Lindahl, T. and McKinnon, P. J. (2000b). Defective neurogenesis resulting from DNA ligase IV deficiency requires Atm. *Genes Dev* **14**, 2576-80.

Leroy, P., Alzari, P., Sassoon, D., Wolgemuth, D. and Fellous, M. (1989). The protein encoded by a murine male germ cell-specific transcript is a putative ATP-dependent RNA helicase. *Cell* **57**, 549-59.

Leung, Y. F. and Cavalieri, D. (2003). Fundamentals of cDNA microarray data analysis. *Trends Genet* **19**, 649-59.

Levy, N. S., Bakalyar, H. A. and Reed, R. R. (1991). Signal transduction in olfactory neurons. *J Steroid Biochem Mol Biol* **39**, 633-7.

Lewcock, J. W. and Reed, R. R. (2004). A feedback mechanism regulates monoallelic odorant receptor expression. *Proc Natl Acad Sci U S A* **101**, 1069-74.

Lewis, S. M., Agard, E., Suh, S. and Czyzyk, L. (1997). Cryptic signals and the fidelity of V(D)J joining. *Mol Cell Biol* **17**, 3125-36.

Li, J., Ishii, T., Feinstein, P. and Mombaerts, P. (2004). Odorant receptor gene choice is reset by nuclear transfer from mouse olfactory sensory neurons. *Nature* **428**, 393-9.

Li, Z., Dordai, D. I., Lee, J. and Desiderio, S. (1996). A conserved degradation signal regulates RAG-2 accumulation during cell division and links V(D)J recombination to the cell cycle. *Immunity* **5**, 575-89.

Liang, H. E., Hsu, L. Y., Cado, D., Cowell, L. G., Kelsoe, G. and Schlissel, M. S. (2002). The "dispensable" portion of RAG2 is necessary for efficient V-to-DJ rearrangement during B and T cell development. *Immunity* **17**, 639-51.

Lieber, M. R., Hesse, J. E., Mizuuchi, K. and Gellert, M. (1987). Developmental stage specificity of the lymphoid V(D)J recombination activity. *Genes Dev* **1**, 751-61.

Lin, W. C. and Desiderio, S. (1993). Regulation of V(D)J recombination activator protein RAG-2 by phosphorylation. *Science* **260**, 953-9.

Lin, W. C. and Desiderio, S. (1994). Cell cycle regulation of V(D)J recombination-activating protein RAG-2. *Proc Natl Acad Sci U S A* **91**, 2733-7.

Lipschitz, D. L. and Michel, W. C. (2002). Amino acid odorants stimulate microvillar sensory neurons. *Chem Senses* **27**, 277-86.

Lo, J., Lee, S., Xu, M., Liu, F., Ruan, H., Eun, A., He, Y., Ma, W., Wang, W., Wen, Z. et al. (2003). 15000 unique zebrafish EST clusters and their future use in microarray for profiling gene expression patterns during embryogenesis. *Genome Res* **13**, 455-66.

Loconto, J., Papes, F., Chang, E., Stowers, L., Jones, E. P., Takada, T., Kumanovics, A., Fischer Lindahl, K. and Dulac, C. (2003). Functional expression of murine V2R pheromone receptors involves selective association with the M10 and M1 families of MHC class Ib molecules. *Cell* **112**, 607-18.

Lou, Z., Kastury, K., Crilley, P., Lasota, J., Druck, T., Croce, C. M. and Huebner, K. (1993). Characterization of human bone marrow-derived closed circular DNA clones. *Genes Chromosomes Cancer* **7**, 15-27.

Lucas, S. M., Rothwell, N. J. and Gibson, R. M. (2006). The role of inflammation in CNS injury and disease. *Br J Pharmacol* **147 Suppl 1**, S232-40.

Maeda, T., Chijiiwa, Y., Tsuji, H., Sakoda, S., Tani, K. and Suzuki, T. (2004). Somatic DNA recombination yielding circular DNA and deletion of a genomic region in embryonic brain. *Biochem Biophys Res Commun* **319**, 1117-23.

Malicki, J. (2000). Harnessing the power of forward genetics--analysis of neuronal diversity and patterning in the zebrafish retina. *Trends Neurosci* **23**, 531-41.

Mathavan, S., Lee, S. G., Mak, A., Miller, L. D., Murthy, K. R., Govindarajan, K. R., Tong, Y., Wu, Y. L., Lam, S. H., Yang, H. et al. (2005). Transcriptome analysis of zebrafish embryogenesis using microarrays. *PLoS Genet* **1**, 260-76.

Matsunami, H. and Buck, L. B. (1997). A multigene family encoding a diverse array of putative pheromone receptors in mammals. *Cell* **90**, 775-84.

Matsuoka, M., Nagawa, F., Okazaki, K., Kingsbury, L., Yoshida, K., Muller, U., Larue, D. T., Winer, J. A. and Sakano, H. (1991). Detection of somatic DNA recombination in the transgenic mouse brain. *Science* **254**, 81-6.

McBlane, J. F., van Gent, D. C., Ramsden, D. A., Romeo, C., Cuomo, C. A., Gellert, M. and Oettinger, M. A. (1995). Cleavage at a V(D)J recombination signal requires only RAG1 and RAG2 proteins and occurs in two steps. *Cell* **83**, 387-95.

Meek, K., Gupta, S., Ramsden, D. A. and Lees-Miller, S. P. (2004). The DNA-dependent protein kinase: the director at the end. *Immunol Rev* **200**, 132-41.

Menco, B. P., Cunningham, A. M., Qasba, P., Levy, N. and Reed, R. R. (1997). Putative odour receptors localize in cilia of olfactory receptor cells in rat and mouse: a freeze-substitution ultrastructural study. *J Neurocytol* **26**, 297-312.

Messier, T. L., O'Neill, J. P., Hou, S. M., Nicklas, J. A. and Finette, B. A. (2003). In vivo transposition mediated by V(D)J recombinase in human T lymphocytes. *Embo J* **22**, 1381-8.

Mizuno, T., Shinya, M. and Takeda, H. (1999). Cell and tissue transplantation in zebrafish embryos. *Methods Mol Biol* **127**, 15-28.

Mizuta, R., Mizuta, M., Araki, S. and Kitamura, D. (2002). RAG2 is down-regulated by cytoplasmic sequestration and ubiquitin-dependent degradation. *J Biol Chem* **277**, 41423-7.

Moens, C. B. and Prince, V. E. (2002). Constructing the hindbrain: insights from the zebrafish. *Dev Dyn* **224**, 1-17.

Mombaerts, P., Iacomini, J., Johnson, R. S., Herrup, K., Tonegawa, S. and Papaioannou, V. E. (1992). RAG-1-deficient mice have no mature B and T lymphocytes. *Cell* **68**, 869-77.

Mombaerts, P., Wang, F., Dulac, C., Chao, S. K., Nemes, A., Mendelsohn, M., Edmondson, J. and Axel, R. (1996). Visualizing an olfactory sensory map. *Cell* **87**, 675-86.

Monroe, R. J., Chen, F., Ferrini, R., Davidson, L. and Alt, F. W. (1999). RAG2 is regulated differentially in B and T cells by elements 5' of the promoter. *Proc Natl Acad Sci U S A* **96**, 12713-8.

Morita, Y. and Finger, T. E. (1998). Differential projections of ciliated and microvillous olfactory receptor cells in the catfish, Ictalurus punctatus. *J Comp Neurol* **398**, 539-50.

Mueller, T. and Wullimann, M. F. (2005). Atlas of Early Zebrafish Brain Development. A Tool for Molecular Neurogenetics. Amsterdam: Elsevier B. V.

Nagawa, F., Yoshihara, S., Tsuboi, A., Serizawa, S., Itoh, K. and Sakano, H. (2002). Genomic analysis of the murine odorant receptor MOR28 cluster: a possible role of gene conversion in maintaining the olfactory map. *Gene* **292**, 73-80.

Nasevicius, A. and Ekker, S. C. (2000). Effective targeted gene 'knockdown' in zebrafish. *Nat Genet* **26**, 216-20.

Neumann, C. J. (2001). Pattern formation in the zebrafish retina. *Semin Cell Dev Biol* **12**, 485-90.

Neumann, C. J. and Nuesslein-Volhard, C. (2000). Patterning of the zebrafish retina by a wave of sonic hedgehog activity. *Science* **289**, 2137-9.

Oettinger, M. A., Schatz, D. G., Gorka, C. and Baltimore, D. (1990). RAG-1 and RAG-2, adjacent genes that synergistically activate V(D)J recombination. *Science* **248**, 1517-23.

Ogiwara, I., Miya, M., Ohshima, K. and Okada, N. (1999). Retropositional parasitism of SINEs on LINEs: identification of SINEs and LINEs in elasmobranchs. *Mol Biol Evol* **16**, 1238-50.

Okazaki, K., Davis, D. D. and Sakano, H. (1987). T cell receptor beta gene sequences in the circular DNA of thymocyte nuclei: direct evidence for intramolecular DNA deletion in V-D-J joining. *Cell* **49**, 477-85.

Okazaki, N., Yan, J., Yuasa, S., Ueno, T., Kominami, E., Masuho, Y., Koga, H. and Muramatsu, M. (2000). Interaction of the Unc-51-like kinase and microtubule-associated protein light chain 3 related proteins in the brain: possible role of vesicular transport in axonal elongation. *Brain Res Mol Brain Res* **85**, 1-12.

Oxtoby, E. and Jowett, T. (1993). Cloning of the zebrafish krox-20 gene (krx-20) and its expression during hindbrain development. *Nucleic Acids Res* **21**, 1087-95.

Ozon, S., El Mestikawy, S. and Sobel, A. (1999). Differential, regional, and cellular expression of the stathmin family transcripts in the adult rat brain. *J Neurosci Res* **56**, 553-64.

Paddock, S. W. (2000). Principles and practices of laser scanning confocal microscopy. *Mol Biotechnol* **16**, 127-49.

Park, H. C., Kim, C. H., Bae, Y. K., Yeo, S. Y., Kim, S. H., Hong, S. K., Shin, J., Yoo, K. W., Hibi, M., Hirano, T. et al. (2000). Analysis of upstream elements in the HuC promoter leads to the establishment of transgenic zebrafish with fluorescent neurons. *Dev Biol* **227**, 279-93.

Peixoto, B. R., Mikawa, Y. and Brenner, S. (2000). Characterization of the recombinase activating gene-1 and 2 locus in the Japanese pufferfish, Fugu rubripes. *Gene* **246**, 275-83.

Pickel, J. M., McCormack, W. T., Chen, C. H., Cooper, M. D. and Thompson, C. B. (1993). Differential regulation of V(D)J recombination during development of avian B and T cells. *Int Immunol* **5**, 919-27.

Prasad, B. C. and Reed, R. R. (1999). Chemosensation: molecular mechanisms in worms and mammals. *Trends Genet* **15**, 150-3.

Qian, F., Zhen, F., Ong, C., Jin, S. W., Meng Soo, H., Stainier, D. Y., Lin, S., Peng, J. and Wen, Z. (2005). Microarray analysis of zebrafish cloche mutant using amplified cDNA and identification of potential downstream target genes. *Dev Dyn* **233**, 1163-72.

Qiu, J. X., Kale, S. B., Yarnell Schultz, H. and Roth, D. B. (2001). Separation-of-function mutants reveal critical roles for RAG2 in both the cleavage and joining steps of V(D)J recombination. *Mol Cell* **7**, 77-87.

Quackenbush, J. (2002). Microarray data normalization and transformation. *Nat Genet* **32 Suppl**, 496-501.

Quetglas, S., Leveque, C., Miquelis, R., Sato, K. and Seagar, M. (2000). Ca2+-dependent regulation of synaptic SNARE complex assembly via a calmodulin- and phospholipid-binding domain of synaptobrevin. *Proc Natl Acad Sci U S A* **97**, 9695-700.

Raghavan, S. C., Swanson, P. C., Wu, X., Hsieh, C. L. and Lieber, M. R. (2004). A non-B-DNA structure at the Bcl-2 major breakpoint region is cleaved by the RAG complex. *Nature* **428**, 88-93.

Ramsay, G. (1998). DNA chips: state-of-the art. *Nat Biotechnol* **16**, 40-4.

Ramsden, D. A., Paull, T. T. and Gellert, M. (1997). Cell-free V(D)J recombination. *Nature* **388**, 488-91.

Reed, R. R. (1992). Signaling pathways in odorant detection. *Neuron* **8**, 205-9.

Ressler, K. J., Sullivan, S. L. and Buck, L. B. (1993). A zonal organization of odorant receptor gene expression in the olfactory epithelium. *Cell* **73**, 597-609.

Restrepo, D., Arellano, J., Oliva, A. M., Schaefer, M. L. and Lin, W. (2004). Emerging views on the distinct but related roles of the main and accessory olfactory systems in responsiveness to chemosensory signals in mice. *Horm Behav* **46**, 247-56.

Rosok, O., Pedeutour, F., Ree, A. H. and Aasheim, H. C. (1999). Identification and characterization of TESK2, a novel member of the LIMK/TESK family of protein kinases, predominantly expressed in testis. *Genomics* **61**, 44-54.

Rubin, B. D. and Katz, L. C. (1999). Optical imaging of odorant representations in the mammalian olfactory bulb. *Neuron* **23**, 499-511.

Rudie Hovland, A., Nahreini, P., Andreatta, C. P., Edwards-Prasad, J. and Prasad, K. N. (2001). Identifying genes involved in regulating differentiation of neuroblastoma cells. *J Neurosci Res* **64**, 302-10.

Rupp, B., Wullimann, M. F. and Reichert, H. (1996). The zebrafish brain: a neuroanatomical comparison with the goldfish. *Anat Embryol (Berl)* **194**, 187-203.

Rupp, R. A., Snider, L. and Weintraub, H. (1994). Xenopus embryos regulate the nuclear localization of XMyoD. *Genes Dev* **8**, 1311-23.

Sacchetti, A., Subramaniam, V., Jovin, T. M. and Alberti, S. (2002). Oligomerization of DsRed is required for the generation of a functional red fluorescent chromophore. *FEBS Lett* **525**, 13-9.

Sadofsky, M. J. (2004). Recombination-activating gene proteins: more regulation, please. *Immunol Rev* **200**, 83-9.

Sadofsky, M. J., Hesse, J. E. and Gellert, M. (1994). Definition of a core region of RAG-2 that is functional in V(D)J recombination. *Nucleic Acids Res* **22**, 1805-9.

Sadofsky, M. J., Hesse, J. E., McBlane, J. F. and Gellert, M. (1993). Expression and V(D)J recombination activity of mutated RAG-1 proteins. *Nucleic Acids Res* **21**, 5644-50.

Salustri, A., Garlanda, C., Hirsch, E., De Acetis, M., Maccagno, A., Bottazzi, B., Doni, A., Bastone, A., Mantovani, G., Beck Peccoz, P. et al. (2004). PTX3 plays a key role in the organization of the cumulus oophorus extracellular matrix and in in vivo fertilization. *Development* **131**, 1577-86.

Santagata, S., Gomez, C. A., Sobacchi, C., Bozzi, F., Abinun, M., Pasic, S., Cortes, P., Vezzoni, P. and Villa, A. (2000). N-terminal RAG1 frameshift mutations in Omenn's syndrome: internal methionine usage leads to partial V(D)J recombination activity and reveals a fundamental role in vivo for the N-terminal domains. *Proc Natl Acad Sci U S A* **97**, 14572-7.

Sato, Y., Miyasaka, N. and Yoshihara, Y. (2005). Mutually exclusive glomerular innervation by two distinct types of olfactory sensory neurons revealed in transgenic zebrafish. *J Neurosci* **25**, 4889-97.

Schatz, D. G. (2004). Antigen receptor genes and the evolution of a recombinase. *Semin Immunol* **16**, 245-56.

Schatz, D. G., Oettinger, M. A. and Baltimore, D. (1989). The V(D)J recombination activating gene, RAG-1. *Cell* **59**, 1035-48.

Scheer, N. and Camnos-Ortega, J. A. (1999). Use of the Gal4-UAS technique for targeted gene expression in the zebrafish. *Mech Dev* **80**, 153-8.

Schena, M., Heller, R. A., Theriault, T. P., Konrad, K., Lachenmeier, E. and Davis, R. W. (1998). Microarrays: biotechnology's discovery platform for functional genomics. *Trends Biotechnol* **16**, 301-6.

Schluter, S. F. and Marchalonis, J. J. (2003). Cloning of shark RAG2 and characterization of the RAG1/RAG2 gene locus. *Faseb J* **17**, 470-2.

Schwarz, K., Gauss, G. H., Ludwig, L., Pannicke, U., Li, Z., Lindner, D., Friedrich, W., Seger, R. A., Hansen-Hagge, T. E., Desiderio, S. et al. (1996). RAG mutations in human B cell-negative SCID. *Science* **274**, 97-9.

Sekiguchi, J. M., Gao, Y., Gu, Y., Frank, K., Sun, Y., Chaudhuri, J., Zhu, C., Cheng, H. L., Manis, J., Ferguson, D. et al. (1999). Nonhomologous end-joining proteins are required for V(D)J recombination, normal growth, and neurogenesis. *Cold Spring Harb Symp Quant Biol* **64**, 169-81.

Serizawa, S., Miyamichi, K., Nakatani, H., Suzuki, M., Saito, M., Yoshihara, Y. and Sakano, H. (2003). Negative feedback regulation ensures the one receptor-one olfactory neuron rule in mouse. *Science* **302**, 2088-94.

Serizawa, S., Miyamichi, K. and Sakano, H. (2004). One neuron-one receptor rule in the mouse olfactory system. *Trends Genet* **20**, 648-53.

Shin, J. T. and Fishman, M. C. (2002). From Zebrafish to human: modular medical models. *Annu Rev Genomics Hum Genet* **3**, 311-40.

Shinkai, Y., Rathbun, G., Lam, K. P., Oltz, E. M., Stewart, V., Mendelsohn, M., Charron, J., Datta, M., Young, F., Stall, A. M. et al. (1992). RAG-2-deficient mice lack mature lymphocytes owing to inability to initiate V(D)J rearrangement. *Cell* **68**, 855-67.

Shkumatava, A., Fischer, S., Muller, F., Strahle, U. and Neumann, C. J. (2004). Sonic hedgehog, secreted by amacrine cells, acts as a short-range signal to direct differentiation and lamination in the zebrafish retina. *Development* **131**, 3849-58.

Shykind, B. M. (2005). Regulation of odorant receptors: one allele at a time. *Hum Mol Genet* **14 Spec No 1**, R33-9.

Shykind, B. M., Rohani, S. C., O'Donnell, S., Nemes, A., Mendelsohn, M., Sun, Y., Axel, R. and Barnea, G. (2004). Gene switching and the stability of odorant receptor gene choice. *Cell* **117**, 801-15.

Silver, D. P., Spanopoulou, E., Mulligan, R. C. and Baltimore, D. (1993). Dispensable sequence motifs in the RAG-1 and RAG-2 genes for plasmid V(D)J recombination. *Proc Natl Acad Sci U S A* **90**, 6100-4.

Singer, M. S., Shepherd, G. M. and Greer, C. A. (1995). Olfactory receptors guide axons. *Nature* **377**, 19-20.

St Johnston, D. (2002). The art and design of genetic screens: Drosophila melanogaster. *Nat Rev Genet* **3**, 176-88.

Stanfield, S. W. and Helinski, D. R. (1986). Multiple mechanisms generate extrachromosomal circular DNA in Chinese hamster ovary cells. *Nucleic Acids Res* **14**, 3527-38.

Stork, O., Zhdanov, A., Kudersky, A., Yoshikawa, T., Obata, K. and Pape, H. C. (2004). Neuronal functions of the novel serine/threonine kinase Ndr2. *J Biol Chem* **279**, 45773-81.

Sumanas, S., Jorniak, T. and Lin, S. (2005). Identification of novel vascular endothelial-specific genes by the microarray analysis of the zebrafish cloche mutants. *Blood* **106**, 534-41.

Tallafuss, A. and Bally-Cuif, L. (2003). Tracing of her5 progeny in zebrafish transgenics reveals the dynamics of midbrain-hindbrain neurogenesis and maintenance. *Development* **130**, 4307-23.

Thiel, G. (1993). Synapsin I, synapsin II, and synaptophysin: marker proteins of synaptic vesicles. *Brain Pathol* **3**, 87-95.

Tomita, K., Ishibashi, M., Nakahara, K., Ang, S. L., Nakanishi, S., Guillemot, F. and Kageyama, R. (1996). Mammalian hairy and Enhancer of split homolog 1 regulates differentiation of retinal neurons and is essential for eye morphogenesis. *Neuron* **16**, 723-34.

Ton, C., Stamatiou, D., Dzau, V. J. and Liew, C. C. (2002). Construction of a zebrafish cDNA microarray: gene expression profiling of the zebrafish during development. *Biochem Biophys Res Commun* **296**, 1134-42.

Tordjman, R., Lepelletier, Y., Lemarchandel, V., Cambot, M., Gaulard, P., Hermine, O. and Romeo, P. H. (2002). A neuronal receptor, neuropilin-1, is essential for the initiation of the primary immune response. *Nat Immunol* **3**, 477-82.

Uchida, N., Takahashi, Y. K., Tanifuji, M. and Mori, K. (2000). Odor maps in the mammalian olfactory bulb: domain organization and odorant structural features. *Nat Neurosci* **3**, 1035-43.

van Beek, J., Elward, K. and Gasque, P. (2003). Activation of complement in the central nervous system: roles in neurodegeneration and neuroprotection. *Ann N Y Acad Sci* **992**, 56-71.

van Loon, N., Miller, D. and Murnane, J. P. (1994). Formation of extrachromosomal circular DNA in HeLa cells by nonhomologous recombination. *Nucleic Acids Res* **22**, 2447-52.

Vassar, R., Ngai, J. and Axel, R. (1993). Spatial segregation of odorant receptor expression in the mammalian olfactory epithelium. *Cell* **74**, 309-18.

Venkatesh, B., Ning, Y. and Brenner, S. (1999). Late changes in spliceosomal introns define clades in vertebrate evolution. *Proc Natl Acad Sci U S A* **96**, 10267-71.

Vicente-Manzanares, M. and Sanchez-Madrid, F. (2004). Role of the cytoskeleton during leukocyte responses. *Nat Rev Immunol* **4**, 110-22.

Villa, A., Sobacchi, C., Notarangelo, L. D., Bozzi, F., Abinun, M., Abrahamsen, T. G., Arkwright, P. D., Baniyash, M., Brooks, E. G., Conley, M. E. et al. (2001). V(D)J recombination defects in lymphocytes due to RAG mutations: severe immunodeficiency with a spectrum of clinical presentations. *Blood* **97**, 81-8.

von Schwedler, U., Jack, H. M. and Wabl, M. (1990). Circular DNA is a product of the immunoglobulin class switch rearrangement. *Nature* **345**, 452-6.

Wakimoto, B. T. (1998). Beyond the nucleosome: epigenetic aspects of position-effect variegation in Drosophila. *Cell* **93**, 321-4.

Walker, J. R., Corpina, R. A. and Goldberg, J. (2001). Structure of the Ku heterodimer bound to DNA and its implications for double-strand break repair. *Nature* **412**, 607-14.

Wang, F., Nemes, A., Mendelsohn, M. and Axel, R. (1998). Odorant receptors govern the formation of a precise topographic map. *Cell* **93**, 47-60.

Wang, X., Su, H. and Bradley, A. (2002). Molecular mechanisms governing Pcdh-gamma gene expression: evidence for a multiple promoter and cis-alternative splicing model. *Genes Dev* **16**, 1890-905.

Wei, X. C., Dohkan, J., Kishi, H., Wu, C. X., Kondo, S. and Muraguchi, A. (2005). Characterization of the proximal enhancer element and transcriptional regulatory factors for murine recombination activating gene-2. *Eur J Immunol* **35**, 612-21.

Wei, X. C., Kishi, H., Jin, Z. X., Zhao, W. P., Kondo, S., Matsuda, T., Saito, S. and Muraguchi, A. (2002). Characterization of chromatin structure and enhancer elements for murine recombination activating gene-2. *J Immunol* **169**, 873-81.

Wekerle, H. (2005). Planting and pruning in the brain: MHC antigens involved in synaptic plasticity? *Proc Natl Acad Sci U S A* **102**, 3-4.

Wess, T. J. (2005). Collagen fibril form and function. *Adv Protein Chem* **70**, 341-74.

Westerfield, M. (2000). The Zebrafish Book. A guide for the laboratory use of zebrafish (Danio rerio). Eugene: University of Oregon Press,.

Whitfield, T. T., Riley, B. B., Chiang, M. Y. and Phillips, B. (2002). Development of the zebrafish inner ear. *Dev Dyn* **223**, 427-58.

Wienholds, E., Schulte-Merker, S., Walderich, B. and Plasterk, R. H. (2002). Target-selected inactivation of the zebrafish rag1 gene. *Science* **297**, 99-102.

Wilkinson, D. G., Bhatt, S., Chavrier, P., Bravo, R. and Charnay, P. (1989). Segment-specific expression of a zinc-finger gene in the developing nervous system of the mouse. *Nature* **337**, 461-4.

Willett, C. E., Cherry, J. J. and Steiner, L. A. (1997). Characterization and expression of the recombination activating genes (rag1 and rag2) of zebrafish. *Immunogenetics* **45**, 394-404.

Wu, Q., Zhang, T., Cheng, J. F., Kim, Y., Grimwood, J., Schmutz, J., Dickson, M., Noonan, J. P., Zhang, M. Q., Myers, R. M. et al. (2001). Comparative DNA sequence analysis of mouse and human protocadherin gene clusters. *Genome Res* **11**, 389-404.

Yagi, T. (2003). Diversity of the cadherin-related neuronal receptor/protocadherin family and possible DNA rearrangement in the brain. *Genes Cells* **8**, 1-8.

Yannoutsos, N., Barreto, V., Misulovin, Z., Gazumyan, A., Yu, W., Rajewsky, N., Peixoto, B. R., Eisenreich, T. and Nussenzweig, M. C. (2004). A cis element in the recombination activating gene locus regulates gene expression by counteracting a distant silencer. *Nat Immunol* **5**, 443-50.

Yoshida, T., Ito, A., Matsuda, N. and Mishina, M. (2002). Regulation by protein kinase A switching of axonal pathfinding of zebrafish olfactory sensory neurons through the olfactory placode-olfactory bulb boundary. *J Neurosci* **22**, 4964-72.

Yoshihara, Y. and Mori, K. (1997). Basic principles and molecular mechanisms of olfactory axon pathfinding. *Cell Tissue Res* **290**, 457-63.

Yu, W., Misulovin, Z., Suh, H., Hardy, R. R., Jankovic, M., Yannoutsos, N. and Nussenzweig, M. C. (1999). Coordinate regulation of RAG1 and RAG2 by cell type-specific DNA elements 5' of RAG2. *Science* **285**, 1080-4.

Yue, G. H. and Orban, L. (2001). Rapid isolation of DNA from fresh and preserved fish scales for polymerase chain reaction. *Mar Biotechnol (NY)* **3**, 199-204.

Yurchenko, V., Xue, Z. and Sadofsky, M. (2003). The RAG1 N-terminal domain is an E3 ubiquitin ligase. *Genes Dev* **17**, 581-5.

Zarrin, A. A., Berinstein, N.L. (1998). A transcriptional silencer may control the expression of human Recombination Activiting Gene-1. In *10th International Congress of Immunology*, (ed., pp. 433-438. New Delhi, India.

Zarrin, A. A., Fong, I., Malkin, L., Marsden, P. A. and Berinstein, N. L. (1997). Cloning and characterization of the human recombination activating gene 1 (RAG1) and RAG2 promoter regions. *J Immunol* **159**, 4382-94.

Zhang, X. and Firestein, S. (2002). The olfactory receptor gene superfamily of the mouse. *Nat Neurosci* **5**, 124-33.

Zon, L. I. and Peterson, R. T. (2005). In vivo drug discovery in the zebrafish. *Nat Rev Drug Discov* **4**, 35-44.

Appendix 1

SOLUTIONS

100x E3 water

29.2 g NaCl, 1.27 g KCl, 4.85 g $CaCl_2 \cdot 2H_2O$, 8.13 g $MgSO_4 \cdot 7H_2O$ in 1 liter

Ringer's solution

116 mM NaCl, 2.9 mM KCl, 1.8 mM $CaCl_2$, 5 mM pH7.2 HEPES (Sigma Cat# H-4034)

Hank's saline

137 mM NaCl, 5.4 mM KCl, 0.25 mM Na_2HPO_4, 0.44 mM KH_2PO_4, 1.3 mM $CaCl_2$, 1.0 mM $MgSO_4$, 4.2 mM $NaHCO_3$

PTU

0.003% 1-phenyl-2-thiourea in 10% Hank's Saline

LB medium

20 g bacto-trypton, 5 g bacto-yeast extract, 0.5 g NaCl, pH7.0 in 1 liter

SOC medium

LB medium plus 20 mM glucose and 10 mM $MgCl_2$

Glycerol solution

65% glycerol, 0.1 M $MgSO_4$, 25 mM Tris-HCl pH8.0

dNTPs

10 mM of each dATP, dCTP, dGTP and dTTP in H_2O

50x TAE

242 g Tris base, 57.1 ml acetic acid, 50 mM EDTA pH8.5 in 1 liter

6x Loading buffer

I. 0.25% orange G, 30% glycerol in water

II. 0.25% bromophenol blue, 0.25% xylene cyanol FF, 30% glycerol in water

10x DNase I buffer

200 mM pH8.0 Tris-HCl, 20 mM $MgCl_2$ and 500mM KCl

PBS

8 g NaCl, 0.2 g KCl, 1.44 g Na_2HPO_4, 0.24 g KH_2PO_4, pH7.4 in 1 liter.

PBST

PBS plus 0.1% Tween-20

20x SSC

3 M NaCl, 0.3 M sodium citrate

SSCT

SSC plus 0.1% Tween-20

Buffer pH9.5

1 M Tris, 1M $MgCl_2$, pH 9.5; add 0.1% Tween-20 before use

4% PFA/PBS

Add 10 g PFA powder and 100 µl 10 M NaOH into 200 ml PBS, heat at 60°C and stir to dissolve the PFA. Then let it cool down to room temperature, adjust the pH to 7.4 with HCl and top up with PBS to 250 ml. Store at 4°C (or -20°C for long time).

Hybridization buffer for in situ

50% Formamide (Sigma Cat# F-9037), 5x SSC, 9.2 mM citric acid pH6.0, 50 µg/ml Heparine (Sigma Cat# H-9399), 500 µg/ml tRNA (Sigma Cat# R-6625), 0.1% Tween-20

TNT

100 mM pH7.5 Tris-HCl, 150 mM NaCl, 0.05% Tween-20

TNB

100 mM pH7.5 Tris-HCl, 150 mM NaCl, 0.5% blocking reagent (NEN)

Appendix 2 Primers for *Rag1* and *Rag2*

PRIMER NAME	DIRECTION	PRIMER SEQUENCE	SOURCE DNA	REMARKES
rag1a	F	CTCTCAATTCATAAAAAATAAATCTTAC	zf Rag1 (U71093)	
rag1b	R	GGTCCACTCTCCCTCGAG	``	Rag1a/b pair, 350bp
Rag1c	F	TCgggCTCAAAAACACAgACTACg	``	Rag1c/d pair, amplify 920bp from
Rag1d	R	TgCCCCggAAgAAgAACCTAAAAg	``	cDNA, 1769bp from genomic DNA
Rag1e	F	CgACgTgAggCTCTATTgAAACTg	``	Rag1e/f pair, 253bp
Rag1f	R	CACTggCCCATgCTCCgATAgACC	``	
Rag1g	F	GCGGTGGAGGCTGTTTG	``	Rag1g/h pair, 465bp
Rag1h	R	TGTGGCTTGCATTGCTTTTACT	``	
Rag1-intron1F	F	GTTTTGGAGGGAAGAGCAAAG	``	Rag1-intron1F/R pair, amplify 147bp
Rag1-intron1R	R	GTGATGGACCTTTAGCCTTCTG	``	from cDNA, 235bp from genome
Rag1E1	F	TCCGGGGCACAGGCTATGATGAGAA	``	
Rag1wt3412R	R	GCTTAGCAGAAACACCTTTGACTCg	``	For allele-specific PCR to detect a
Rag1mut3412R	R	GCTTAGCAGAAACACCTTTGACTCa	``	point mutation at 4312nt
Rag1-endR-BamH I	R	cgggatcccAAAAATCTGGAACATCAAGACTGTT	``	For clone the Rag1 full length cDNA
zfRag1 site-mut F	F	GCAGACGAACTGCGTGACtGAGTCAAAGGTGTTTCTGCTAAG	yinyi's full zf Rag1	To introduce the stop codon in the
zfRag1 site-mut R	R	CTTAGCAGAAACACCTTTGACTCaGTCACGCAGTTCGTCTGC	``	zf Rag1fullcDNA
Rag2c	F	TCTgggAgCCCTACTATTCTACTg	zf Rag2 (U71094)	
Rag2d	R	CTTgCggTgggTCATCTTCATT	``	
Rag2.Eag1	R	CAACggCCgCTTTTTgAAggTAgCTgTgTAAA	``	Matches to 5' of Rag2 ATG and contains a Eag1 site
Rag-inter 1	R	TCTGCATGAATTCGTGAAGGTGT	z.RAG intergenic region (U69610)	Give a band together with Rag1e but not Rag2e
Rag-inter.2	F	ACCCCgCggCTTTgATTgACTTTCTTTAATggACC	``	with Sac II site
Rag-inter.3	R	ACCCCgCggTTTgTTCTTCTTTTCTCTTCACATgg	``	with Sac II site

Appendix 3 Primers for General Use

PRIMER NAME	DIRECTION	PRIMER SEQUENCE	Tm	SOURCE DNA	REMARKES
T3		AATTAACCCTCACTAAAggg	56		
T7		TAATACgACTCACTATAggg	56		
SP6		ATTTAggTgACACTATAg	48		
M13 Reward	R	ggAAACAgCTATgACCATg	56	pGET-T, pGEM-T easy	
M13-20 Forward	F	gTAAAACgACggCCAgT	56	pGET-T, pGEM-T easy	
SV40-R	R	gTTCAgggggAggTgTgggAggTT	64	pFBD (pFastBacDual)	can be used for clontech vector
HSV-R	R	AATggggTCTCggTggggTATCg	64	pFBD (pFastBacDual)	
pEGFP-N	R	CgTCgCCgTCCAgCTCgACCAg	68	Clontech EGFP	also matches to ECFP and EYFP
pEGFP-N2	R	CTgCTTCATgTggTCggggTAg	58.1	Clontech EGFP	also matches to ECFP and EYFP
pEGFP-C	F	CATggTCCTgCTggAgTTCgTg	59	Clontech EGFP	also matches to ECFP and EYFP
pDsRed-N	R	gTACTggAACTgggggACAg	55	Clontech DsRed1	
pDsRed-C	F	gCTgCCCggCTACTACTACg	66	Clontech DsRed2	
GFPmut3-1	F	TgAAggTgAAggTgATgC	54	GFPmut3 (U73901)	for Suo Lin's Rag1-GFP fish
GFPmut3-2	R	CATgggTAATACCAgCAgC	58	GFPmut3 (U73901)	for Suo Lin's Rag1-GFP fish
WtGFP-end	R	gctctagaTTATTTgTATAgTTCATCCATgCC		Wt-GFP (AF302837)	with a XbaI site; also matches to GFPmut3
5smart3	F	AAgCAgTggTATCAACgCAgAgT	55		
smart3	F	AAgCAgTggTATCAACgCAgAgTggCCATTATggCCggg	79		the 3 "g" at 3' end are rGTP
Oligo dT20-VN		TTTTTTTTTTTTTTTTTTTTVN			V for A, C or G; N for A, T, C or G

Appendix 4

Primers for 12158 locus characterization

PRIMER NAME	PRIMER SEQUENCE	REMARKS
12158-F	AACCGAAGCACCTGGAGGAT	12158
12158-R	AGTCCCACGTTGTATTTCTTTATTTG	``
12158A-F1	AGTCCCACGGTTTAGTCTCG	``
12158A-F2	GGCCCTTTTCAACCTTTTCACT	``
12158A-R	AATACTCTGCAGCCATACGGTTCT	``
12158B-F1	GCAGAGTACGCGGGCAGATTAG	``
12158B-F2	ATAAACCACGGCGAATGAAT	``
12158-R2	GTTCCGTTGTTATCACCAGTTAGC	``
12158-R3	GCCTTTGTTCGCGTGGGTAT	``
12158-rpF2	TGCCCAACTGAGTCTGGTTC	for Real-Time PCR
12158-rpR	TTAATCATTACTGAGAGTTCAAACACTG	``
12158-rtF	TTGAATTGAATGACTTACAGAGCA	``
12158-rtR	GTTCCGTTGTTATCACCAGTTAG	``
actin-rtF	TCGAGCAGGAGATGGGAACC	``
actin-rtR	CTCGTGGATACCGCAAGATTC	``

Appendix 5

The 341 Significants in Adult OE Microarray

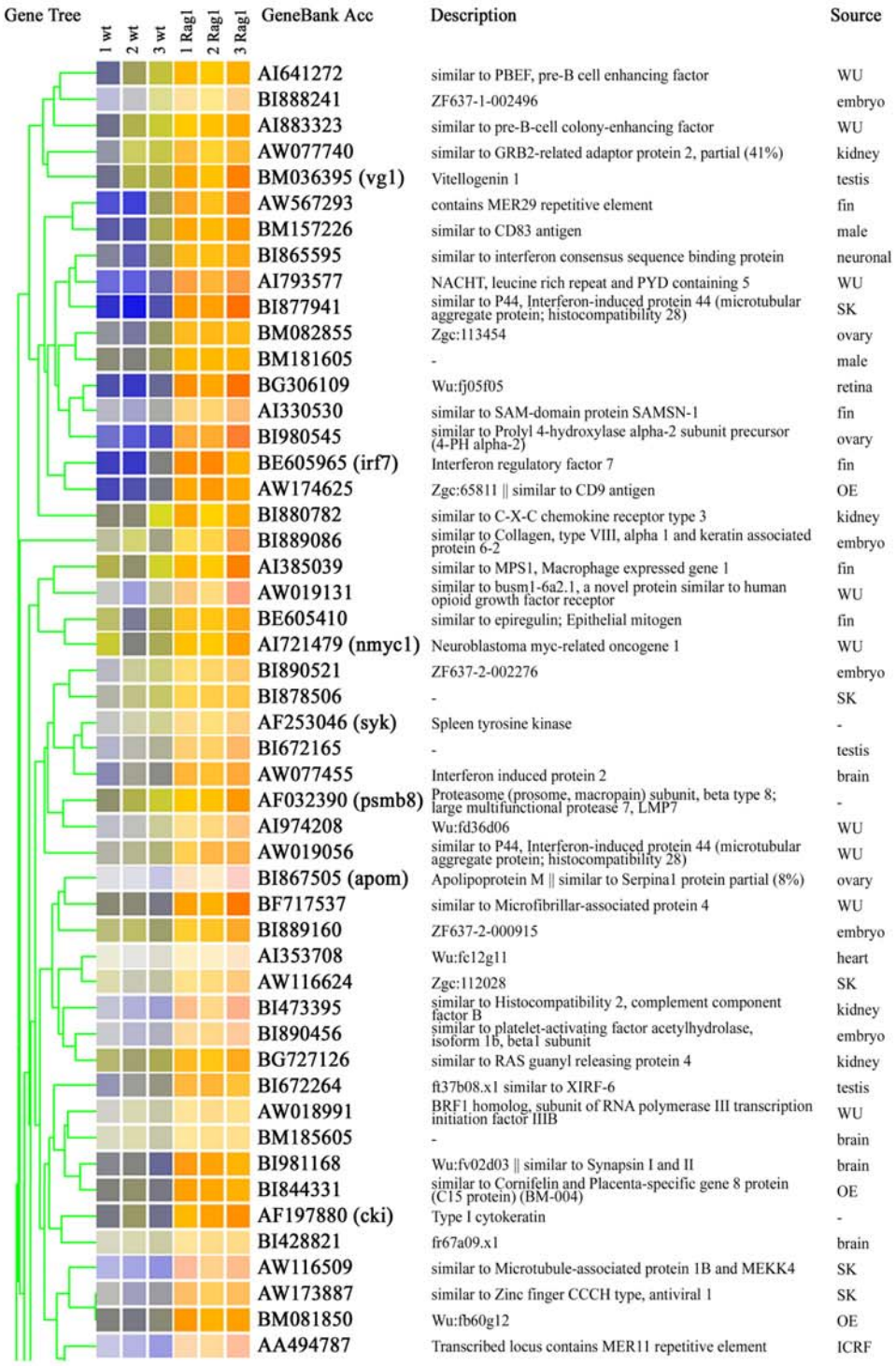

Gene Tree	1 wt	2 wt	3 wt	1 Rag1	2 Rag1	3 Rag1	GeneBank Acc	Description	Source
							AI641272	similar to PBEF, pre-B cell enhancing factor	WU
							BI888241	ZF637-1-002496	embryo
							AI883323	similar to pre-B-cell colony-enhancing factor	WU
							AW077740	similar to GRB2-related adaptor protein 2, partial (41%)	kidney
							BM036395 (vg1)	Vitellogenin 1	testis
							AW567293	contains MER29 repetitive element	fin
							BM157226	similar to CD83 antigen	male
							BI865595	similar to interferon consensus sequence binding protein	neuronal
							AI793577	NACHT, leucine rich repeat and PYD containing 5	WU
							BI877941	similar to P44, Interferon-induced protein 44 (microtubular aggregate protein; histocompatibility 28)	SK
							BM082855	Zgc:113454	ovary
							BM181605	-	male
							BG306109	Wu:fj05f05	retina
							AI330530	similar to SAM-domain protein SAMSN-1	fin
							BI980545	similar to Prolyl 4-hydroxylase alpha-2 subunit precursor (4-PH alpha-2)	ovary
							BE605965 (irf7)	Interferon regulatory factor 7	fin
							AW174625	Zgc:65811 || similar to CD9 antigen	OE
							BI880782	similar to C-X-C chemokine receptor type 3	kidney
							BI889086	similar to Collagen, type VIII, alpha 1 and keratin associated protein 6-2	embryo
							AI385039	similar to MPS1, Macrophage expressed gene 1	fin
							AW019131	similar to busm1-6a2.1, a novel protein similar to human opioid growth factor receptor	WU
							BE605410	similar to epiregulin; Epithelial mitogen	fin
							AI721479 (nmyc1)	Neuroblastoma myc-related oncogene 1	WU
							BI890521	ZF637-2-002276	embryo
							BI878506	-	SK
							AF253046 (syk)	Spleen tyrosine kinase	-
							BI672165	-	testis
							AW077455	Interferon induced protein 2	brain
							AF032390 (psmb8)	Proteasome (prosome, macropain) subunit, beta type 8; large multifunctional protease 7, LMP7	-
							AI974208	Wu:fd36d06	WU
							AW019056	similar to P44, Interferon-induced protein 44 (microtubular aggregate protein; histocompatibility 28)	WU
							BI867505 (apom)	Apolipoprotein M || similar to Serpina1 protein partial (8%)	ovary
							BF717537	similar to Microfibrillar-associated protein 4	WU
							BI889160	ZF637-2-000915	embryo
							AI353708	Wu:fc12g11	heart
							AW116624	Zgc:112028	SK
							BI473395	similar to Histocompatibility 2, complement component factor B	kidney
							BI890456	similar to platelet-activating factor acetylhydrolase, isoform 1b, beta1 subunit	embryo
							BG727126	similar to RAS guanyl releasing protein 4	kidney
							BI672264	ft37b08.x1 similar to XIRF-6	testis
							AW018991	BRF1 homolog, subunit of RNA polymerase III transcription initiation factor IIIB	WU
							BM185605	-	brain
							BI981168	Wu:fv02d03 || similar to Synapsin I and II	brain
							BI844331	similar to Cornifelin and Placenta-specific gene 8 protein (C15 protein) (BM-004)	OE
							AF197880 (cki)	Type I cytokeratin	-
							BI428821	fr67a09.x1	brain
							AW116509	similar to Microtubule-associated protein 1B and MEKK4	SK
							AW173887	similar to Zinc finger CCCH type, antiviral 1	SK
							BM081850	Wu:fb60g12	OE
							AA494787	Transcribed locus contains MER11 repetitive element	ICRF

(Continued)

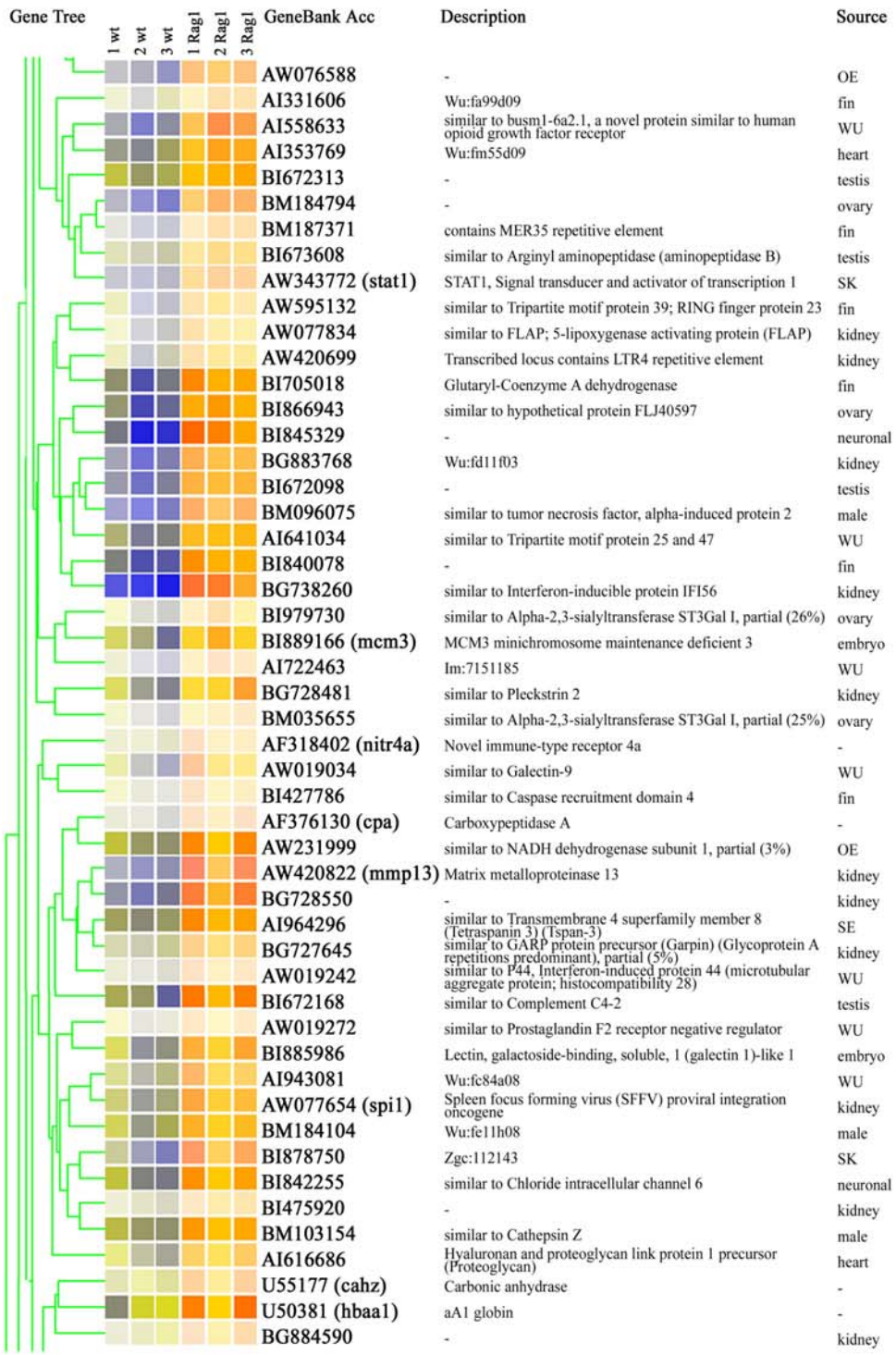
Gene Tree
1 wt
2 wt
3 wt
1 Rag1
2 Rag1
3 Rag1
GeneBank Acc
Description
Source
AW076588 - OE
AI331606 Wu:fa99d09 fin
AI558633 similar to busm1-6a2.1, a novel protein similar to human opioid growth factor receptor WU
AI353769 Wu:fm55d09 heart
BI672313 - testis
BM184794 - ovary
BM187371 contains MER35 repetitive element fin
BI673608 similar to Arginyl aminopeptidase (aminopeptidase B) testis
AW343772 (stat1) STAT1, Signal transducer and activator of transcription 1 SK
AW595132 similar to Tripartite motif protein 39; RING finger protein 23 fin
AW077834 similar to FLAP; 5-lipoxygenase activating protein (FLAP) kidney
AW420699 Transcribed locus contains LTR4 repetitive element kidney
BI705018 Glutaryl-Coenzyme A dehydrogenase fin
BI866943 similar to hypothetical protein FLJ40597 ovary
BI845329 - neuronal
BG883768 Wu:fd11f03 kidney
BI672098 - testis
BM096075 similar to tumor necrosis factor, alpha-induced protein 2 male
AI641034 similar to Tripartite motif protein 25 and 47 WU
BI840078 - fin
BG738260 similar to Interferon-inducible protein IFI56 kidney
BI979730 similar to Alpha-2,3-sialyltransferase ST3Gal I, partial (26%) ovary
BI889166 (mcm3) MCM3 minichromosome maintenance deficient 3 embryo
AI722463 Im:7151185 WU
BG728481 similar to Pleckstrin 2 kidney
BM035655 similar to Alpha-2,3-sialyltransferase ST3Gal I, partial (25%) ovary
AF318402 (nitr4a) Novel immune-type receptor 4a -
AW019034 similar to Galectin-9 WU
BI427786 similar to Caspase recruitment domain 4 fin
AF376130 (cpa) Carboxypeptidase A -
AW231999 similar to NADH dehydrogenase subunit 1, partial (3%) OE
AW420822 (mmp13) Matrix metalloproteinase 13 kidney
BG728550 - kidney
AI964296 similar to Transmembrane 4 superfamily member 8 (Tetraspanin 3) (Tspan-3) SE
BG727645 similar to GARP protein precursor (Garpin) (Glycoprotein A repetitions predominant), partial (5%) kidney
AW019242 similar to P44, Interferon-induced protein 44 (microtubular aggregate protein; histocompatibility 28) WU
BI672168 similar to Complement C4-2 testis
AW019272 similar to Prostaglandin F2 receptor negative regulator WU
BI885986 Lectin, galactoside-binding, soluble, 1 (galectin 1)-like 1 embryo
AI943081 Wu:fc84a08 WU
AW077654 (spi1) Spleen focus forming virus (SFFV) proviral integration oncogene kidney
BM184104 Wu:fe11h08 male
BI878750 Zgc:112143 SK
BI842255 similar to Chloride intracellular channel 6 neuronal
BI475920 - kidney
BM103154 similar to Cathepsin Z male
AI616686 Hyaluronan and proteoglycan link protein 1 precursor (Proteoglycan) heart
U55177 (cahz) Carbonic anhydrase -
U50381 (hbaa1) aA1 globin -
BG884590 - kidney

(Continued)

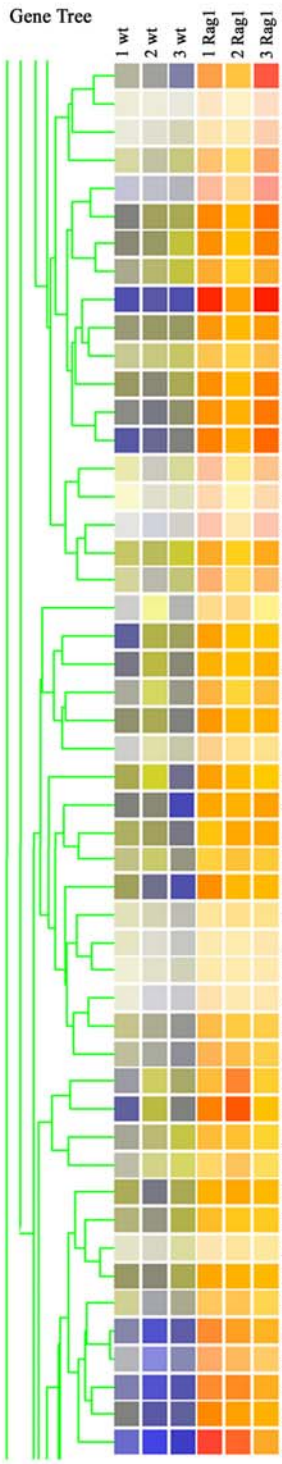

GeneBank Acc	Description	Source
AW184745	-	OE
AA497156	Complement protein component C7	ICRF
BG303313	similar to Coagulation factor XIII, A1 subunit	SK
BM155827	Lectin, galactoside-binding, soluble, 1 (galectin 1)-like 1	embryo
AF349034 (mpx)	Myeloid-specific peroxidase	-
BE557057	similar to cornifelin [Homo sapiens]; PLAC8-like 1	fin
BG727173	-	kidney
BI885361	-	kidney
AF402599 (lyz)	Lysozyme	-
BG728378	-	kidney
BI473291	similar to septin 3	kidney
AW203093	similar to Regulator of G-protein signaling 2	OE
BI672130	Similar to PHD finger protein 6	testis
BI672148	similar to Mucin 2 precursor (Intestinal mucin 2)	testis
AW420589	-	kidney
AI497271	similar to Beta-microseminoprotein	WU
AW305943 (mmp13)	Matrix metalloproteinase 13	kidney
BG727595	similar to Cytochrome c oxidase polypeptide III (74%) and mitotic checkpoint protein kinase Bub1	kidney
AW595495	similar to intestinal mucin-like protein	fin
AW171357	similar to KIAA1018 protein [Homo sapiens]	SK
AA495032	similar to PBEF, pre-B cell enhancing factor	ICRF
AW232046 (env)	Envelope protein	OE
AI882824	similar to tartrate resistant acid phosphatase 5 precursor	SK
BI475655	similar to Complement component 1, q subcomponent, gamma polypeptide	OE
AW466712	similar to Epiprofin	fin
AI722545	similar to Prosaposin	SK
AI641426	similar to Repetitively Interspersed Family	WU
AF327410 (caspb)	Caspase b	-
BI890108 (mcm6)	MCM6 minichromosome maintenance deficient 6, mitotin	embryo
BI876813	-	SK
AF164776	similar to Lyn protein tyrosine kinase, partial (49%)	kidney
AW116315	similar to Complement C4-1	SK
BM185873	similar to Erythrocyte membrane protein band 4.1-like 3	brain
AW018956	Transcribed locus contains MER30 repetitive element	WU
AW777978	-	embryo
AI794490	Wu:fc45a07	WU
AF286374 (atp1a1a.2)	ATPase, Na+/K+ transporting, alpha 1a.2 polypeptide	-
BI475857	Wu:fj65c07	kidney
AI883105	similar to pre-B-cell colony-enhancing factor	SK
BI474937	similar to Rho-related BTB domain-containing protein 1	kidney
BM095893	similar to Interferon-stimulated transcription factor 3	male
BI533933	similar to osteoprotegerin, Tumor necrosis factor receptor 11b	fin
BM081830	similar to NACHT, leucine rich repeat and PYD containing 5, contains MER17 repetitive element	OE
BM103998	similar to Cathepsin Z, partial (97%)	male
BI473402	similar to VHSV-induced protein (80%); estrogen-responsive B box protein and Tripartite motif-containing 16	kidney
AI331286	-	fin
AW019087	similar to Ubiquitin-protein ligase E3A	WU
AI331579	similar to Mov10, Moloney leukemia virus 10	fin
AW420718	Lectin, galactoside-binding, soluble, 9 (galectin 9)-like 1	kidney
AW019716	Similar to novel radical SAM superfamily protein, Viperin	WU

(Continued)

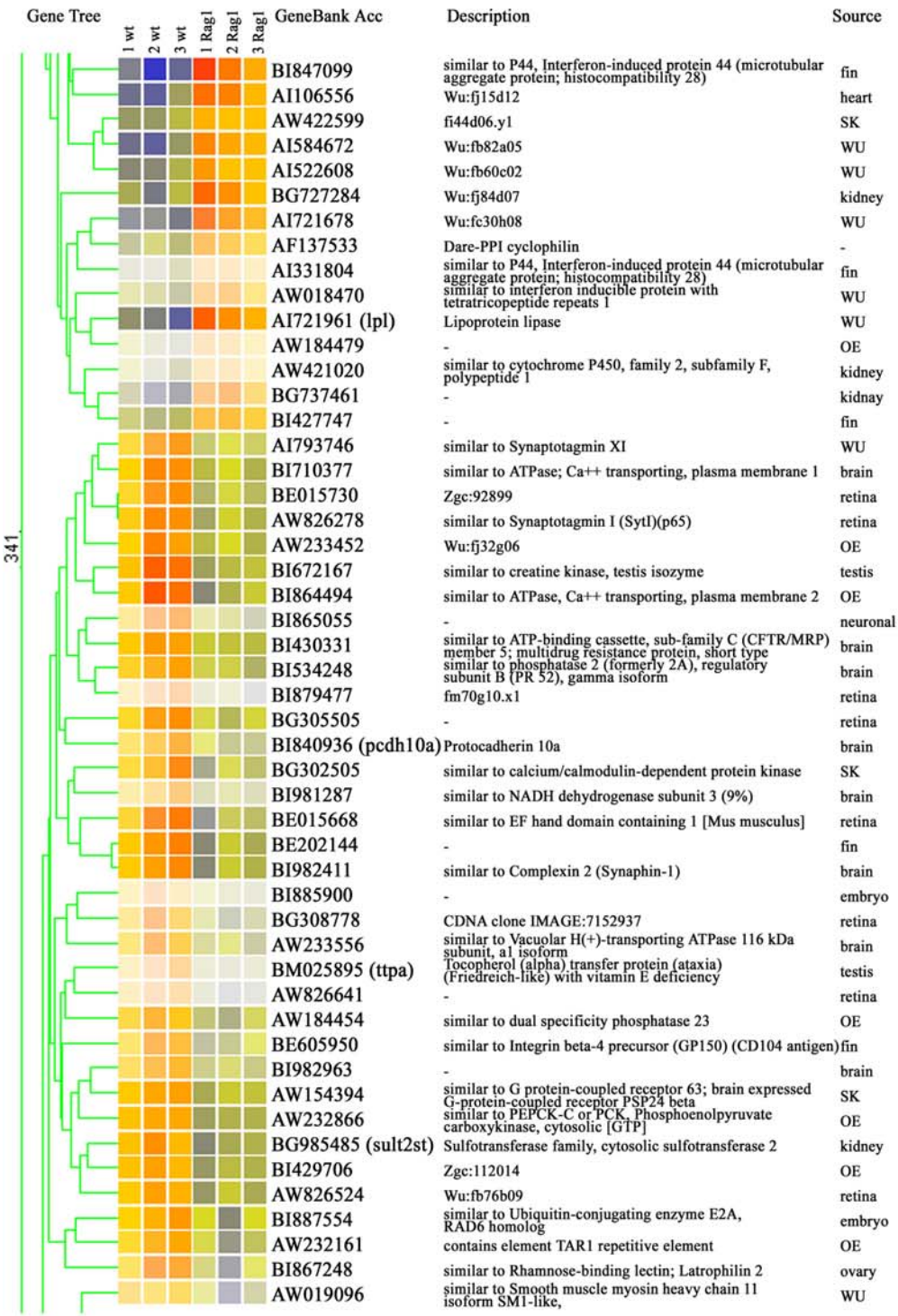
Gene Tree
1 wt
2 wt
3 wt
1 Rag1
2 Rag1
3 Rag1
GeneBank Acc
Description
Source
341
BI847099 similar to P44, Interferon-induced protein 44 (microtubular aggregate protein; histocompatibility 28) fin
AI106556 Wu:fj15d12 heart
AW422599 fi44d06.y1 SK
AI584672 Wu:fb82a05 WU
AI522608 Wu:fb60c02 WU
BG727284 Wu:fj84d07 kidney
AI721678 Wu:fc30h08 WU
AF137533 Dare-PPI cyclophilin -
AI331804 similar to P44, Interferon-induced protein 44 (microtubular aggregate protein; histocompatibility 28) fin
AW018470 similar to interferon inducible protein with tetratricopeptide repeats 1 WU
AI721961 (lpl) Lipoprotein lipase WU
AW184479 - OE
AW421020 similar to cytochrome P450, family 2, subfamily F, polypeptide 1 kidney
BG737461 - kidnay
BI427747 - fin
AI793746 similar to Synaptotagmin XI WU
BI710377 similar to ATPase; Ca++ transporting, plasma membrane 1 brain
BE015730 Zgc:92899 retina
AW826278 similar to Synaptotagmin I (SytI)(p65) retina
AW233452 Wu:fj32g06 OE
BI672167 similar to creatine kinase, testis isozyme testis
BI864494 similar to ATPase, Ca++ transporting, plasma membrane 2 OE
BI865055 - neuronal
BI430331 similar to ATP-binding cassette, sub-family C (CFTR/MRP) member 5; multidrug resistance protein, short type brain
BI534248 similar to phosphatase 2 (formerly 2A), regulatory subunit B (PR 52), gamma isoform brain
BI879477 fm70g10.x1 retina
BG305505 - retina
BI840936 (pcdh10a) Protocadherin 10a brain
BG302505 similar to calcium/calmodulin-dependent protein kinase SK
BI981287 similar to NADH dehydrogenase subunit 3 (9%) brain
BE015668 similar to EF hand domain containing 1 [Mus musculus] retina
BE202144 - fin
BI982411 similar to Complexin 2 (Synaphin-1) brain
BI885900 - embryo
BG308778 CDNA clone IMAGE:7152937 retina
AW233556 similar to Vacuolar H(+)-transporting ATPase 116 kDa subunit, a1 isoform brain
BM025895 (ttpa) Tocopherol (alpha) transfer protein (ataxia) (Friedreich-like) with vitamin E deficiency testis
AW826641 - retina
AW184454 similar to dual specificity phosphatase 23 OE
BE605950 similar to Integrin beta-4 precursor (GP150) (CD104 antigen) fin
BI982963 - brain
AW154394 similar to G protein-coupled receptor 63; brain expressed G-protein-coupled receptor PSP24 beta SK
AW232866 similar to PEPCK-C or PCK, Phosphoenolpyruvate carboxykinase, cytosolic [GTP] OE
BG985485 (sult2st) Sulfotransferase family, cytosolic sulfotransferase 2 kidney
BI429706 Zgc:112014 OE
AW826524 Wu:fb76b09 retina
BI887554 similar to Ubiquitin-conjugating enzyme E2A, RAD6 homolog embryo
AW232161 contains element TAR1 repetitive element OE
BI867248 similar to Rhamnose-binding lectin; Latrophilin 2 ovary
AW019096 similar to Smooth muscle myosin heavy chain 11 isoform SM1-like, WU

(Continued)

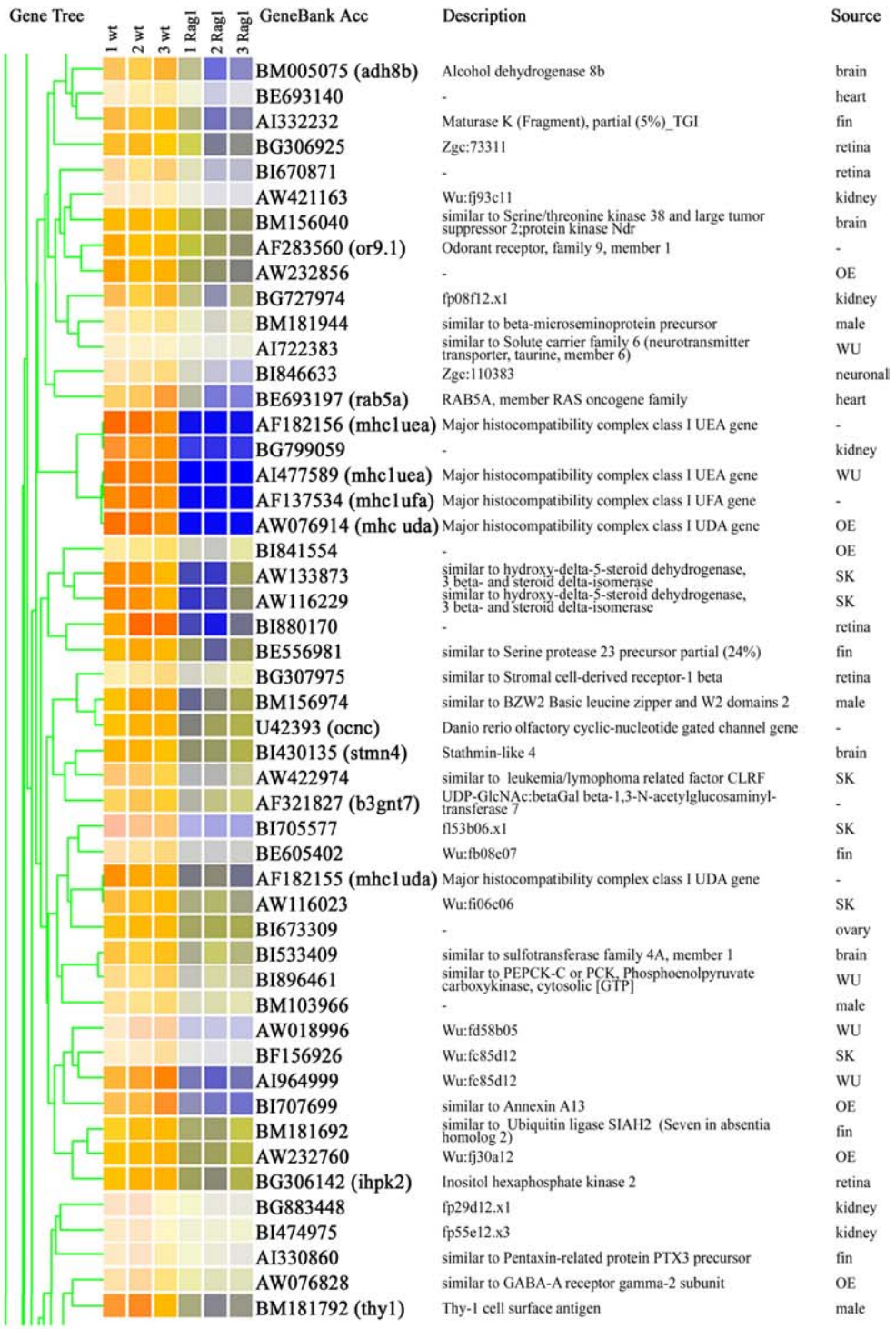
Gene Tree
1 wt
2 wt
3 wt
1 Rag1
2 Rag1
3 Rag1
GeneBank Acc
Description
Source
BM005075 (adh8b) Alcohol dehydrogenase 8b brain
BE693140 - heart
AI332232 Maturase K (Fragment), partial (5%)_TGI fin
BG306925 Zgc:73311 retina
BI670871 - retina
AW421163 Wu:fj93c11 kidney
BM156040 similar to Serine/threonine kinase 38 and large tumor suppressor 2;protein kinase Ndr brain
AF283560 (or9.1) Odorant receptor, family 9, member 1 -
AW232856 - OE
BG727974 fp08f12.x1 kidney
BM181944 similar to beta-microseminoprotein precursor male
AI722383 similar to Solute carrier family 6 (neurotransmitter transporter, taurine, member 6) WU
BI846633 Zgc:110383 neuronal
BE693197 (rab5a) RAB5A, member RAS oncogene family heart
AF182156 (mhc1uea) Major histocompatibility complex class I UEA gene -
BG799059 - kidney
AI477589 (mhc1uea) Major histocompatibility complex class I UEA gene WU
AF137534 (mhc1ufa) Major histocompatibility complex class I UFA gene -
AW076914 (mhc uda) Major histocompatibility complex class I UDA gene OE
BI841554 - OE
AW133873 similar to hydroxy-delta-5-steroid dehydrogenase, 3 beta- and steroid delta-isomerase SK
AW116229 similar to hydroxy-delta-5-steroid dehydrogenase, 3 beta- and steroid delta-isomerase SK
BI880170 - retina
BE556981 similar to Serine protease 23 precursor partial (24%) fin
BG307975 similar to Stromal cell-derived receptor-1 beta retina
BM156974 similar to BZW2 Basic leucine zipper and W2 domains 2 male
U42393 (ocnc) Danio rerio olfactory cyclic-nucleotide gated channel gene -
BI430135 (stmn4) Stathmin-like 4 brain
AW422974 similar to leukemia/lymophoma related factor CLRF SK
AF321827 (b3gnt7) UDP-GlcNAc:betaGal beta-1,3-N-acetylglucosaminyl-transferase 7 -
BI705577 fl53b06.x1 SK
BE605402 Wu:fb08e07 fin
AF182155 (mhc1uda) Major histocompatibility complex class I UDA gene -
AW116023 Wu:fi06c06 SK
BI673309 - ovary
BI533409 similar to sulfotransferase family 4A, member 1 brain
BI896461 similar to PEPCK-C or PCK, Phosphoenolpyruvate carboxykinase, cytosolic [GTP] WU
BM103966 - male
AW018996 Wu:fd58b05 WU
BF156926 Wu:fc85d12 SK
AI964999 Wu:fc85d12 WU
BI707699 similar to Annexin A13 OE
BM181692 similar to Ubiquitin ligase SIAH2 (Seven in absentia homolog 2) fin
AW232760 Wu:fj30a12 OE
BG306142 (ihpk2) Inositol hexaphosphate kinase 2 retina
BG883448 fp29d12.x1 kidney
BI474975 fp55e12.x3 kidney
AI330860 similar to Pentaxin-related protein PTX3 precursor fin
AW076828 similar to GABA-A receptor gamma-2 subunit OE
BM181792 (thy1) Thy-1 cell surface antigen male

(Continued)

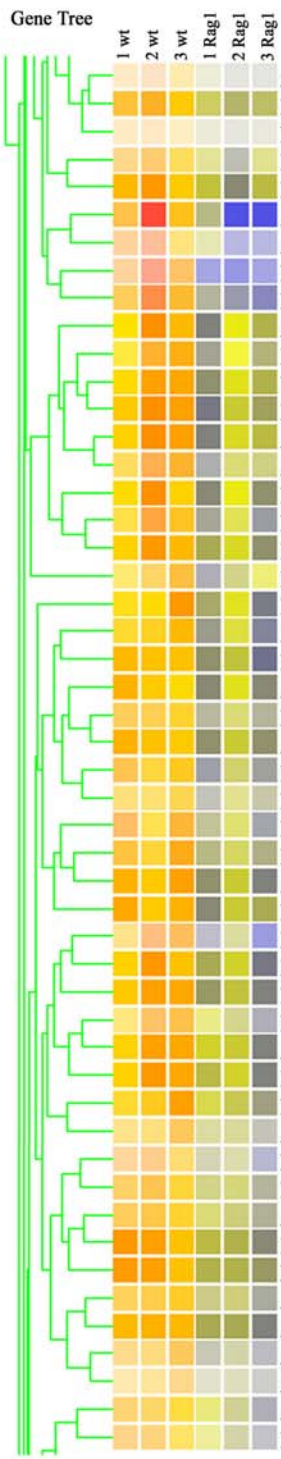

GeneBank Acc	Description	Source
AI641158	similar to ATPASE 6; contains L1 repetitive element	WU
BI672376	similar to Tubulin, beta 2	testis
BI877868	fl67d01.x1	SK
BI888606	similar to NF-YB, Nuclear transcription factor Y subunit beta	embryo
BI865041	-	neuronal
AI601338	Wu:fc10a01	WU
AI522693	-	WU
BG883345	-	kidney
BG308888	similar to KIAA0553 protein	retina
AW076585	similar to S-100 protein, alpha chain	WU
BM035348 (vamp2)	Vesicle-associated membrane protein 2	brain
U72685 (or3.1)	Danio rerio odorant receptor 3 (ZOR3) gene, partial cds.	-
BI429738	Hypothetical protein LOC553446	OE
AW184252	fj11c05.y1	OE
AI957754 (cdo1)	Cysteine dioxygenase, type I	WU
BI839526 (ivns1abpa)	Influenza virus NS1A binding protein a	brain
BM103356	fv20d06.x1	brain
BI879868	Wu:fj48a08	retina
BI670974	similar to Synaptophysin	OE
BI882244	similar to sulfide quinone reductase-like, partial (83%)	fin
AW203029 (chga)	Chromogranin A	OE
BM024532	-	brain
AI959474	similar to Retinoblastoma binding protein 6	WU
BI878329 (eno2)	Enolase 2	retina
AW826462	similar to embigin [Homo sapiens] and teratocarcinoma glycoprotein GP-70 precursor - mouse	retina
BI890046 (otop1)	Otopetrin 1	embryo
BI844904	similar to Pl10	brain
BI427769	-	fin
BI887892	similar to plakophilin 1 isoform 1b [Homo sapiens]	embryo
AI544512 (otop1)	Otopetrin 1	WU
BG308711	-	retina
BG305588	fm06a08.x1	retina
BI865609 (atp1b2a)	ATPase, Na+/K+ transporting, beta 2a polypeptide and heterogeneous nuclear ribonucleoprotein C isoform b	neuronal
BI534285	-	brain
BI888989	similar to Phosphoribosyl-ATP pyrophosphatase (PRA-PH)	embryo
AF012748 (or2.1)	Odorant receptor, family 2, member 1	-
BI878898 (nsf)	N-ethylmaleimide-sensitive factor	SK
BI879589	similar to KIAA1582 protein and Probable tolQ-type transport protein (8%)	retina
AF012761 (or2.7)	Danio rerio olfactory receptor protein 2.7 gene, complete cds.	-
BM080877	-	ovary
BI979865	CDNA clone MGC:110128 IMAGE:7286967	ovary
AI884262 (dnmt3bl)	similar to DNA (cytosine-5-)-methyltransferase 3 beta	WU
BG305533 (vamp2)	Vesicle-associated membrane protein 2	retina
X97333 (her6)	Hairy-related 6	-
AF425590 (trac)	T cell receptor alpha constant	-
AW305605 (vamp2)	Vesicle-associated membrane protein 2	brain
AW233752	Wu:fj41f10	brain
AI958242	similar to Telomerase associated protein 1	WU
AI641534	CpG DNA methylase (cytosine-specific methyltransferase)	WU
BI886668	similar to Calcineurin B subunit	embryo

(Continued)

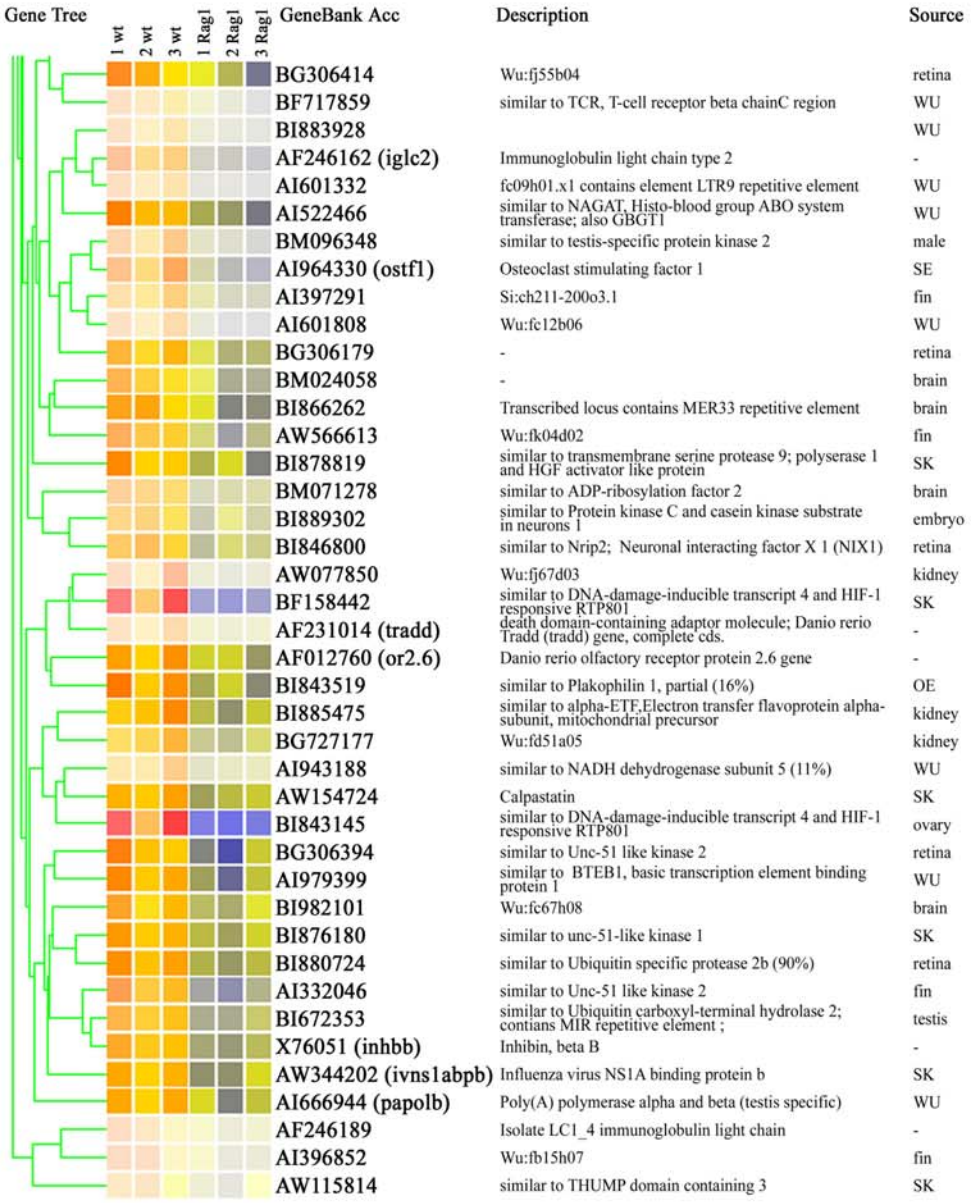

Gene Tree	1 wt	2 wt	3 wt	1 Rag1	2 Rag1	3 Rag1	GeneBank Acc	Description	Source
							BG306414	Wu:fj55b04	retina
							BF717859	similar to TCR, T-cell receptor beta chainC region	WU
							BI883928		WU
							AF246162 (iglc2)	Immunoglobulin light chain type 2	-
							AI601332	fc09h01.x1 contains element LTR9 repetitive element	WU
							AI522466	similar to NAGAT, Histo-blood group ABO system transferase; also GBGT1	WU
							BM096348	similar to testis-specific protein kinase 2	male
							AI964330 (ostf1)	Osteoclast stimulating factor 1	SE
							AI397291	Si:ch211-200o3.1	fin
							AI601808	Wu:fc12b06	WU
							BG306179	-	retina
							BM024058	-	brain
							BI866262	Transcribed locus contains MER33 repetitive element	brain
							AW566613	Wu:fk04d02	fin
							BI878819	similar to transmembrane serine protease 9; polyserase 1 and HGF activator like protein	SK
							BM071278	similar to ADP-ribosylation factor 2	brain
							BI889302	similar to Protein kinase C and casein kinase substrate in neurons 1	embryo
							BI846800	similar to Nrip2; Neuronal interacting factor X 1 (NIX1)	retina
							AW077850	Wu:fj67d03	kidney
							BF158442	similar to DNA-damage-inducible transcript 4 and HIF-1 responsive RTP801	SK
							AF231014 (tradd)	death domain-containing adaptor molecule; Danio rerio Tradd (tradd) gene, complete cds.	-
							AF012760 (or2.6)	Danio rerio olfactory receptor protein 2.6 gene	-
							BI843519	similar to Plakophilin 1, partial (16%)	OE
							BI885475	similar to alpha-ETF,Electron transfer flavoprotein alpha-subunit, mitochondrial precursor	kidney
							BG727177	Wu:fd51a05	kidney
							AI943188	similar to NADH dehydrogenase subunit 5 (11%)	WU
							AW154724	Calpastatin	SK
							BI843145	similar to DNA-damage-inducible transcript 4 and HIF-1 responsive RTP801	ovary
							BG306394	similar to Unc-51 like kinase 2	retina
							AI979399	similar to BTEB1, basic transcription element binding protein 1	WU
							BI982101	Wu:fc67h08	brain
							BI876180	similar to unc-51-like kinase 1	SK
							BI880724	similar to Ubiquitin specific protease 2b (90%)	retina
							AI332046	similar to Unc-51 like kinase 2	fin
							BI672353	similar to Ubiquitin carboxyl-terminal hydrolase 2; contians MIR repetitive element ;	testis
							X76051 (inhbb)	Inhibin, beta B	-
							AW344202 (ivns1abpb)	Influenza virus NS1A binding protein b	SK
							AI666944 (papolb)	Poly(A) polymerase alpha and beta (testis specific)	WU
							AF246189	Isolate LC1_4 immunoglobulin light chain	-
							AI396852	Wu:fb15h07	fin
							AW115814	similar to THUMP domain containing 3	SK